

An Investigation into a Class of Fractional Order Analog Circuits

Submitted in partial fulfilment of the requirements for the award of the degree

of

Doctor of Philosophy

by

MANOJ KUMAR

Roll. No. 2K15/Ph.D/EE/07

Under the Supervision of

Prof. Pragati Kumar

Department of Electrical Engineering

Delhi Technological University

New Delhi-110042

Prof. D. R. Bhaskar

Department of Electrical Engineering

Delhi Technological University

New Delhi-110042



Department of Electrical Engineering

Delhi Technological University

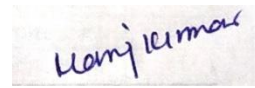
Shahabad Daulatpur, Main Bawana Road,

Delhi-110042

February, 2021

DECLARATION

I hereby declare that the work which is being presented in this thesis entitled “**An Investigation into a Class of Fractional Order Analog Circuits**” being submitted by me for fulfilment of the requirements for the award of the degree of Doctor of Philosophy to Delhi Technological University, Delhi, is a bonafide record of my own work carried out under the guidance and supervision of Prof. Pragati Kumar and Prof. D. R. Bhaskar, Electrical Engineering Department, Delhi Technological University. The matter presented in this thesis has not been submitted elsewhere in part or fully to any other University or Institute for award of any degree.



(Manoj Kumar)

Roll No. 2K15/Ph.D/EE/07

CERTIFICATE

This is to certify that the thesis entitled “**An Investigation into a Class of Fractional Order Analog Circuits**” being submitted by Manoj Kumar (Roll No. 2K15/Ph.D/EE/07) to the Delhi Technological University, Delhi for the award of degree of Doctor of Philosophy is the record of the bonafide research work carried by him under our guidance and supervision. He has fulfilled the requirements which to our knowledge have reached the requisite standard for the submission of this thesis. It is further certified that the work embodied in this thesis has neither partially nor fully submitted to any other University or Institution for the award of any degree or diploma.



Prof. (Dr.) Pragati Kumar

Supervisor

Department of Electrical Engineering

Delhi Technological University

New Delhi-1140042



Prof. (Dr.) D. R. Bhaskar

Supervisor

Department of Electrical Engineering

Delhi Technological University

New Delhi-1140042

ACKNOWLEDGEMENTS

I take this opportunity to express my significant indebtedness, most profound sense of gratitude and heartiest thanks towards my supervisors, Prof. Pragati Kumar and Prof. D. R. Bhaskar, who kindly accepted to be my thesis supervisors and supported me with warm encouragement, patient guidance and fruitful discussions during the entire course of the present research work. Their humanistic and warm personal approaches in all aspects, have given me the strength to carry out this research work on a steady and smooth course. I humbly acknowledge lifetime gratitude to them.

I would like to express my thanks to Prof. Uma Nangia, HOD, Electrical Engineering, Delhi Technological University, New Delhi, for her kind support.

I would like to express my sincere thanks to Prof. Raj Senani, NSUT, New Delhi and Prof. Madhusudan Singh, Department of Electrical Engineering, Delhi Technological University, New Delhi, for giving me continuous moral boosting, helpful advice and constructive suggestions during the course of the research work.

I would also like to express my sincere thanks to Dr. Ram Bhagat, Ms. Garima, Department of Electrical Engineering, Delhi Technological University, New Delhi and Mr. Ajishek Raj, research scholar, in the Department of Electrical Engineering, Delhi Technological University, New Delhi EED, DTU, Delhi for rendering valuable help throughout the present work. I would also like to thank Dr. A. K. Singh from ECE Department, Delhi Technological University, New Delhi, Prof. Y. Singh, Prof. A. K. Gautam and Mr. Sandeep Kumar (Registrar) from GBPIET, Pauri (Uttarakhand), Dr. Ram Pratap, Dr. Abhishek Kumar, Dr. Rahul Bansal and Mr. Anil

Kumar Rajak for their encouragement, help and support throughout the course of my research work.

Also, I would like to extend my thanks to Mr. Upendra Kumar, Mr. Jagvir Singh, Mr. Anil Butola and Mr. Abhishek for providing and arranging all necessary help in Analog Signal Processing research Lab, Department of Electrical Engineering, Delhi Technological University, New Delhi, during the course of the research work.

Finally, I would never forget the deepest concern of my parents, my wife Shashibala, my son Hrishikesh, my brothers, my brothers-in-laws and all my family members for their forever love, care and beliefs during overall journey of my Ph. D research work.

(Manoj Kumar)

Table of Contents

DECLARATION	i
CERTIFICATE	ii
ACKNOWLEDGEMENTS	iii
TABLE OF CONTENTS	v
Chapter 1	
Introduction	
1.1. Research Objectives	2
1.2. Organization of Thesis	4
Chapter 2	
Overview of Structures and Methods for the Realization of Fractional order Elements	
2.1. Fundamental Relations in Fractional Order Calculus	27
2.2. Fractional Order Laplacian Operator	29
2.3. Fractional Order Element	30
2.3.1. Single Component-Based Realization of the FOE/FC.....	33
2.3.2. Multi Components-Based Realization of FOE/FC	36
2.3.3. FOE Implemented with Passive Components.....	37
2.3.4. FOE Implemented with Active Components.....	42
2.4. Implementation of Fractional Order Capacitor Using Valsa, Dvorak and Friedl Method.....	43
2.4.1. Design Procedure	46
2.4.2. PSPICE Simulations of Fractional Order Capacitors	49
2.5. Implementation of Fractional Order Capacitor Using Oustaloup, Levron, Mathieu and Nanot Method.....	52
2.5.1. Design of Fractional Order Capacitor.....	54
2.5.2. PSPICE Simulations of Fractional Order Capacitors	55
2.6. Conclusions	56
References.....	57

Chapter 3

Current Feedback Operational Amplifier Based Fractional Order Filters

3.1. Fractional Order Filters	60
3.2. Methods for Realization of Fractional Order Filters	61
3.2.1. Fractional Order Filters Using Single Fractance Device	62
3.2.1.1. Fractional Order Low Pass Filter	62
3.2.1.2. Fractional Order High Pass Filter	66
3.2.1.3. Fractional Order Band Pass Filter.....	69
3.2.1.4. Fractional Order All Pass Filter	72
3.2.2. Fractional Order Filters Using Two Fractance Device	74
3.2.2.1. Fractional Order Low Pass Filter.....	75
3.2.2.2. Fractional Order High Pass Filter	78
3.2.2.3. Fractional Order Band Pass Filter.....	80
3.2.2.4. Fractional Order Band Reject Filter.....	83
3.2.2.5. Fractional Order All Pass Filter	85
3.2.3. Realization of Fractional Order Filters Using Rational Approximation of Fractional Order Laplacian Operator	87
3.2.3.1. Fractional Order Low Pass Filter	88
3.3. Literature Overview of Fractional Order Filters	89
3.4. Voltage Mode Fractional Order Filters Employing a Single CFOA	103
3.4.1. First Structure of Fractional Order Filter	104
3.4.1.1. PSPICE and MATLAB Simulation Results	106
3.4.1.2. Experimental Results of the Proposed FOFs	110
3.4.2. Second Structure of Fractional Order Filter.....	114
3.4.2.1. MATLAB and PSPICE Simulation Results	116
3.5. Current Mode Fractional Order Filter Configuration Using a Single CFOA 120	
3.5.1. MATLAB and PSPICE Simulation Results	122
3.6. Conclusions	125

Chapter 4

Realization of Fractional Order Inverse Filters

4.1. Fractional Order Inverse Filters	138
4.1.1. Fractional Order Inverse Low Pass Filter	139
4.1.2. Fractional Order Inverse High Pass Filter	142
4.1.3. Fractional Order Inverse Band Pass Filter	145
4.1.4. Fractional Order Inverse Band Reject Filter	147
4.2. Literature Overview of Conventional Inverse Active Filters	150
4.3. Fractional Order Inverse Active Filters using an Operational Amplifier ..	152
4.3.1. Fractional Order Inverse Active Filters Employing an Op-amp.....	152
4.3.1.1. Inverting Mode Multifunctional Fractional Order Inverse Filter Configuration.....	152
4.3.1.2. Non-Inverting Fractional Order Inverse Filter Configuration	161
4.3.2. Minimal Realization of Fractional Order Inverse Filters.....	167
4.3.2.1. PSPICE and MATLAB Simulation Results	169
4.3.2.2. Experimental Results of the Proposed FOIFs.....	173
4.3.2.3. Sensitivity Analysis of the Proposed Fractional Order Inverse Active Filters	177
4.4. Fractional Order Inverse Active Filters using Current Feedback Operational Amplifiers	179
4.4.1. Generalized (Inverting Mode) Fractional Order Inverse Active Filter Configuration	180
4.4.1.1. PSPICE and MATLAB Simulation Results	182
4.4.2. Generalized (Non-Inverting Mode) Fractional Order Inverse Active Filter Configuration	184
4.4.2.1. PSPICE and MATLAB Simulation Results	186
4.5. Fractional Order Inverse Active Filters using a Single Operational Trans- resistance Amplifier	188
4.5.1. Operational Trans-Resistance Amplifier	189
4.5.2. Proposed Fractional Order Inverse Filter Structure	190

4.5.3. PSPICE and MATLAB Simulation Results	192
4.6. Stability Analysis of Fractional Order Inverse Active Filters.....	196
4.7. Conclusions	202
Chapter 5	
Realization of Fractional Order Sinusoidal Oscillators Using a Single Analog Active Building Block	
5.1. Fractional Order Sinusoidal Oscillators	208
5.1.1. Design Procedure of Fractional Order Sinusoidal Oscillators.....	209
5.2. Literature Overview of Fractional Order Sinusoidal Oscillators.....	210
5.3. Realization of Fractional Order Sinusoidal Oscillator Employing Single Operational Trans-Resistance Amplifier.....	216
5.3.1. Proposed Structure of Fractional Order Oscillator	216
5.3.2. Simulation and Numerical Results.....	219
5.3.3. Operation of the Proposed Fractional Order Oscillator as SRCO	223
5.4. Fractional Order Sinusoidal Oscillator Implemented with a Single CFOA and Two Fractional Order Capacitors	224
5.4.1. Proposed Single CFOA Based FOSO Circuit.....	225
5.4.2. PSPICE Simulation and Numerical Results	227
5.4.3. Experimental Results of Proposed Fractional Order Sinusoidal Oscillator.....	231
5.5. Stability Analysis	233
5.6. Conclusions	238
Chapter 6	
Conclusions and Future Scope	
6.1. Summary	244
6.2. Future Scope	247
Appendix I: Realization of FC and Fractional Order Filter and Inverse Filter... ..	250
List of Research Papers in Journals and Conferences	259

LIST OF FIGURES

Figure No.	Title of Figures	Page No.
Figure 2.1	Classification of fractional-order element [5]	31
Figure 2.2	Different structures of various RC networks approximating the FC	41
Figure 2.3	(a) grounded CPE (b) floating CPE	42
Figure 2.4	Capacitor less fractional order differentiators/integrators [28]	43
Figure 2.5	R-C ladder structure of CPE	44
Figure 2.6	Modified R-C network of FC	46
Figure 2.7	Magnitude and phase responses of fractional order capacitor of value $0.382 \mu\text{F}/\text{sec}^{(\alpha-1)}$ (a) Magnitude response (b) Phase response	50
Figure 2.8	Magnitude and phase response of fractional order capacitor of value $0.0955 \mu\text{F}/\text{sec}^{(\alpha-1)}$ (a) Magnitude response (b) Phase response	50
Figure 2.9	Magnitude and phase response of fractional order capacitor of value $1\text{nF}/\text{sec}^{(\alpha-1)}$ (a) Magnitude response (b) Phase response	51
Figure 2.10	Experimentally obtained magnitude and phase responses of fractional order capacitor of value $0.382 \mu\text{F}/\text{sec}^{(\alpha-1)}$	
Figure 2.11	Fractional order capacitor network	54
Figure 2.12	Magnitude and phase response of fractional order capacitor of value $10\text{nF}/\text{sec}^{(\alpha-1)}$ (a) Magnitude response (b) Phase response	56
Figure 3.1	Magnitude and phase responses of FOLP (a) Magnitude response (b) Phase response	65
Figure 3.2	Magnitude and phase responses of FOHP (a) Magnitude response (b) Phase response	68
Figure 3.3	Magnitude and phase responses of FOBP (a) Magnitude response (b) Phase response	71
Figure 3.4	Magnitude and phase responses of FOAP (a) Magnitude response (b) Phase response	74
Figure 3.5	Magnitude and phase responses of FOLP (a) Magnitude response (b) Phase response	77
Figure 3.6	Magnitude and phase responses of FOHP (a) Magnitude response (b) Phase response	80
Figure 3.7	Magnitude and phase responses of FOBP (a) Magnitude response (b) Phase response	82
Figure 3.8	Magnitude and phase responses of FOBR (a) Magnitude	85

	response (b) Phase response	
Figure 3.9	Magnitude and phase responses of FOAP (a) Magnitude response (b) Phase response	87
Figure 3.10	Circuit symbol of CFOA	104
Figure 3.11	First configuration of FOFs	105
Figure 3.12	RC ladder structure used to realize fractional order capacitors for the value of $0.382 \mu\text{F}/\text{sec}^{(\alpha-1)}$	107
Figure 3.13	Frequency responses of FOFs (a) FOLP (b) FOBP (c) FOHP	109
Figure 3.14	(a) Experimental results and Frequency responses (a) Experimental setup (b) FOLP response (c) FOBP response (d) FOHP response	112
Figure 3.15	Experimental results superimposed on PSPICE and MATLAB results for $\alpha=0.7$ (a) FOLP (b) FOBP (c) FOHP	114
Figure 3.16	Proposed second configuration of FOFs	115
Figure 3.17	Frequency responses of FOFs using PSPICE (a) FOLP filter (b) FOBP filter (c) FOHP filter	118
Figure 3.18	Frequency responses of FOFs using MATLAB (a) FOLP filter (b) FOBP filter (c) FOHP filter	119
Figure 3.19	Proposed current mode fractional order generalized filter structure	121
Figure 3.20	PSPICE and MATLAB simulation results of current mode FOFs (a) FOLP filter (b) FOBP filter (c) FOHP filter	124
Figure 4.1	MATLAB simulations of FOILP (a) Magnitude responses (b) Phase responses	141
Figure 4.2	MATLAB simulations of FOIHP (a) Magnitude responses (b) Phase responses	144
Figure 4.3	MATLAB simulations of FOIBP (a) Magnitude responses (b) Phase responses	147
Figure 4.4	MATLAB simulations of FOIBR (a) Magnitude responses (b) Phase responses	149
Figure 4.5	Inverting mode multifunctional FOIF configuration	153
Figure 4.6	R-C ladder structure used to realize fractional order capacitors for the values $0.382 \mu\text{F}/\text{sec}^{(\alpha-1)}$ and $0.0955 \mu\text{F}/\text{sec}^{(\alpha-1)}$	156
Figure 4.7	Frequency responses of proposed FOIFs using PSPICE (i) FOILP (ii) FOIHP (iii) FOIBP	158
Figure 4.8	Frequency responses of proposed FOIFs using PSPICE (i) FOILP (ii) FOIHP (iii) FOIBP	159
Figure 4.9	Proposed non-inverting multifunctional FOIF configuration	161

Figure 4.10	Frequency responses of FOIFs using PSPICE (i) FOILP (ii) FOIBP (iii) FOIHP filter	165
Figure 4.11	Frequency responses of FOIFs using MATLAB (i) FOILP (ii) FOIBP (iii) FOIHP filter	166
Figure 4.12	Proposed structure of multifunctional FOIFs	168
Figure 4.13	Phase responses of fractional order capacitor of value $0.382 \mu\text{F}/\text{sec}^{(\alpha-1)}$ for different values of α	170
Figure 4.14	Frequency responses of FOIFs (a) Magnitude responses of FOILP (b) Magnitude responses of FOIHP (c) Magnitude responses of FOIBP filter (d) Phase responses of FOILP (e) Phase responses of FOIHP (f) Phase responses of FOIBP	171
Figure 4.15	Experimental setup for FOILP filter for $\alpha = 0.7$	175
Figure 4.16	Experimental result of FOILP filter	175
Figure 4.17	Frequency responses of proposed FOIFs superimposed on MATLAB and PSPICE obtained results for $\alpha = 0.7$ (a)FOILP (b) FOIHP (c) FOIBP filter	177
Figure 4.18	Sensitivity of magnitude of transfer functions for the proposed FOIFs	178
Figure 4.19	Circuit symbol of CFOA	181
Figure 4.20	Proposed generalized FOIF structure	181
Figure 4.21	Frequency responses of FOIFs of Fig. 4.20 (i) FOILP (ii) FOIBP (iii) FOIHP filter	184
Figure 4.22	Proposed generalized FOIF structure	186
Figure 4.23	Frequency responses of proposed FOIFs (i) FOILP (ii) FOIBP (iii) FOIHP filter	189
Figure 4.24	(a) Symbolic representation (b) Equivalent circuit of OTRA	191
Figure 4.25	Proposed structure of OTRA based FOIFs	192
Figure 4.26	Exemplary CMOS OTRA proposed by Mostafa and Soliman [27]	194
Figure 4.27	Frequency responses of OTRA-based FOIFs using PSPICE (i) FOILP (ii) FOIBP (iii) FOIHP	196
Figure 4.28	Frequency responses of OTRA-based FOIFs using MATLAB (i) FOILP (ii) FOIBP (iii) FOIHP	197
Figure 4.29	Stability analysis of fractional order system (a) s-plane (b) w-plane	199
Figure 4.30	Polar plots of CE of FOIBP filter of Fig. 4.5 in w-plane for $\alpha = 0.9$	201
Figure 4.31	Polar plots of CE of FOIBP filter of Fig. 4.9 in w-plane for	201

	$\alpha = 0.9$	
Figure 4.32	Polar plots of CE of FOIBP filter of Fig. 4.20 in w-plane for $\alpha = 0.9$	202
Figure 4.33	Polar plots of CE of FOIBP filter of Fig. 4.22 in w-plane for $\alpha = 0.9$	202
Figure 4.34	Minimum absolute root angles for fractional order inverse filters: (a) $b = 4$, $a = 2.0, 2.5, 3.0, 3.5, 4.0$ (b) for $a = 4$ and $b = 2, 3, 4, 5, 6$	204
Figure 5.1	The proposed OTRA based fractional order oscillator	219
Figure 5.2	CMOS OTRA circuit proposed by Mostafa and Soliman [32]	222
Figure 5.3	R-C ladder circuit of fractional order capacitor	222
Figure 5.4	Transient responses and frequency spectra of proposed fractional order oscillator	225
Figure 5.5	Variation of FO with R_2 (a) $\alpha = \beta = 0.9$ (b) $\alpha = \beta = 0.8$ (c) $\alpha = 0.9, \beta = 0.8$	226
Figure 5.6	Proposed configuration of single CFOA based fractional order oscillator	227
Figure 5.7	R-C ladder circuit to realize fractional order capacitors	229
Figure 5.8	Transient responses and frequency spectra of proposed fractional order oscillator of Fig. 5.6	232
Figure 5.9	Experimentally obtained transient response and frequency spectrum of the oscillator of Fig. 5.6	234
Figure 5.10	Polar plot of the poles of the CE in w-plane of the oscillator of Fig. 5.1	237
Figure 5.11	Polar plot of the poles of the CE in w-plane of the oscillator of Fig. 5.6	240

LIST OF TABLES

Table No.	Title of Table	Page No.
Table 2.1	Component values for realization of fractional of Fig. 2.6	48
Table 2.2	Component values of FC of value $1nF/\sec^{(\alpha-1)}$	49
Table 2.3	Obtained values of ω'_k and ω_k	54
Table 2.4	Component values of FC for $\alpha = 0.8$	55
Table 2.5	Component values of FC for $\alpha = 0.9$	55
Table 3.1	The values of magnitude and phase of FOLP filter for different values of ω	64
Table 3.2	Parameters of FOLP filter	66
Table 3.3	The values of magnitude and phase of FOHP filter for different values of ω	67
Table 3.4	Parameters of FOHP filter	69
Table 3.5	The values of magnitude and phase of FOBP filter for different values of ω	70
Table 3.6	Filter parameters of FOBP filter	72
Table 3.7	The values of magnitude and phase of FOAP filter for different values of ω	73
Table 3.8	Parameters of FOAP filter	74
Table 3.9	Various parameters of FOLP filter obtained from MATLAB simulations	78
Table.3.10	Various parameters of FOHP filter obtained from MATLAB simulations	80
Table 3.11	Various parameters of FOBP filter obtained from MATLAB simulations	83
Table 3.12	Various parameters of FOBR filter obtained from MATLAB simulations	85
Table 3.13	Various parameters of FOAP filter obtained from MATLAB simulations	87
Table 3.14	Various fractional order filter transfer functions derived from equation (3.41)	105
Table.3.15	Mapping of the coefficients of the characteristic equation with the passive components of the fractional order filters	105

Table.3.16	Component values for the realization of fractional order filter used in PSPICE simulation	107
Table 3.17	Component values for the realization of FCs	107
Table 3.18:	Simulation results for half power/maximum frequency (kHz)	109
Table.3.19	Simulation results for stop band attenuation (dB/decade)	110
Table 3.20	Half power/maximum frequencies of proposed FOFs for $\alpha = 0.7$	114
Table 3.21	Various fractional order filter transfer function derived from equation (3.45)	115
Table.3.22	Mapping of the coefficients of the characteristic equation with the passive components of the fractional order filters	116
Table.3.23	Component values for the realization of fractional order filter used in PSPICE simulation	116
Table 3.24	Simulation results for half power/maximum frequency (kHz)	119
Table 3.25	Simulation results for stop band attenuation (dB/decade)	120
Table.3.26	Various fractional order filter transfer function derived from equation (3.46)	121
Table.3.27	Mapping of the coefficients of the characteristic equation with the passive components of the fractional order filters	122
Table 3.28	Component values for the realization of fractional order filter used in PSPICE simulation	122
Table 3.29	Simulation results for half power/maximum frequency (kHz)	124
Table 3.30	Simulation results for stop band attenuation (dB/decade)	124
Table 4.1	Various parameters of FOILP filter	142
Table 4.2	Various parameters of FOIHP filter	145
Table 4.3	Various parameters of FOIBP filter	147
Table 4.4	Peak frequency (ω_p) for FOIBR for different values of ' α '	150
Table 4.5	Transfer functions of the proposed FOIFs structure shown in Fig. 4.5	153
Table 4.6	Mapping of the coefficients of the characteristic equation with the passive components of the fractional order inverse filters	154
Table 4.7	Component values used in PSPICE simulations	155
Table 4.8	Components value for the realization of FCs	156

Table 4.9	Summary of the simulation results for ω_h and ω_m for the FOIF of Fig. 4.5	160
Table 4.10	Summary of the simulation results for stopband attenuation (dB/decade)	160
Table 4.11	Branch admittances and transfer functions of FOIFs realized from Fig. 4.9	162
Table 4.12	Mapping of the coefficients of the characteristic equation with the passive components of the fractional order inverse filters	162
Table 4.13	Components value used in PSPICE simulations	163
Table 4.14	Summary of the simulation results for ω_h and ω_m (Hz)	166
Table 4.15	Summary of the simulation results for stopband attenuation (dB/decade)	167
Table 4.16	Various fractional order inverse filter transfer function derived from equation (4.25)	168
Table 4.17	Mapping of the coefficients of the characteristic equation with the passive components of the fractional order inverse filters	169
Table 4.18	Component values for the realization of fractional order inverse filters used in PSPICE	170
Table 4.19	PSPICE, MATLAB and theoretical results for half power/minimum frequency (Hz)	172
Table 4.20	Summary of the simulation results for stopband attenuation (dB/decade)	172
Table 4.21	IMD results of the proposed FOIBP filter for $\alpha = 0.7$	174
Table 4.22	Summary of results of FOIs for $\alpha = 0.7$	176
Table 4.23	Sensitivity of the proposed fractional order inverse filters	179
Table 4.24	Various fractional order inverse filter transfer functions derived from equation (4.29)	182
Table 4.25	Mapping of the coefficients of the characteristic equation with the passive components of the fractional order inverse filters	182
Table 4.26	Component values used in the design of FOIFs	183
Table 4.27	Half power frequency and maximum frequency (Hz) of proposed FOIFs of Fig. 4.20	184
Table 4.28	Stop band attenuation (dB/decade) of proposed FOIFs	185
Table 4.29	Transfer functions of proposed FOIFs	186
Table 4.30	Mapping of the coefficients of the characteristic equation with the passive components of the fractional order inverse filters	187
Table 4.31	Component values used in the design of FOIFs	187

Table 4.32	Half power frequency and minimum frequency (Hz) of proposed FOIFs of Fig. 4.20	189
Table 4.33	Stop band attenuation (dB/decade) of proposed FOIFs	189
Table 4.34	Transfer functions of proposed FOIFs	192
Table 4.35	Mapping of the coefficients of the characteristic equation with the passive components of the fractional order inverse filters	193
Table 4.36	Aspect ratios of various MOSFETs for the OTRA circuit of Fig. 4.26	194
Table 4.37	Component values used in the design of FOIFs	194
Table 4.38	PSPICE and MATLAB simulations results for half power and maximum frequency (Hz)	197
Table 4.39	Stop band attenuation (dB/decade) of proposed FOIFs	197
Table 5.1	Component values of FC for ($\alpha = \beta = 0.8, 0.9$)	220
Table 5.2	Simulation and theoretical results of fractional order sinusoidal oscillator	224
Table 5.3	Component values of FC for $\alpha = 0.8$ and 0.9	229
Table 5.4	Simulation and theoretical results of fractional order sinusoidal oscillator	232
Table 5.5	Frequency of oscillation and phase difference between the outputs of fractional order oscillator for $\alpha = \beta = 0.8$	234

LIST OF SYMBOLS

ω	Angular Frequency (in Radian per second)
φ	Phase angle
$\Gamma(\cdot)$	Gamma Function
ω_h	Half Power Frequency
ω_o	Pole Frequency
ω_{rp}	Right Phase Frequency
ω_l	Minimum Frequency
ω_b	Maximum Frequency
θ_p	Root Angle
θ_w	Root Angle in w-plane
θ_s	Root Angle in s-plane
ω_m	Maximum Frequency/Minimum Frequency
ω_p	Peak Frequency

LIST OF ABBREVIATIONS

ABB	Analog Building Block
ACA	Adjustable Current Amplifier
AMS	Austrian Micro Systems
BPF	Band Pass Filter
CBO	Colliding Bodies Optimisation
CC	Current Conveyor
CCII	Current Conveyor Second Generation
CDBA	Current Differencing Buffer Amplifier
CDTA	Current Differencing Trans-conductance Amplifier
CE	Characteristic Equation
CFE	Continued Fraction Expansion
CFOA	Current Feedback Operational Amplifier
CFTA	Current Feedback Trans-conductance Amplifier
CM	Current Mode
CO	Condition of Oscillation
CPE	Constant Phase Element
DDCC	Differential Difference Current Conveyor
DVCC	Differencing Voltage Current Conveyor
FBWF	Fractional Butterworth Like Filter
FC	Fractional Capacitor
FD	Fractance Device
FI	Fractional Order Inductor
FM	Frequency Modulation
FO	Frequency of Oscillation
FOAP	Fractional Order All Pass
FOBP	Fractional Order Band Pass
FOBR	Fractional Order Band Reject
FOC	Fractional Order Capacitor
FOF	Fractional Order Filter
FOHP	Fractional Order High Pass

FOSO	Fractional Order Sinusoidal Oscillator
FOTF	Fractional Order transfer Function
FOIBP	Fractional Order Inverse Band Pass
FOIBR	Fractional Order Inverse Band Reject
FOIF	Fractional Order Inverse Filter
FOIHP	Fractional Order Inverse High Pass
FOILP	Fractional Order Inverse Low Pass
FPAA	Field Programmable Analogue Array
GSA	Gravitational Search Algorithm
IFLF	Inverse Follow Leader Feedback
IIMC	Inverted Impedance Multiplier Circuit
IMD	Inter Modulation Distortion
KHN	Kerwin-Heulsman-Newcomb
MIMO	Multiple Input Multiple Output
MMCC	Multiplication Mode Current Conveyor
OTA	Operational Trans-conductance Amplifier
OTRA	Operational Trans-Resistance Amplifier
PSO	Particle Swarm Optimization
SISO	Single Input Single Output
SM	Simulation Result
SRCO	Single Resistance Controlled Oscillator
TH	Theoretical Result
VCVS	Voltage Controlled Voltage Source
VM	Voltage Mode

Chapter 1

Introduction

This thesis presents “An investigation into a class of fractional order analog circuits”. The class of circuits investigated includes, fractional order inverse filters, fractional order conventional filters and fractional order oscillators.

Though, the calculus involving derivatives and integrations of non-integer order has been in existence for more than 300 years and the suitability of these fractional order derivatives in modelling of several engineering and non-engineering phenomenon has been well known since long [1]-[3], fractional order analog circuits have started attracting renewed interest during the last few decades. Fractional order analog circuits comprise of one or more active building blocks, at least one fractional order immittance, sometimes known as fractance and few other conventional passive elements. During the decades of fifties and sixties, several works [4-6] were reported on passive realization of an immittance function whose argument remained constant over an extended range of frequencies. Since, in such immittance functions, the phase response remains bound within a specified tolerance band around “ $\alpha \frac{\pi}{2}$ ” radian, these passive elements are also popularly referred to as constant phase elements. The parameter ‘ α ’ which characterizes the fractance device present in the circuit provides an extra degree of freedom in the design and control of various parameters of the designed circuits. Though, a fractional order element, either capacitor or inductor, with arbitrarily specified value of ‘ α ’ is not yet available commercially, efforts are

being directed towards the development of a fractance device as a ‘two-terminal’ element which can be used directly as a fractance device in the design of analog circuits. Notwithstanding the non-availability of a standard two-terminal, fractance element, lots of research work is currently being carried out in the area of design and analysis of fractional order active analog filters [7]-[96], fractional order oscillators [97]-[117], fractional order PID controllers [118]-[133] and fractional order analog inverse filters [134]-[135]. The fractance device used in most of the works involving analog circuit realization of fractional order circuits, has been simulated by Foster/Cauer-type RC networks [4]-[6], [136]-[144] which emulates the behaviour of the specified fractional order element in pre-defined frequency range by using different approximation techniques for approximating an irrational Laplacian operator. Alternate realizations of fractance devices using active building blocks [145]-[146] and single component-based realizations [147]-[153] have also been attempted.

1.1. Research Objectives

From an exhaustive literature survey of the analog circuit implementation of fractional order analog circuits, it was found that no work was available in open literature on the realization of fractional order inverse filters, prior to the commencement of this work. Also, most of the works presented on fractional order filters were based on (i) generalization of existing integer order circuits, wherein, an existing integer order filter circuit/topology, viz. Sallen and Key, KHN, Tow-Thomas, etc. realized with different amplifiers were converted into fractional order filters by replacing the standard capacitors by fractional order capacitors (FCs), which in turn, were realized with Foster/Cauer type of RC networks approximating the fractional

order capacitor in a specified frequency band and (ii) realization of an integer order transfer function, approximating the prototype fractional order filter transfer function, obtained by replacing the fractional order operator ' s^α ' using some standard approximation techniques. Very few circuits were realized, ab-initio, in fractional order domain. In addition, very few circuits were realized in fractional order domain in which the realized structure employed minimum number of components. Also compared to the realization of fractional order filters and fractional order elements, relatively less attention has been paid on the realization of fractional order oscillators with modern active building blocks. Motivated by these facts, in this thesis, we have proposed novel realizations of fractional order filters, fractional order inverse filters and fractional order oscillators realized with various types of traditional as well as modern active building blocks viz. operational amplifiers (op-amps), operational trans-resistance amplifiers (OTRAs) and current feedback operational amplifiers (CFOAs).

The main goal of this thesis is divided into the following objectives:

1. Realization of fractional order filters, both in voltage mode (VM) and current mode (CM) using a single CFOA.
2. To implement fractional order inverse filters using different active devices such as operational amplifiers, current feedback operational amplifiers and operational trans-resistance amplifiers.
3. Minimal realization of high input impedance fractional order inverse filters.
4. Realization of fractional order sinusoidal oscillators using single active device such as OTRA and CFOA.

1.2. Organization of Thesis

The work presented in the thesis has been organized as follows:

Chapter 1 highlighted the necessary mathematical background of fractional order calculus and its association with the fractance device. We have also presented some of the fundamental concepts related to fractional order systems in general and fractional order filters, fractional order inverse filters and fractional order oscillators in particular to articulate the research gap and subsequently set the objective of the thesis work.

Chapter 2 dealt with an overview of methods of approximations and structures used for the implementation of fractional order element (FOE). The details of some of the important works dealing with the realizations of the FOEs using single as well as the multi-component based realizations of the FOEs have been presented. We have also described the methodology and design of the fractional order capacitors, which we have used for the realization of various analog circuits in this thesis. PSPICE simulations of the magnitude and the phase responses of proposed FOCs realized with these methods have been presented. Experimentally obtained frequency response characteristics of a fractional order capacitor have also been presented.

In **Chapter 3**, we have presented the theoretical formulations of fractional order filters realized with a single fractance device as well as two fractance devices. The frequency response characteristics of the prototype transfer functions have also been plotted using MATLAB for different values of the order of the fractional order capacitors. A detailed review of fractional order filters realized with different active

building blocks has been presented before presenting fractional order multifunction filter circuits operating in voltage/current modes using a single current feedback operational amplifier. PSPICE and MATLAB simulation results are given to validate the theoretical findings. Experimental results for an exemplary single CFOA based fractional order filter operating in voltage mode (for $\alpha = \beta = 0.7$) have also been presented.

Chapter 4 discusses the fundamental concepts related with inverse analog filters in general and the same has been extended to non-integer order domain. The frequency response characteristics of the prototype fractional order inverse filters of various types have been derived and plotted using MATLAB. Several new inverse filter circuits¹ realized with operational amplifiers, and other modern active building blocks like current feedback amplifiers and the operational transresistance amplifiers have also been presented. Performance of all the proposed analog circuits has been evaluated using PSPICE and MATLAB simulations. Experimental results for an exemplary single operational amplifier based fractional order inverse filter, which is a minimal realization in which different inverse filter responses can be obtained by appropriate selection(s) of different admittances have also been presented.

Chapter 5: After presenting a detailed summary of the research work reported by various researchers on the realization of fractional order oscillators realized with different active building blocks, we have presented a new circuit of fractional order sinusoidal oscillator realized with operational trans-resistance amplifier and two

¹ Prior to the publication of the work presented in "Fractional order inverse filters using operational amplifiers" by D. R. Bhaskar, Manoj Kumar and P. Kumar, in Analog Integrated Circuits and Signal Processing, vol. 97, no. 1, pp. 149-158, 2018, no work on the realization of analog inverse active filters in fractional order domain was available in open literature.

fractance devices. We have also presented a single CFOA-based fractional order sinusoidal oscillator using two fractional order capacitors. The experimental results for an exemplary single CFOA-based fractional order sinusoidal oscillator for $\alpha = \beta = 0.8$ has also been presented.

Chapter 6: In this chapter, a summary of the work presented in this thesis and some suggestions for further research work on the ideas explored are given.

References

- [1] K. Oldham and J. Spanier, "The Fractional Calculus: Theory and Applications of Differentiation and Integration to Arbitrary Order", New York: Academic Press, 1974.
- [2] K. Miller and B. Ross, "An Introduction to the Fractional Calculus and Fractional Differential Equations", New York: Wiley, 1993.
- [3] S. Das, "Functional Fractional Calculus," Springer, Berlin Heidelberg, 2011, DOI: <http://doi.org/10.1007/987-3-642-20545-3>
- [4] K. Steiglitz, "An RC impedance approximation to $s^{(-1/2)}$," IEEE Trans. Circuits Syst., vol. CT-11, pp. 160–161, Apr. 1964.
- [5] G. E. Carlson and C. A. Halijak, "Approximation of fractional capacitors $(1/s)^{(1/n)}$ by a regular Newton process," IEEE Trans. Circuit Theory, vol. 11, no. 2, pp. 210–213, Jun.1964.
- [6] S. C. Dutta Roy, "On the realization of a constant-argument immittance or fractional operator," IEEE Trans. Circuits Systems, vol. CAS-14, no. 3, pp. 264–274, Sep. 1967.

- [7] A. G. Radwan, A. M. Soliman and A. S. Elwakil, "First-order filters generalized to the fractional domain," *J. Circ. Syst. Comput.* vol. 17, no. 1, pp. 55–66. July 2008.
- [8] A. G. Radwan, A. M. Soliman and A. S. Elwakil, "On the generalization of second-order filters to the fractional-order domain," *J. Circ. Syst. Comput.* vol.18, no. 2, pp. 361–386, Mar. 2009.
- [9] T. J. Freeborn, B. Maundy and A. S. Elwakil, "Towards the realization of fractional step filters," *IEEE Int. Symp. Circuits Syst. (ISCAS)*, pp. 1037–1040, May-June 2010.
- [10] T. J. Freeborn, B. Maundy and A. S. Elwakil, "Field programmable analogue array implementation of fractional step filters," *IET Circ. Devices Syst.*, vol. 4, no. 6, pp. 514-524, Nov. 2010.
- [11] B. Maundy, A.S. Elwakil and T. J. Freeborn, "On the practical realization of higher-order filters with fractional stepping," *Signal Process.*, vol. 91, no. 3, pp. 484–491, Mar. 2011.
- [12] A. Soltan, A. G. Radwan and A. M. Soliman, "Fractional order filters with two fractional elements of dependent orders," *Microelectron. J.*, vol. 43, no. 11, pp. 818–827, Nov. 2012.
- [13] P. Ahmadi, B. Maundy, A. S. Elwakil and L. Belostotski, "High-quality factor asymmetric-slope band-pass filters: a fractional-order capacitor approach," *IET Circ. Devices Syst.*, vol. 6, no. 3, pp. 187-197, May. 2012.
- [14] M. C. Tripathy, K. Biswas and S. Sen, "A design example of a fractional-order Kerwin-Huelsman-Newcomb biquad filter with two fractional capacitors of different order," *Circ. Syst. Signal Process*, vol. 32, no. 4, pp. 1523-1536, Aug. 2013.

- [15] A. S. Ali, A. G. Radwan and A. M. Soliman, "Fractional order Butterworth filter: active and passive realizations," *IEEE J. Emerging Selected topics Circ. syst.*, vol. 3, no. 3, pp. 346–354, Jun. 2013.
- [16] A. Soltan, A. G. Radwan and A. M. Soliman, "CCII based KHN fractional order filter," *Midwest Symp. Circ. Syst. (MWSCAS)*, pp. 197-200, 2013.
- [17] A. Soltan, A. G. Radwan and A. M. Soliman, "CCII based fractional filters of different orders," *J. Advanced Research*, vol. 5, no. 2, pp. 157-164, Mar. 2014.
- [18] M. C. Tripathy, "Experimental Realization of Fractional order filter using PMMA coated constant phase elements," *Int. J. Engineering and Advanced Research Technology (IJEART)*, vol. 1, no. 5, pp.14-17, Nov. 2015.
- [19] D. Kubanek, J. Koton, J. Jerabek, P. Ushakov and A. Shadrin, "Design and properties of fractional order multifunction filter with DVCCs," *Int. Conf. Telecommunications and Signal Process. (TSP)*, pp. 620-624, Jun. 2016
- [20] F. Khateb, D. Kubanek, G. Tsirimokou, and C. Psychalinos, "Fractional order filters based on low-voltage DDCCs," *Microelectron. J.*, vol. 50, pp. 50-59, Apr. 2016.
- [21] J. Koton, O. Sladok, J. Salasek and P. Ushakov, "Current-mode fractional low- and high pass filters using current conveyors", *Int. Congress on Ultra-Modern Telecommunications and Control Systems and Workshops — ICUMT*, Lisbon, Portugal, pp. 231–234, 18–20 Oct. 2016.
- [22] L. A. Said, S. M. Ismail, A. G. Radwan, A. H. Median, El Yazeed MFA and A. M. Soliman, "On the optimization of fractional order low pass filter," *Circ. Syst. Signal Process.* vol. 35, no. 6, pp. 2017–2039, Jun. 2016.

- [23] C. Psychalinos, G. Tsirimokou and A. S. Elwakil, "Switched-Capacitor Fractional-Step Butterworth Filter Design," *Circ. Syst. Signal Process.* vol. 35, pp. 1377-1393, Apr. 2016.
- [24] T. J. Freeborn, "Comparison of $(1+\alpha)$ fractional-order transfer functions to approximate low pass Butterworth magnitude responses," *Circ. Syst Signal Process.* vol. 35, no. 6, 1983–2002, Jun. 2016.
- [25] G. Tsirimokou, S. Koumoussi and C. Psychalinos "Design of fractional-order filters using current feedback operational amplifiers," *J. Eng. Sci. Technol. Rev,* vol. 9, no. 4, pp. 77–81, Jan. 2016.
- [26] R. Verma, N. Pandey and R. Pandey, "Realization of a higher fractional order element based on novel OTA based IIMC and its application in filter," *Analog Integ. Circuits Signal Process.* vol. 97, pp. 177–191, Oct. 2018.
- [27] T. Suksang, V. Pirajanchai and W. Loedhammacakra, "Tunable OTA Low Pass Filter with the Fractional-Order step Technique," *Int. Conf. Advances in Electron Electr. Engg. (AEEEE)*, pp. 29-32, 2012.
- [28] J. Jerabek, R. Sotner, J. Dvorak, J. Polak, D. Kubanek, N. Herencsar and J. Koton, "Reconfigurable fractional-order filter with electronically controllable slope of attenuation, pole frequency and type of approximation," *J. Circ. Syst. Comput.*, vol. 26, no. 10, pp. 1–21, Oct. 2017.
- [29] J. Koton, D. Kubanek, O. Sladok and K. Vrba, "Fractional-order low- and high-pass filters using UVCs," *J. Circ. Syst. Comput.*, vol. 26, no. 12, pp. 1–23, Dec. 2017.
- [30] G. Tsirimokou, C. Psychalinos, and A. S. Elwakil, "Fractional-order electronically controlled generalized filters," *Int. J. Circ. Theor. Appl.*, vol. 45, pp. 595–612, May. 2017.

- [31] G. Kaur, A. Q. Ansari and M. S. Hashmi, "Fractional order multifunction filter with 3degrees of freedom," *AEU-Int. J. Electron. Commun.*, vol. 82, pp. 127–35, Dec. 2017.
- [32] L. Langhammer, J. Dvorak, R. Sotner and J. Jerabek, "Electronically tunable fully differential fractional-order low-pass filter," *Elektron Elektrotech*, vol. 23, no. 3, pp. 47-54, Jun. 2017.
- [33] R. Verma, N. Pandey and R. Pandey, "Electronically tunable fractional order all pass filter," *IOP Conf. Ser. Mater Sci. Eng.*, vol. 225, pp. 1–9, Aug. 2017.
- [34] P. Bertias, F. Khateb, D. Kubanek, F. A. Khanday, and C. Psychalinos, "Capacitorless digitally programmable fractional-order filters," *AEU-Int. J. Electron. Commun.*, vol. 78, pp. 228-237, Aug. 2017.
- [35] J. Baranowski, M. Pauluk and A. Tutaj, "Analog realization of fractional filters: Laguerre approximation approach," *AEU-Int. J. Electron. Commun*, vol. 81, pp. 1–11, Nov. 2017.
- [36] E. M. Hamed, A. M. Abdelaty, L. A. Said and A. G. Radwan, "Effect of Different Approximation Techniques on Fractional-Order KHN Filter Design," *Circ. Syst Signal Process.*, vol. 37, pp. 5222–5252, Dec. 2018
- [37] D. Kubanek and T. Freeborn, " $(1+\alpha)$ Fractional-order transfer functions to approximate low-pass magnitude responses with arbitrary quality factor," *AEU-Int. J. Electron. Commun.*, vol. 83, pp. 570-578, Jun. 2018.
- [38] S. Mahata, R. Kar and D. Mandal, "Optimal fractional-order high pass Butterworth magnitude characteristics realization using current mode filter," *AEU-Int. J. Electron. Commun.*, vol. 102, pp. 78-89, Apr. 2019.

- [39] N. A. Khalil, L. A. Said, A. G. Radwan and A. M. Soliman, "Generalized two-port network based fractional order filters," *AEU-Int. J. Electron. Commun.*, vol. 104, pp. 128-146, May. 2019.
- [40] D. Kubanek, T. Freeborn and J. Koton, "Fractional-order band-pass filter design using fractional-characteristic specimen functions," *AEU-Int. J. Electron. Commun.*, vol. 86, pp. 77-86, Apr. 2019.
- [41] R. Verma, N. Pandey and R. Pandey, "CFOA based low pass and high pass fractional step filter realization," *AEU-Int. J. Electron. Commun.*, vol. 99, pp. 161-176, Feb. 2019.
- [42] A. G. Radwan, A. M. Soliman, A. S. Elwakil and A. Sedeek, "On the stability of linear systems with fractional-order elements," *Chaos, Solutions Fractals*, vol. 40, no. 5, pp. 2317-2328, Oct. 2009.
- [43] R. Verma, N. Pandey and R. Pandey, "Electronically tunable fractional order filter," *Arabian J. Science and Engineering*, vol. 42, no. 8, pp. 3409-3422, Aug. 2017.
- [44] S. K. Mishra, M. Gupta and D. K. Upadhyay, "Active realization of fractional order Butterworth lowpass filter using DVCC," *J. King Saud University Engineering Sciences*, vol. 32, no. 2, pp. 158-165, 2020.
- [45] J. Koton, D. Kubanek, O. Sladok and K. Vrba, "Fractional-order low- and high-pass filters using UVCs," *J. Circ. Syst. Comput.*, vol. 26, no. 12, pp. 1-23, Dec. 2017.
- [46] G. Tsirimokou, C. Psychalinos, and A. S. Elwakil, "Fractional-order electronically controlled generalized filters," *Int. J. Circ. Theor. Appl.*, vol. 45, pp. 595-612, May. 2017..

- [47] L. Langhammer, J. Dvorak, R. Sotner and J. Jerabek, "Electronically tunable fully differential fractional-order low-pass filter," *Elektron Elektrotech*, vol. 23, no. 3, pp. 47-54, Jun. 2017.
- [48] G. Kaur, A. Q. Ansari, and M. S. Hashmi, "Fractional order high pass filter based on operational transresistance amplifier with three fractional capacitors of different order," *Advances in Electrical and Electronic Engineering*, vol. 17 no. 2, pp. 155–166, 2019.
- [49] E. M. Hamed, A. M. Abdelaty, L. A. Said and A. G. Radwan, "Effect of Different Approximation Techniques on Fractional-Order KHN Filter Design," *Circ. Syst Signal Process.*, vol. 37, pp. 5222–5252, Dec. 2018
- [50] G. Kaur, A. Q. Ansari and M. S. Hashmi, "Analysis and investigation of CDBA based Fractional order filters," *Analog Integ. Circ. Signal Process.*, vol. 105, pp. 11-124, 2020.
- [51] S. Mahata, R. Kar and D. Mandal, "Optimal fractional-order highpass Butterworth magnitude characteristics realization using current mode filter," *AEU-Int. J. Electron. Commun.*, vol. 102, pp. 78-89, Apr. 2019.
- [52] N. A. Khalil, L. A. Said, A. G. Radwan and A. M. Soliman, "Generalized two-port network based fractional order filters," *AEU-Int. J. Electron. Commun.*, vol. 104, pp. 128-146, May. 2019.
- [53] D. Kubanek, T. Freeborn and J. Koton, "Fractional-order band-pass filter design using fractional-characteristic specimen functions," *AEU-Int. J. Electron. Commun.*, vol. 86, pp. 77-86, Apr. 2019.
- [54] K. Sengar and A. Kumar, "Fractional order capacitor in first order and second order filter," *Micro and Nano Systems*, vol. 12, no. 2, pp.1-4, 2020

- [55] L. Langhammer, J. Dvorak, R. Sotner, J. Jerabek and P. Bertias, "Reconnection-less reconfigurable low pass-filtering technology suitable for higher order fractional order design," *J. Advanced Research*, vol.25, pp. 257-274, 2020
- [56] G. Varshney, N. Pandey and R. Pandey, " Electronically tunable multifunction transadmittance mode fractional order filter," *Arabian J. Science and Engineering*, 2020, <https://doi.org/10.1007/s13369-020-04841-8>.
- [57] I. E. Sacu and M. Alci, "A Current Mode Design of Fractional Order Universal Filter," *Advances in Electrical and Computer Engineering*, vol.19, no.1, pp.71-78, 2019, doi:10.4316/AECE.2019.01010
- [58] E. Kaskouta, T. Kamilaris, R. Sotner, J. Jerabek and C. Psychalinos, "Single-Input Multiple-Output and Multiple-Input Single-Output Fractional-Order Filter Designs," *Int. Conf. Telecommunications and Signal Process. (TSP)*, Athens, 2018, pp. 1-4, doi: 10.1109/TSP.2018.8441348.
- [59] A. Tutaj, P. Piątek, W. Bauer, J. Baranowski, T. Petropoulos, G. Moustos, P. Bertias and C. Psychalinos, "Approximating Fractional Filters With Analogue Active Filter Structures," *Int. Conf. Telecommunications and Signal Process. (TSP)* pp. 440-444, doi: 10.1109/TSP.2019.8768817
- [60] G. Singh, Garima and P. Kumar, "Fractional Order Capacitors Based Filters Using Three OTAs," *Control Automation and Robotics (ICCAR) 2020 6th International Conference on*, pp. 638-643, 2020.
- [61] C. Matos and M. D. Ortigueira, "Fractional filters: an optimization approach," *Emerging Trends in Technological Innovation, Series: IFIP Advances in Information and Communication Technology*, vol. 314, pp. 361-366, 2010.
- [62] A. G. Radwan and K. N. Salama, "Passive and active elements using fractional $L_\beta C_\alpha$ circuit," *IEEE Trans. Circ. Syst.*, vol. 58, pp. 2388–2397, 2011.

- [63] A. Soltan, A. G. Radwan and A. M. Soliman, "Butterworth passive filter in the fractional order," Int. Conf. Microelectronics (ICM). pp. 1–4, 19-22 December 2011.
- [64] S. Mahata, R. Kar and D. Mandal, "Optimal approximation of asymmetric type fractional order band passes Butterworth filter using decomposition Technique," Int. J. Circ. Theor. Appl., pp. 1-7, 2017.
- [65] Y. Zhang and J. Li, "An improvement method of fractional order filter approximation," Advanced Research on Computer Education, Simulation and Modeling, Series: Communications in Computer and Information Science, vol. 176, pp. 101-106, 2011.
- [66] A. Pakhira, S. Das, A. Acharya, I. Pan and S. Saha, "Optimized quality factor of fractional order analog filters with band-pass and band-stop characteristics," Int. Conf. Computing, Communication and Networking Technologies (ICCCNT'12), July 2012.
- [67] A. Acharya, S. Das, I. Pan and S. Das, "Extending the concept of analog Butterworth filter for fractional order systems," Signal Process., vol. **94**, pp.409–420, 2013.
- [68] T. Comedang and P. Intani, " $A \pm 0.2$ V, 0.12 μ W CCTA using VT MOS and an application fractional-order universal filter," J. Circ. Syst. Comp., vol. 23, no. 8, 2014.
- [69] L.A Said, S. M. Ismail, A. G. Radwan, A. H. Madian, M. F. Abu El Yazeed and A. M. Soliman, "On the optimization of fractional order low pass filters," Circ. Syst. Signal Process., vol. 35, no. 6, pp. 2017–2039, 2016.

- [70] A. Soltan, A. G. Radwan and A. M. Soliman, "Fractional order Sallen–Key and KHN filters: stability and poles allocation," *Circ. Syst. Signal Process.*, vol. 34, no. 5, pp. 1461–1480, 2015.
- [71] T. J Freeborn, B. Maundy and A. S. Elwakil, "Approximated fractional-order Chebyshev low pass filters," *Math. Prob. Eng.*, vol. 2015, Article ID 832468, pp.1-7, 2015.
- [72] G. Tsirimokou, C. Laoudias and C. Psychalinos, "0.5-V fractional-order companding filters," *Int. J. Circ. Theory Appl.*, vol. 43, no. 9, pp. 1105–1126, 2015.
- [73] T. J. Freeborn, A.S Elwakil and B. Maundy, "Approximated fractional-order inverse Chebyshev lowpass filters," *Circ. Syst. Signal Process.*, vol. 35, no.6, pp. 1973–1982, 2015.
- [74] M. C. Tripathy, D. Mondal, K. Biswas and S. Sen, "Experimental studies on realization of fractional inductors and fractional-order bandpass filters," *Int. J. Circ. Theory Appl.*, vol. 43, no. 9, pp. 1183–1196, 2015.
- [75] T. Khanna, and D. K. Upadhyay, "Design and realization of fractional order butterworth low pass filters," *Int. Conf. Signal Process. Computing and Control*, vol. 978, no.1, pp. 356-361, 2015.
- [76] J. Koton, O. Sladok, J. Salasek and P. Ushakov, "Current-mode fractional low- and high pass filters using current conveyors," *Int. Congress on Ultra Modern Telecommunications and Control Systems and Workshops (ICUMT)*, Lisbon, Portugal. 18-20 October 2016, pp. 231–234, 2016.

- [77] J. Koton, D. Kubanek, K. Vrba, A. Shadrin and P. Ushakov, "Universal voltage conveyors in fractional-order filter design," *Int. Conf. Telecommun. Signal Process., (TSP)*, Vienna, Austria. June 2016, pp. 1–5, 2016.
- [78] J. Jerabek, R. Sotner, J. Dvorak, L. Langhammer and J. Koton, "Fractional-order high pass filter with electronically adjustable parameters," *Int. Conf. Applied Electron., (APPEL)*, 6–7 September 2016, Pilsen, Czech Republic, pp. 111–116, 2016.
- [79] P. Rani and R. Pandey, "Voltage differencing transconductance amplifier based fractional order multiple input single output universal filter," *Solid State Electron. Lett.*, 1, pp. 110-118, 2019
- [80] R. Tanwar and Sanjay Kumar, "Analysis and design of Fractance based Fractional order filter," *Int. J. Innovative Research in Electrical, Electron. Instrumentation and Control Engineering.*, vol.1, no.3, 2013
- [81] A. G. Radwan and M. E. Fouda, "Optimization of fractional-order RLC filters," *Circ. Syst. Signal Process.*, vol. 32, pp. 2097–2118, 2013
- [82] A. Marathe, B. Maundy and A.S. Elwakil, "Design of fractional notch filter with asymmetric slopes and large values of notch magnitude," *Int. Midwest Symp. Circuits Syst. (MWSCAS).*, pp. 388–391, 2013
- [83] T. Helie, "Simulation of fractional-order low-pass filters," *IEEE/ACM Trans. Audio Speech Lang. Process.*, vol. 22, no. 11, pp. 1636–1647, 2014.
- [84] M. C. Tripathy, D. Mondal, K. Biswas and S. Sen, "Design and performance study of phase-locked loop using fractional-order loop filter," *Int. J. Circ. Theo. Applications*, vol. 43, pp. 773-792, 2014, doi:10.1002/cta.1972.

- [85] P. Bertias, C. Psychalinos, A. S. Elwakil and K. Biswas, "Single transistor fractional order filter using multi-walled carbon nanotube device," *Analog Integ. Circ. Signal Process.*, vol. 100, pp. 215-219, 2018.
- [86] J. Dvorak, L. Langhammer, J. Jerabek, J. Koton, R. Sotner, and J. Polak, "Synthesis and analysis of electronically adjustable fractional-order low-pass filter," *J. Circ. Syst. Comp.*, vol. 27, no. 02, article no1850032, p.p 1-18, 2018.
- [87] M. R. Dar, N. A. Kant, F. A. Khanday and C. Psychalinos, "Fractional-order filter design for ultra-low frequency applications," *Int. Conf. Recent Trends in Electron. Information & Commun. Techn. (RTEICT)*, pp. 1727-1730, 2016.
- [88] J. Dvorak, J. Jerabek, Z. Polesakova, D. Kubanek and P. Blazek, "Multifunctional Electronically Reconfigurable and Tunable Fractional-Order Filter," *Elektronika ir Elektrotechnika*, vol. 25, no. 1, pp.26-30, 2019.
- [89] P. Bertias, C. Psychalinos, A. S. Elwakil and B. J. Maundy, "Simple Multi-Function Fractional-Order Filter Designs," *Int. Conf. Modern Circ. Syst. Technologies (MOCASST)*, pp. 1-4, 2019.
- [90] E. Kaskouta, T. Kamilaris, R. Sotner, J. Jerabek and C. Psychalinos, "Single-Input Multiple-Output and Multiple-Input Single-Output Fractional-Order Filter Designs," *Int. Conf. Telecommun. Signal Process. (TSP)*, Athens, 2018, pp. 1-4, doi: 10.1109/TSP.2018.8441348.
- [91] S. Mahata, S. K. Saha, R. Kar, and D. Mandal, "Optimal design of fractional order low pass Butterworth filter with accurate magnitude response," *Digital Signal Process.*, vol. 72, pp. 96-114, 2018.

- [92] G. Tsirimokou, C. Psychalinos and A. S. Elwakil, "Digitally programmed fractional-order Chebyshev filters realizations using current-mirrors," *Int. Symp. Circ. Systems (ISCAS)*, pp. 2337-2340, 2015.
- [93] D. Kubanek, T. Freeborn and J. Koton, "Fractional-order band-pass filter design using fractional-characteristic specimen functions," *AEU-Int. J. Electron. Commun.*, vol. 86, pp. 77-86, Apr. 2019.
- [94] A. M. AbdelAty, A. Soltan, W. A. Ahmed and A. G. Radwan, "On the analysis and design of fractional-order Chebyshev complex filter," *Circ. Syst. Signal Process.*, vol. 37, no. 3, pp.915-938, 2018.
- [95] D. Kubanek, T. J. Freeborn, J. Koton, and J. Dvorak, "Validation of fractional-order lowpass elliptic responses of $(1+\alpha)$ -Order analog filters," *Applied Sciences*, vol. 8, no. 2603, pp. 1-17, 2018.
- [96] P. Bertias, C. Psychalinos, A. S. Elwakil and K. Biswas, "Single transistor fractional-order filter using a multi-walled carbon nanotube device," *Analog Integ. Circ. Signal Process.*, vol. 100, no. 1, pp.215-219, 2019.
- [97] A. Oustaloup, "Fractional order sinusoidal oscillators: optimization and their use in highly linear FM modulation," *IEEE Trans. Circ. Syst.*, vol. 28, no. 10, pp. 1007-1009, 1981.
- [98] W. Ahmad, R. El-Khazali, and A. S. Elwakil. "Fractional-order Wien-bridge oscillator," *Electron. Lett.*, vol. 37, no.18, pp. 1110-1112, 2001.
- [99] A. G. Radwan, A. S. Elwakil and A. M. Soliman, "Fractional-order sinusoidal oscillators: design procedure and practical examples," *IEEE Tran. Circ. Syst., I: Regular Papers*, vol. 55, no. 7, pp. 2051-2063, 2008

- [100] A. G. Radwan, A. M. Soliman and A. S. Elwakil, "Design equations for fractional-order sinusoidal oscillators: four practical circuits examples," *Int. J. Circ. Theo. Appl.*, vol. 36, pp. 473-492, 2007.
- [101] L.A. Said, A. G. Radwan, A.H. Madian and A. M. Soliman, "Fractional order two port network oscillator with equal order," *Int. Conf. Microelectron. (ICM)*, pp. 156-159, 2014.
- [102] L. A. Said, A. H. Madian, A. G. Radwan and A. M. Soliman, "Current feedback operational amplifier (CFOA) based fractional order oscillators," *Int. Conf. Electron. Circ. Syst. (ICECS)*, Marseille, 2014, pp. 510-513, doi: 10.1109/ICECS.2014.7050034.
- [103] L. A. Said, A. G. Radwan A. H. Madian, and A. M. Soliman, "Fractional order Oscillators Based on Operational Transresistance Amplifiers," *AEÜ-Int. J. Electron. Comm.*, vol.69, pp. 988-1003, 2015.
- [104] L. A. Said, A. G. Radwan, A. H. Madian and A. M. Soliman, "Fractional-order oscillator based on single CCII," *Int. Conf. Telecommun. Signal Processing (TSP)*, Vienna, 2016, pp. 603-606, doi: 10.1109/TSP.2016.7760952.
- [105] T. Comedang and P. Intani, "Current-Controlled CFTA Based Fractional Order Quadrature Oscillators," *Circ. Syst.*, vol. 7, pp. 4201-4212, 2016. doi: 10.4236/cs.2016.713345.
- [106] L. A. Said, A. G. Radwan, A. H. Madian and A. M. Soliman, "Fractional order oscillator design based on two-port network," *Circ. Syst. Signal Process.*, vol. 35 pp. 3086–3112, 2016.

- [107] D. Kubánek, F. Khateb, G. Tsirimokou, and C. Psychalinos, "Practical design and evaluation of fractional-order oscillator using differential voltage current conveyors," *Circ. Syst. Signal Process.*, vol. 35, no. 6, pp. 2003-2016, 2016.
- [108] L. A. Said, A. H. Madian, A. G. Radwan and A. M. Soliman, "Fractional order oscillator with independent control of phase and frequency," *Int. Conf. Electron. Design (ICED)*, Penang, 2014, pp. 224-229, doi: 10.1109/ICED.2014.7015803.
- [109] A. Kartci, N. Herencsar, J. Koton and C. Psychalinos, "Compact MOS-RC voltage-mode fractional-order oscillator design," *European Conf. Circ. Theo. and Design (ECCTD)*, Catania, 2017, pp. 1-4, doi: 10.1109/ECCTD.2017.8093281.
- [110] A. M. EL-Naggar, L. A. Said, A. G. Radwan, A. H. Madian, A. M. Soliman, "Fractional order four-phase oscillator based on double integrator topology," *Int. Conf. Modern Circ. and Syst. Technologies*, pp. 1-4, 2017.
- [111] A. Kartci, N. Herencsar, J. Koton, L. Brancik, K. Vrba, G. Tsirimokou, C. Psychalinos, "Fractional-order oscillator design using unity-gain voltage buffers and OTAs," *Int. Midwest Symp. Circ. Syst., (MWSCAS)*, Boston, MA, 2017, pp. 555-558, doi: 10.1109/MWSCAS.2017.8052983.
- [112] L. A. Said, A. G. Radwan, A. H. Madian and A. M. Soliman, "Generalized family of fractional-order oscillators based on single CFOA and RC network," *Int. Conf. Modern Circ. Syst. Technologies (MOCAS)*, pp. 1-4, 2017.
- [113] L. A. Said, A. G. Radwan, A. H. Madian and A. M. Soliman, "Three fractional-order-capacitors-based oscillators with controllable phase and frequency," *J. Circ. Syst. Comp.*, vol. 26, no. 10, 1750160, 2017.

- [114] S. K. Mishra, D. K. Upadhyay and M. Gupta, "An approach to improve the performance of fractional-order sinusoidal oscillators," *Chaos, Solitons & Fractals*, 116(C), pp. 126-135, 2018.
- [115] S. K. Mishra, M. Gupta and D. K. Upadhyay, "Design and implementation of DDCC-based fractional-order oscillator," *Int. J. Electron.*, vol. 106, no. 4, pp.581-598, 2019.
- [116] A. Pradhan and R. K. Sharma, "Generalized Fractional-Order Oscillators using OTA," *Int. Conf. Signal Process. Integ. Networks (SPIN)*, pp. 402-406, 2018.
- [117] A. Pradhan, K. S. Subhadhra, N. Atique, R. K. Sharma and S. S. Gupta, "MMCC-based current-mode fractional-order voltage-controlled oscillators," *Int. Conf. Inventive Syst. Control (ICISC)*, pp. 763-768, 2018.
- [118] I. Podlubny, L. Dorcak and I. Kostial, "On fractional derivatives, fractional-order dynamic systems and PID-controller," *Conference on Decision & Control San Diego. December 1997*, pp. 4985-4990
- [119] I. Petras, "The fractional order controllers methods for their synthesis and application," *J. Electrical Engineering*, vol. 50, no. 10, pp. 284–288, 1999
- [120] I. Podlubny, "Fractional-order systems and $PI^{\lambda}D^{\mu}$ controllers," *IEEE Trans. Automatic control*, vol. 44, no. 1, pp. 208–214, 1999.
- [121] I, Podlubny, I. Petras, B.M. Vinagre, P. Oleary, and L. Dorcak, "Analogue realizations of fractional order controllers," *Nonlinear Dynamics*, vol. 29, no. 2, pp. 281–296, 2002
- [122] J. A. T. Machado, "Discrete time fractional-order controllers," *Fract. Calc. Appl. Anal.*, vol. 4, pp.47–66, 2001.

- [123] C. Jun-Yi. And C. Bing-Gang, “Design of fractional order controller based on particle swarm optimization,” *Int. J. Control, Automation, and Syst.*, vol. 4, no.6, pp. 775-781, 2006.
- [124] A. Charef, “Analogue realization of fractional order integrator differentiator and fractional $PI^\lambda D^\mu$ controller,” *IEE Proc. Control Theory Applications*. vol. 153, no.6, pp.714–720, 2006.
- [125] Y. Luo, Y. Q. Chen and C. Y. Wang, “Tuning fractional order proportional integral controllers for fractional order systems,” *J. Process Control*. vol. 20, no. 7, pp.823-831, 2010.
- [126] F. Padula and V. Antonio, “Tuning rules for optimal PID and fractional-order PID controllers,” *J. Process Control*, vol. 21, no. 1, pp. 69–81, 2011.
- [127] A. Tepljakov, E. Petlenkov and J. Belikov, “Application of Newton’s method to analog and digital realization of fractional-order controllers,” *Int. J. Microelectron. Comput. Sci.*, vol. 3, no. 2, pp. 45–52, 2012.
- [128] D. S. Karanjkar, S. Chatterji and P. R. Venkateswaran, “Trends in fractional order controllers,” *Int. J. Emerging Technology and Advanced Engineering*, vol. 2, no. 3, pp. 383-389, 2012.
- [129] T. Suksang, W. Loedhammacakra and V. Pirajanchai, “Implement the Fractional Order, Half Integrator and Differentiator on the OTA Based $PI^\lambda D^\mu$ Controller Circuit,” *IEEE Conference on ECTICON*, pp. 1-4, 2012.
- [130] A. Tepljakov, E. Petlenkov and J. Belikov, “Efficient analog implementations of fractional-order controllers,” *Int. Carpathian Control Conf.*, Rytro, Poland, pp. 377–382, 2013.

- [131] S. Pandey, P. Dwivedi and A.S. Junghare, "A novel 2-DOF fractional-order $PI^{\lambda}D^{\mu}$ controller with inherent anti-windup capability for a magnetic levitation system," *AEU-Int. J. Electron. Commun.*, vol. 79, pp.158-171, 2017.
- [132] A. Kumar and V. Kumar, "Hybridized ABC-GA optimized fractional order fuzzy pre-compensated FOPID Control design for 2-DOF robot manipulator," *Int. J. Electron. Commun.*, vol. 79, pp. 219-23, 2017.
- [133] G.W. Bohannan, "Analog fractional order controller in temperature and motor control applications," *J. Vibration and Control*, vol. 14, no. 9-10, pp. 1487–1498, 2008.
- [134] E. M. Hamed, L. A. Said, H. M. Ahmed and A. G. Radwan, "On the Approximations of CFOA-Based Fractional-Order Inverse Filters," *Circ. Syst. Signal Process.*, vol. 39, pp. 2-29, 2019.
- [135] N. A. Khalil, L. A. Said, A. G. Radwan and A. M. Soliman, "Fractional Order Inverse Filters Based on CCII Family," *Int. Conf. Advances in Computational Tools for Engineering Applications (ACTEA)*, Beirut, Lebanon, pp. 1-4, Sep. 2019.
- [136] B.T. Krishna and K.V.V.S. Reddy, "Active and Passive Realization of Fractance Device of Order 1/2," *Active and Passive Electronic Components*, vol. 2008, no. 369421, 2008.
- [137] M. Sugi, Y. Hirano, Y.F. Miura, K. Saito, "Frequency behavior of self-similar ladder circuits," *Colloids Surfaces Physicochem. Eng. Aspect.*, vol. 198–200, pp. 683–688, 2002.
- [138] A. Charef, , H. H. Sun, Y. Y. Tsao and B. Onaral, "Fractal system as represented by singularity function," *IEEE Trans. Automatic Control*, vol. 37, no. 9, pp. 1465-1470, 1992.

- [139] A. Oustaloup, F. Levron, B. Mathieu and F. M. Nanot, "Frequency-band complex noninteger differentiator: characterization and synthesis," *IEEE Trans. Circ. Syst. I: Fundamental Theo. Applications*, vol. 47 no. 1, pp. 25-39, 2000.
- [140] K. Matsuda and F. Hironori, " H_∞ optimized wave-absorbing control-Analytical and experimental results," *J. Guidance, Control, and Dynamics*, vol. 16, no. 6, pp. 1146-1153, 1993.
- [141] M. Nakagawa and K. Sorimachi, "Basic characteristic of fractance devices," *IEICE Trans. Fund.*, vol. E75-A, no. 12, pp. 1814–1819, 1992.
- [142] J. Valsa, P. Dvorak and M. Friedl, "Network model of the CPE," *Radioengineering*, vol. 20, no. 3, pp. 619–626, 2011.
- [143] G. Tsirimokou, C. Psychalinos and A.S Elwakil, "Emulation of a constant phase element using operational transconductance amplifiers," *Analog Integ. Circ. Signal Process.*, vol. 85, pp. 413–423, 2015
- [144] I. Dimeas, G. Tsirimokou, C. Psychalinos and A. Elwakil, "Realization of fractional-order capacitor and inductor emulators using current feedback operational amplifiers", *Int. Symp. Nonlinear Theo. Applic. (NOLTA 2015)*, Hong Kong, China, pp. 237-240, Dec. 2015.
- [145] A. Agambayev, M. Farhat, S.P. Patole, A.H. Hassan, H. Bagci and K.N. Salama, "An ultra-broadband single-component fractional-order capacitor using MoS_2 -ferroelectric polymer composite," *Appl. Phys. Lett.*, vol. 113, no. 9, 093505, 2018.
- [146] K. Biswas, S. Sen and P. K. Dutta, "Realization of a constant phase element and its performance study in a differentiator circuit," *IEEE Trans. Circ. Syst. II*, vol. 53, no. 9, pp. 802–806, 2006.

- [147] G.W. Bohannan, “Application of Fractional Calculus to Polarization Dynamics in Solid Dielectric Materials,” Montana State University Bozeman, Montana, November 2000. Ph.D. Thesis. (Accessed 4 April 2018).
- [148] R. Caponetto, S. Graziani, F.L. Pappalardo and F. Sapuppo, “Experimental characterization of ionic polymer metal composite as a novel fractional-order element,” *Adv. Math. Phys.*, vol. 2013, pp. 1–10, 2013.
- [149] A. Buscarino, R. Caponetto, G. Di Pasquale, L. Fortuna, S. Graziani and A. Pollicino, “Carbon Black based capacitive Fractional-order Element towards a new electronic device,” *AEU-Int. J. Electr. Commun.*, vol. 84, pp. 307–312, 2018.
- [150] M. El shurafa, N. Almadhoun, K. Salama and H. Alshareef, “Microscale electrostatic fractional-order capacitors using reduced graphene oxide percolated polymer composites,” *Appl. Phys. Lett.*, vol. 102, no. 23, pp. 232901–232904, 2013.
- [151] A. Adhikary, M. Khanra, S. Sen and K. Biswas, “Realization of a Carbon Nanotube Based Electrochemical Fractor,” *Int. Symp. Circ. Syst. (ISCAS)*, pp. 2329-2332, 2015, doi: 978-1-4799-8391-9/15/\$31.00.
- [152] D. A. John, S. Banerjee, G. W. Bohannan and K. Biswas, “Solid-state fractional-order capacitor using MWCNT-epoxy nanocomposite,” *Appl. Phys. Lett.*, vol. 110, 163504, 2017.
- [153] A. Agambayev, S. Patole, H. Bagci, K.N. Salama, Tunable fractional-order capacitor using layered ferroelectric polymers, *AIP Adv.* 7, 095202, 2017.

- [154] G. Tsirimokou, C. Psychalinos and A. Elwakil, "Design of CMOS Analog Integrated Fractional-Order Circuits: Applications in Medicine and Biology," 2017, DOI:10.1007/978-3-319-55633-8.
- [155] El-Khazali, Reyad. "On the biquadratic approximation of fractional-order Laplacian operators." *Analog Integ. Circ. Signal Process.*, vol. 82, no. 3, pp. 503-517, 2015.

Chapter 2

Overview of Structures and Methods for the Realization of Fractional Order Elements

In this chapter, we present some of the fundamental concepts of fractional order calculus and their utilization in the design of fractional order elements. Later on, an overview of methods and structures for the realization of fractional order elements (FOEs) in general and fractional order capacitors in particular have been introduced.

2.1. Fundamental Relations in Fractional Order Calculus

Fractional order calculus is a branch of mathematics, which deals with differentiation and integration of non-integer order. Its origin goes back to the seventeenth century. In a communication in 1695, between L'Hospital and Leibniz regarding n^{th} derivative of function $f(x)$, $\left(\frac{d^n}{dx^n} f(x)\right)$, which has now become signature statement of any publication on fractional order calculus, pondering over the question: what will be the result when $n = \frac{1}{2}$, Leibniz had replied that it was a paradox from which one day useful inferences will be drawn [1-4]. Previously, fractional order calculus was popular among mathematicians only, but over the last few years, it has become popular in the field of science and engineering because it can model several real life problems more accurately [2-3]. Fractional order calculus deals with the differentiation and integration of arbitrary order. It is the super subset of classical calculus, as classical calculus is a special case of fractional order calculus. Since the proclamation of 'fractional order calculus' word in 1695, many mathematicians have proposed definitions of the fractional order differentiation and integration, but three

definitions namely Riemann-Liouville (R-L), Grunwald-Letnikov (G-L) and Caputo have become very popular and useful. These definitions are used in various fields of science and engineering. Definitions of fractional order derivatives are based on two approaches. In the first approach, differentiation and integration are considered as cut-off point of finite differences, while, the other approach generalizes the convolution type representation of repeated integration. While the Grunwald-Letnikov (G-L) definition is based on the first approach, the other two definitions, namely, the Riemann-Liouville (R-L) and Caputo are based on the second approach.

According to R-L definition [2] the fractional order differ-integral of any function $f(t)$ can be expressed as:

$${}_n D_t^\alpha f(t) = \frac{1}{\Gamma(n-\alpha)} \frac{d^n}{dt^n} \int_a^t (t-\tau)^{n-\alpha-1} f(\tau) d\tau; (n-1 \leq \alpha < n) \quad (2.1)$$

where n is an integer, ' α ' is a real number, $f(t)$ is an integrable function in interval ' a ' and ' t ' and $\Gamma(\bullet)$ is the Euler's Gamma function.

The fractional derivative of a function $f(t)$ as defined by Caputo [2] can be expressed as:

$${}_a D_t^\alpha f(t) = \frac{1}{\Gamma(n-\alpha)} \int_a^t \frac{f^{(n)}(\tau)}{(t-\tau)^{\alpha+1-n}} d\tau; (n-1 << \alpha < n) \quad (2.2)$$

where n is an integer, and ' α ' is a real number.

Under homogenous initial conditions, the R-L and Caputo derivatives are equivalent [4].

According to G-L definition [4], fractional differ-integral of any function $f(t)$ can be written as:

$${}_a D_t^\alpha f(t) = \lim_{h \rightarrow 0} \frac{1}{h^\alpha} \sum_{n=0}^{\lfloor \frac{t-a}{h} \rfloor} (-1)^n \binom{\alpha}{n} f(t - nh) \quad (2.3)$$

where 'a' is lower limit and $\binom{\alpha}{n}$ is the binomial coefficient, $\binom{\alpha}{n} = \frac{\alpha!}{n!(\alpha-n)!}$.

2.2. Fractional Order Laplacian Operator

The Laplace transform is a very useful mathematical tool in the analysis and design of electronic circuits. It transforms the circuit from time domain to frequency domain. This transform is widely used in the design and analysis of electronic circuits (filters, oscillators, control systems etc.) as analysis of any linear time invariant circuits is easier in frequency domain as compared to time domain. The Laplace transforms of derivative and integral of any time varying function can be expressed (assuming zero initial conditions) as:

$$L \left\{ \frac{d}{dt} f(t) \right\} = sF(s) \quad (2.4)$$

$$L \left\{ \int f(t) dt \right\} = \frac{F(s)}{s} \quad (2.5)$$

The Laplace transforms of equations (2.1)-(2.3) lead to the following definitions of the fractional order Laplacian operator [3] (considering zero initial conditions).

$$L \left\{ \frac{d^\alpha}{dt^\alpha} f(t) \right\} = s^\alpha F(s) \quad (2.6)$$

$$L\{D^{-\alpha}f(t)\} = \frac{1}{s^\alpha}F(s) \quad (2.7)$$

It may, however, be pointed out that no physical interpretation of the initial condition exists for the differ-integral given in equation (2.1). On the other hand, the Caputo definition of the fractional order derivative is more restrictive as it requires the n^{th} order derivative of $f(t)$ to be absolutely integrable. However, initial conditions for the differ-integral equation based on this definition are of the same form as those of their integer order counterparts.

2.3. Fractional Order Element

The fractional order element (FOE) is an important and useful two terminal electrical element, which is used for the design and implementation of fractional order analog circuits. The commonly used fractional order elements, namely, fractional order capacitor (FC) and fractional order inductor (FI) are characterised by the following time domain terminal characteristics:

$$i(t) = C_\alpha \frac{d^\alpha v(t)}{dt^\alpha} \quad (2.8)$$

$$v(t) = L_\alpha \frac{d^\alpha i(t)}{dt^\alpha} \quad (2.9)$$

where $\alpha \in (0,1)$ is the ‘order’ of the FOE characterising the fractance device, C_α and L_α are known as pseudo capacitance and pseudo inductance, respectively. The units of C_α and L_α are $\text{F}/\text{sec}^{\alpha-1}$ and $\text{H}/\text{sec}^{\alpha-1}$ respectively. Using the Laplace transform of the fractional order derivative, the impedance of a FOE can be expressed as:

$$Z(s) = Ds^\alpha \quad (2.10)$$

where ‘D’ is a constant and ‘ α ’ is the order of FOE.

$Z(s)$ is proportional to the fractional order Laplacian operator s^α . Depending upon the values of ‘ α ’, fractance devices are classified into several categories such as (i) resistor, if $\alpha = 0$ (ii) inductor, when $\alpha = 1$ (iii) capacitor for $\alpha = -1$ (iv) fractional order inductor for $0 < \alpha < 1$ (v) fractional order capacitor for $-1 < \alpha < 0$ (vi) frequency dependent negative resistor, if $\alpha = -2$. The classification of these elements is depicted in Fig 2.1[5].

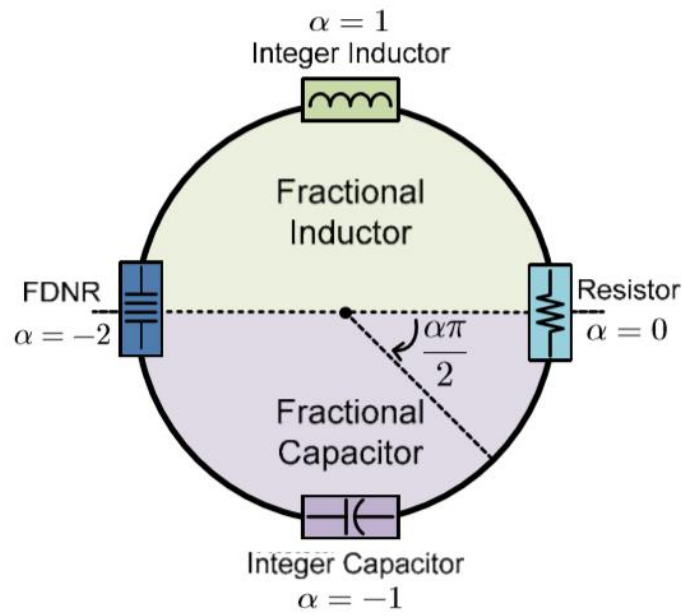


Figure.2.1 Classification of fractional-order element [5]

The impedance of a fractional capacitor can be expressed as:

$$Z(s) = \frac{1}{C_f s^\alpha} \quad (2.11)$$

where variable ‘ α ’ ($0 < \alpha < 1$) is the order of fractional order capacitor (FC) and C_f is pseudo capacitance, expressed in $F/\text{sec}^{\alpha-1}$. The value of frequency dependent capacitance (C) of fractional order element in Farad can be calculated as $C = \frac{C_f}{\omega^{1-\alpha}}$.

Similarly, the impedance of a fractional order inductor (FI) can be given by:

$$Z(s) = L_f s^\alpha \quad (2.12)$$

and relation between pseudo inductor (L_f) and conventional inductor (L) is given by:

$$L = \frac{L_f}{\omega^{1-\alpha}}.$$

The phase of FOE is constant, independent of ω (angular frequency) and equal to $\alpha \frac{\pi}{2}$ (where ' α ' is the order of FOE). For this reason, fractional order immittances are also called constant phase elements (CPE). The magnitude of $Z(s)$ will decrease or increase, according to the sign of ' α ' with angular frequency (ω).

As the CPEs are not available as standard devices, the characteristics of these factors have been simulated/emulated by circuit designers using a variety of methods. The existing implementation of the CPEs may be categorized into two different classes [6]: (i) single component- based realizations and (ii) multiple components-based realizations. The multiple components based realizations can be further sub-divided into active and passive realizations. The single component-based realizations [7]-[15] mainly comprise of the electrochemical realizations or solid state realizations. These realizations are generally available for a fixed value of the fractional order parameter ' α ' and the designs are customized, and not suitable for general purpose circuit applications. On the other hand, the passive, multi components-based realizations, which are most commonly used for the implementation of various fractional order filters and oscillators, are Foster/Cauer-like structures, approximating the driving point immittances of the CPEs whose immittances are expressed as $F(s) = Ks^\alpha$, over a specified range of frequencies. The values of the passive components employed in these realizations are calculated according to the approximation methods [16]-[25] used to approximate the fractional order Laplacian operator s^α . This approach is preferred over the single component-based realization from the circuit point of

view because CPEs with arbitrary values of α can be emulated by choosing the appropriate values of the passive components used in the network emulating the CPEs. Active realizations of the CPEs [26]-[28] employ cascade connection of second/higher order transfer functions approximating the fractional order Laplacian operator s^α followed by a voltage to current or current to voltage converter.

In the following, we present the details of some of the important works dealing with the realizations of the FOEs using, single as well as the multi component-based realizations. We have also discussed the details of the methodology and design of the fractional order capacitors, which we have used for the realization of various analog circuits in this thesis. The methods suggested by Valsa, Dovrak, and Friedel [24] and Oustaloup, Levron, Mathieu and Nanot [21], have been used to design the fractional order capacitors used for the implementation of all the proposed fractional order circuits in this thesis. PSPICE simulations of the magnitude and the phase responses of the FCs realized with these methods have also been presented.

2.3.1. Single Component-Based Realization of the FOE/FC

The aim of single component-based realizations of the FOE is to develop a compact two-terminal element similar to the standard two-terminal passive circuit element which can be used as an off-the-shelf component, available for implementation of any analog signal processing circuit. The research work in this area is still in infancy stage. In the following, we present the details of some of the important works in this area.

In [7], Agambayer, Farhat, Patole, Hassan, Bagci and Salama have fabricated a fractional order capacitor (FC) with a molybdenum disulphide (MoS_2)-ferroelectric

polymer composite. The fabricated FC has constant phase angle in the frequency range of 100Hz to 10MHz with variation of $\pm 4^\circ$. The value of phase angle of this FC can be adjusted from -80° to -58° by changing the ferroelectric polymer in composite and the volume ratio of MoS₂.

Krishna, Das, Biswas and Goswami have proposed a porous polymer material based fractional order capacitor in [8]. The capacitor of predefined specifications was fabricated by dipping a capacitive type probe, coated with a porous film of poly methyl methacrylate (PMMA) of particular thickness into a polarizable medium. Fractional order capacitor having phase angles of -15° to -60° was realized in the frequency range of 20 Hz to 200 kHz.

An ionic gel-Cu electrode based fractional order capacitor has been reported by Bohannan in [9]. The FC was developed by sandwiching a copper (Cu) plate (25mm x 25mm) coated with Lithium Nitrate and tetra-ethyl orthosilicate gel between two square Cu electrodes and packaged by Plexiglas plate. Fractional order capacitor having phase angle of 45° in the frequency range of 20 Hz to 200 KHz was obtained with a ripple of $\pm 5^\circ$.

In [10], Caponetto, Graziani, Pappalardo and Sapuppo have shown that ionic polymer metal composite (IPMC) can act as FOE. IPMC materials are made by metallization of thin membranes of ionic polymer. Through metal coating thickness, order of FOE (α) can be varied between 0.05 to 0.3 in two constant phase (CP) zones 10 mHz to 10Hz and 1Hz to 100Hz. CPE of this form is more suitable for low frequency applications.

A carbon black polymer dielectric base FOE is reported by Buscarino in [11], in which nanometre size particles of carbon black polymer composite is used as dielectric of capacitor. The value of pseudo capacitor ranges from 25 pF to 207 pF was measured, where order of capacitor varies from 0.77 to 0.86. The constant phase frequency zone of 100 kHz to 1000 MHz was observed for the fabricated FOE.

A Grapheme polymer dielectric based FOE was proposed by Shurafa in [12], in which grapheme polymer composite is used as dielectric material between two electrodes of the capacitor terminal. The order of fabricated capacitor varies between 0.77 to 0.86 in the frequency range of 400 Hz to 2 MHz. The main feature of this FOE is that it is compact and compatible for PCB fabrication.

In [13], Adhikary, Khanra, Sen and Biswas have reported carbon nanotube based single component FOE. This type of FOE has been developed by coating a polymer-carbon nanotube (CNT) composite over Cu clad epoxy block and putting the block in polarizing solution. Two different types of FOEs have been obtained by varying the percentage of CNT in polymer-CNT composite and nature of polarized solution. This FOE has constant phase of -31° over the frequency range of 20 Hz to 2MHz with phase error of $\pm 2^\circ$. While the other type of FOE developed, has two ranges of frequency bands 20 Hz to 8 kHz and 70 kHz to 2 MHz for $-33^\circ (\pm 1.5^\circ)$ and $-20^\circ (\pm 1^\circ)$ respectively.

A solid state based- FOE was fabricated using multi walled carbon nanotubes (MWCNTs) by John, Banerjee, Bohannan and Biswas in [14]. By increasing the loading of MWCNT in composite material the phase angle of FOE can be adjusted

from -80° to -45° in the frequency zone above 100Hz. The fabricated device is compact and easily integrable with electronic circuits.

In [15], Agambayer, Farhat, Patole, Hassan, Bagci and Salama have used pairs of various poly-vinylidene fluoride (PVDF)-based polymers in the fabrication of fractional order capacitor. Bi-layers of polymer were deposited on Ti/Au electrodes of FC using a drop casting approach. The phase of FC can be tuned in the range of -83° to -65° for the frequency band of 150 KHz to 10 MHz by changing the thickness ratio of the layers. The main features of this proposed FC are (i) low cost and (ii) straightforward fabrication method for designing a PCB compatible FC with a tunable CPA in a wide range of operational frequency.

2.3.2. Multi Components-Based Realization of FOE/FC

The single component-based realizations of the FOE are in the developing stage and not a single prototype has been developed so far, which can be mass produced. Also, from the very nature of the prototype designs discussed above, it emerges that each FOE is a customized designed for a fixed value of ' α '. For changing the value of ' α ', the complete hardware needs redesign. Such an FOE, obviously, is not suitable for analog signal processing because the circuits cannot be tested in simulations. Also, there are issues of portability, aging and degradation. Thus, many circuit designers, working in the field of analog realization of fractional order circuits have utilized various approximation methods developed over a period of time to approximate the fractional order Laplacian operator s^α by a rational function of higher order and developed network models of the fractional order capacitors which approximate the behaviour of the fractional order elements (FC/FI) over some specified frequency

range [16]-[25]. In the following, we present an account of the multi component-based FOEs. The design methodology of multi component FOEs is categorised into two sub categories [6]: (i) FOEs implemented with passive components and (ii) FOEs implemented with active components

2.3.3. FOE Implemented with Passive Components

Heaviside, in 1922, showed that the input impedance of an infinite RC cable was an irrational function of the complex frequency variable 's'. It was shown that the input impedance was proportional to $\frac{1}{\sqrt{s}}$ [17]. The term 'fractional order capacitor' was first coined by Cole and Cole in [29], wherein, the dispersion and absorption characteristics of various dielectrics were investigated. The mathematical modelling of the experimental results showed that the dissipative and charge storage component constituted complex impedance whose argument remain constant at all frequencies. The phase angle depended on a constant 'α' that was different for different dielectrics.

Various passive realizations of fractional order capacitors have appeared in literature and many of these research works have used similar design rules which were used in realizing driving point impedance proportional to $s^{\pm\frac{1}{2}}$. The corresponding network realizations comprised of cascaded or parallel connection of RC networks arranged in the form of 'T' or symmetrical lattices. In the following, we present a brief review of the important passive component-based realizations of fractional order capacitors/fractional order elements.

Calson and Halijac proposed an approximation method for $(1/s)^{1/n}$ for any integer value of $n > 1$ in [16]. Regular Newton process was used in this approximation

method. R-C networks have been used for fractional order capacitors of order $1/3$ and $1/4$ designed using the proposed approximation method.

Dutta Roy [17] proposed two methods for realization of an immittance whose argument is approximately equal to $\pm\alpha/2$, where $0 < \alpha < 1$, over an extended frequency range. The first approximation method was based on the continued fraction expansion of the irrational driving point function of a uniform distributive R-C network. In the other method, elliptic functions were used to describe the phase characteristics of the FOE. The resulting FOE can then be synthesized as an RC-impedance or an RL admittance function, which can finally be realized as a Foster/Cauer network.

The rational approximation of fractional differ-integral operator was attempted using Cole-Cole dispersion method by Charef, Sun, Tsao and Onard in [18]. The approximated fractional order function was synthesized using R-C network consisting of series connection of 'm' cell of parallel R and C, and these components were arranged in geometric progression.

Nakagawa and Sorimachi [19] presented a recursive electric circuit of a fractal structure consisting of resistors and capacitors. Proposed R-C network has magnitude and phase properties similar to a fractance device of order $-1/2$. The proposed fractance device was tested numerically and experimentally for number of stages of fractance circuits ($N = 1, 5, 10, 100$ and ∞ for numerical simulations and $N = 5$ for experimental). Experimentally, the proposed fractance device was also tested on integrator as well as differentiator circuits designed using op-amp.

In [20], Matsuda and Hironori proposed an approximation method of fractional differential operator utilizing the concept of continued fraction expansion technique. This approximation process was completed in two stages, first the rational model of irrational function was obtained by the continued fraction expansion technique, then its poles and zeros were fitted in logarithmically spaced points. The phase error can be reduced by increasing the order of approximation.

Oustaloup, Leveron, Mathieu and Nanot proposed an approximation method for fractional order operator to convert the irrational transfer function into rational transfer function in [21]. A recursive distribution of poles and zeros was utilized for the approximation. This method was applied to approximate the fractional order operator s^α ($0 < \alpha < 1$) into integer order rational form within a specified frequency band. The phase and magnitude error, in this approximation method can be reduced by increasing the order of approximation. This method is widely used in fractional order control systems.

Self-similar RC network has been simulated for α , varying from 0.25 to 0.75, using 18 or less rungs by Sugi, Hirano, Miura, Saito in [22], where the term ‘rung’ is employed for a set of R and C elements. The components of consecutive rungs are arranged in geometric progression. The proposed fractional order capacitor has constant phase zone over five decades of frequency with ripple of $\pm 0.5^\circ$.

Krishna and Reddy reported the realization of a fractance device of order $\frac{1}{2}$ in [23] using continued fraction expansion method. A rational approximation for \sqrt{s} is deduced using CFE method, which, then was realized using R-C ladder network. The

results obtained from this method were compared with Oustaloup approximation considerable improvements were reported.

An R-C ladder structure of fractional order capacitor was proposed in 2011 by Valsa, Dvorak and Friedl [24], wherein, a systematic process for simulation of CPE in a desired frequency range for arbitrary orders was described. The design method is quite simple and approximates the ideal behaviour of CPE in specified frequency range with acceptable tolerance.

In [25], Reyad EI- Khazali proposed a biquadratic approximation of fractional order differ-integral operators. The equivalent circuit was synthesized with series R-C and R-L networks. The performance of proposed structure has better results than equi-ripple and Oustaloup approximations.

In Fig.2.2, we have shown the structures of the various RC networks, which may be used for the implementation of fractional order elements, resulting from the above discussed methods/techniques.

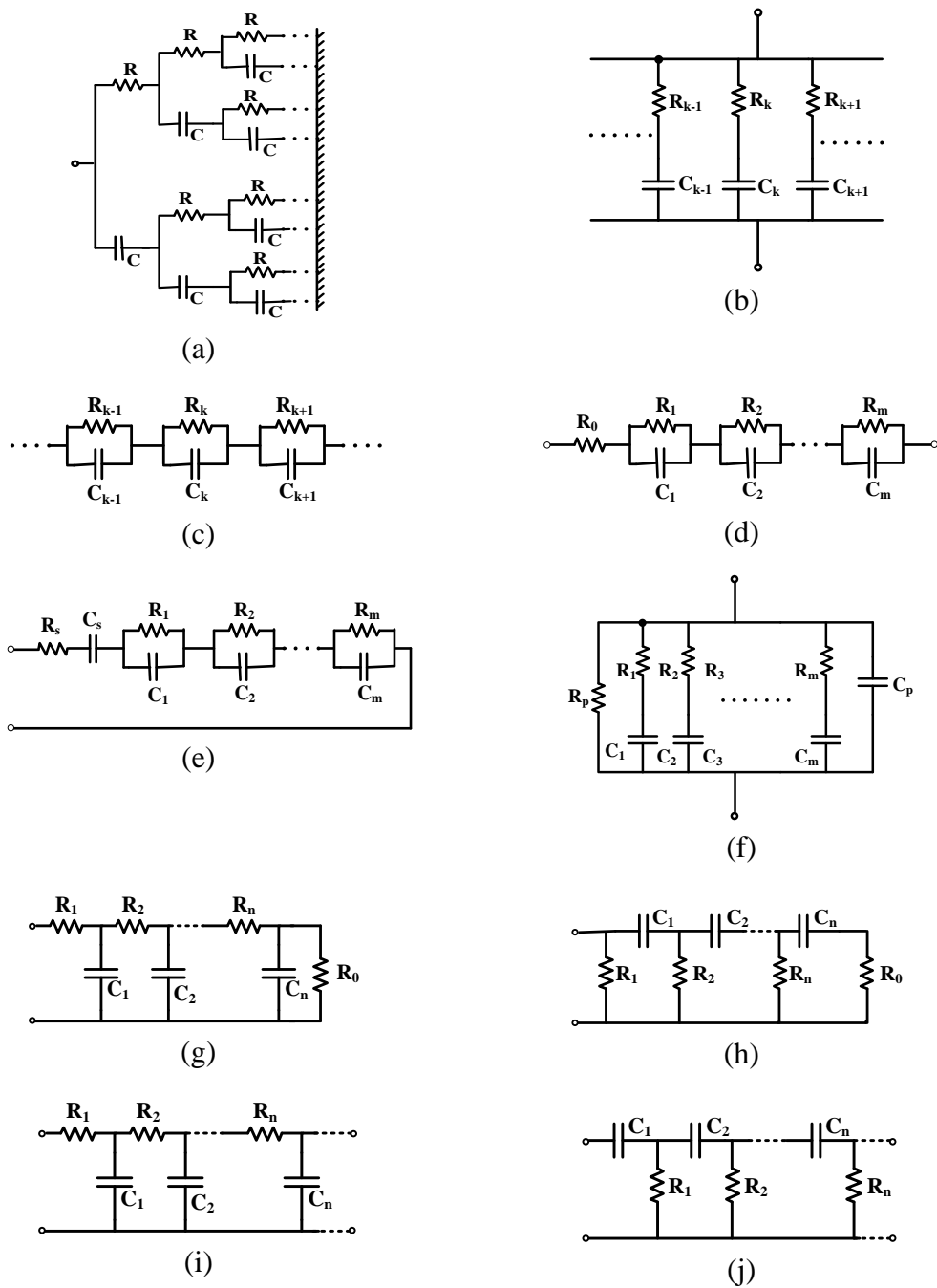


Figure.2.2 Different structures of various RC networks approximating the FC (a) Nakagawa and Sorimachi [18] (b-c) Sugi, Hirano, Miura and Saito [21] (d) Oustaloup, Levron, Maithieu and Nanot [20] (e-f) Valsa, Dvorak and Friedl [23] (g-h) Cauer I and II [25] (i-j) S. C. Dutta Roy [16]

2.3.4. FOE Implemented with Active Components

The active realizations of FOEs are based on cascading a fractional order integrator/differentiator stage followed by a voltage to current converter [26]. The fractional order differentiator/integrator in all such realizations may be designed using any of the popular approximation techniques, mostly, the continued fraction expansion method [26] and subsequently implemented with different types of amplifiers viz. the operational transconductance amplifiers (OTA) [26], [28], current feedback amplifiers (CFOA) [27] etc. The scheme for active realization of a fractional order element is represented below in Fig. 2.2 [26]-[28].

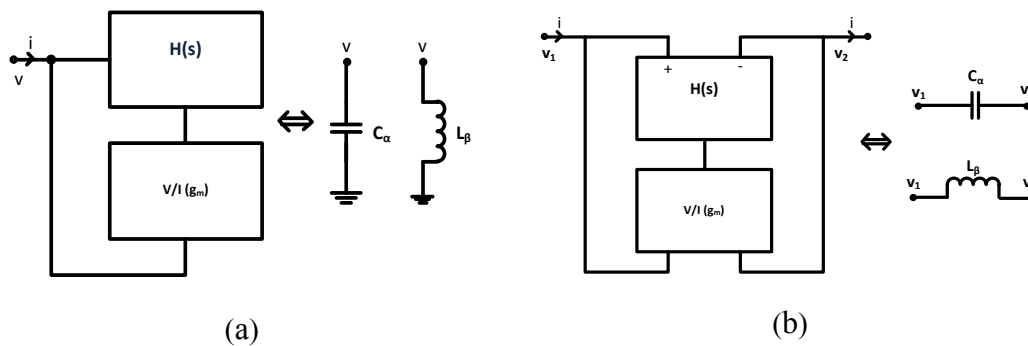


Figure.2.3 (a) Grounded CPE (b) Floating CPE

The realized circuits can operate in low and high frequency range depending on the implementation. The circuit can be implemented in fully integrated circuit form subject to the availability of suitable capacitors. The external capacitors used in the realization of the fractional order differentiators/integrators can be replaced if one uses MOS capacitors. Bertias, Psychalinos, Elwakil and Maundy [28] presented a capacitor less emulator for fractional order capacitors and integrators in which current mirrors and MOSFETS were used as capacitors. The scheme is shown below in Fig. 2.3

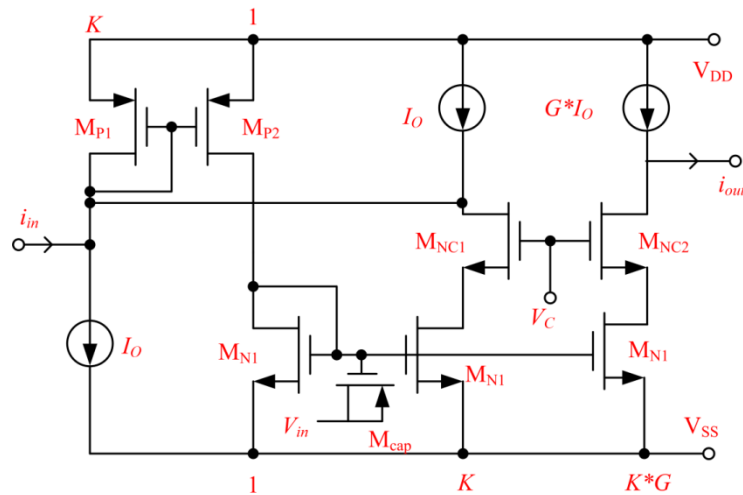


Figure.2.4 Capacitorless fractional order differentiator/integrator [28]

OTA-based implementation of FOE was proposed by Tsirimokou, Psychalinos, Freeborn and Elwakil in [26], while CFOA-based implementation was reported by Dimeas, Tsirimokou, Psychalinos and Elwakil in [27].

In this thesis, we have used the methods proposed in [21] and [24] to design the various fractional order capacitors in the implementation of the proposed circuits of fractional order filters, fractional order inverse filters and fractional order sinusoidal oscillators.

2.4. Implementation of Fractional Order Capacitor Using Valsa, Dvorak and Friedl Method

The R-C ladder structure of fractional order capacitor was proposed in 2011, by Valsa, Dvorak and Friedl [24]. A systematic process for simulation of CPE in a desired frequency range for arbitrary orders was described. The design method is quite simple and approximates the ideal behaviour of CPE in specified frequency

range with acceptable tolerance. The basic network model of CPE contains m cell of series R-C branches connected in parallel, which is shown in Fig. 2.5.

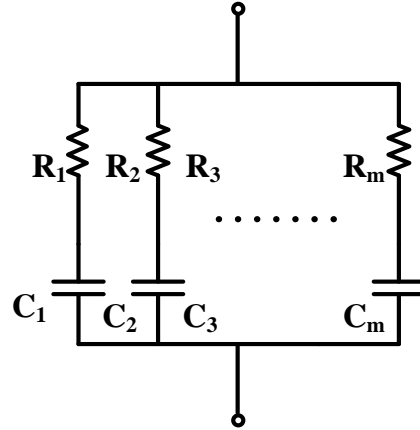


Figure 2.5 R-C ladder structure of CPE

The values of resistances and capacitances of branches form a geometric sequence and represented as

$$R_k = R_1 a^{k-1}, C_k = C_1 b^{k-1}, \text{ where } k = 1, 2, \dots, m \quad (2.13)$$

The coefficients 'a' and 'b' lie between 0 and 1 ($0 < a < 1$ and $0 < b < 1$).

The input impedance of network shown in Fig.2.5 can be represented as

$$Z(s) = \frac{1}{Y(s)} \quad (2.14)$$

where $Y(s)$ is input admittance and it is equal to the sum of the admittances of individual branch i.e.

$$Y(s) = \sum_{k=1}^m \frac{sb^{k-1}C_1}{1 + s(ab)^{k-1}R_1C_1} \quad (2.15)$$

The input impedance $Z(s)$ has zeros at the breaking points and expressed as:

$$Z_k = \frac{1}{R_1C_1(ab)^{k-1}} \quad (2.16)$$

Further, poles and zeros can be calculated as:

$$P_k = \frac{Z_k}{b} \text{ and } Z_{k+1} = \frac{P_k}{a}$$

Now, after replacing $s = j\omega$ in equation (2.15), we have:

$$Y(j\omega) = \sum_{k=1}^m \frac{j\omega b^{k-1} C_1}{1 + j\omega (ab)^{k-1} R_1 C_1} \quad (2.17)$$

$$Z(j\omega) = \frac{1}{Y(j\omega)}$$

Argument of $Z(j\omega)$ in degrees can be expressed as:

$$\varphi(\omega) = \frac{180}{\pi} \tan^{-1} \left(\frac{\text{Imag}(Z)}{\text{Real}(Z)} \right) \quad (2.18)$$

The average value of the phase angle can be given by:

$$\varphi_{av} = 90^\circ \alpha = 90^\circ \frac{\log(a)}{\log(a) + \log(b)} = 90^\circ \frac{\log(a)}{\log(ab)} \quad (2.19)$$

The phase characteristic passes value φ_{av} in points of $\omega_{av}(k) = Z_k(a/b)^{1/4}$ and reaches at extreme values at $\omega_{\varphi_{min}}(k) = Z_k(a)^{1/2}$ and $\omega_{\varphi_{max}}(k) = P_k(b)^{1/2}$

The ω_{av} can be expressed as:

$$\omega_{av} = \sqrt{\omega_{\varphi_{max}} * \omega_{\varphi_{min}}} \quad (2.20)$$

For a good approximation of CPE in the specified frequency range, the R-C model of CPE as given in Fig. 2.5 must have relatively higher number of sections (m should be very high). This introduces complexity in network model of CPE. Thus, to reduce this complexity one section of parallel R-C is added in network and the values of parallel resistance (R_p) and capacitance (C_p) are given by:

$R_p = R_1 \frac{1-a}{a}$, $C_p = C_1 \frac{b^m}{1-b}$, where, m is number of cell, and the values of a, b are determined, as explained next.

The resultant R-C network is thus obtained shown in Fig. 2.6

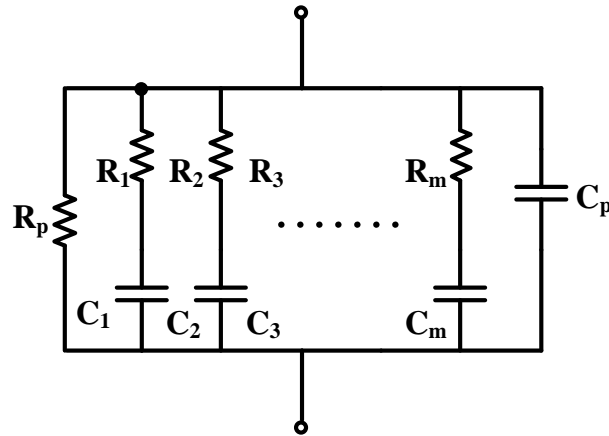


Figure 2.6 Modified R-C network of FC

2.4.1. Design Procedure

For the given data of $\tau_1 = R_1 C_1$, φ_{av} , $\Delta\varphi$, m and D_p , R-C network of a fractional order capacitor can be implemented using the following steps:

Step1: Determination of product of a and b as:

$$ab = \frac{0.24}{1+\Delta\varphi}, \Delta\varphi \text{ is phase error } (\Delta\varphi = 0.5^\circ, 1^\circ, 2^\circ)$$

Step2: Determination of the lower and upper frequency as:

$$\omega_l = \frac{1}{\tau_1}, \omega_u = \frac{\omega_l}{(ab)^m}$$

Step 3: Determination of the values of 'a' and 'b' as:

$$\alpha = \frac{\varphi_{av}}{90}, a = 10^{\log(\alpha)}, b = \frac{ab}{a}$$

Step 4: Determination of values of components of R-C ladder circuit as:

$$R_p = R_1 \frac{1-a}{a}, C_p = C_1 \frac{b^m}{1-b} \quad \text{and} \quad R_k = R_1 a^{k-1}, C_k = C_1 b^{k-1} \quad \text{where } k = 1, 2, 3, \dots, m$$

Step 5: For the given value of R_1 and C_1 , the input admittance of R-C network can be expressed as:

$$Y(j\omega_{av}) = \frac{1}{R_p} + j\omega_{av}C_p + \sum_{k=1}^m \frac{j\omega_{av}C_k}{1 + j\omega_{av}R_kC_k}$$

$$\text{where } \omega_{av} = Z_k \sqrt{a} = \frac{1}{R_1 C_1 (ab)^{k-1}} \sqrt{a}, \quad \text{where } k = \text{int}\left(\frac{m}{2}\right)$$

Step 6: Calculation of D as: $D = Z_{av} \omega_{av}^{-\alpha}$.

If the value of D as obtained above is different from required D_p , then resistors R_k and R_p are multiplied with ratio D_p/D , while C_k and C_p are divided by the same ratio to keep same frequency range.

we have calculated the values of capacitances and resistances for ladder structure of CPE for FCs of the value $0.382\mu\text{F}/\text{sec}^{(\alpha-1)}$ and $0.955\mu\text{F}/\text{sec}^{(\alpha-1)}$, when ' α ' was varied from 0.5 to 0.9 in step of 0.1. Also, the ladder element values for $1\text{nF}/\text{sec}^{(\alpha-1)}$ for $\alpha = 0.9$ and 0.8 , have been determined. These FCs were designed for $f_{\min} = 10$ Hz, $f_{\max} = 1$ MHz and phase error of $\Delta\phi = 2^\circ$ (except FCs of $1\text{nF}/\text{sec}^{(\alpha-1)}$ which has $f_{\max} = 100$ kHz). These values are given in Table 2.1 and Table 2.2 respectively.

Table 2.1 Component values for realization of fractional of Fig. 2.6

' α '	$C_f = 0.0955 \mu\text{F}/\text{sec}^{(\alpha-1)}$	
	Resistors	Capacitors
0.9	$R_a = 676.34, R_b = 69.65, R_c = 7.17,$ $R_d = 0.74, R_e = 0.08, R_p = 5890.9$	$C_a = 14.79, C_b = 11.49, C_c = 8.92,$ $C_d = 6.93, C_e = 5.38, C_p = 18.736$
0.8	$R_a = 569.89, R_b = 75.56, R_c = 10.02,$ $R_d = 1.33, R_e = 0.18, R_p = 3728.7$	$C_a = 17.55, C_b = 10.59, C_c = 6.39,$ $C_d = 3.86, C_e = 2.33, C_p = 3.5397$
0.7	$R_a = 662.09, R_b = 113, R_c = 19.29,$ $R_d = 3.29, R_e = 0.56, R_p = 3217.2$	$C_a = 15.1, C_b = 7.08, C_c = 3.32, C_d =$ $1.56, C_e = 0.73, C_p = 0.6429$
0.6	$R_a = 897.74, R_b = 197.24, R_c = 43.34,$ $R_d = 9.52, R_e = 2.09, R_p = 3188.2$	$C_a = 11.14, C_b = 4.06, C_c = 1.48, C_d =$ $0.54, C_e = 0.2, C_p = 0.11211$
0.5	$R_a = 1355.8, R_b = 383.5, R_c = 108.5,$ $R_d = 30.7, R_e = 8.7, R_p = 3437.8$	$C_a = 7.375, C_b = 2.086, C_c = 0.59, C_d =$ $0.167, C_e = 0.047, C_p = 0.018617$
' α '	$C_f = 0.382 \mu\text{F}/\text{sec}^{(\alpha-1)}$	
	Resistors	Capacitors
0.9	$R_a = 168.95, R_b = 17.40, R_c = 1.79,$ $R_d = 0.18, R_e = .019, R_p = 1471.36$	$C_a = 59, C_b = 46, C_c = 35,$ $C_d = 27, C_e = 21, C_p = 75$
0.8	$R_a = 142.47, R_b = 8.89, R_c = 2.5,$ $R_d = 0.33, R_e = 0.04, R_p = 932.16$	$C_a = 70.19, C_b = 42.35, C_c = 25.56,$ $C_d = 15.42, C_e = 9.31, C_p = 14.15$
0.7	$R_a = 165.52, R_b = 28.25, R_c = 4.82,$ $R_d = 0.82, R_e = 0.14, R_p = 804.3$	$C_a = 60.41, C_b = 28.32, C_c = 13.27,$ $C_d = 6.22, C_e = 2.92, C_p = 2.57$
0.6	$R_a = 224.43, R_b = 49.31, R_c = 10.83,$ $R_d = 2.38, R_e = .52, R_p = 797.06$	$C_a = 44.56, C_b = 16.22, C_c = 5.91,$ $C_d = 2.15, C_e = 0.78, C_p = 0.48$
0.5	$R_a = 338.96, R_b = 95.87, R_c = 27.12,$ $R_d = 7.67, R_e = 2.17, R_p = 859.45$	$C_a = 29.5, C_b = 8.34, C_c = 2.36,$ $C_d = 0.67, C_e = 0.19, C_p = .074$

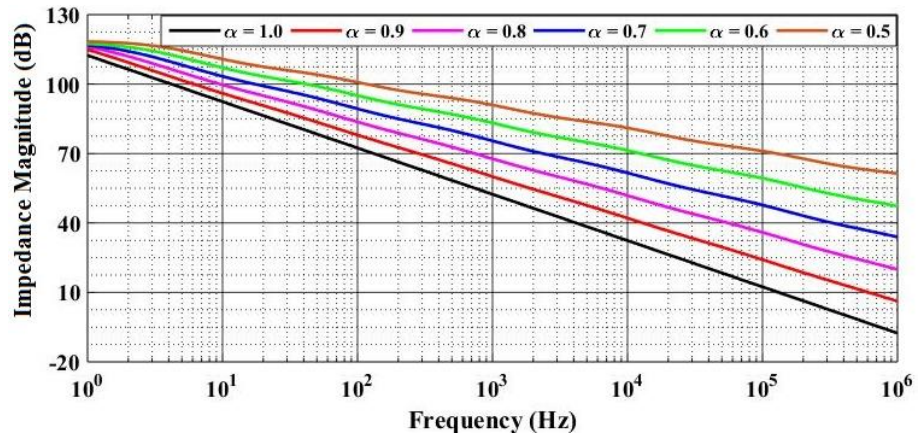
All resistances are in $k\Omega$ and capacitors are in nF

Table.2.2 Component values of FC of value $1\text{nF}/\text{sec}^{(\alpha-1)}$

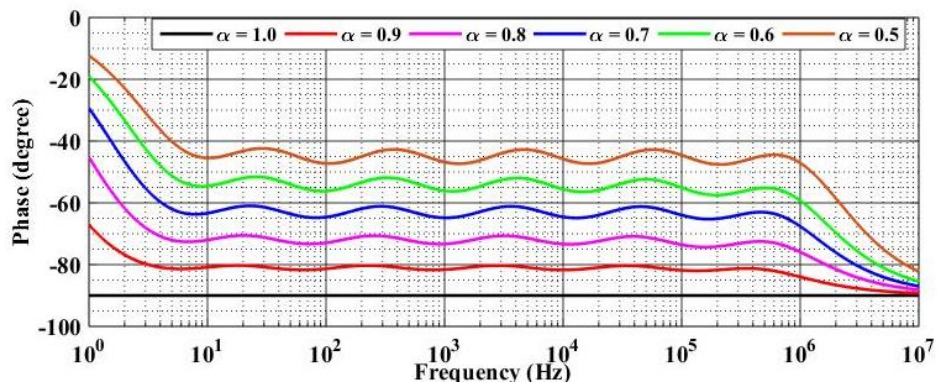
Order	$C_f = 1\text{nF}/\text{s}^{(\alpha-1)}$	
	Resistors	Capacitors
0.9	$R_a = 76.44\text{M}\Omega, R_b = 11.339\text{M}\Omega$ $R_c = 1.682\text{M}\Omega, R_d = 0.25\text{M}\Omega$ $R_e = 0.037\text{M}\Omega, R_p = 436.86\text{M}\Omega$	$C_a = 0.138\text{nF}, C_b = 0.1058\text{nF}$ $C_c = 0.856\text{nF}, C_d = 0.0693\text{nF}$ $C_e = 0.056\text{nF}, C_p = 0.2372\text{nF}$
0.8	$R_a = 64.029\text{M}\Omega, R_b = 11.471\text{M}\Omega$ $R_c = 2.153\text{M}\Omega, R_d = 0.395\text{M}\Omega$ $R_e = 0.072\text{M}\Omega, R_p = 285.14\text{M}\Omega$	$C_a = 0.156\text{nF}, C_b = 0.15058\text{nF}$ $C_c = 0.0669\text{nF}, C_d = 0.0438\text{nF}$ $C_e = 0.0286\text{nF}, C_p = 0.0542\text{nF}$

2.4.2. PSPICE Simulations of Fractional Order Capacitors

Using PSPICE simulations, the designed fractional order capacitor, whose structure is shown in Fig. 2.6, has been tested using passive components as given in Table 2.1 and Table 2.2 respectively. The magnitude and phase responses of fractional order capacitors of values $0.382 \mu\text{F}/\text{sec}^{(\alpha-1)}$, $0.0955 \mu\text{F}/\text{sec}^{(\alpha-1)}$ for different values of α , varying from 0.5 to 0.9 in step of 0.1 and $1\text{nF}/\text{sec}^{(\alpha-1)}$ for different values of α , varying from 0.8 to 0.9 in step of 0.1 along with passive capacitors ($\alpha = 1$) are shown in Fig. 2.7, Fig. 2.8 and Fig. 2.9 respectively.

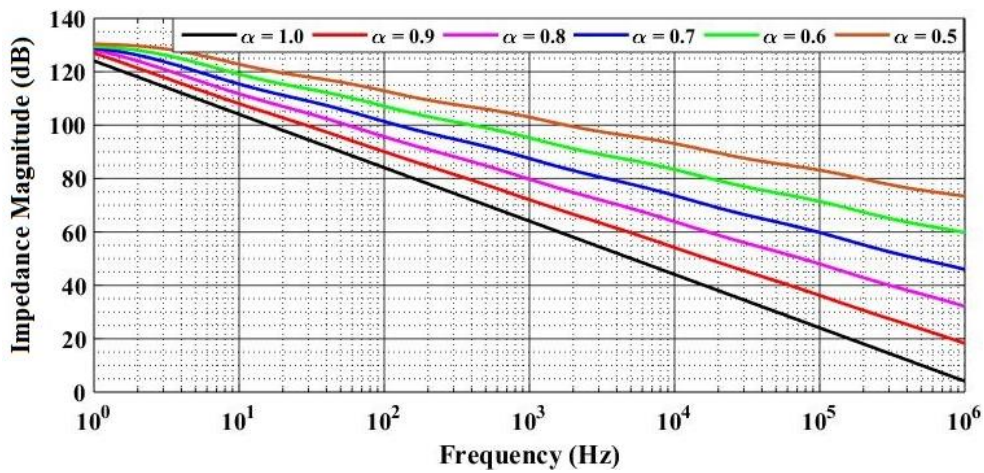


(a)

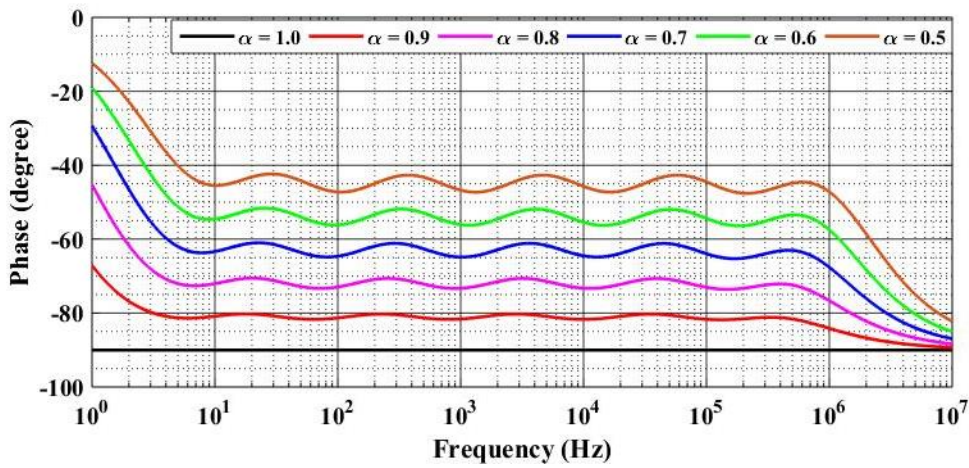


(b)

Figure 2.7 Magnitude and phase responses of fractional order capacitor of value $0.382 \mu\text{F}/\text{sec}^{(\alpha-1)}$ (a) Magnitude response (b) Phase response

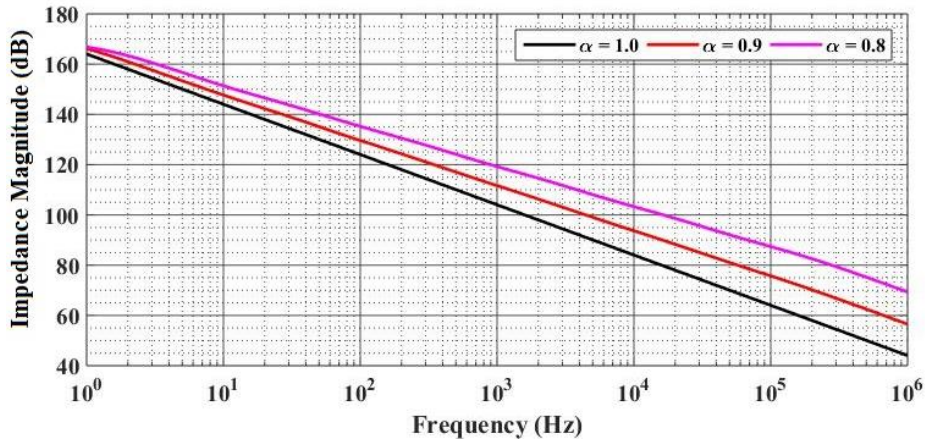


(a)



(b)

Figure 2.8 Magnitude and phase response of fractional order capacitor of value $0.0955 \mu\text{F}/\text{sec}^{(\alpha-1)}$ (a) Magnitude response (b) Phase response



(a)

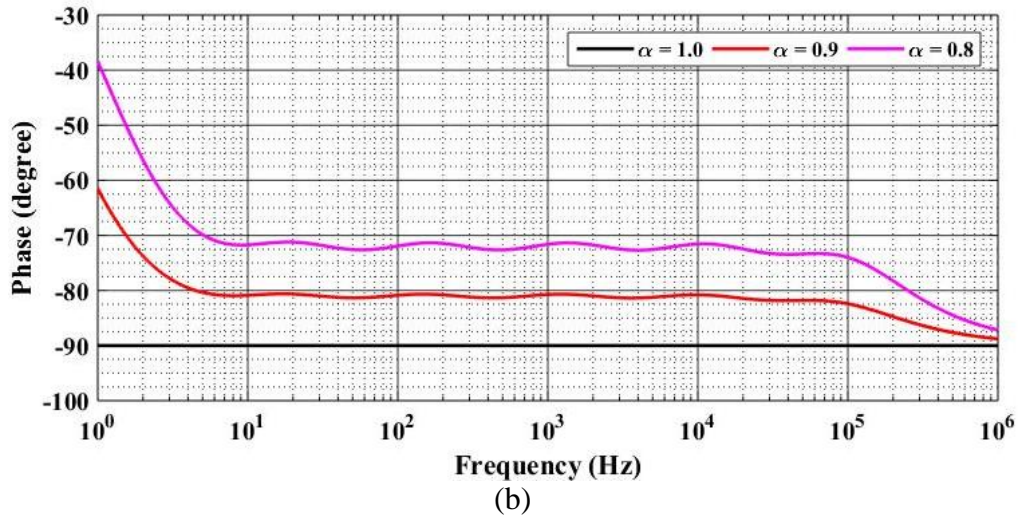


Figure 2.9 Magnitude and phase responses of fractional order capacitor of value $1\text{nF}/\text{sec}^{(\alpha-1)}$ (a) Magnitude response (b) Phase response

From the phase responses of FCs, it is noted that, the phase of fractional order capacitors of value $0.382\mu\text{F}/\text{sec}^{(\alpha-1)}$ and $0.0955\mu\text{F}/\text{sec}^{(\alpha-1)}$ are constant in the frequency range of 10 Hz to 1 MHz, while the phase of fractional order capacitor of value $1\text{nF}/\text{sec}^{(\alpha-1)}$ is constant in the frequency range of 10 Hz to 100 kHz and remains within the tolerance band $\Delta\phi$ as designed. The constant value of phases are approximately equal to $\frac{\alpha\pi}{2}$ or $90^\circ\alpha$, where $0 < \alpha < 1$.

For experimental verification, the fractional capacitor of value $0.382\mu\text{F}/\text{sec}^{(\alpha-1)}$ for $\alpha = 0.7$ was bread-boarded using discrete components whose values are given in Table 2.1. The experimentally obtained magnitude and phase responses of same FC have been demonstrated in Fig. 2.10 using Keysight E4990 impedance analyser.

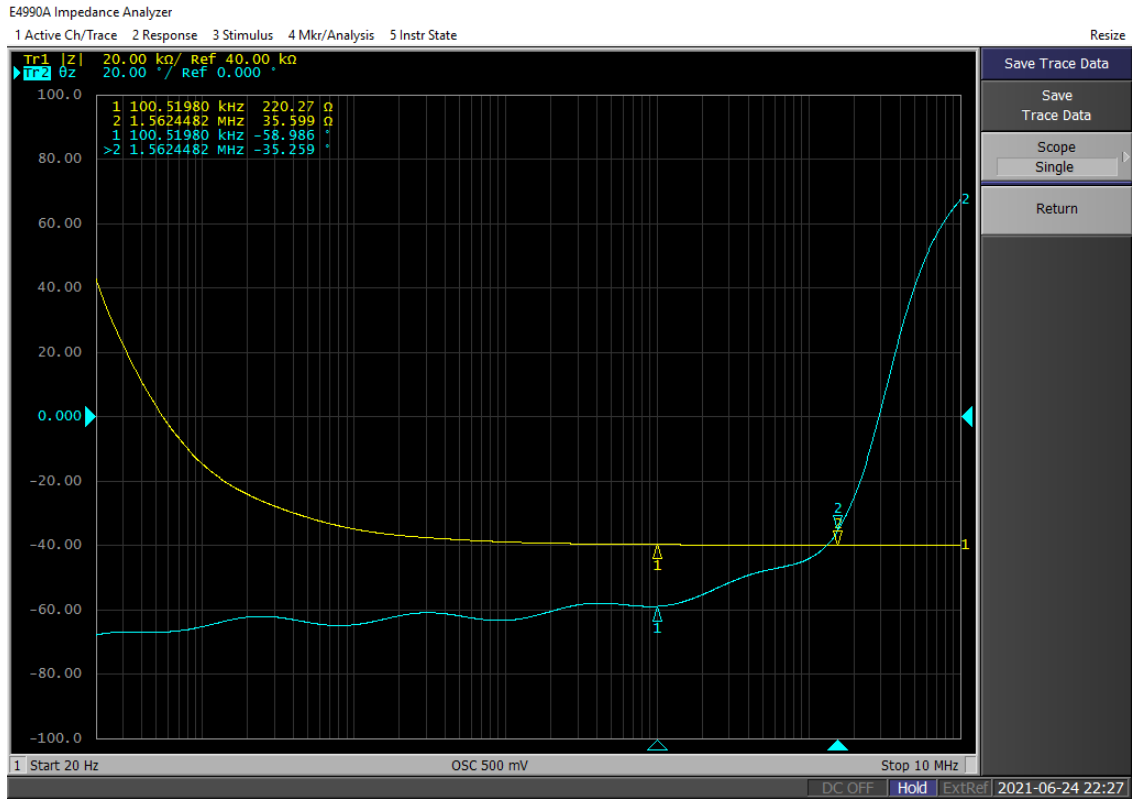


Figure 2.10 Experimentally obtained magnitude and phase responses of fractional order capacitor of order 0.7 and value $0.382 \mu\text{F}/\text{sec}^{(0.7)}$

2.5. Implementation of Fractional Order Capacitor Using Oustaloup, Levron, Mathieu and Nanot Method

This approximation method was proposed by Oustaloup, Leveron, Mathieu and Nanot [20] to approximate the fractional order Laplacian operator s^α in the form of rational function of 's'. In the following, we explain this method with a design example. The method approximates the operator ' s^α ' for non-integer values of the exponent ' α ' by a rational function given below:

$$s^\alpha = c \prod_{k=1}^{k=N} \frac{1+s/\omega_k'}{1+s/\omega_k} \quad (2.21)$$

where N, is the order of the approximation and 'c' is a constant whose value depends upon the maximum frequency up to which the approximation is valid.

$$c = (\omega_{\max})^\alpha \quad (2.22)$$

ω_{\max} = maximum frequency range,

ω_{\min} = minimum frequency range

$$\omega'_k = \omega_{\min} \left(\frac{\omega_{\max}}{\omega_{\min}} \right)^{(2k-1-\alpha)/(2N)} \quad (2.23)$$

$$\omega_k = \omega_{\min} \left(\frac{\omega_{\max}}{\omega_{\min}} \right)^{(2k-1+\alpha)/(2N)} \quad (2.24)$$

The fractional order Laplacian operator s^α , thus is expressed by the following rational function, if the values of α (minimum and maximum frequency) are specified

$$s^\alpha = \frac{N(s)}{D(s)} \quad (2.25)$$

The above rational function, when representing the immittances of a fractional order element (FOE), can be realized either by partial fraction expansion (Foster-I/II forms) or continued fraction expansion (Cauer-I/II forms). An exemplary realization in the Foster form has been shown in Fig 2.11 whose driving point impedance is given by:

$$Z(s) = \frac{1}{s^\alpha C_\alpha} = R_0 + \sum_{n=1}^N \frac{1}{s + \frac{1}{C_n R_n}} \quad (2.26)$$

R_0 = series resistor

R_n, C_n = resistors and capacitors in parallel network

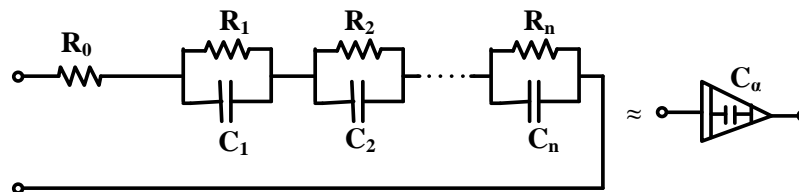


Figure 2.11 Fractional order capacitor network

2.5.1. Design of Fractional Order Capacitor

We have used the above discussed method to design the FC of the value 10^{-8} F/sec^($\alpha-1$) for ω_{\min} and ω_{\max} as specified below, by 8th order ladder, for $\alpha = 0.8$.

Design example: Let $\alpha = 0.8$, $\omega_{\min} = 6.48 \times 10$ rad/sec, $\omega_{\max} = 6.48 \times 10^8$ rad/sec, $C_\alpha = 10^{-8}$ F/sec^($\alpha-1$), $N = 8$, then from equation 2.26, we obtain:

$$Z(s) = \frac{1}{C_\alpha s^\alpha} = \frac{1}{10^{-8} \times s^\alpha}$$

Substituting the Laplacian operator s^α of equation (2.21) in the above equation, we obtain

$$Z(s) = \frac{1}{10^{-8} \times s^\alpha} = \frac{1}{10^{-8} \times c \prod_{k=1}^N \frac{1 + \frac{s}{\omega_k}}{1 + \frac{s}{\omega'_k}}} = \frac{1}{10^{-8} \times c} \prod_{k=1}^N \frac{1 + \frac{s}{\omega_k}}{1 + \frac{s}{\omega'_k}}$$

For the given values of ω_{\min} , ω_{\max} , N and α , using equations (2.22 - 2.24), we obtain $c = 11201082.72$ and the values of ω'_k and ω_k are given in Table 2.3.

Table 2.3 Obtained values of ω'_k and ω_k

Value of k	ω_k (rad/sec)	ω'_k (rad/s)
1	397.36	79.2638
2	2979	594.39
3	22340	4457.3
4	167520	33425
5	1256200	250650
6	9420500	1879600
7	70644000	14095000
8	529750000	105700000

The driving point impedance, thus, turns out to be:

$$Z(s) = \frac{8.928s^8 + 5.457 \times 10^9 s^7 + 3.925 \times 10^{17} s^6 + 3.706 \times 10^{24} s^5 + 4.657 \times 10^{30} s^4 + 7.8 \times 10^{35} s^3 + 1.738 \times 10^{40} s^2 + 5.087 \times 10^{43} s^1 + 1.738 \times 10^{46}}{s^8 + 1.22 \times 10^8 s^7 + 1.75 \times 10^{15} s^6 + 3.298 \times 10^{21} s^5 + 8.268 \times 10^{26} s^4 + 2.763 \times 10^{31} s^3 + 1.229 \times 10^{35} s^2 + 7.173 \times 10^{37} s^1 + 1.738 \times 10^{46} + 4.927 \times 10^{39}}$$

The values of resistors and capacitors of the ladder of FC of value 10^{-8} F/sec^($\alpha-1$) for order $\alpha = 0.8$ have been found (employing Foster-I method on Z(s)) and are given in Table 2.4.

Table 2.4 Component values of FC for $\alpha = 0.8$

Order	$C_f = 10\text{nF/s}^{(\alpha-1)}$			
	Resistors		Capacitors	
0.8	$R_0 = 8.957\Omega$	$R_1 = 12.89\Omega$	$C_1 = 0.757\text{nF}$	$C_2 = 1.0009\text{nF}$
	$R_2 = 72.56\Omega$	$R_3 = 368.96\Omega$	$C_3 = 1.48\text{nF}$	$C_4 = 2.22\text{nF}$
	$R_4 = 1.85\text{K}\Omega$	$R_5 = 9.3\text{K}\Omega$	$C_5 = 3.319\text{nF}$	$C_6 = 4.918\text{nF}$
	$R_6 = 47.1\text{K}\Omega$	$R_7 = 254.4\text{K}\Omega$	$C_7 = 6.82\text{nF}$	$C_8 = 3.9\text{nF}$
	$R_8 = 3.33\text{M}\Omega$			

Similarly, we have calculated the values of resistors and capacitors of the ladder of FC for the value of 10^{-8} F/sec^($\alpha-1$) and 0.9, and presented them in Table 2.5.

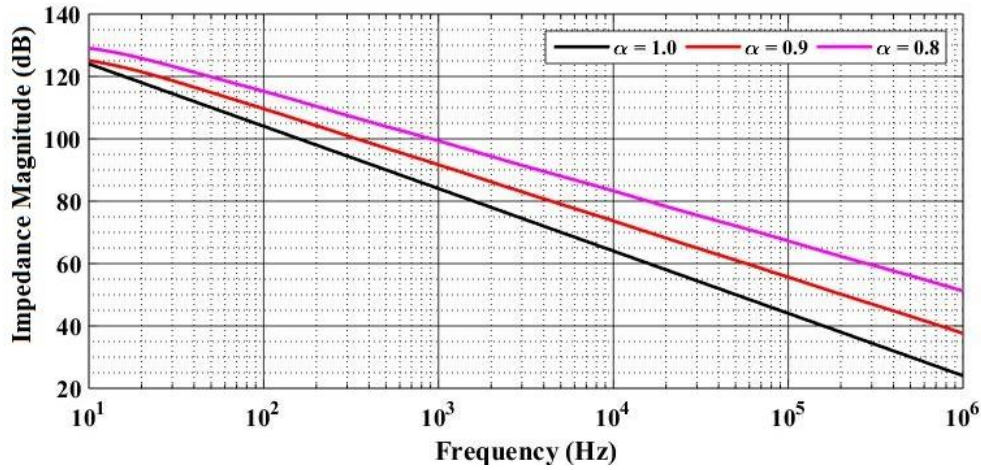
Table 2.5 Component values of FC for $\alpha = 0.9$

Order	$C_f = 10\text{nF/s}^{(\alpha-1)}$			
	Resistors		Capacitors	
0.9	$R_0 = 1.20\Omega$	$R_1 = 1.116\Omega$	$C_1 = 9.25\text{nF}$	$C_2 = 10.03\text{nF}$
	$R_2 = 8.07\Omega$	$R_3 = 50.23\Omega$	$C_3 = 12.08\text{nF}$	$C_4 = 14.75\text{nF}$
	$R_4 = 308.66\Omega$	$R_5 = 1.895\text{K}\Omega$	$C_5 = 18.00\text{nF}$	$C_6 = 21.75\text{nF}$
	$R_6 = 11.76\text{K}\Omega$	$R_7 = 79.52\text{K}\Omega$	$C_7 = 24.14\text{nF}$	$C_8 = 6.21\text{nF}$
	$R_8 = 2.315\text{M}\Omega$			

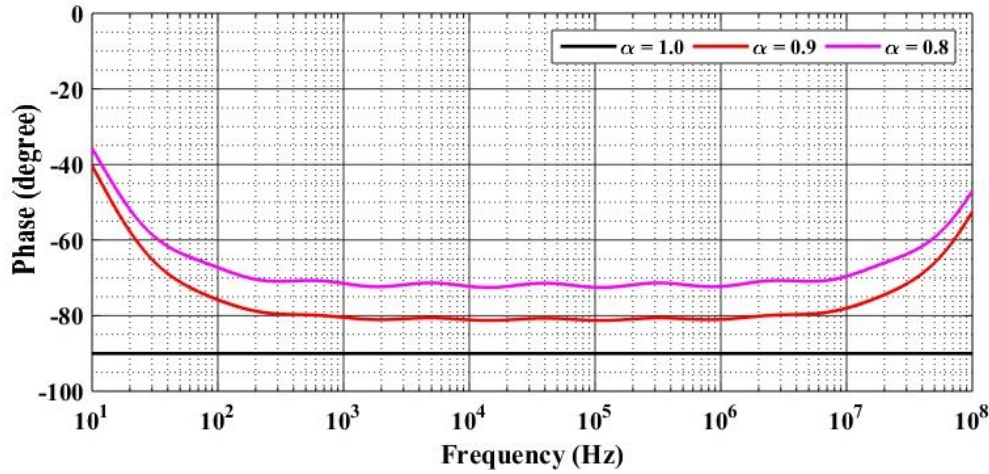
2.5.2. PSPICE Simulations of Fractional Order Capacitors

To validate the functionality of the designed FC of Fig. 2.11 (for $\alpha = 0.8, 0.9$ and 1), PSPICE simulations have been carried out. The passive component values used in the simulation are taken from Table 2.3 and Table 2.4.

The magnitude and phase responses of FC thus obtained are displayed in Fig. 2.12.



(a)



(b)

Figure. 2.12 Magnitude and phase response of fractional order capacitor of value $10\text{nF}/\text{sec}^{(\alpha-1)}$ (a) Magnitude response (b) Phase response

From the phase responses of FCs, it is observed that, the phase of fractional order capacitor of value $10\text{nF}/\text{sec}^{(\alpha-1)}$ in the frequency range of 100 Hz to 10 MHz remains approximately equal to $\frac{\alpha\pi}{2}$ or $90^\circ\alpha$.

2.6. Conclusions

In this chapter, we have presented some of the fundamental concepts of fractional order calculus and their utilization in the design of fractional order elements. A review of some of the important research works dealing with the realizations of the fractional order elements in general and fractional order capacitors in particular, using single as

well as the multi component-based realizations have also been presented. We have also discussed the details of the methodology and design of the fractional order capacitors, which we have used for the realization of various analog circuits in this thesis. Valsa, Dvorak and Friedl and Oustaloup, Leveron, Mathieu and Nanot approximation methods of fractional order capacitors have been used for determining the component values of R-C ladder networks. Fractional order capacitors of values $0.382\mu\text{F}/\text{sec}^{(\alpha-1)}$, $0.0955\mu\text{F}/\text{sec}^{(\alpha-1)}$ and $1\text{nF}/\text{sec}^{(\alpha-1)}$ for different values of α are designed using the method proposed by Valsa, Dvorak and Friedl while, fractional order capacitors of value $10\text{nF}/\text{sec}^{(\alpha-1)}$ for $\alpha = 0.9$ and $\alpha = 0.8$ are designed using Oustaloup, Leveron, Mathieu and Nanot's method. PSPICE simulation results showing the magnitude and phase responses of the designed fractional order capacitors for different values of α have been presented. The magnitude and phase responses of a fractional order capacitor of value $0.382\mu\text{F}/\text{sec}^{(\alpha-1)}$ for $\alpha = 0.7$) has also been tested experimentally using KEYSIGHT E4990A impedance analyser.

References

- [1] K. Oldham and J. Spanier, "The Fractional Calculus: Theory and Applications of Differentiation and Integration to Arbitrary Order", New York: Academic Press, 1974.
- [2] K. Miller and B. Ross, "An Introduction to the Fractional Calculus and Fractional Differential Equations," New York: Wiley, 1993.
- [3] S. Das, "Functional Fractional Calculus," Springer, Berlin Heidelberg, 2011, DOI: <http://doi.org/10.1007/987-3-642-20545-3>
- [4] I. Petráš I, "Fractional-Order Nonlinear Systems", Nonlinear Physical Science. Springer, Berlin, Heidelberg. https://doi.org/10.1007/978-3-642-18101-6_3.
- [5] Tsirimokou, C. Psychalinos and A. Elwakil, "Design of CMOS Analog Integrated Fractional-Order Circuits: Applications in Medicine and Biology, 2017, DOI:10.1007/978-3-319-55633-8.
- [6] Z. M. Shah, M. Y. Kathjoo, F. A. Khanday, K. Biswas and C. Psychalinos, "A survey of single and multi-component Fractional-Order Elements (FOEs) and their applications," Microelectron. J., vol. 84, pp. 9-25, 2019.

- [7] A. Agambayev, M. Farhat, S.P. Patole, A.H. Hassan, H. Bagci and K.N. Salama, "An ultra-broadband single-component fractional-order capacitor using MoS₂-ferroelectric polymer composite," *Appl. Phys. Lett.*, vol. 113, 093505, 2018.
- [8] M. S. Krishna, S. Das, K. Biswas and B. Goswami, "Fabrication of a Fractional Order Capacitor with Desired Specifications: A Study on Process Identification and Characterization," *IEEE Trans. Electron Devices*, vol. 58, pp. 4067-4073, 2011.
- [9] G.W. Bohannon, "Application of Fractional Calculus to Polarization Dynamics in Solid Dielectric Materials," Montana State University Bozeman, Montana, November 2000. Ph.D. Thesis. (Accessed 4 April 2018).
- [10] R. Caponetto, S. Graziani, F. L. Pappalardo and F. Sapuppo, "Experimental characterization of ionic polymer metal composite as a novel fractional-order element," *Adv. Math. Phys.*, 2013, pp. 1-10, 2013.
- [11] A. Buscarino, R. Caponetto, G. Di Pasquale, L. Fortuna, S. Graziani, and A. Pollicino, "Carbon Black based capacitive Fractional-order Element towards a new electronic device," *AEU-Int. J. Electr. Commun.*, vol. 84, pp. 307–312, 2018.
- [12] M. El shurafa, N. Almadhoun, K. Salama and H. Alshareef, "Microscale electrostatic fractional-order capacitors using reduced graphene oxide percolated polymer composites," *Appl. Phys. Lett.*, vol. 102, no. 23, pp. 232901–232904, 2013.
- [13] A. Adhikary, M. Khanra, S. Sen and K. Biswas, "Realization of a Carbon Nanotube Based Electrochemical Fractor," In 2015 IEEE International Symposium on Circuits and Systems (ISCAS), pp. 2329-2332, 2015, doi: 978-1-4799-8391-9/15/\$31.00.
- [14] D. A. John, S. Banerjee, G. W. Bohannon and K. Biswas, "Solid-state fractional-order capacitor using MWCNT-epoxy nanocomposite," *Appl. Phys. Lett.*, vol. 110, 163504, 2017.
- [15] A. Agambayev, S. Patole, H. Bagci and K.N. Salama, "Tunable fractional-order capacitor using layered ferroelectric polymers," *AIP Adv.* 7, 095202, 2017.
- [16] G. E. Carlson and C. A. Halijak, "Approximation of fractional capacitors $(1/s)^{(1/n)}$ by a regular Newton process," *IEEE Trans. Circuit Theo.*, vol. 11, no. 2, pp. 210–213, Jun.1964.
- [17] S. C. Dutta Roy, "On the realization of a constant-argument immittance or fractional operator," *IEEE Trans. Circ. Syst.*, vol. CAS-14, no. 3, pp. 264–274, Sep. 1967.
- [18] A. Charef, H. H. Sun, Y. Y. Tsao, and B. Onaral, "Fractal system as represented by singularity function," *IEEE Trans. Automatic Control*, vol. 37, no. 9, pp. 1465-1470, 1992.
- [19] M. Nakagawa and K. Sorimachi, "Basic characteristic of fractance devices," *IEICE Trans. Fund.*, vol. E75-A, no. 12, pp. 1814–1819, Dec. 1992.

- [20] K. Matsuda, and F. Hironori, " H_∞ optimized wave-absorbing control-Analytical and experimental results," *J. Guidance, Control, and Dynamics*, vol. 16, no. 6, pp. 1146-1153, 1993.
- [21] A. Oustaloup, F. Levron, B. Mathieu and F. M. Nanot, "Frequency-band complex noninteger differentiator: characterization and synthesis," *IEEE Trans. Circ. Syst. I: Fundamental Theory and Applications*, vol. 47 no. 1, pp. 25-39, 2000.
- [22] M. Sugi, Y. Hirano, Y.F. Miura and K. Saito, "Frequency behavior of self-similar ladder circuits," *Colloids Surfaces A: Physicochem. Eng. Aspect.*, vol. 198–200, pp. 683–688, 2002.
- [23] B.T. Krishna and K.V.V.S. Reddy, "Active and Passive Realization of Fractance Device of Order $1/2$," *Active and Passive Electronic Components*, vol. 2008, no. 369421, 2008.
- [24] J. Valsa, P. Dvorak and M. Friedl, "Network model of the CPE," *Radioengineering*, vol. 20, no. 3, pp. 619–626, 2011.
- [25] R. El-Khazali, "On the biquadratic approximation of fractional-order Laplacian operators," *Analog Integ. Circ. Signal Process.*, vol. 82, no. 3, pp. 503-517, 2015.
- [26] K. S. Cole and R. H. Cole, "Dissipation and absorption in dielectrics", *J. Chemical Physics*, vol. 9, pp. 341-351, 1941.
- [27] G. Tsirimokou, C. Psychalinos, and A.S Elwakil, "Emulation of a constant phase element using operational transconductance amplifiers," *Analog Integ. Circ. Signal Process.*, vol. 85, pp. 413–423, 2015
- [28] I. Dimeas, G. Tsirimokou, C. Psychalinos and A. Elwakil, "Realization of fractional-order capacitor and inductor emulators using current feedback operational amplifiers," *Proc. Int. Symp. Nonlinear Theo. its Appl. (NOLTA 2015)*, Hong Kong, China, pp. 237-240, Dec. 2015.
- [29] P. Bertias, C. Psychalinos, A. S. Elwakil and B. Maundy, "Current-mode capacitorless integrators and differentiators for implementing emulators of fractional-order elements," *AEU-Int. J. Electr. Commun.*, vol. 80, pp. 94-103, 2017

Chapter 3

Current Feedback Operational Amplifier Based Fractional Order Filters

In the previous chapter, an introductory idea about the fractional calculus and its utilization in the design of fractance devices are described. In this chapter, we describe the basic concepts related with fractional order filters and implementation of fractional order analog active filters (FOFs) using fractance device(s). Subsequently, we have proposed three structures of single CFOA-based FOFs. Two of the proposed FOFs operate in voltage mode while the third structure operates in current mode.

3.1. Fractional Order Filters

The fractional order filters (FOFs) have been developed as a new research area during the last two decades. The first systematic paper on generalization of first order filters into fractional order domain was published in 2008 [1] in which a fractional order filter using a single fractance device was introduced by Radwan, Soliman and Elwakil. Subsequently, this work was extended to cover circuits with two identical fractance devices [2], wherein, design and simulation of Sallen-Key and Kerwin-Huelsman-Newcomb (KHN) type bi-quad filter topologies was presented in fraction order domain along with the experimental results of KHN bi-quad filters using real fractional order capacitors of order 0.5. After that, several fractional order filters [2-87] have been proposed in open literature using either fractance devices (FC/FI) or rational approximation of fractional order filter's transfer function. Most of the fractional order

filters have been realized by replacing the conventional capacitor(s) in an existing integer order filter, few fractional order filters have been designed ab-initio in fractional order domain. Various active building blocks such as op-amps [2-17, 19-29, 85-86], current feedback operational amplifiers (CFOAs) [30-32], current conveyors (CCs) [33-40], current differencing buffered amplifiers (CDBAs) [41], operational trans-resistance amplifiers (OTRAs) [42], operational trans-conductance amplifiers (OTAs) [43-59, 83] and other active building blocks [60-82, 84, 87] have been used in the design and implementation of fractional order active filters with different characteristic and properties.

Since this thesis deals with fractional order filters, in the following, we present a quantitative overview of some of the fundamental concepts related with fractional order analog filters.

3.2. Methods for Realization of Fractional Order Filters

Generally, two methods have been used for the implementation of analog fractional order filters. In the first method, FOF is realized by replacing capacitor(s) of an existing integer order filter with fractional order capacitors thereby generalizing the design of an integer order filter, while in the second method, transfer function of a prototype fractional order filter is converted into a higher order integer transfer function, by replacing the fractional order Laplacian operator s^α with its equivalent second order or higher order rational approximation. The resulting integer order transfer function can then be realized using some active building block, passive resistors and capacitors. The frequency response of the filter thus realized, approximates the frequency response of

prototype FOF in the given frequency band. In this thesis, fractional order filters are realized using the first approach.

A fractional order filter can be realized using a single fractance device or more than one fractance devices. In the following, we present the fundamental concepts and necessary analytical framework, supported with MATLAB simulations using which fractional order analog filters are realized with single fractance device and two fractance devices.

3.2.1. Fractional Order Filters Using Single Fractance Device

A fractional order filter may be realized with single fractance device, if the order of this filter lies between 0 to 1 [1]. The generalized transfer function [1] of FOF can be represented as:

$$T(s) = \frac{as^\beta + b}{s^\alpha + c} \quad (3.1)$$

where a, b and c are constants. The cut-off frequency (pole frequency) ω_0 of the filter is defined as $\omega_0 = (c)^{\frac{1}{\alpha}}$

From equation (3.1), four different responses of fractional order filters viz. fractional order low pass (FOLP), fractional order band pass (FOBP), fractional order high pass (FOHP) and fractional order all pass (FOAP) can be derived by appropriate selection(s) the coefficients (a, b and c) as given below.

3.2.1.1. Fractional Order Low Pass Filter

The transfer function of a FOLP filter [1] can be derived from equation (3.1), if we select the coefficient a = 0 as:

$$T(s)_{\text{FOLP}} = \frac{b}{s^\alpha + c} \quad (3.2)$$

The magnitude and phase of the above transfer function can be represented as:

$$|T(j\omega)_{\text{FOLP}}| = \frac{b}{\sqrt{\omega^{2\alpha} + 2c\omega^\alpha \cos\left(\frac{\alpha\pi}{2}\right) + c^2}} \quad (3.3a)$$

$$\angle T(j\omega)_{\text{FOLP}} = -\tan^{-1}\left(\frac{\omega^\alpha \sin\left(\frac{\alpha\pi}{2}\right)}{\omega^\alpha \cos\left(\frac{\alpha\pi}{2}\right) + c}\right) \quad (3.3b)$$

The important critical frequencies viz cut-off frequency ω_0 , maxima frequency ω_m (at which the peak, if, any of the magnitude response occurs), right phase frequency ω_{rp} (the frequency at which the phase of the FOLP becomes equal to $\frac{\pi}{2}$ radian) and half power frequency ω_h (the frequency at which the magnitude of FOLP become $\frac{1}{\sqrt{2}}$ times of the DC gain of FOLP) can be derived from equation (3.3) as:

$$\omega_0 = (c)^{\frac{1}{\alpha}} \quad (3.4a)$$

$$\omega_m = \left(-c \cos\left(\frac{\alpha\pi}{2}\right)\right)^{\frac{1}{\alpha}} \quad (3.4b)$$

$$\omega_{rp} = \left(-c \sec\left(\frac{\alpha\pi}{2}\right)\right)^{\frac{1}{\alpha}} \quad (3.4c)$$

$$\omega_h = \left(-c \left(\sqrt{1 + \cos^2\left(\frac{\alpha\pi}{2}\right)} - \cos\left(\frac{\alpha\pi}{2}\right)\right)\right)^{\frac{1}{\alpha}} \quad (3.4d)$$

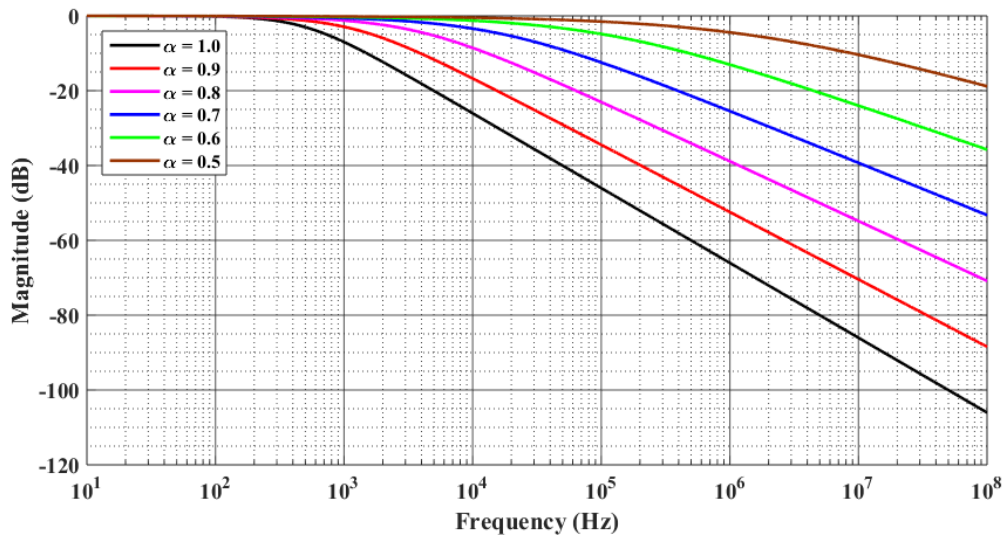
From equation (3.4b), it may be noted that the magnitude response will have a peak iff the value of α is greater than 1. Similarly from equation (3.4c), it is observed that the

phase response will have a value of $\frac{\pi}{2}$ iff the value of α is greater than 1. The magnitude and phase of FOLP filter for different values of ω are given in Table 3.1

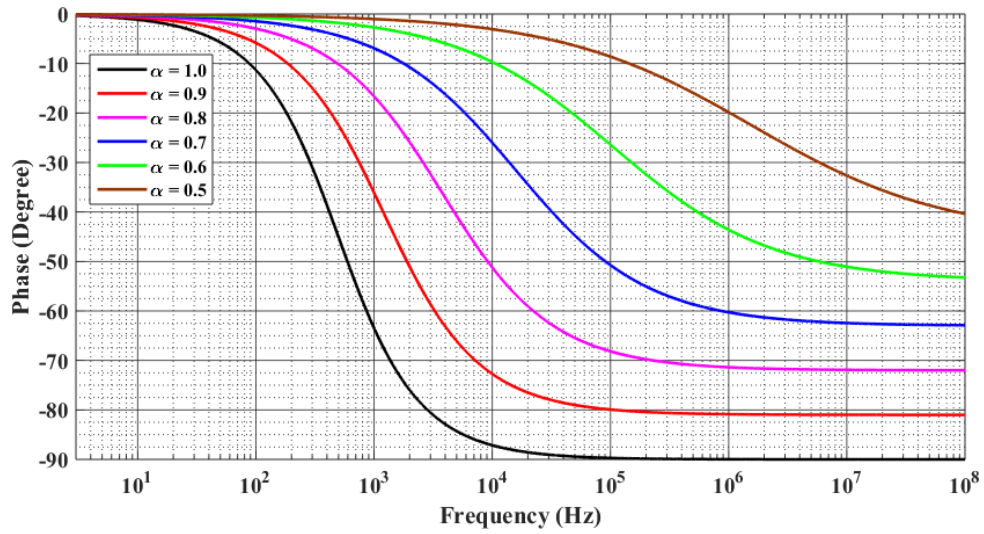
Table 3.1 The values of magnitude and phase of FOLP filter for different values of ω

The values of ω	$ T(j\omega)_{\text{FOLP}} $	$\angle T(j\omega)_{\text{FOLP}}$
0	$\frac{b}{c}$	0
ω_0	$\frac{b}{2c \cos\left(\frac{\alpha\pi}{2}\right)}$	$-\frac{\alpha\pi}{4}$
∞	0	$\frac{-\alpha\pi}{2}$
ω_m	$\frac{b}{c \sin\left(\frac{\alpha\pi}{2}\right)}$	$\frac{(1-\alpha)\pi}{2}$
ω_h	$\frac{1}{\sqrt{2}} \frac{b}{c}$	$\tan^{-1}\left(\frac{\sin\left(\frac{\alpha\pi}{2}\right)}{2\cos\left(\frac{\alpha\pi}{2}\right) + \sqrt{1 + \cos^2\left(\frac{\alpha\pi}{2}\right)}}\right)$
ω_{rp}	$\frac{b}{c \cot\left(\frac{\alpha\pi}{2}\right)}$	$\frac{\pi}{2}$

A FOLP filter was designed using equation (3.3) for a cut-off frequency of 500 Hz (for $\alpha = 1$) and DC gain equal to 1 by choosing $b = c = 2\pi \times 500 = 3140$. MATLAB simulations were performed for different values of α to validate the workability of the FOLF plotted using MATALB for different valued of α . Fig. 3.1 shows the magnitude and the phase responses of the designed FOLP.



(a)



(b)

Figure 3.1 Magnitude and phase responses of FOLP (a) Magnitude response (b) Phase response

The slope of the magnitude response and half power frequency as obtained from Fig. 3.1 are given in Table 3.2, from where it may be noted that the slope of the magnitude characteristics and the half power frequency may be varied by the values of α . In contrast, for an integer order filter, the slope and the half power frequency can not be varied.

Table 3.2 Parameters of FOLP filter

Order of FOLP	Parameters	
	Half power frequency (Hz)	Attenuation (dB/decade)
$\alpha = 1.0$	500	20
$\alpha = 0.9$	1027	18
$\alpha = 0.8$	2552	16
$\alpha = 0.7$	8390	14
$\alpha = 0.6$	41980	12
$\alpha = 0.5$	416900	10

3.2.1.2. Fractional Order High Pass Filter

If we take $b = 0$ and $\beta = \alpha$ in equation (3.1), The transfer function of the FOHP filter can be obtained as:

$$T(s)_{\text{FOHP}} = \frac{as^\alpha}{s^\alpha + c} \quad (3.5)$$

where 'a' and 'c' are constants.

The magnitude and phase of above transfer function can be expressed as:

$$|T(j\omega)_{\text{FOHP}}| = \frac{a\omega^\alpha}{\sqrt{\omega^{2\alpha} + 2c\omega^\alpha \cos\left(\frac{\alpha\pi}{2}\right) + c^2}} \quad (3.6a)$$

$$\angle T(j\omega)_{\text{FOHP}} = \frac{\alpha\pi}{2} - \tan^{-1}\left(\frac{\omega^\alpha \sin\left(\frac{\alpha\pi}{2}\right)}{\omega^\alpha \cos\left(\frac{\alpha\pi}{2}\right) + c}\right) \quad (3.6b)$$

The important critical frequencies viz cut-off frequency (ω_0), maxima frequency (ω_m), right phase frequency (ω_{rp}) and half power frequency (ω_h)of FOHP filter [1] can be derived from equation (3.6) as:

$$\omega_0 = (c)^{\frac{1}{\alpha}} \quad (3.7a)$$

$$\omega_m = \left(-c \sec\left(\frac{\alpha\pi}{2}\right)\right)^{\frac{1}{\alpha}} \quad (3.7b)$$

$$\omega_{rp} = \left(-c \cos\left(\frac{\alpha\pi}{2}\right)\right)^{\frac{1}{\alpha}} \quad (3.7c)$$

$$\omega_h = \left(-c \left(\sqrt{1 + \cos^2\left(\frac{\alpha\pi}{2}\right)} + \cos\left(\frac{\alpha\pi}{2}\right)\right)\right)^{\frac{1}{\alpha}} \quad (3.7d)$$

From equation (3.7b), it may be observed that the magnitude response will have a peak iff, the value of α is greater than 1. Similarly from equation (3.7c) it is observed that the phase response will have a value of $\frac{\pi}{2}$ iff, the value of α is greater than 1.

The values of magnitude and phase of the FOHP filter for different values of ω are given in Table 3.3

Table 3.3 The values of magnitude and phase of FOHP filter for different values of ω		
ω	$ T(j\omega)_{\text{FOHP}} $	$\angle T(j\omega)_{\text{FOHP}}$
0	0	$\frac{\alpha\pi}{2}$
ω_0	$\frac{1}{2 \cos\left(\frac{\alpha\pi}{4}\right)}$	$\frac{3\alpha\pi}{4}$
∞	a	0
ω_m	$\frac{a}{1 + \cos\left(\frac{\alpha\pi}{2}\right)}$	$\frac{(\alpha - 1)\pi}{2}$
ω_h	$\frac{a}{\sqrt{2}}$	$\frac{\alpha\pi}{2} - \tan^{-1}\left(\frac{\sin\left(\frac{\alpha\pi}{2}\right) \cos\left(\frac{\alpha\pi}{2}\right) + \sin\left(\frac{\alpha\pi}{2}\right) \sqrt{1 + \cos^2\left(\frac{\alpha\pi}{2}\right)}}{\cos^2\left(\frac{\alpha\pi}{2}\right) + \cos\left(\frac{\alpha\pi}{2}\right) \sqrt{1 + \cos^2\left(\frac{\alpha\pi}{2}\right)} + 1}\right)$
ω_{rp}	$-a \cot\left(\frac{\alpha\pi}{2}\right)$	$\frac{\pi}{2}$

MATLAB simulations have been carried out for the magnitude and phase responses of a FOHP filter designed to have a high frequency gain of 1 and cut-off frequency of $(2\pi \times 500)$ rad/s (for $\alpha = 1$) when α is varied from 0.1 to 0.5 in step of 0.1. The frequency response plots are displayed in Fig. 3.2.

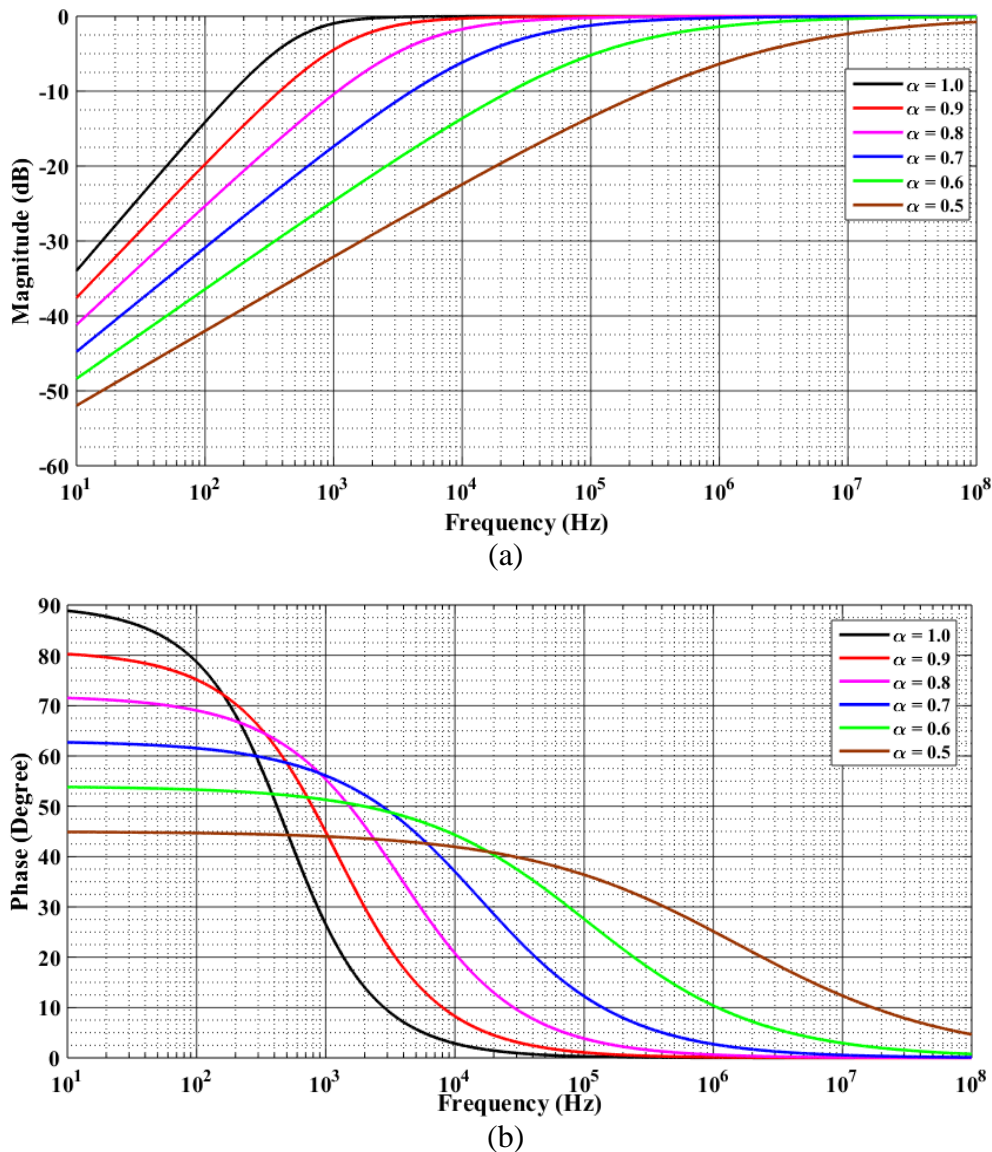


Figure 3.2 Magnitude and phase responses of FOHP (a) Magnitude response (b) Phase response

The half power frequency and stop band attenuation of FOHP for different values of α have been calculated down from Fig. 3.2 and tabulated in Table 3.4. From Fig.3.2 and Table 3.4, it may be noted that, both half power frequency and stop band attenuation may

be varied by varying the values of α . This type of variation is not possible in its integer order counterpart.

Table 3.4 Parameters of FOHP filter

Order of FOHP	Parameters	
	ω_h (Hz)	Attenuation (dB/decade)
$\alpha = 1.0$	500	20
$\alpha = 0.9$	1452	18
$\alpha = 0.8$	5471	16
$\alpha = 0.7$	29.58k	14
$\alpha = 0.6$	272.9k	12
$\alpha = 0.5$	5.879M	10

3.2.1.3. Fractional Order Band Pass Filter

The expression for the transfer function of a FOBP filter [1] can be obtained from equation (3.1) by selecting $b = 0$ and $\alpha > \beta$ as:

$$T(s)_{\text{FOBP}} = \frac{as^\beta}{s^\alpha + c} \quad (3.8)$$

The magnitude and phase of transfer function as given in equation (3.8), have been derived as:

$$|T(j\omega)_{\text{FOBP}}| = \frac{a\omega^\beta}{\sqrt{\omega^{2\alpha} + 2c\omega^\alpha \cos\left(\frac{\alpha\pi}{2}\right) + c^2}} \quad (3.9a)$$

$$\angle T(j\omega)_{\text{FOBP}} = \frac{\beta\pi}{2} - \tan^{-1}\left(\frac{\omega^\alpha \sin\left(\frac{\alpha\pi}{2}\right)}{\omega^\alpha \cos\left(\frac{\alpha\pi}{2}\right) + c}\right) \quad (3.9b)$$

The magnitude and phase of FOBP filter at $\omega = 0$, $\omega = \omega_0$ and $\omega = \infty$ as obtained from equation (3.9) are given in Table 3.5

Table 3.5 The values of magnitude and phase of FOBP filter for different values of ω

ω	$ T(j\omega)_{\text{FOBP}} $	$\angle T(j\omega)_{\text{FOBP}}$
0	0	$\frac{\beta\pi}{2}$
ω_0	$\frac{a(c)^\beta}{2c \cos\left(\frac{\alpha\pi}{4}\right)}$	$\frac{\beta\pi}{2} - \frac{\alpha\pi}{4}$
∞	$a\omega^{\beta-\alpha}$	$\frac{(\beta - \alpha)\pi}{2}$

It may be noted from the above table that unless $\beta < \alpha$, the transfer function given in equation (3.8) can not represent a band pass filter as magnitude will become infinite at $\omega = \infty$ for $\beta > \alpha$. The peak frequency (ω_p) of FOBP can be calculated from the equation $\frac{d}{d\omega}|T(j\omega)_{\text{FOBP}}|_{\omega=\omega_p} = 0$ and expressed as:

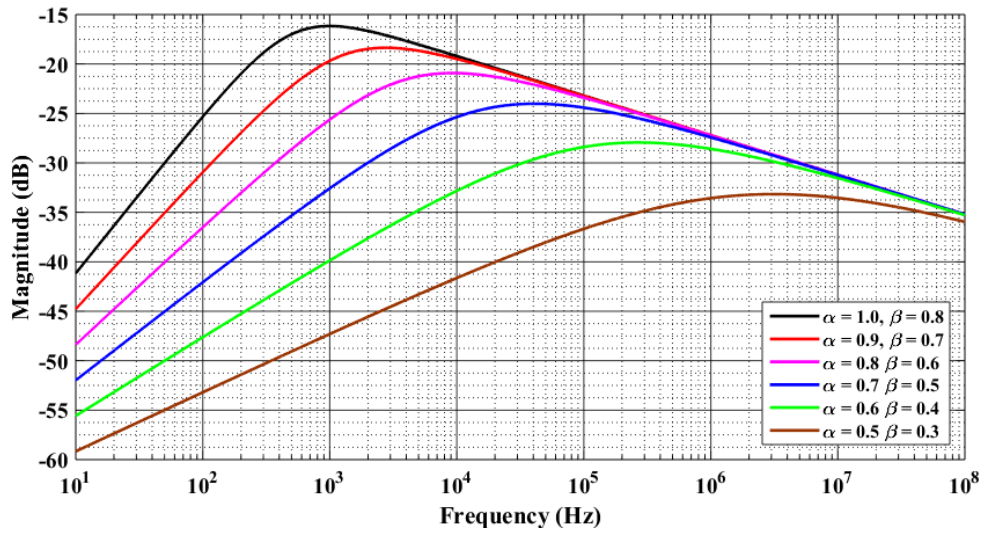
$$\omega_p = \left(c \frac{\cos\left(\frac{\alpha\pi}{2}\right) \left[(2\beta - \alpha) + \sqrt{\alpha^2 + 4\beta(\alpha - \beta)\tan^2\left(\frac{\alpha\pi}{2}\right)} \right]}{2(\alpha - \beta)} \right)^{\frac{1}{\alpha}} \quad (3.10)$$

When $\alpha = 1$, the expression for ω_p , derived from equation (3.10) can be expressed as

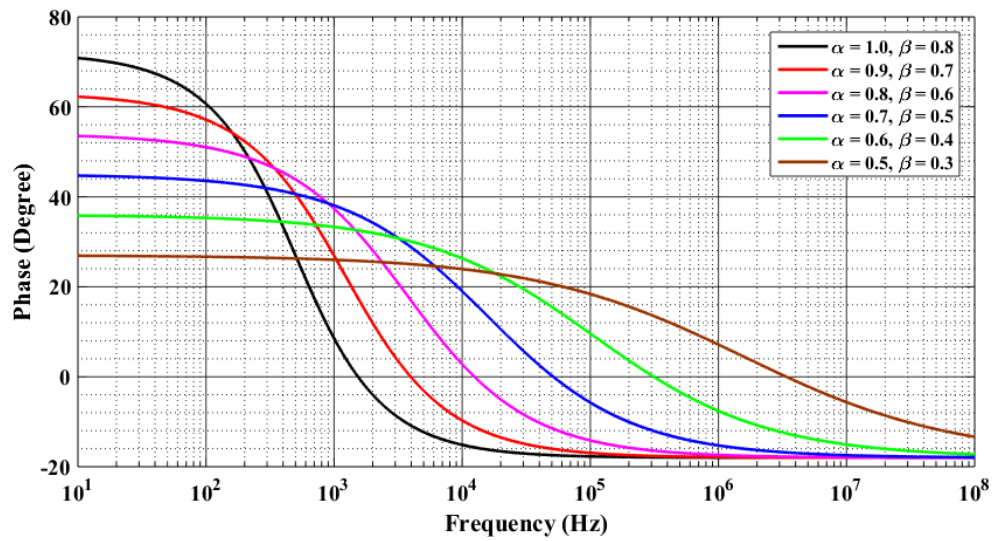
$$\omega_p = c \sqrt{\frac{\beta}{1 - \beta}} \quad (3.11)$$

If $\alpha = 2\beta$, then $\omega_p = \omega_0 = (c)^\frac{1}{\alpha}$ rad/s and frequency in Hz i.e $f_p = (0.159 \times \omega_p)$ Hz

A fractional order band pass filter was designed to have a peak frequency of 2000π rad/s for $\alpha = 1.0$ and $\beta = 0.8$, selecting $c = 3140$ and $a = 1$. Using MATLAB simulations, the magnitude and phase responses for different values of α (from 1.0 to 0.5 in step of 0.1) and β (from 0.8 to 0.3 in step of 0.1) have been plotted and shown in Fig. 3.3.



(a)



(b)

Figure 3.3 Magnitude and phase responses of FOBP (a) Magnitude response (b) Phase response

From Fig 3.3 (a), the peak frequency, attenuation gradients at lower frequency (equal to 6β dB/octave) and higher frequency (equal to $-6(\alpha-\beta)$ dB/octave) [88] for different values of α and β have been noted down and given in Table 3.6.

Table 3.6 Filter parameters of FOBP filter

Values of α and β of FOBP	Parameters		
	f_p (Hz)	Attenuation (dB/octave) at Low Frequency	Attenuation (dB/octave) at High Frequency
$\alpha = 1.0, \beta = 0.8$	1000	4.84	1.19
$\alpha = 0.9, \beta = 0.7$	2900	4.22	1.20
$\alpha = 0.8, \beta = 0.6$	9866	3.62	1.19
$\alpha = 0.7, \beta = 0.5$	43.56k	3.02	1.15
$\alpha = 0.6, \beta = 0.4$	262.1k	2.41	1.06
$\alpha = 0.5, \beta = 0.3$	3.076M	1.81	0.85

3.2.1.4. Fractional Order All Pass Filter

The transfer function of fractional order allpass filter (FOAPF) [1] can be expressed using equation (3.1) as:

$$T(s)_{\text{FOAP}} = b \frac{s^\alpha - c}{s^\alpha + c} \quad (3.12)$$

where c and b are constants and $0 < \alpha < 1$. From equation (3.12), the magnitude and phase of FOAP can also be expressed as:

$$|T(j\omega)_{\text{FOAP}}| = b \sqrt{\frac{\omega^{2\alpha} - 2c\omega^\alpha \cos\left(\frac{\alpha\pi}{2}\right) + c^2}{\omega^{2\alpha} + 2c\omega^\alpha \cos\left(\frac{\alpha\pi}{2}\right) + c^2}} \quad (3.13a)$$

$$\angle T(j\omega)_{\text{FOAP}} = \tan^{-1}\left(\frac{\omega^\alpha \sin\left(\frac{\alpha\pi}{2}\right)}{\omega^\alpha \cos\left(\frac{\alpha\pi}{2}\right) - c}\right) - \tan^{-1}\left(\frac{\omega^\alpha \sin\left(\frac{\alpha\pi}{2}\right)}{\omega^\alpha \cos\left(\frac{\alpha\pi}{2}\right) + c}\right) \quad (3.13b)$$

The half power frequency of FOAP filter [1] derived from equation (3.13a) can be written as:

$$\omega_h = \left(c \left(\sqrt{4\cos^2\left(\frac{\alpha\pi}{2}\right) - 1} + 2\cos\left(\frac{\alpha\pi}{2}\right) \right) \right)^{\frac{1}{\alpha}} \quad (3.14a)$$

While the right phase frequency(ω_{rp}), minimum/maximum frequency (ω_m) and cut-off frequency are equal and can be given as:

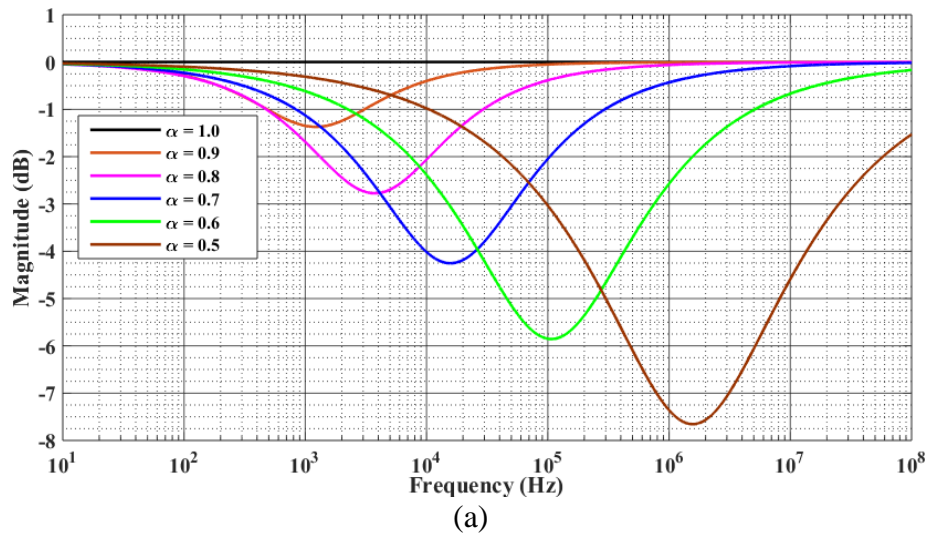
$$\omega_m = \omega_{rp} = \omega_0 = (c)^{\frac{1}{\alpha}} \quad (3.14b)$$

It is worth mentioning here that the magnitude response will have a maxima at ω_0 for $\alpha > 1$ and minima when $\alpha < 1$ [1]. The magnitude and phase of filter at different values of ω are shown in Table 3.7.

Table 3.7 The values of magnitude and phase of FOAP filter for different values of ω

Ω	$ \mathbf{T}(\mathbf{j}\omega)_{\text{FOAP}} $	$\angle \mathbf{T}(\mathbf{j}\omega)_{\text{FOAP}}$
0	b	π
ω_0	$b \tan\left(\frac{\alpha\pi}{4}\right)$	$\frac{\pi}{2}$
∞	b	0

In Fig. 3.4, we have shown the magnitude and phase responses of a fractional order all pass filter designed for a cutoff frequency of $(2\pi \times 3140)$ rad/s for $\alpha = 1$, by selecting $c = 3140$ and $b = 1$ for different values of α (from 1.0 to 0.5 in step of 0.1) using MATLAB.



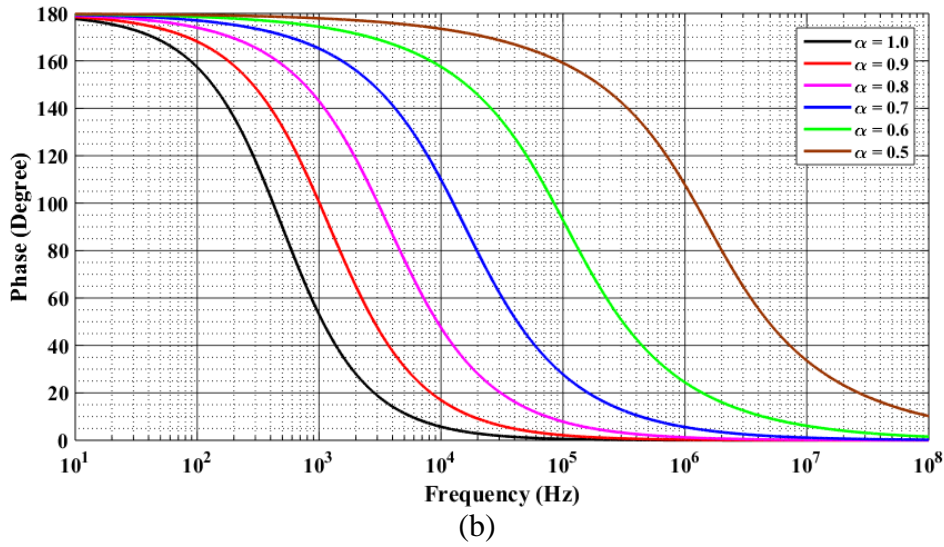


Figure 3.4 Magnitude and phase responses of FOAP (a) Magnitude response (b) Phase response

From Fig 3.4, filter parameters such as peak frequencies (ω_p) and right phase frequencies (ω_{rp}) for different values of α (from 1.0 to 0.5) have been obtained and provided in Table 3.8.

Table 3.8 Parameters of FOAP filter

α	Filter's parameters	
	Peak frequency (Hz)	Right phase frequency (Hz)
$\alpha = 1.0$	499	499
$\alpha = 0.9$	1221	1221
$\alpha = 0.8$	3730	3730
$\alpha = 0.7$	15.7k	15.7k
$\alpha = 0.6$	107k	107k
$\alpha = 0.5$	1.56M	1.56M

We now present the general theory and some sample simulations of fractional order filters realized with two fractance devices.

3.2.2. Fractional Order Filters Using Two Fractance Device

The generalized form of fractional order filters, implemented with two fractance devices of order α and β can be expressed [2] as:

$$T(s) = \frac{As^{\alpha+\beta} + Bs^\beta + C}{s^{\alpha+\beta} + Ds^\beta + E} \quad (3.15)$$

where ‘ α ’ and ‘ β ’ ($0 < \alpha < 1, 0 < \beta < 1$) are the order of two fractance devices used in the design of fractional order filters. In a fractional order filter realized with two fractance devices, arbitrary values of stop band attenuation in the range of 20dB-40dB/decades can be achieved by appropriate selection of ‘ α ’ and ‘ β ’. This feature is not available in integer order filters realized with two conventional capacitors. Different responses of fractional order filter viz. FOLP, FOBP, FOHP, FOBR and FOAP filters can be derived from equation (3.15) as illustrated in following sections.

3.2.2.1. Fractional Order Low Pass Filter

The transfer function of a fractional order low pass (FOLP) filter can be derived from equation (3.15) if we take $A = 0$ and $B = 0$ as:

$$T(s)_{\text{FOLP}} = \frac{C}{s^{\alpha+\beta} + Ds^\beta + E} \quad (3.16)$$

The magnitude and phase responses can be obtained from equation (3.16) and expressed as:

$$|T(j\omega)_{\text{FOLP}}| = \frac{C}{\left[\omega^{2(\alpha+\beta)} + 2D\omega^{(\alpha+2\beta)} \cos\left(\frac{\alpha\pi}{2}\right) + D^2\omega^{2\beta} + 2E\omega^{(\alpha+\beta)} \cos\left(\frac{(\alpha+\beta)\pi}{2}\right) + 2DE\omega^\beta \cos\left(\frac{\beta\pi}{2}\right) + E^2 \right]^{\frac{1}{2}}} \quad (3.17a)$$

$$\angle T(j\omega)_{\text{FOLP}} = -\tan^{-1} \left(\frac{\omega^{(\alpha+\beta)} \sin\left(\frac{(\alpha+\beta)\pi}{2}\right) + D\omega^\beta \sin\left(\frac{\beta\pi}{2}\right)}{\omega^{(\alpha+\beta)} \cos\left(\frac{(\alpha+\beta)\pi}{2}\right) + D\omega^\beta \cos\left(\frac{\beta\pi}{2}\right) + E} \right) \quad (3.17b)$$

The low frequency gain (DC gain) of FOLP filter is $\frac{C}{E}$. The half power frequency is the frequency at which gain of transfer function become $\frac{1}{\sqrt{2}}$ times the low frequency gain of

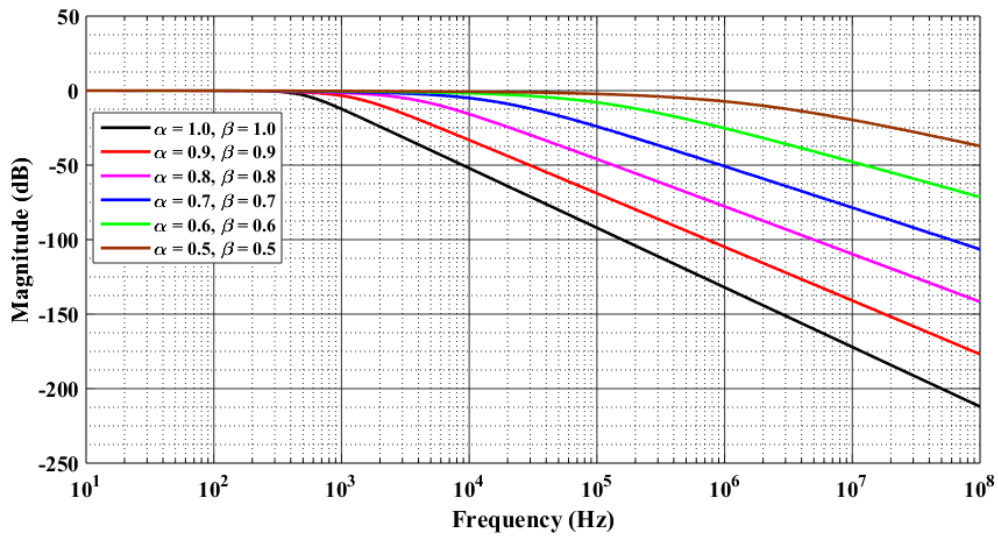
transfer function i.e. $\frac{1}{\sqrt{2}} \frac{C}{E}$ and the right phase frequency is the frequency at which phase of transfer function becomes $\pm \frac{\pi}{2}$ radians. These frequencies for a fractional order low pass filter can be evaluated by solving the following equations:

$$\omega_h^{2(\alpha+\beta)} + 2D\omega_h^{(\alpha+2\beta)} \cos\left(\frac{\alpha\pi}{2}\right) + D^2\omega_h^{2\beta} + 2E\omega_h^{(\alpha+\beta)} \cos\left(\frac{(\alpha+\beta)\pi}{2}\right) + \quad (3.18a)$$

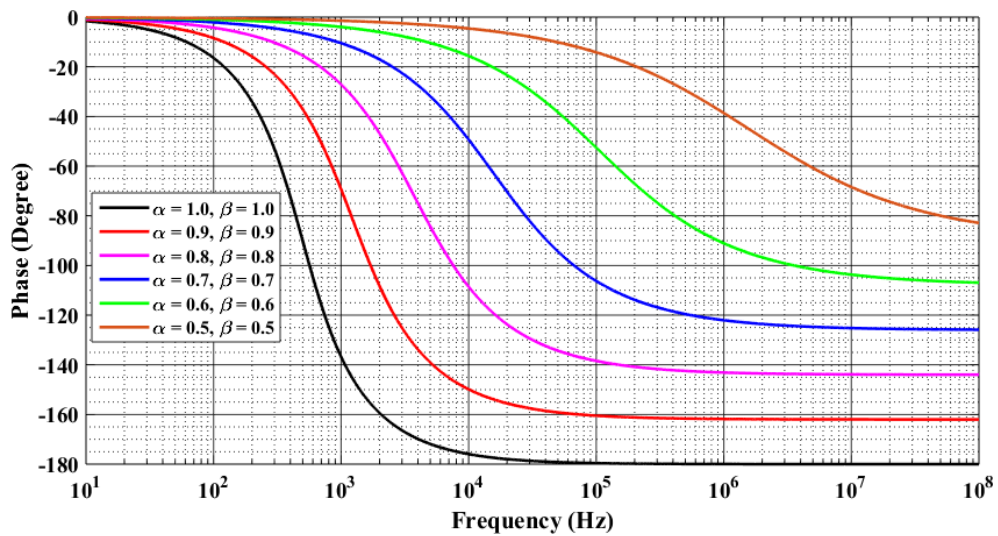
$$2DE\omega_h^\beta \cos\left(\frac{\beta\pi}{2}\right) - E^2 = 0$$

$$-\tan^{-1}\left(\frac{\omega_{rp}^{(\alpha+\beta)} \sin\left(\frac{(\alpha+\beta)\pi}{2}\right) + D\omega_{rp}^\beta \sin\left(\frac{\beta\pi}{2}\right)}{\omega_{rp}^{(\alpha+\beta)} \cos\left(\frac{(\alpha+\beta)\pi}{2}\right) + D\omega_{rp}^\beta \cos\left(\frac{\beta\pi}{2}\right) + E}\right) = \pm \frac{\pi}{2} \quad (3.18b)$$

It may be mentioned here that the slope of the attenuation characteristics in the stop band for very high frequencies will be $-20(\alpha+\beta)$ dB/decade. The magnitude and phase responses, as given in equation (3.17) have been plotted, using MATLAB, for a FOLP designed to have a half power frequency of 500Hz (for $\alpha = 1$, $\beta = 1$), by selecting the coefficients C, D, and E as 9859600, 4439.94 and 9859600 respectively, so that the response is maximally flat. The magnitude and phase responses for different values of α and β are depicted in Fig. 3.5.



(a)



(b)

Figure 3.5 Magnitude and phase responses of FOLP (a) Magnitude response (b) Phase response

The slope of the magnitude response in stopband, half power frequency and right phase frequency as obtained from Fig. 3.5 are given below in Table 4.9, from where it may be noted that the slope of the magnitude characteristics and the characterising frequency may be varied between -20db/decade to -40dB/decade by appropriately choosing the values of α and β . In contrast, for an integer order filter with two poles, the slope and the half power frequency always remains fixed at -40dB/decades.

Table. 3.9 Various parameters of FOLP filter obtained from MATLAB simulations

Value of α and β	Parameters		
	Half power frequency (Hz)	Right phase frequency (Hz)	Attenuation (dB/decade)
$\alpha = \beta = 1.0$	500	500	40
$\alpha = \beta = 0.9$	936.6	1426	36
$\alpha = \beta = 0.8$	2001	5761	32
$\alpha = \beta = 0.7$	5553	41.22k	28
$\alpha = \beta = 0.6$	22.86k	904k	24
$\alpha = \beta = 0.5$	180k	-	20

3.2.2.2. Fractional Order High Pass Filter

The transfer function of FOHP filter can be obtained from equation 3.15 by taking $B = 0$ and $C = 0$ as:

$$T(s)_{\text{FOHP}} = \frac{As^{\alpha+\beta}}{s^{\alpha+\beta} + Ds^\beta + E} \quad (3.19)$$

From equation (3.19), the expressions for magnitude and phase can be derived as:

$$|T(j\omega)_{\text{FOHP}}| = \frac{A\omega^{(\alpha+\beta)}}{\left[\begin{array}{l} \omega^{2(\alpha+\beta)} + 2D\omega^{(\alpha+2\beta)} \cos\left(\frac{\alpha\pi}{2}\right) + D^2\omega^{2\beta} + \\ 2E\omega^{(\alpha+\beta)} \cos\left(\frac{(\alpha+\beta)\pi}{2}\right) + 2DE\omega^\beta \cos\left(\frac{\beta\pi}{2}\right) + E^2 \end{array} \right]^{\frac{1}{2}}} \quad (3.20a)$$

$$\angle T(j\omega)_{\text{FOHP}} = \frac{(\alpha+\beta)\pi}{2} - \tan^{-1} \left(\frac{\omega^{(\alpha+\beta)} \sin\left(\frac{(\alpha+\beta)\pi}{2}\right) + D\omega^\beta \sin\left(\frac{\beta\pi}{2}\right)}{\omega^{(\alpha+\beta)} \cos\left(\frac{(\alpha+\beta)\pi}{2}\right) + D\omega^\beta \cos\left(\frac{\beta\pi}{2}\right) + E} \right) \quad (3.20b)$$

From equation 3.20, the slope of the magnitude characteristics in the stopband for low frequencies will be $+20(\alpha+\beta)$ dB/decade. The high frequency gain of FOLP filter is $\frac{A}{E}$.

The half power frequency is the frequency at which gain of transfer function become $\frac{1}{\sqrt{2}}$

times the high frequency gain of transfer function i.e. $\frac{1}{\sqrt{2}} \frac{A}{E}$ and the right phase frequency

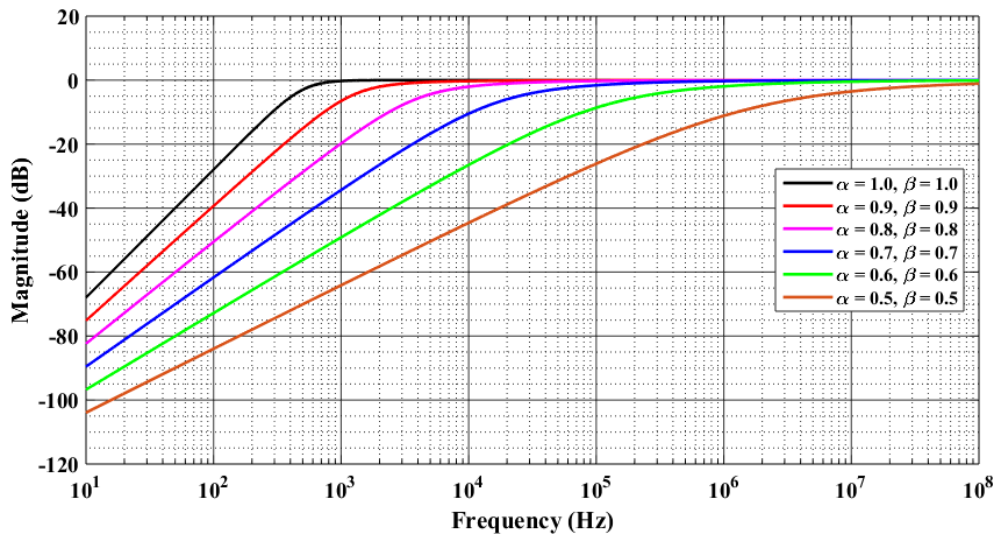
is the frequency at which phase of transfer function becomes $\pm \frac{\pi}{2}$ radians. These

frequencies for a FOHP filter can be evaluated by solving the following equations:
respectively

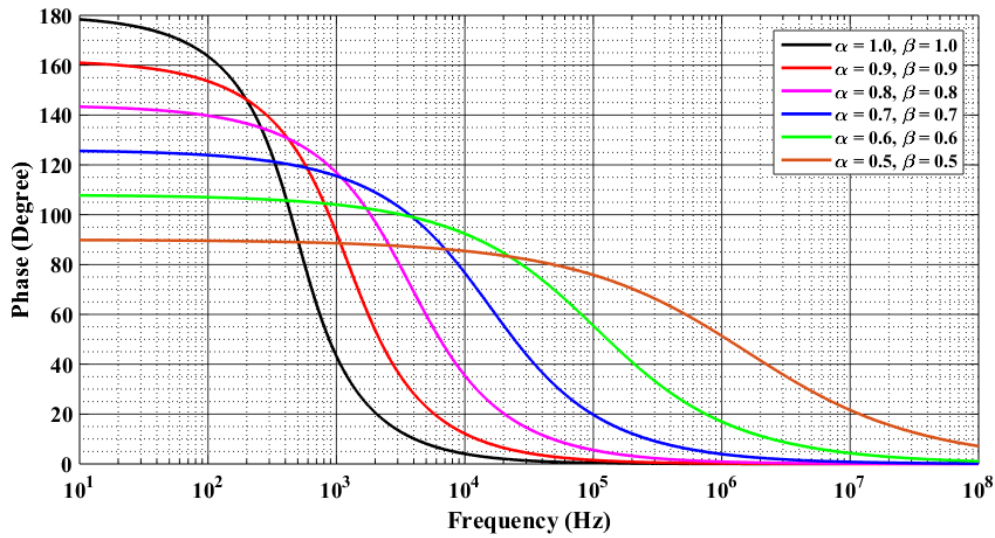
$$D^2\omega_h^{2\beta} + 2D\omega_h^{(\alpha+2\beta)}\cos\left(\frac{\alpha\pi}{2}\right) + 2E\omega_h^{(\alpha+\beta)}\cos\left(\frac{(\alpha+\beta)\pi}{2}\right) + 2DE\omega_h^\beta\cos\left(\frac{\beta\pi}{2}\right) + E^2 - \omega_h^{2(\alpha+\beta)} = 0 \quad (3.21a)$$

$$(\alpha+\beta)\frac{\pi}{2} - \tan^{-1}\left(\frac{\omega_{rp}^{(\alpha+\beta)}\sin\left(\frac{(\alpha+\beta)\pi}{2}\right) + D\omega_{rp}^\beta\sin\left(\frac{\beta\pi}{2}\right)}{\omega_{rp}^{(\alpha+\beta)}\cos\left(\frac{(\alpha+\beta)\pi}{2}\right) + D\omega_{rp}^\beta\cos\left(\frac{\beta\pi}{2}\right) + E}\right) = \pm\frac{\pi}{2} \quad (3.21b)$$

The magnitude and phase response, as given in equation (3.20) have been plotted using MATLAB for a FOHP filter, designed to have a half power frequency of 500 Hz (for $\alpha = 1, \beta = 1$), by selecting the coefficients A, D, and E as 1, 4439.96 and 9859600 respectively. The magnitude and phase response for different values of α and β are displayed in Fig. 3.6.



(a)



(b)

Figure 3.6 Magnitude and phase responses of FOHP (a) Magnitude response (b) Phase response

The slope of the magnitude response, half power frequency and right phase frequency as obtained from Fig. 3.6 are given in Table 3.10, from where it may be noted that the slope of the magnitude characteristics and the characterising frequency may be varied by appropriate selection of the values of α and β .

Table 3.10 Various parameters of FOHP filter obtained from MATLAB simulations

Values of α and β	Parameters		
	Half power frequency (Hz)	Right phase frequency (Hz)	Attenuation (dB/decade)
$\alpha = \beta = 1.0$	500	500	40
$\alpha = \beta = 0.9$	1598	1051	36
$\alpha = \beta = 0.8$	6997	2430	32
$\alpha = \beta = 0.7$	45.11k	6033	28
$\alpha = \beta = 0.6$	503.1k	12.75k	24
$\alpha = \beta = 0.5$	13.66M	-	20

3.2.2.3. Fractional Order Band Pass Filter

A fractional order band pass function can be obtained from equation (3.15) if we select $A = 0$ and $C = 0$ as:

$$T(s)_{\text{FOBP}} = \frac{Bs^\beta}{s^{\alpha+\beta} + Ds^\beta + E} \quad (3.22)$$

From above equation (3.22), the magnitude and phase responses of FOBP filter may be expressed as:

$$|T(j\omega)_{\text{FOBP}}| = \frac{B\omega^\beta}{\left[\begin{array}{l} \omega^{2(\alpha+\beta)} + 2D\omega^{(\alpha+2\beta)} \cos\left(\frac{\alpha\pi}{2}\right) + D^2\omega^{2\beta} + \\ 2E\omega^{(\alpha+\beta)} \cos\left(\frac{(\alpha+\beta)\pi}{2}\right) + 2DE\omega^\beta \cos\left(\frac{\beta\pi}{2}\right) + E^2 \end{array} \right]^{\frac{1}{2}}} \quad (3.23a)$$

$$\angle T(j\omega)_{\text{FOBP}} = \frac{\beta\pi}{2} - \tan^{-1} \left(\frac{\omega^{(\alpha+\beta)} \sin\left(\frac{(\alpha+\beta)\pi}{2}\right) + D\omega^\beta \sin\left(\frac{\beta\pi}{2}\right)}{\omega^{(\alpha+\beta)} \cos\left(\frac{(\alpha+\beta)\pi}{2}\right) + D\omega^\beta \cos\left(\frac{\beta\pi}{2}\right) + E} \right) \quad (3.23b)$$

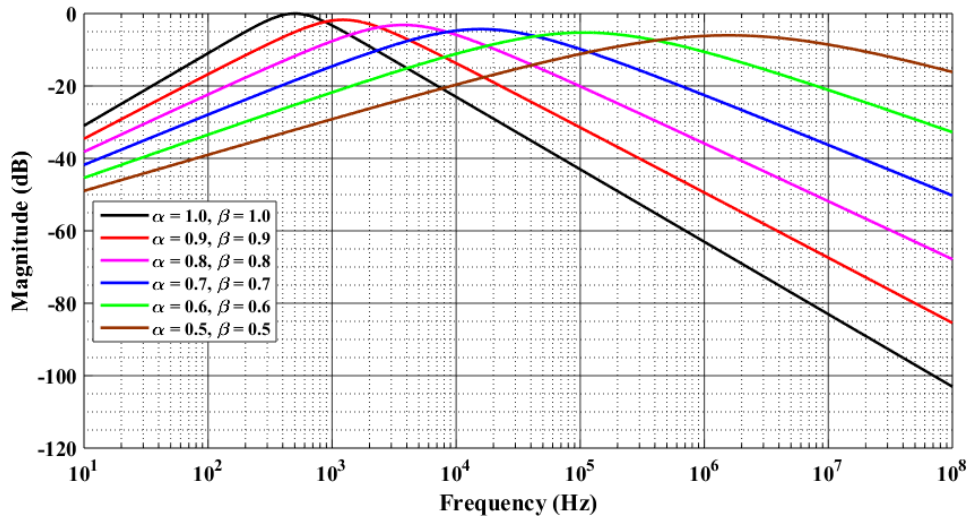
It may be mentioned here that the slope of the attenuation characteristics in the stopband for lower frequency will be $+20\beta$ db/decade, while higher frequency be -20α dB/decade. From equation (3.23a), the high frequency gain as well as DC gain of FOBP filter is found to be zero, while maximum/peak frequency gain is found to be $\frac{B}{D}$ (for $\alpha = \beta = 1$). The maximum frequency ω_m of fractional order band pass filter is the frequency at which magnitude response of fractional order band pass filter attains a maxima. This frequency is given by:

$$\omega_m = E^{\frac{1}{(\alpha+\beta)}} \quad (3.24)$$

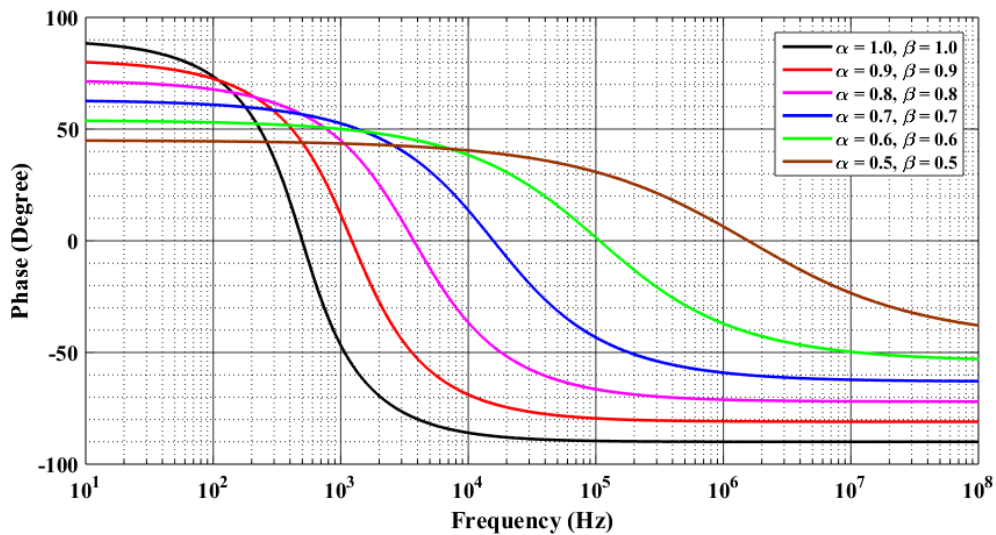
The right phase frequency ω_{rp} , on the other hand may be obtained by equating the equation (3.23b) with $\pm \frac{\pi}{2}$ radian. The solution of the following equation thus, gives the value of ω_{rp} as:

$$\omega_{rp}^{\alpha+\beta} \sin\left(\frac{(1-\alpha)\pi}{2}\right) E + D\omega_{rp}^\alpha + E \sin\left(\frac{(\beta+1)\pi}{2}\right) = 0 \quad (3.25)$$

The frequency responses of a FOBP filter designed to have a maximum/peak frequency of 500 Hz (for $\alpha = 1, \beta = 1$), designed, choosing the coefficients B, D, and E as 4439.96, 4439.96 and 9859600 respectively have been plotted using MATLAB for different values of α and β and shown in Fig.3.7.



(a)



(b)

Figure 3.7 Magnitude and phase responses of FOBP (a) Magnitude response (b) Phase response

From frequency responses as shown in Fig.3.7, the different parameters such as peak frequencies and stop band attenuations are noted and presented in Table 3.11.

Table. 3.11 Various parameters of FOBP filter obtained from MATLAB simulations

Values of α and β	Parameters		
	Peak frequency (Hz)	Maximum Phase (degree)	Attenuation (dB/decade)
$\alpha = \beta = 1.0$	500	89.7	20
$\alpha = \beta = 0.9$	1219	80.79	18
$\alpha = \beta = 0.8$	3743	71.8	16
$\alpha = \beta = 0.7$	15.67k	62.83	14
$\alpha = \beta = 0.6$	108k	53.88	12
$\alpha = \beta = 0.5$	1.58M	44.5	10

From Fig. 3.7 and Table 3.11, it may be noted that various parameters of FOBP filter viz. peak frequency, stop band attenuation and maximum phase vary with the values of α and β as per the theoretical formulations presented above.

3.2.2.4. Fractional Order Band Reject Filter

The fractional order band reject (FOBR) filter response can be obtained from equation (3.15) for $B = 0$ and $C = A.C$, as:

$$T(s)_{\text{FOBR}} = \frac{A(s^{\alpha+\beta} + C)}{s^{\alpha+\beta} + Ds^{\beta} + E} \quad (3.26)$$

From above transfer function of FOBR filter, the magnitude and phase of fractional order band reject filter can be found as:

$$|T(j\omega)_{\text{FOBR}}| = A \left[\frac{\omega^{2(\alpha+\beta)} + 2C\omega^{(\alpha+\beta)} \cos\left(\frac{(\alpha+\beta)\pi}{2}\right) + C^2}{\omega^{2(\alpha+\beta)} + 2D\omega^{(\alpha+2\beta)} \cos\left(\frac{\alpha\pi}{2}\right) + D^2\omega^{2\beta} + 2E\omega^{(\alpha+\beta)} \cos\left(\frac{(\alpha+\beta)\pi}{2}\right) + 2DE\omega^{\beta} \cos\left(\frac{\beta\pi}{2}\right) + E^2} \right]^{\frac{1}{2}} \quad (3.27a)$$

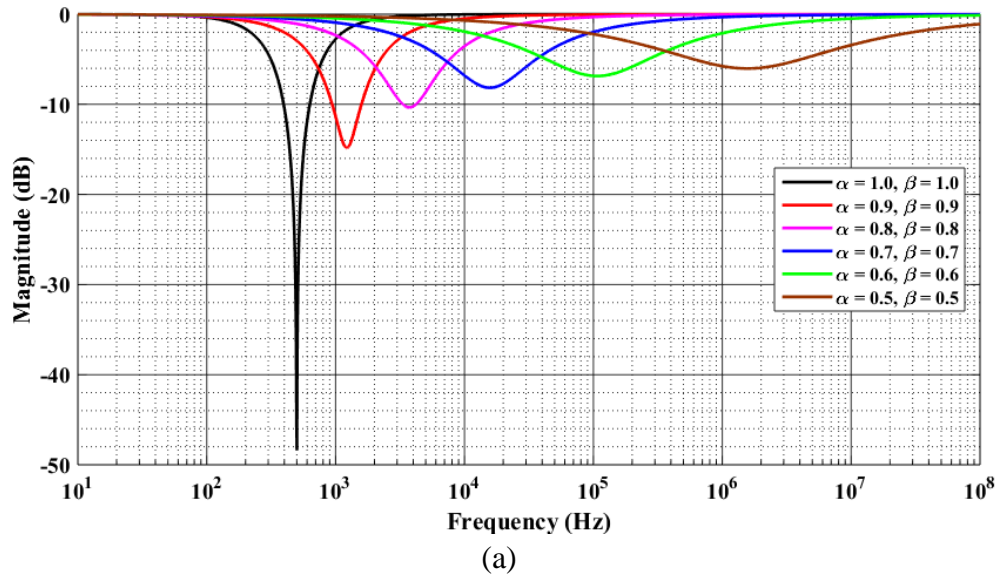
$$\angle T(j\omega)_{\text{FOBR}} = \tan^{-1} \left(\frac{\omega^{(\alpha+\beta)} \sin \left(\frac{(\alpha+\beta)\pi}{2} \right)}{\omega^{(\alpha+\beta)} \cos \left(\frac{(\alpha+\beta)\pi}{2} \right) + C} \right) \quad (3.27b)$$

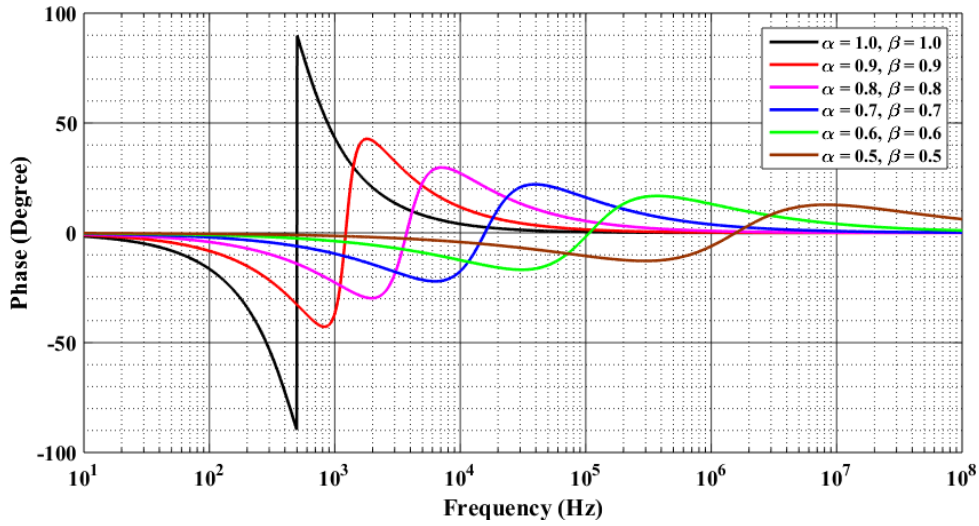
$$- \tan^{-1} \left(\frac{\omega^{(\alpha+\beta)} \sin \left(\frac{(\alpha+\beta)\pi}{2} \right) + D\omega^\beta \sin \left(\frac{\beta\pi}{2} \right)}{\omega^{(\alpha+\beta)} \cos \left(\frac{(\alpha+\beta)\pi}{2} \right) + D\omega^\beta \cos \left(\frac{\beta\pi}{2} \right) + E} \right)$$

The high frequency gain of FOBR filter is A and DC gain is $\frac{AC}{E}$. The frequency ω_m at which the minima of the magnitude response occurs is given by:

$$\omega_m = E^{\frac{1}{\alpha+\beta}} \quad (3.28)$$

The frequency response of a FOBR filter designed for minimum frequency of 500 Hz (for $\alpha = \beta = 1$), by selecting $A = 1$, $C = E = 3140$, has been plotted from equation (3.27) using MATLAB and shown in Fig.3.8. The minimum frequency and maximum phases obtained from Fig.3.8 for different values of α and β are tabulated in Table 3.12.





(b)

Figure 3.8 Magnitude and phase responses of FOBR (a) Magnitude response (b) Phase response

Table 3.12 Various parameters of FOBR filter obtained from MATLAB simulations

Values of α and β	ω_m (Hz)	Maximum Phase (degree)
$\alpha = \beta = 1.0$	500	90.00
$\alpha = \beta = 0.9$	1227	42.78
$\alpha = \beta = 0.8$	3719	29.75
$\alpha = \beta = 0.7$	15.77k	22.00
$\alpha = \beta = 0.6$	107k	16.70
$\alpha = \beta = 0.5$	1.5M	12.78

The minima frequency and maximum phase shift of FOBR filter can be varied with the variation of α and β , which can be observed from Fig.3.8 and Table 3.12.

3.2.2.5. Fractional Order All Pass Filter

For $A = 1$, $B = -D$ and $C = E$, the transfer function given in equation (3.15) will represent a fractional order all pass (FOAP) filter.

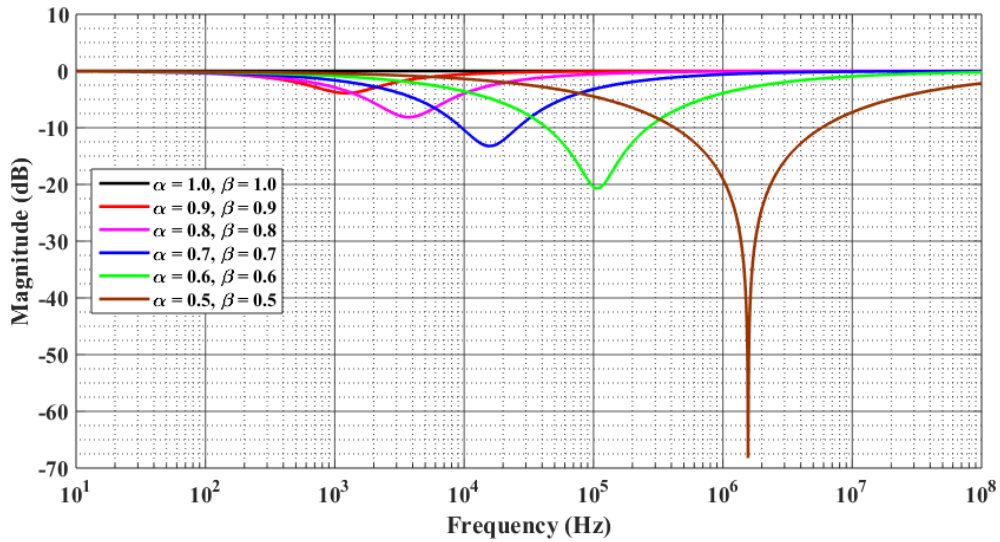
$$T(s)_{\text{FOAP}} = \frac{s^{\alpha+\beta} - Ds^{\beta} + E}{s^{\alpha+\beta} + Ds^{\beta} + E} \quad (3.29)$$

Using equation (3.29), the magnitude and phase of FOAP filter may be derived as:

$$|T(j\omega)_{\text{FOAP}}| = \left[\frac{\omega^{2(\alpha+\beta)} - 2D\omega^{(\alpha+2\beta)} \cos\left(\frac{\alpha\pi}{2}\right) + D^2\omega^{2\beta} + 2E\omega^{(\alpha+\beta)} \cos\left(\frac{(\alpha+\beta)\pi}{2}\right) - 2DE\omega^\beta \cos\left(\frac{\beta\pi}{2}\right) + E^2}{\omega^{2(\alpha+\beta)} + 2D\omega^{(\alpha+2\beta)} \cos\left(\frac{\alpha\pi}{2}\right) + D^2\omega^{2\beta} + 2E\omega^{(\alpha+\beta)} \cos\left(\frac{(\alpha+\beta)\pi}{2}\right) + 2DE\omega^\beta \cos\left(\frac{\beta\pi}{2}\right) + E^2} \right]^{\frac{1}{2}} \quad (3.30a)$$

$$\begin{aligned} \angle T(j\omega)_{\text{FOAP}} = & \tan^{-1} \left(\frac{\omega^{(\alpha+\beta)} \sin\left(\frac{(\alpha+\beta)\pi}{2}\right) - D\omega^\beta \sin\left(\frac{\beta\pi}{2}\right)}{\omega^{(\alpha+\beta)} \cos\left(\frac{(\alpha+\beta)\pi}{2}\right) - D\omega^\beta \cos\left(\frac{\beta\pi}{2}\right) + E} \right) \\ & - \tan^{-1} \left(\frac{\omega^{(\alpha+\beta)} \sin\left(\frac{(\alpha+\beta)\pi}{2}\right) + D\omega^\beta \sin\left(\frac{\beta\pi}{2}\right)}{\omega^{(\alpha+\beta)} \cos\left(\frac{(\alpha+\beta)\pi}{2}\right) + D\omega^\beta \cos\left(\frac{\beta\pi}{2}\right) + E} \right) \end{aligned} \quad (3.30b)$$

The high frequency gain and DC gain are unity. It may be noted that unlike a integer order all pass filter of order 2, the magnitude response of FOAP filter realized with two fractance devices, may have a maxima/minima and the FOAP filter may not be a true all pass filter [2]. The magnitude and phase plots of the FOAP filter using MATLAB are shown in Fig.3.9, while frequencies (ω_m) for different values of α and β are given in Table 3.13.



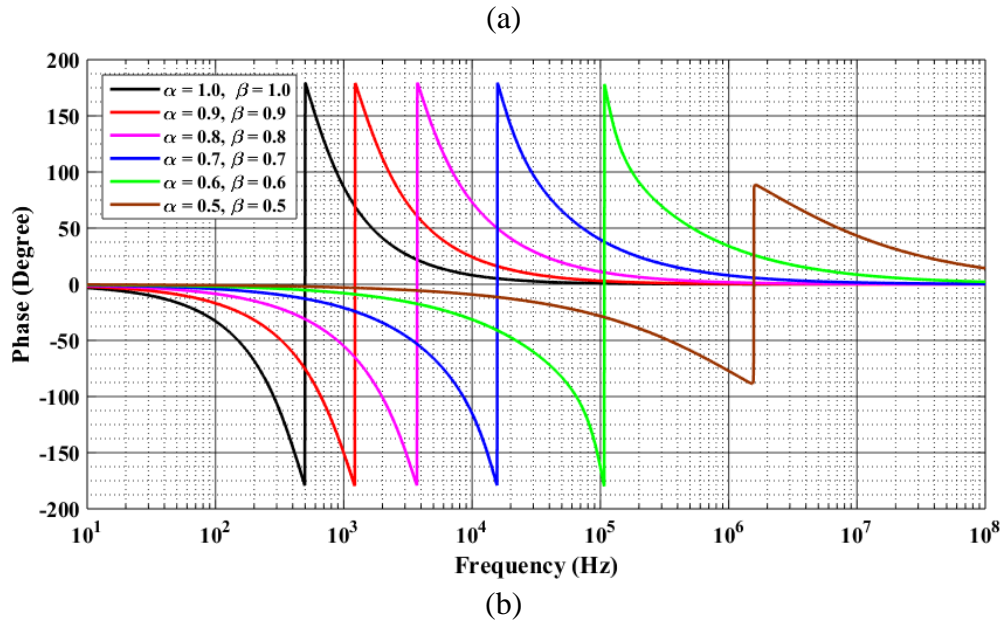


Figure 3.9 Various parameters of FOAP filter obtained from MATLAB simulations

Table. 3.13 Various parameters of FOAP obtained from MATLAB simulations

Values of α and β	Minimum frequency (Hz)	Maximum Phase (degree)
$\alpha = \beta = 1.0$	500	179.6
$\alpha = \beta = 0.9$	1227	179.3
$\alpha = \beta = 0.8$	3743	179.3
$\alpha = \beta = 0.7$	15.77k	179.7
$\alpha = \beta = 0.6$	107k	178.4
$\alpha = \beta = 0.5$	1.56M	88.59

3.2.3. Realization of Fractional Order Filters Using Rational Approximation of Fractional Order Laplacian Operator

In this approach, using a rational approximation of s^α , based on continued fraction expansion of $(1+x)^\alpha$ (which converges in the finite complex s-plane, along with the negative real axis from $(x = -\infty$ to $x = -1)$), substituting $x=s-1$ and retaining first four terms in the expansion [89], the fractional order Laplacian operator s^α is approximated by

$$S^\alpha = \frac{a_0 s^2 + a_1 s + a_2}{a_2 s^2 + a_1 s + a_0} \quad (3.31)$$

Where a_0 , a_1 and a_2 can be given by following equation

$$a_0 = (\alpha^2 + 3\alpha + 2), a_1 = (8 - 2\alpha^2) \text{ and } a_2 = (\alpha^2 - 3\alpha + 2). \quad (3.32)$$

Because of this approximation, the transfer function of FOFs is converted into integer order transfer function. If the continued fraction expansion is terminated with higher number of terms then the rational order approximation will be of higher order, resulting into a still higher integer order for the approximated transfer function.

Thus, equivalent integer order transfer function for the FOFs can be obtained using equations 3.15 and rational approximation of s^α , to realize the FOLP, FOHP and FOBP responses of FOFs. In the following, we have illustrated the concept by taking an example of the realization of fractional order low pass filter's transfer function.

3.2.3.1. Fractional Order Low Pass Filter

The transfer function of a prototype fractional order low pass filter realized with two fractance devices can be expressed as:

$$T(s)_{\text{FOLP}} = \frac{C}{s^{\alpha+\beta} + Ds^\beta + E} = \frac{C}{s^\alpha s^\beta + Ds^\beta + E} \quad (3.33)$$

Using a rational approximation of s^α based on continued fraction expansion of $(1 + x)^\alpha$ (which converges in the finite complex s -plane, along with the negative real axis from $(x = -\infty$ to $x = -1)$), substituting $x = s - 1$ and retaining first four terms in the expansion [88], this transfer function may be converted into an integer order transfer function by substituting $s^\alpha = \frac{a_0 s^2 + a_1 s + a_2}{a_2 s^2 + a_1 s + a_0}$ and $s^\beta = \frac{b_0 s^2 + b_1 s + b_2}{b_2 s^2 + b_1 s + b_0}$ in the transfer function given in equation (3.33). The resulting integer order transfer function may be expressed as:

$$T(s)_{FOLP} = \frac{C(N_4s^4 + N_3s^3 + N_2s^2 + N_1s + N_0)}{D_4s^4 + D_3s^3 + D_2s^2 + D_1s + D_0} \quad (3.34)$$

$$\begin{aligned} N_0 &= a_0b_0 & D_0 &= a_2b_2 + Da_0b_2 + Ea_0b_0 \\ N_1 &= a_1b_0 + a_0b_1 & D_1 &= a_1b_2 + a_2b_1 + D(a_0b_1 + a_1b_2) + E(a_1b_0 + a_0b_1) \\ N_2 &= a_1b_1 + a_2b_0 + a_0b_2 & D_2 &= a_0b_2 + a_1b_1 + a_2b_0 + D(a_0b_0 + a_1b_1 + a_2b_2) + E(a_2b_0 + a_1b_1 + a_0b_2) \\ N_3 &= a_2b_1 + a_1b_2 & D_3 &= a_0b_1 + a_1b_0 + D(a_1b_0 + a_2b_1) + E(a_2b_1 + a_1b_2) \\ N_4 &= a_2b_2 & D_4 &= a_0b_0 + Da_2b_0 + Ea_2b_2 \end{aligned}$$

The transfer function represented by equation (3.34) can now be realized using any of the standard methods available for realization of a rational transfer function using some active building block(s), resistors and conventional capacitors. It may be mentioned here that the rational function approximation method results into a similar integer order transfer function for FOLP, FOBP, FOHP and FOBR filters. Depending on the numerical values of the coefficients of the numerator and denominator polynomial, the response represents different filters [89].

3.3. Literature Overview of Fractional Order Filters

During the last couple of years, a very large number of contributions have been made on the realization of fractional order analog filters, in the following, we present a detailed account of the major contributions made by various researchers in the field of fractional order analog filters, so that the work presented in this chapter may be put in proper perspective.

The main work on the realization of fractional order filters started with the paper of Radwan, Soliman and Elwakil [1] wherein fractional order low pass (FOLP), fractional order high pass (FOHP), fractional order band pass (FOBP) and fractional

order all pass (FOAP) filters were reported using a single fractance device. The expressions for different critical frequencies viz. pole frequency, the right phase frequency, half power frequency and the quality factor were derived. Passive proto types of these fractional order filters were simulated in which the fractional order capacitors were realized by an approximation method presented in [2]. Numerical simulations were also carried out to verify the proposed theory. Subsequently, this work was extended to cover circuits with two identical fractance devices, wherein, design and simulation of Sallen-Key and KHN bi-quad filter topologies were presented in fractional domain along with the experimental results of KHN bi-quad filters using real fractional order capacitors of order 0.5.

Freeborn, Maundy and Elwakil [3-4,57] have used the approach of approximating the Laplacian operator s^α by an integer order approximation, and, thus converting the fractional order transfer function into an integer order transfer function and then realizing the transfer function with standard analog hardware and passive components. In all these research works the coefficients of the fractional order transfer functions were chosen in such a way so as to result in frequency responses which were maximally flat in pass band. Specifically, fractional order low pass filter of order $(1+\alpha)$, α varying in steps from 0.1 to 0.9 was presented in [3] while in [57], the authors reported the use of field programmable analogue arrays (FPAA) hardware to implement an approximated fractional step transfer function of order $(n+\alpha)$, where n is an integer and $0 < \alpha < 1$. In [4], $(5+\alpha)$ order low pass and band pass fractional order filters using op-amp MC-1458 were presented.

Fractional order filters using two fractional capacitors of dependent orders ($\alpha = k\beta$) to realize the FOLP, FOHP and FOBP responses were reported in [5]. Numerical and ADS simulation results of fractional order KHN bi-quad filters were provided to validate the theoretical findings. The stability conditions for designed filters have also been described.

In [6], two transfer functions have been presented, one realized by RCD structure while the other uses a series capacitor with a parallel LC tank circuit in which the series capacitors have been replaced by fractional order capacitors for realizing high-quality factor asymmetric-slope FOBP filters. SPICE and experimental results have been provided to verify the theory.

In [7], authors have proposed the use of fractional order capacitors in Tow-Thomas bi-quad to realize both fractional low pass and asymmetric band pass filters of order $0 < (\alpha_1 + \alpha_2) < 2$. PSPICE and MATLAB simulation results of first order fractional-step low pass and band pass filters of order 1.1, 1.5 and 1.9 have been provided as examples. The results of fractional order low pass filter of order 1.5 are experimentally verified using silicon fabricated fractional order capacitor of order 0.5.

Design of KHN bi-quad filters using fractional order capacitors of order α and β has been reported in [8]. The frequency responses of these proposed filters obtained experimentally are compared with simulated results of PSPICE and MATLAB. The sensitivity analysis and stability of presented filters have also been examined.

In [9], authors have described a general procedure to obtain Butterworth filter specifications in the fractional-order domain with the necessary and sufficient condition for getting maximally flat response with a specified cut off frequency. As an example,

fractional order KHN and Sallen–Key filters using fractional order capacitors have been designed.

Soltan, Radwan and Soliman [10], [30] have described the general design procedure for fractional order analog filters in terms of various critical frequencies namely maximum/minimum/half power of the filters and the transfer function coefficients taking into consideration the stability of the realized filters, showing the flexibility in the design procedure because of extra degree of freedom provided by the fractional parameters. Design examples of KHN and Tow-Thomas filters using second generation current conveyors have also been presented.

A fractional order low pass filter having Butterworth characteristic was implemented for the first time using the concept of switched capacitor filters [11]. Fractional order low pass filters of order $(1+\alpha)$ and $(3+\alpha)$ were designed and verified using transistor level simulations using AMS $0.35\mu\text{m}$ CMOS process.

Fractional order KHN type filters with two different PMMA coated constant phase elements have been presented in [12], and experimental results have also been compared with PSPICE and MATLAB simulation results.

Freeborn in [13] has shown that using a MATLAB based optimization approach, the transfer function coefficients of $(1+ \alpha)$ order FOLP filter can be obtained more accurately for specified least square error in the pass band, cut-off frequency, stability margin etc. Numerical simulations and circuit simulations of Tow-Thomas biquad realization for three different order FOLP filters have been presented.

Laguerre impulse response approximation method has been used for implementation of fractional order filters in [14]. A method based on optimization of fractional characteristics specimen function has been proposed in [15] to determine the coefficients of the fractional order band pass filter transfer function with asymmetric stop band characteristics using MATLAB. Experimental and simulation results for fractional order Tow-Thomas bi-quad structure have also been presented.

Soltan, Radwan and Soliman have presented a passive fractional order Butterworth low pass filter in [18]. The series connection of R-L-C circuit is used to study the two different cases of fractional order low pass filter.

A metaheuristic optimization algorithm based approach to design $(1 + \alpha)$ order low pass Butterworth filter in terms of an integer order continuous-time filter of third order was proposed in [24]. Due to the improved search efficiency of the search agents in exploring and exploiting the non-uniform and multimodal error surface, the proposed gravitational search algorithm (GSA) based designs achieve the best magnitude responses in a consistent and computationally proficient manner as compared with the fractional order low pass Butterworth filter (FOLBFs) based on RGA and PSO.

In [25], the concept of fractional order complex Chebyshev filter was introduced. A fractional variation of Chebyshev differential equations was introduced based on Caputo fractional operator. The proposed equation was solved using fractional Taylor power series method.

In [26], fractional order transfer functions to approximate the pass band and stop band ripple characteristics of a second-order elliptic low pass filter were designed and validated. The necessary coefficients for these transfer functions were determined

through the application of a least squares fitting process. These fittings were applied to symmetrical and asymmetrical frequency ranges to evaluate how the selected approximated frequency band impacts the determined coefficients using this process and the transfer function magnitude characteristics.

Design of a CFOA-based fractional order filter with low pass magnitude response optimized for minimum error in the frequency response, utilizing the decomposition of an approximated integer order transfer function representing a low pass fractional order filter of order $(1+\alpha)$ has been presented in [27].

CFOA-based fractional order filters utilizing an approximated integer order transfer function implemented with functional block diagram approach is presented in [28] for the realization of $(1+\alpha)$ and $(5+\alpha)$ order filters.

A detailed stability analysis of fractional order Sallen-Key and KHN type filters with two different fractional order elements has been presented in [31]. The relationship between transfer function parameters and the singularities of the system along with several stability contours for the various values of the coefficients of transfer function has also been presented.

A Fractional order low pass and high pass filters of order $(1+\alpha)$ in current mode with Butterworth characteristics realized with second generation multi-output current conveyors and DDCCs have been presented in [32].

A multi objective optimization approach implemented in MATLAB for designing a FOLP filter with specified cut off frequency, stop band frequency (transition bandwidth) and pass band attenuation, determining the optimized values of α and the

transfer function coefficients has been presented in [33]. Two fractional order filters of order 1.6 and 3.6 are implemented using CCII. Experimental and simulation results are provided to validate the proposed design approach.

A general design procedure for prototype fractional order filter utilizing two port network concept has been proposed in [35]. The general transfer function along with the necessary network condition, critical frequency and stability condition are also derived for the forty six presented fractional order filters.

Effect of four different approximation techniques for the realization of s^α , namely, Oustaloup, Matsuda, CFE and Valsa on the performance of KHN bi-quad filters in respect of various critical parameters of the fractional order filters has been investigated in [36]. Experimental results of a fractional order KHN bi-quad filter in which the fractional order capacitors have been realized using Valsa method have also been presented.

CFOAs based fractional order filters have been reported in [37] with inverting and non-inverting modes of operations. SPICE simulations have been performed for fractional order low pass, high pass and band pass filter responses.

A multifunction fractional order filter based on single CDBA using five fractional order capacitors (three of them are of same order and two of different orders) was presented in [38]. Numerical simulations using FOCOM toolbox of MATLAB and SPICE based circuit simulations have been carried out to validate the workability of these filters.

Inverted impedance multiplier circuit (IIMC) employing OTAs has been used to realize fractional order inductors (FI) and fractional order capacitors (FC) for $\alpha > 1$ in

[40]. The applications of realized FC and FI in the design of higher order FOLP, FOHP, and FOBP filters have also been presented. Experimental verification of proposed IIMC was performed using LM 13600N dual OTAs IC.

An approach for designing FOLP and FOHP filters using OTAs and current amplifiers with standard capacitors and without using any passive resistors were reported in [41]. The realized filter structures were reconfigurable in which the order of the filter and the coefficients of the filter transfer function determining the performance of the filter can be controlled electronically. SPICE simulations and experimental results are provided to validate the proposed fractional order filters.

Suksang, Pirajnanchai and Loedhammacakra [42] have reported a tunable OTA low pass filter using fractional-order step technique. The proposed structure has employed an IC LT1228 to realize the said filter.

A generalized fractional order filter structure using OTAs, which can realize FOLP, FOHP, FOBP, FOAP and fractional order band stop filter responses have been presented in [43], wherein resistor less realization of these fractional order filters having all grounded capacitors and electronically controllable parameters like cut-off frequency and order of filter have been proposed. The simulation results of fractional order filters of order 0.5, 1.2, 1.5 and 1.8 were also presented.

In [44], a $(1+\alpha)$ order fully differential low pass filter using OTAs, adjustable current amplifiers (ACAs) and fully differential current conveyors has been reported. The proposed filter structure is based on inverse follow the leader feedback (IFLF) topology. The order ' α ' of the filter as well as the cut-off frequency are electronically controllable.

An electronically tunable fractional order all pass filter using two OTAs and one fractional order capacitor has been proposed in [45]. In [48], trans-admittance mode fractional order filter topology has been reported. Fractional order low pass, high pass and all pass filters were realized with two OTAs and one fractional order capacitor. Through PSPICE simulations as well as experimentally, the proposed fractional order filters were verified.

Single-input multiple-output and multiple-input single-output fractional-order filter topologies were reported in [50], constructed from two fractional order integrators with appropriate feedback and feed-forward paths, as well as from summation stages.

Multi-input single-output fractional order filter structure using three OTAs was proposed in [51]. Fractional order low pass, band pass, high pass, band reject and all pass filters can be realized with the same topology. PSPICE simulation results are provided to validate the proposed fractional order filter structure.

An ultra-low sub-hertz range frequency fractional order filter scheme was presented in [53]. In addition to low frequency design, the filter offers the features of electronic tunability.

In [54], the authors proposed a multifunctional reconfigurable fractional-order filter having low-pass, high-pass, band-pass and band-reject transfer functions. The circuit has provision to provide the electronic control of the pole frequency and quality factor.

A multi-function fractional-order filter topology, constructed from 2 MOS transistors only, was introduced in [55]. The main attractive feature was the significant reduction of MOS transistor count and, consequently, the reduced power dissipation.

Design procedure for the realization of FOLP and FOBP filters with Butterworth type characteristics, in which the values of passive elements can be calculated in terms of cut-off frequency using two differential voltage current conveyors has been reported in [57].

In [58], differential difference current conveyors (DDCCs) based realization of $(1+\alpha)$ order FOLP filter approximated by second order approximation of the Laplacian operator has been proposed.

In [59], authors have outlined the use of universal voltage conveyors (UVCs) in the design of FOLP and FOHP filters. FOLP and FOHP transfer functions were approximated by integer order transfer functions of third order, using continued fraction expansion (CFE) method. The resultant transfer functions of FOLP and FOHP filters were implemented using UVCs devices. The PSPICE simulation results of FOLP and FOHP filters of order 1.3, 1.5 and 1.7 were provided to validate the theoretical findings.

Capacitor-less lossy and lossless integrators using current mirrors have been employed in [60] to propose MOS only structure of FOLP, FOBP, FOHP and fractional order band reject filters based on IFLF topology realizing integer order approximation of these filters. Various filter parameters of these fractional order filters can be controlled digitally.

Kubanek and Freeborn in [61] have determined the coefficients of three different fractional $(1+\alpha)$ order low pass transfer functions by minimizing the error between these fractional order transfer functions and the second order transfer function using least square optimization with `fminsearch` function of MATLAB. Simulations of fractional order low pass filter (order 1.5) using two DVCCs and one fractional order capacitor were carried out to validate the theoretical findings.

A new family of low-pass filters has been proposed in [66], which allows the tuning of the cut-off frequency between 20 Hz and 20 kHz and that of the filter attenuation between 0 and -6 Decibels per octave, separately and independently from one another.

A low-pass fractional order filter topology based on a single MOSFET was presented in [67]. The filter was realized using a fractional order capacitor fabricated using multi-walled carbon nanotubes. The electronic tuning capability of the filter's frequency characteristics was achieved through a biasing current source.

In [68], authors introduced the proposal of the fractional order low pass filter, operating in current mode and providing the ability to electronically adjust the order and pole frequency by changing values of the individual transfers. Simulation and experimental results of the electronically controlled order and pole frequency were compared.

Fractional-order filter realizations with Chebyshev characteristics, approximated by appropriate integer-order topologies, were realized in [69]. The employed active building blocks were current-mirrors and the derived filters were capable of operating in a low-voltage environment and resistor-less realization.

In [70], six optimal fractional order transfer functions (FOTF) approximating the magnitude characteristics of a fractional-order high pass Butterworth filter were presented. A novel cost function was proposed which specifically considers the characteristics of an ideal $(1 + \alpha)$ order ($0 < \alpha < 1$), high pass Butterworth filter over the pass band as well as the stop band. One of these transfer functions (current mode fractional order high pass) is implemented using CCIIIs.

In [71], a new kind of fractional order Butterworth-like filter has been designed using the consideration of poles lying on a circle in the transformed w -plane and also using the concept of stability in complex w -plane. The obtained fractional Butterworth-like filters were analysed from the nature of poles, as well as in the time and frequency domains.

A fractional order differential operator had been simulated in MATLAB for different input signals and different values of α (fractional order) in [72]. The simulated results showed that the response of the system was noticeably different for the integer and non-integer values and it was observed that for gradual change of α from 0 to 1, the fractional order system resulted in gradual change in the output response.

Optimal integer-order transfer function approximations to model the single fractance element-based fractional order low-pass filter for any arbitrary order ' α ', where, $0 < \alpha < 1$, was proposed in [73] with ' α ' varying from 0.01 to 0.99 in steps of 0.01.

A fractional order Chua's circuit based on a new look at Chua's chaotic oscillator where the circuit has been regarded as an interconnection between an oscillator, a passive low pass filter and an active load was presented in [74].

In [75], the fractional order model of a phantom electroencephalographic system, at various distances between electrodes, was realized using appropriate decomposition of the rational transfer function which approximated the high pass filter that describes its dynamics.

A multi-function fractional order filter topology realized, utilizing the partial fraction expansion tool, was introduced in [76]. The implementation of the filter functions, offers reduced circuit complexity without losing the important benefit of the electronic tuning of the frequency characteristics.

A fractional order Wiener filter was proposed in [77], for restoring reference objects in a fractional correlation system. In [78], a current differencing buffered amplifier based current mode universal filter with fractional order capacitor was proposed. A piecewise frequency control (PFC) strategy was proposed in [79] for coordinating vibration isolation and positioning of supporting systems under complex disturbance conditions, such as direct and external disturbances. This control strategy was applied in an active-passive parallel supporting system, where relative positioning feedback for positioning and absolute velocity feedback for active vibration isolation was used.

An application of PSO algorithm for fractional order filter function discretization for digital signal processing applications was presented in [80]. The proposed method contributes to digital filter design.

In [81], multiple methods to generate $(1 + \alpha)$ order FOHP, FOBP filter transfer functions from their FOLP counterparts were presented.

A new approach to design fractional order low pass Butterworth filters (FOLPBF) in terms of integer order rational approximations meeting an accurate magnitude response was proposed in [82].

In [83], a novel solution of a fully differential $(1+\alpha)$ fractional-order filter was reported. The filter can provide low-pass, high-pass, band-pass and band-stop transfer functions without a change in circuit topology.

In [84], the design method of IIR filters, using an improved genetic algorithm to optimize the coefficients of fractional order differentiator was introduced. Experimental results were given to show that the algorithm can deal with all cases of fractional differentiator design problem, and made even more outstanding than the traditional design method results.

In [85], Soni and Gupta have reported the approximated behaviour of low pass Bessel filter of Tow-Thomas filter configuration. Interior search algorithm (ISA) was used for the approximation of the behaviour of proposed fractional order filter. $(1+\alpha)$ order low pass filters were analysed with MATLAB and PSPICE software tools.

Soni and Gupta in [86], have proposed the fractional order low pass Chebyshev filter using Tow-Thomas filter configuration. Three optimization techniques namely simulated annealing (SA), non-linear least square (NLS) and interior search algorithm (ISA) were used to optimize the proposed filters.

The design and realization of fractional order Butterworth low pass filter of order $(1+\alpha)$, with $0 < \alpha < 1$, optimized employing a speed enhanced series combination of two meta-heuristic algorithms namely cuckoo search algorithm (CSA) and ISA was presented by Soni, Sreejeth, Saxena and Gupta in [87].

After presenting a detailed account of important works reported on the realization of fractional order filters, we now present new structures of fractional order filters realized with current feedback operational amplifier (CFOA) with two/three fractance devices.

3.4. Voltage Mode Fractional Order Filters Employing a Single CFOA

Current feedback operational amplifier or the trans-impedance amplifier with an externally accessible compensation pin, such as AD844, is a very versatile analog circuit building block for analog circuit design, as compared to conventional voltage mode op-amp in many signals processing as well as signal generation applications. CFOAs are receiving considerable attention in analog circuit design as they offer two significant advantages over op-amps namely, very high slew rates and a constant bandwidth which is independent of the gain [90]. They have been extensively used for the realization of various analog signal processing circuits both in integer order domain as well as in fractional order domain.

The CFOA is a four terminal analog active building block characterized by the hybrid matrix equation (3.39):

$$\begin{bmatrix} i_y \\ v_x \\ i_z \\ V_w \end{bmatrix} = \begin{bmatrix} 0 & 0 & 0 \\ 1 & 0 & 0 \\ 0 & 1 & 0 \\ 0 & 0 & 1 \end{bmatrix} \begin{bmatrix} V_y \\ i_x \\ V_z \\ i_w \end{bmatrix} \quad (3.39)$$

From matrix equation (3.39), terminal equations can be deduced as:

$$i_y = 0, v_x = v_y, i_z = I_x \text{ and } v_w = v_z \quad (3.40)$$

The circuit symbol of CFOA is shown in Fig. 3.10.

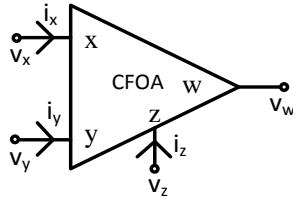


Figure 3.10 Circuit symbol of CFOA

In the following, we introduce two new circuits of single CFOA-based fractional order filters (FOFs) operating in voltage mode. With appropriate choice(s) of branch admittance(s), fractional order low pass filter, fractional order band pass filter and fractional order high pass filter responses can be derived from the same configuration. Two identical fractional order capacitors have been used the design of fractional order filters (FOFs).

3.4.1. First Structure of Fractional Order Filter²

Fig. 3.11 shows the first proposed generalized configuration of the proposed FOFs. Assuming an ideal CFOA ($i_y = 0, v_x = v_y, i_z = i_x$ and $v_w = v_z$), the transfer function is found to be:

$$\frac{V_0}{V_{in}} = - \frac{y_1 y_2}{y_4 (y_1 + y_2 + y_3)} \quad (3.41)$$

where $y_i, i=1-4$ are the branch admittances.

² The work presented in this section has been published in : Manoj kumar, D. R. Bhaskar and P. Kumar, "A multifunctional voltage mode fractional order filters using a single CFOA," International Journal of Innovative and Technology Exploring Engineering, vol. 9, no. 4, pp. 687-691, 2020.

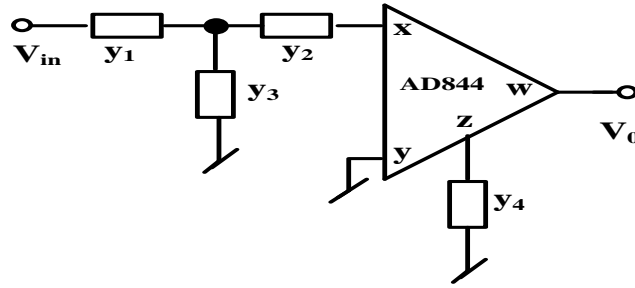


Figure 3.11 First Configuration of FOFs

The various filters responses viz. FOLP, FOBP and FOHP can be obtained from equation (3.41) by appropriate choice(s) of different branch admittances. Table 3.14 shows the selection of branch admittances to realise various fractional order filters.

Table 3.14 Various fractional order filter transfer functions derived from equation (3.41)

Filter	y_1	y_2	y_3	y_4	$\frac{V_0}{V_{in}}$
FOLP	$\frac{1}{R_1}$	$\frac{1}{R_2}$	$s^\alpha C_3$	$s^\alpha C_4 + \frac{1}{R_4}$	$-\frac{K_1}{D_1(s)}$
FOBP	$\frac{1}{R_1}$	$s^\alpha C_2$	$\frac{1}{R_3}$	$s^\alpha C_4 + \frac{1}{R_4}$	$-\frac{K_2 s^\alpha}{D_2(s)}$
FOHP	$s^\alpha C_1$	$s^\alpha C_2$	$\frac{1}{R_3}$	$s^\alpha C_4 + \frac{1}{R_4}$	$-\frac{K_3 s^{2\alpha}}{D_3(s)}$

where $D_1(s) = s^{2\alpha} + a_1 s^\alpha + b_1$, $D_2(s) = s^{2\alpha} + a_2 s^\alpha + b_2$, $D_3(s) = s^{2\alpha} + a_3 s^\alpha + b_3$ and
 $K_1 = \frac{1}{R_1 R_2 C_3 C_4}$, $K_2 = \frac{1}{R_1 C_4}$ and $K_3 = \frac{C_1 C_2}{C_4 (C_1 + C_2)}$

The coefficients a_1 - a_3 and b_1 - b_3 for the FOLP, FOBP and FOHP filters are mapped with the values of various passive elements as given below in Table 3.15.

Table 3.15 Mapping of the coefficients of the characteristic equation with the passive components of the fractional order filters

Filter Coefficients			
a_1	$\frac{1}{C_3} \left(\frac{1}{R_1} + \frac{1}{R_2} \right) + \frac{1}{R_4 C_4}$	b_1	$\frac{1}{C_3 C_4 R_4} \left(\frac{1}{R_1} + \frac{1}{R_2} \right)$
a_2	$\frac{1}{C_2} \left(\frac{1}{R_1} + \frac{1}{R_3} \right) + \frac{1}{R_4 C_4}$	b_2	$\frac{1}{C_2 C_4 R_4} \left(\frac{1}{R_1} + \frac{1}{R_3} \right)$

a_3	$\frac{1}{R_4 C_4} + \frac{1}{R_3 (C_1 + C_2)}$	b_3	$\frac{1}{R_3 R_4 C_4 (C_1 + C_2)}$
-------	-------------------------------------------------	-------	-------------------------------------

Thus, from Table 3.14, it is seen that the FOLP and FOBP can be realized using three resistors and two fractional order capacitors ($0 < \alpha < 1$), while for FOHP, two resistors and three fractional order capacitors are needed.

The ω_h of fractional order low pass and high pass filters, and maximum frequency (ω_m) can be obtained from following equations:

FOLP:

$$\omega_h^{4\alpha} + 2a_1\omega_h^{3\alpha}\cos\left(\frac{\alpha\pi}{2}\right) + \omega_h^{2\alpha}(a_1^2 + 2b_1\cos(\alpha\pi)) + 2a_1b_1\omega_h^\alpha\cos\left(\frac{\alpha\pi}{2}\right) - b_1^2 = 0 \quad (3.42)$$

FOHP:

$$b_3^2 + 2a_3\omega_h^{3\alpha}\cos\left(\frac{\alpha\pi}{2}\right) + \omega_h^{2\alpha}(a_3^2 + 2b_3\cos(\alpha\pi)) + 2a_3b_3\omega_h^\alpha\cos\left(\frac{\alpha\pi}{2}\right) - \omega_h^{4\alpha} = 0 \quad (3.43)$$

FOBP:

$$\omega_m = (b_2)^{\frac{1}{2\alpha}} \quad (3.44)$$

3.4.1.1. PSPICE and MATLAB Simulation Results

PSPICE simulations of the proposed FOFs as shown in Fig.3.11 have been carried out for FOLP, FOBP and FOHP responses. In the simulations PSPICE macro-model of AD844 supplied by Analog Devices has been used along with two/three simulated fractional order capacitors and three/two conventional resistors to verify the workability of the proposed FOF circuits. The component values (the value of resistors and FCs), required to realize the FOLP, FOBP and FOHP responses of FOFs for a half power frequency/ maximum frequency of 500 Hz (for $\alpha = 1$) are given in Table 3.16.

Table 3.16. Component values for the realization of fractional order filter used in PSPICE simulation

Type of filter	Resistor	Fractional Capacitor
FOLP	$R_1 = 690\Omega$ $R_2 = 690\Omega$ $R_4 = 690\Omega$	$C_3 = 0.382\mu\text{F}/\text{sec}^{(\alpha-1)}$ $C_4 = 0.382\mu\text{F}/\text{sec}^{(\alpha-1)}$
FOBP	$R_1 = 1120\Omega$ $R_3 = 1120\Omega$ $R_4 = 1120\Omega$	$C_2 = 0.382\mu\text{F}/\text{sec}^{(\alpha-1)}$ $C_4 = 0.382\mu\text{F}/\text{sec}^{(\alpha-1)}$
FOHP	$R_1 = 1000\Omega$ $R_4 = 1000\Omega$	$C_2 = 0.382\mu\text{F}/\text{sec}^{(\alpha-1)}$ $C_1 = 0.382\mu\text{F}/\text{sec}^{(\alpha-1)}$ $C_4 = 0.382\mu\text{F}/\text{sec}^{(\alpha-1)}$

The fractional order capacitors, used to realize the FOFs have been designed using a method proposed by Valsa, Dvorak and Friedl [89]. The R-C ladder structure along with symbolic representation of FC are shown in Fig. 3.12, while the passive components used in the design of the FC, for various values of the fractional order parameters are provided in Table 3.17

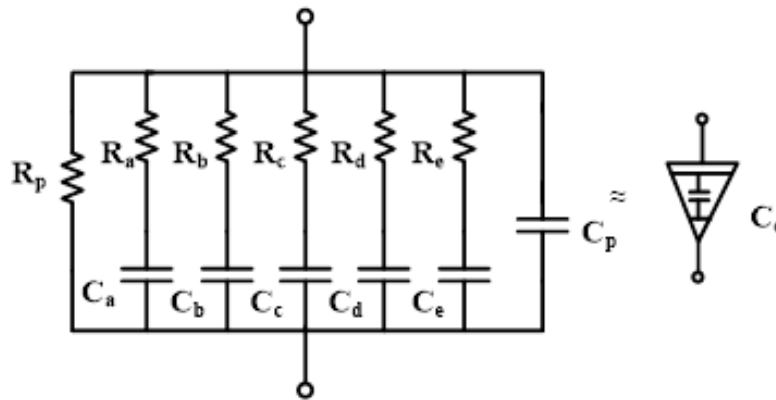


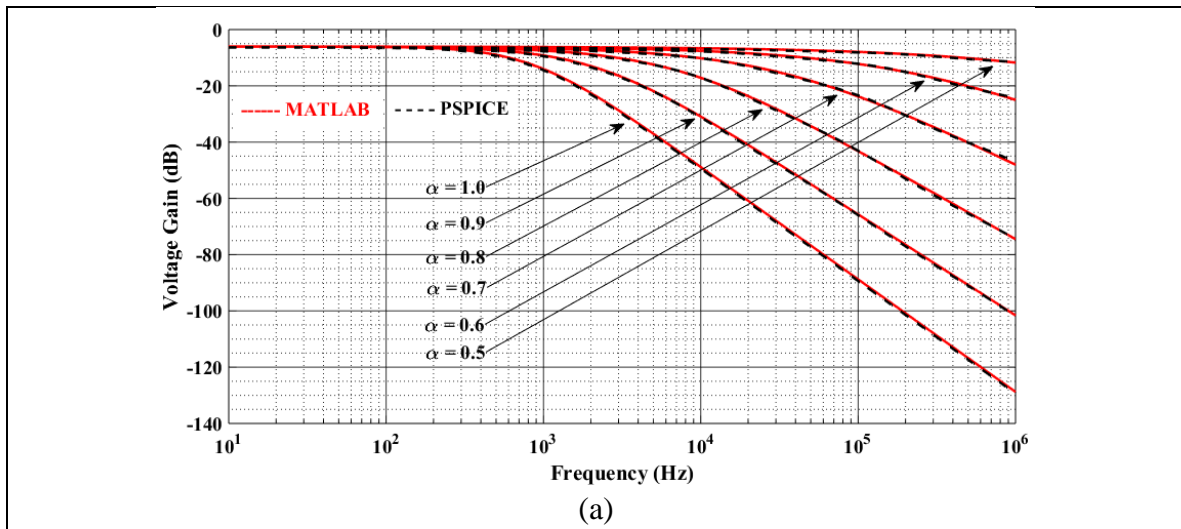
Figure 3.12 RC ladder structure used to realize fractional order capacitors for the value of $0.382 \mu\text{F}/\text{sec}^{(\alpha-1)}$

Table 3.17 Component values for the realization of FCs

' α '	$C_f = 0.382 \mu\text{F}/\text{sec}^{(\alpha-1)}$	
	Resistors	Capacitors
0.9	$R_a=168.95, R_b = 17.40, R_c = 1.79,$ $R_d = 0.18, R_e = .019, R_p = 1471.36$	$C_a = 59, C_b = 46, C_c = 35, C_d = 27, C_e = 21,$ $C_p = 75$
0.8	$R_a=142.47, R_b = 8.89, R_c = 2.5,$ $R_d = 0.33, R_e = 0.04, R_p = 932.16$	$C_a = 70.19, C_b = 42.35, C_c = 25.56, C_d = 15.42$ $C_e = 9.31, C_p = 14.15$
0.7	$R_a=165.52, R_b = 28.25, R_c = 4.82,$	$C_a = 60.41, C_b = 28.32, C_c = 13.27, C_d = 6.22,$

	$R_d = 0.82, R_e = 0.14, R_p = 804.3$	$C_e = 2.92, C_p = 2.57$
0.6	$R_a = 224.43, R_b = 49.31, R_c = 10.83,$ $R_d = 2.38, R_e = .52, R_p = 797.06$	$C_a = 44.56, C_b = 16.22, C_c = 5.91, C_d = 2.15,$ $C_e = 0.78, C_p = 0.48$
0.5	$R_a = 338.96, R_b = 95.87, R_c = 27.12,$ $R_d = 7.67, R_e = 2.17, R_p = 859.45$	$C_a = 29.5, C_b = 8.34, C_c = 2.36, C_d = 0.67, C_e =$ $0.19, C_p = .074$
All resistors are in $k\Omega$ and capacitors are in nF .		

Using same component values (as used in PSPICE simulations), the transfer function of FOFs given in Table 3.14 have also been simulated using MATLAB for different values of α (from 0.5 to 1.0). The frequency responses of FOFs obtained from PSPICE and MATLAB simulations are shown in Fig. 3.13, while the obtained numerical results are provided in Table 3.18 (for frequency) and Table 3.19 (for stop band attenuation) respectively. Thus, workability of proposed FOFs has been tested through PSPICE as well as MATLAB simulations.



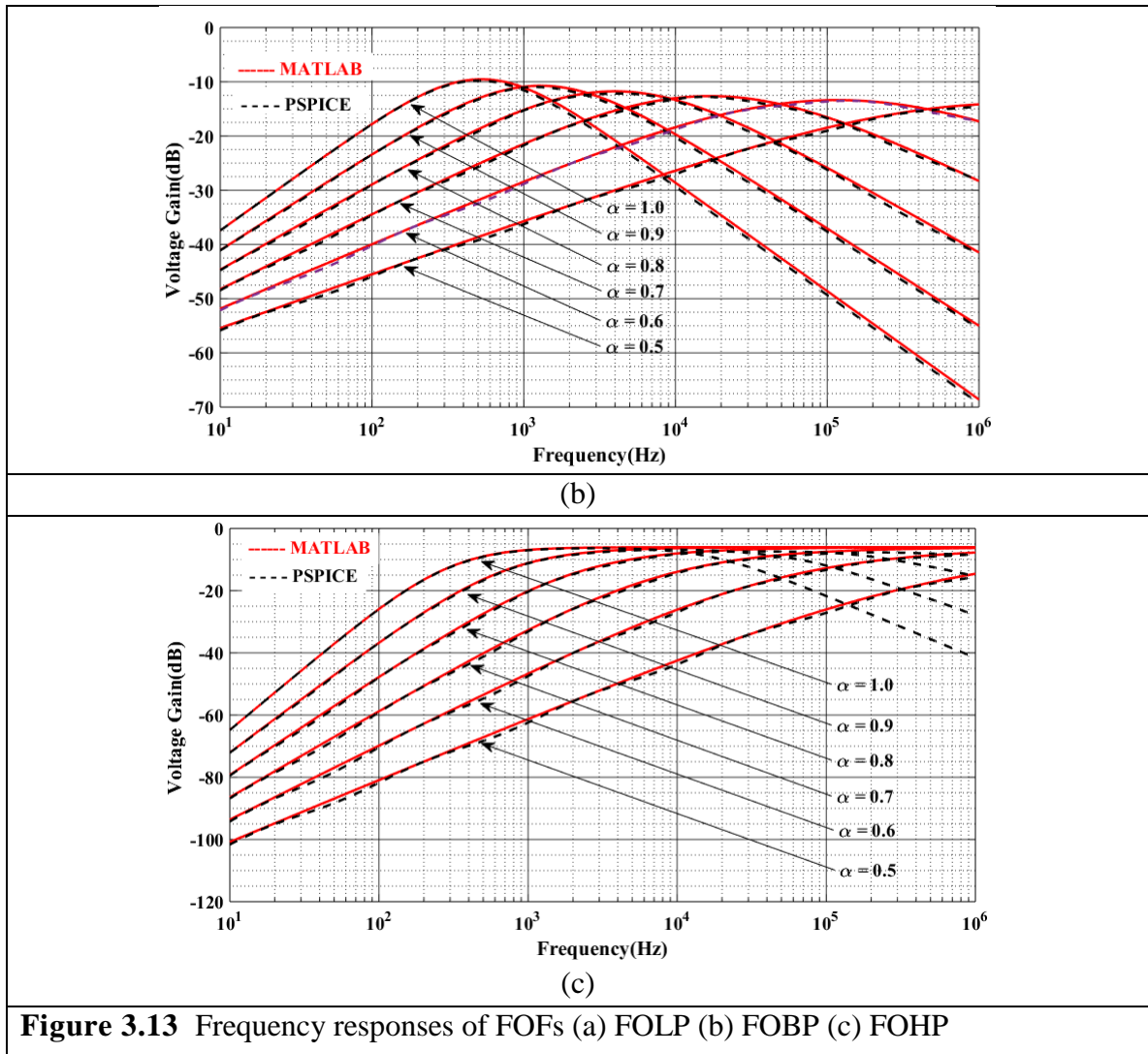


Table 3.18 Simulation results for half power/maximum frequency (kHz)

Frequency (in kHz)		Value of α					
		1.0	0.9	0.8	0.7	0.6	0.5
Half power frequency (FOLP)	PSPICE	0.49	0.972	2.21	7.03	28.0	273
	MATLAB	0.50	1.10	2.35	7.07	29.3	280
	Theoretical	0.51	0.955	2.16	6.455	29.11	254.48
Half power frequency (FOHP)	PSPICE	0.501	1.66	7.24	38.9	397	-
	MATLAB	0.498	1.57	6.60	38.89	400	9.8M
	Theoretical	0.497	1.57	6.51	38.78	398.47	9.79M

Maximum frequency (FOBP)	PSPICE	0.501	1.20	4.26	15.49	134.8	1.0M
	MATLAB	0.525	1.26	4.10	15.89	122.0	1.6M
	Theoretical	0.525	1.29	3.98	16.9	116.59	1.73M

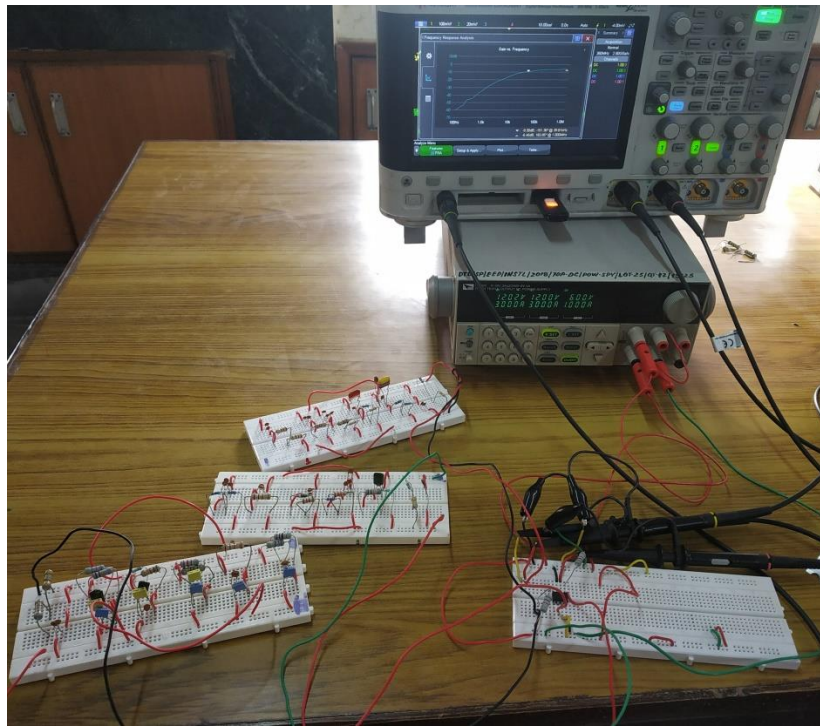
Table 3.19 Simulation results for stop band attenuation (dB/decade)

Attenuation (dB/decades)		Value of α					
		1.0	0.9	0.8	0.7	0.6	0.5
Attenuation (FOLP)	PSPICE	39.96	36.96	32.42	27.46	21.93	14.32
	MATLAB	39.70	35.24	31.79	26.43	32.70	18.24
	Theoretical	40.00	36.00	32.00	28.00	24.00	20.00
Attenuation (FOHP)	PSPICE	38.46	35.26	31.67	27.87	23.94	19.95
	MATLAB	39.29	35.51	31.66	27.82	23.85	19.92
	Theoretical	40.00	36.00	32.00	28.00	24.00	20.00
Attenuation (FOBP)	PSPICE	19.75	17.80	15.87	13.93	11.95	9.95
	MATLAB	19.88	18.05	15.91	13.57	11.82	9.97
	Theoretical	20	18	16	14	12	10

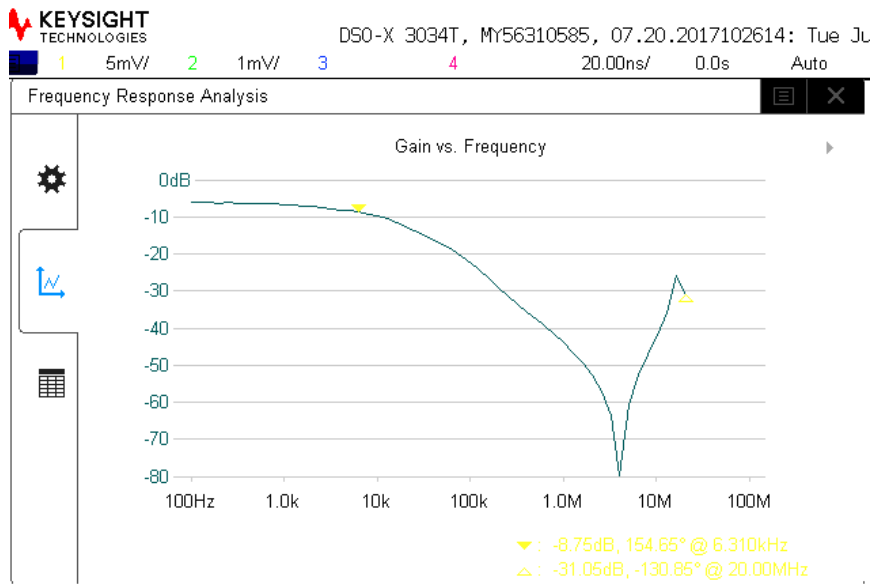
From the Tables 3.18 and 3.19, it may be noticed that both the PSPICE and MATLAB simulation results of the proposed FOFs are in good agreement with the theoretical values.

3.4.1.2. Experimental Results of the Proposed FOFs

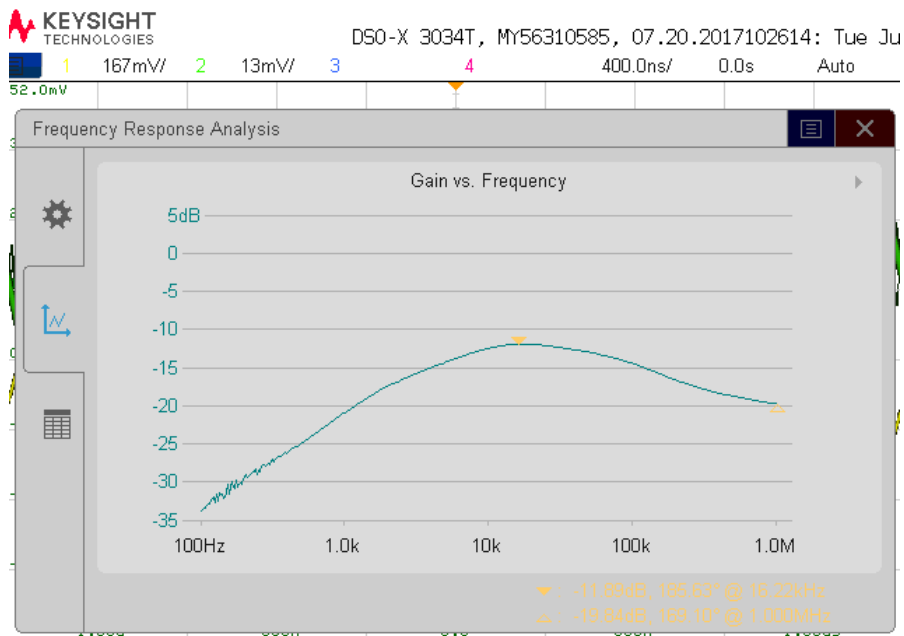
The workability of proposed FOFs has also been corroborated experimentally using AD844, resistors and fractional order capacitors. To examine the performance of FOLP, FOBP and FOHP filters, we have bread-boarded the circuits as given in Fig.3.11 using discrete components whose values are given in Table 3.16 for $\alpha = 0.7$. The DC power supply voltages of ± 12 V were used to bias the AD844. All three responses (FOLP, FOBP and FOHP) of FOFs are obtained separately using KEYSIGHT DSOX-3034T and these are shown in Fig. 3.14 along with one snapshot of experimental set up.



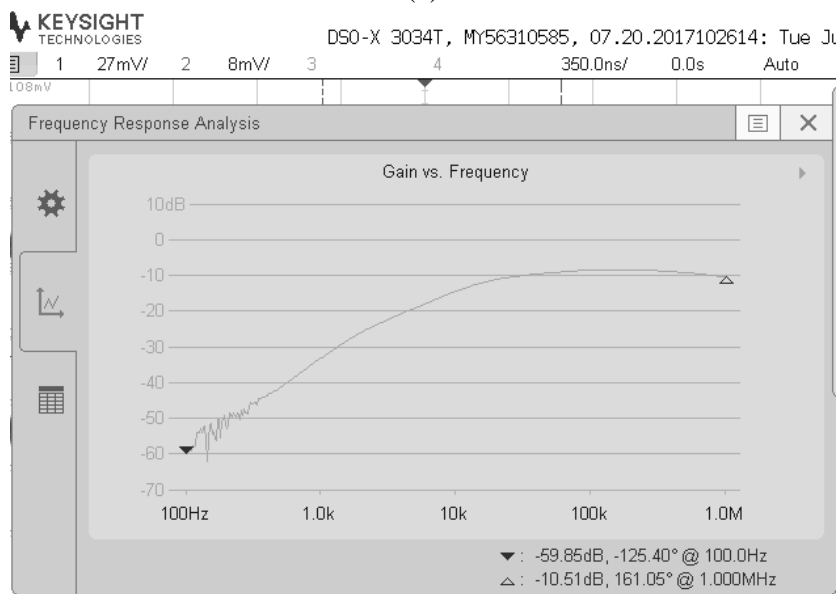
(a)



(b)



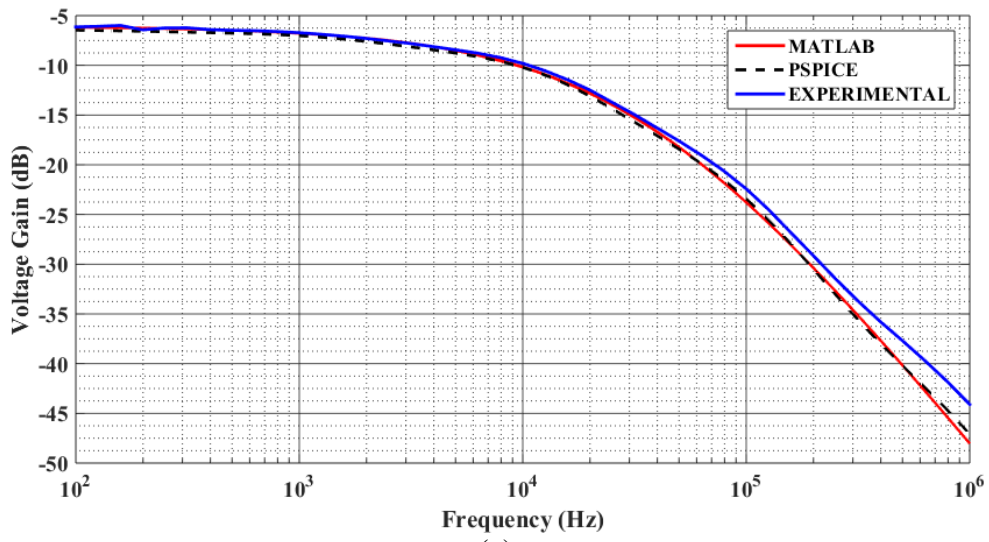
(c)



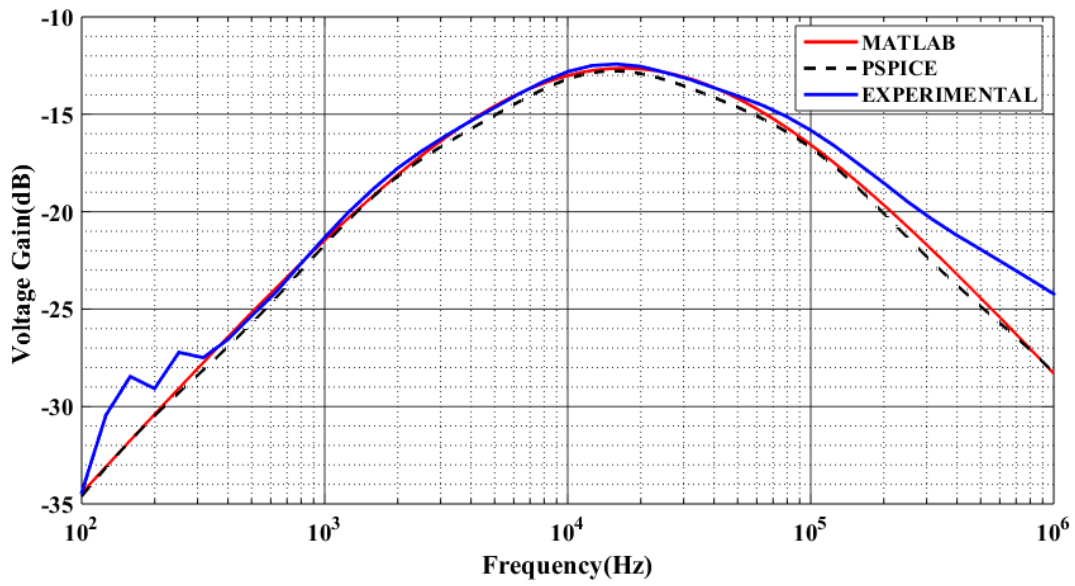
(d)

Figure 3.14 (a) Experimental results and Frequency responses (a) Experimental setup (b) FOLP response (c) FOBP response (d) FOHP response

The experimentally acquired frequency responses of proposed FOFs along with responses obtained using PSPICE and MATLAB are shown in Fig. 3.15, while the numerical values of the half power frequencies and maximum frequencies are provided in Table 3.20



(a)



(b)

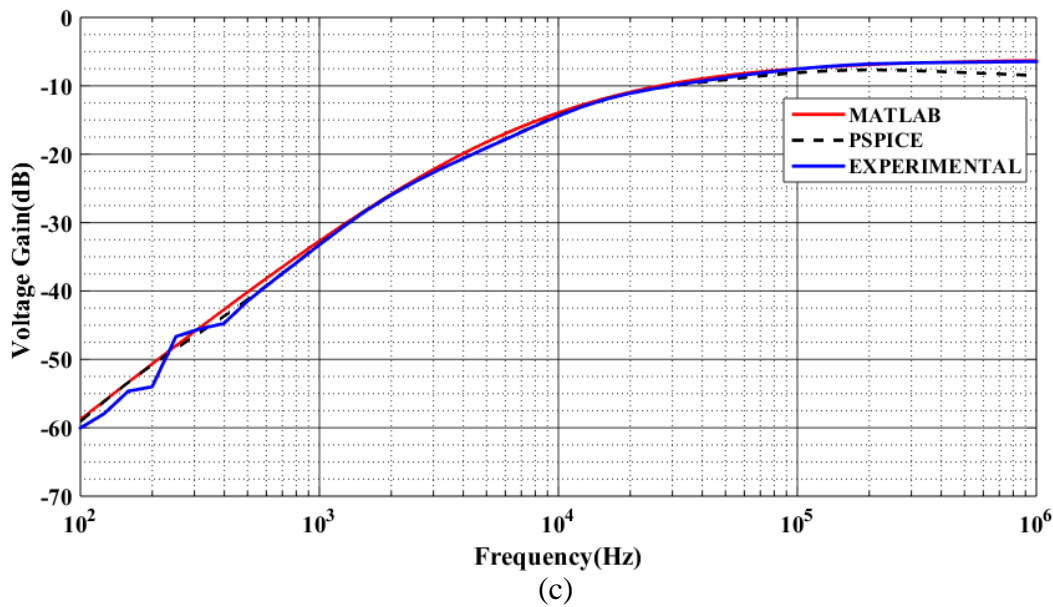


Figure 3.15 Experimental results superimposed on PSPICE and MATLAB results for $\alpha=0.7$ (a) FOLP (b) FOBP (c) FOHP

Table 3.20 Half power/maximum frequencies of proposed FOFs for $\alpha = 0.7$

Type of FOFs	Frequency (kHz)
FOLP	Half power frequency (kHz)
MATLAB	7.07
PSPICE	7.03
Experimental	7.50
FOBP	Minimum Frequency (kHz)
MATLAB	15.49
PSPICE	15.89
Experimental	15.39
FOHP	Half power Frequency (kHz)
MATLAB	38.89
PSPICE	38.98
Experimental	39.80

From the above results, it may be observed that the experimental results corroborate the results obtained from PSPICE simulations and MATLAB evaluations.

3.4.2. Second Structure of Fractional Order Filter

The second proposed multifunction fractional order filter structure is shown in Fig. 3.16

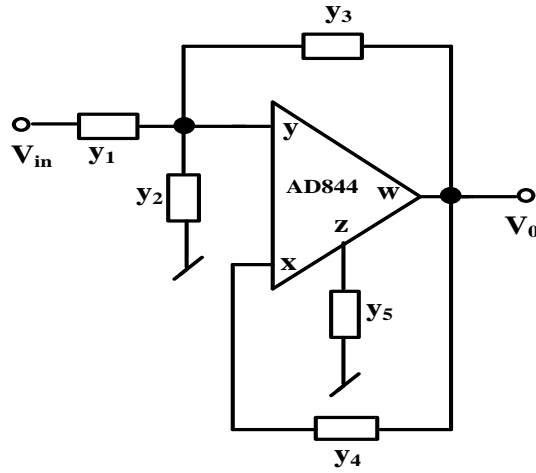


Figure 3.16 Proposed second configuration of FOFs

A routine circuit analysis (assuming ideal CFOA) of the structure of Fig.3.16 yields the following transfer function:

$$\frac{V_0}{V_{in}} = \frac{y_1 y_4}{y_5 (y_1 + y_2 + y_3) + y_4 (y_1 + y_2)} \quad (3.45)$$

where $y_i, i=1-4$ are the branch admittances.

From equation (3.45), various fractional order filters viz. FOLP, FOBP and FOHP can be realized with appropriately selecting the various branch admittances as given in Table 3.21.

Table 3.21 Various fractional order filter transfer function derived from equation (3.45)

FOFs	y_1	y_2	y_3	y_4	y_5	$\frac{V_0}{V_{in}}$
FOLP	$\frac{1}{R_1}$	$\frac{1}{R_2}$	$s^\alpha C_3$	$\frac{1}{R_4}$	$s^\alpha C_5$	$\frac{K_1}{D_1(s)}$
FOBP	$\frac{1}{R_1}$	$s^\alpha C_2$	$\frac{1}{R_3}$	$s^\alpha C_4$	$\frac{1}{R_5}$	$\frac{K_2 s^\alpha}{D_2(s)}$
FOHP	$s^\alpha C_1$	$\frac{1}{R_2}$	$\frac{1}{R_3}$	$s^\alpha C_4$	$\frac{1}{R_5}$	$\frac{K_3 s^{2\alpha}}{D_3(s)}$

where $D_1(s) = s^{2\alpha} + a_1s^\alpha + b_1$, $D_2(s) = s^{2\alpha} + a_2s^\alpha + b_2$, $D_3(s) = s^{2\alpha} + a_3s^\alpha + b_3$ and $K_1 = \frac{1}{R_1R_4C_3C_5}$, $K_2 = \frac{1}{R_1C_2}$ and $K_3 = 1$

The coefficients a_1 - a_3 and b_1 - b_3 for the FOLP, FOBP and FOHP filters are mapped with the values of various passive components as given below in Table 3.22.

Table 3.22 Mapping of the coefficients of the characteristic equation with the passive components of the fractional order filters

a_1	$\frac{1}{C_3} \left(\frac{1}{R_1} + \frac{1}{R_2} \right)$	b_1	$\frac{1}{C_3C_5R_4} \left(\frac{1}{R_1} + \frac{1}{R_2} \right)$
a_2	$\frac{1}{R_5C_4} + \frac{1}{R_1C_2}$	b_2	$\frac{1}{C_2C_4R_5} \left(\frac{1}{R_1} + \frac{1}{R_3} \right)$
a_3	$\frac{1}{R_5C_4} + \frac{1}{R_2C_1}$	b_3	$\frac{1}{R_5C_1C_4} \left(\frac{1}{R_2} + \frac{1}{R_3} \right)$

Thus, from Table 3.22, it is seen that the FOLP, FOBP and FOHP can be realized using three resistors and two fractional order capacitors ($0 < \alpha < 1$). The half power frequency (ω_h) of FOLP and FOHP filters and maximum frequency (ω_m) of FOBP filter can be obtained from equations (3.42), (3.43) and (3.44) respectively

3.4.2.1. MATLAB and PSPICE Simulation Results

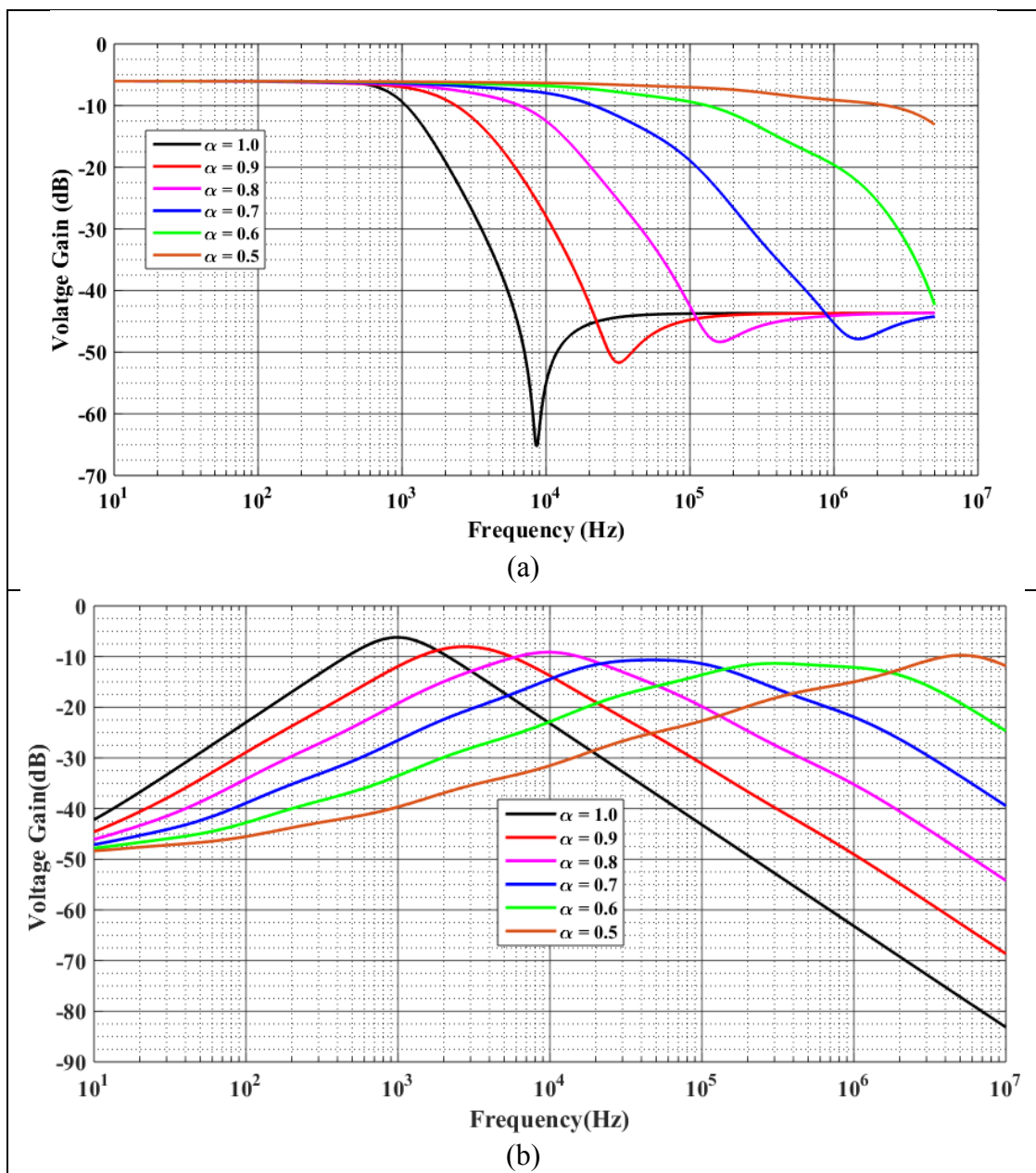
The fractional order filters realised from Fig. 3.16 have been simulated in PSPICE. The proposed circuits were validated using macro-model of AD844 CFOA and also validated through MATLAB simulations. The component values which are used in the design of fractional order filters are given below in Table 3.23.

Table 3.23 Component values for the realization of fractional order filter used in PSPICE simulation

Type of filter	Resistors	Fractional Capacitors
FOLP	$R_3 = 2.26K\Omega$ $R_4 = 2.26K\Omega$ $R_5 = 2.26K\Omega$	$C_1 = 0.0955\mu F/sec^{(\alpha-1)}$ $C_2 = 0.0955\mu F/sec^{(\alpha-1)}$

FOBP	$R_1 = 2.34\text{K}\Omega$ $R_3 = 2.34\text{K}\Omega$ $R_5 = 2.34\text{K}\Omega$	$C_2 = 0.0955\mu\text{F}/\text{sec}^{(\alpha-1)}$ $C_4 = 0.0955\mu\text{F}/\text{sec}^{(\alpha-1)}$
FOHP	$R_2 = 2.35\text{K}\Omega$ $R_3 = 2.35\text{K}\Omega$ $R_5 = 2.35\text{K}\Omega$	$C_1 = 0.0955\mu\text{F}/\text{sec}^{(\alpha-1)}$ $C_4 = 0.0955\mu\text{F}/\text{sec}^{(\alpha-1)}$

The PSPICE simulation and MATLAB results of the proposed fractional order filters of Fig. 3.16 are displayed in Fig. 3.17 and Fig. 3.18 respectively.



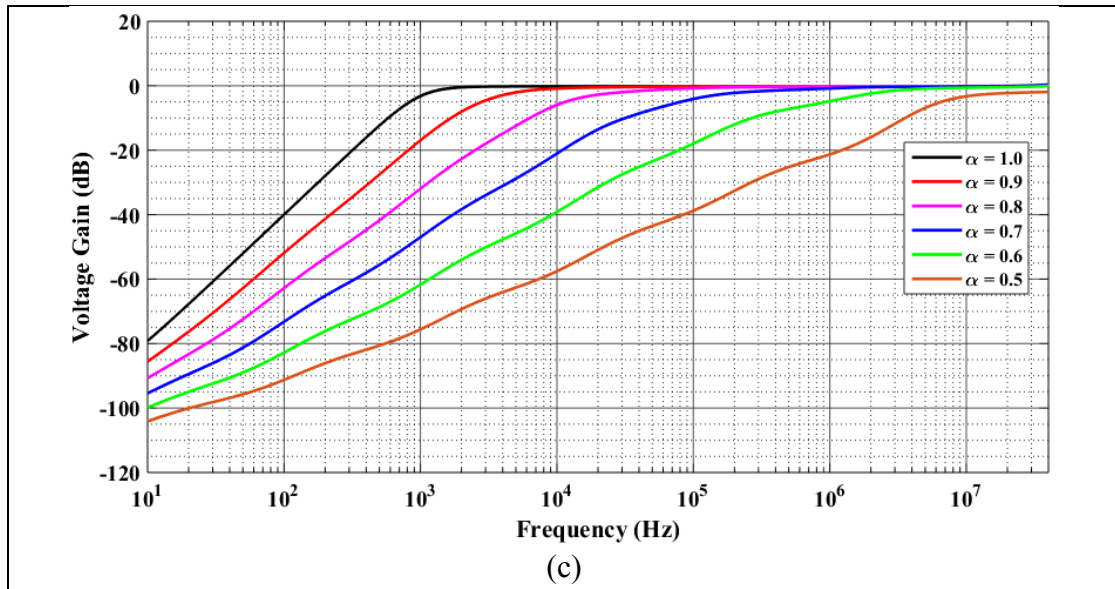
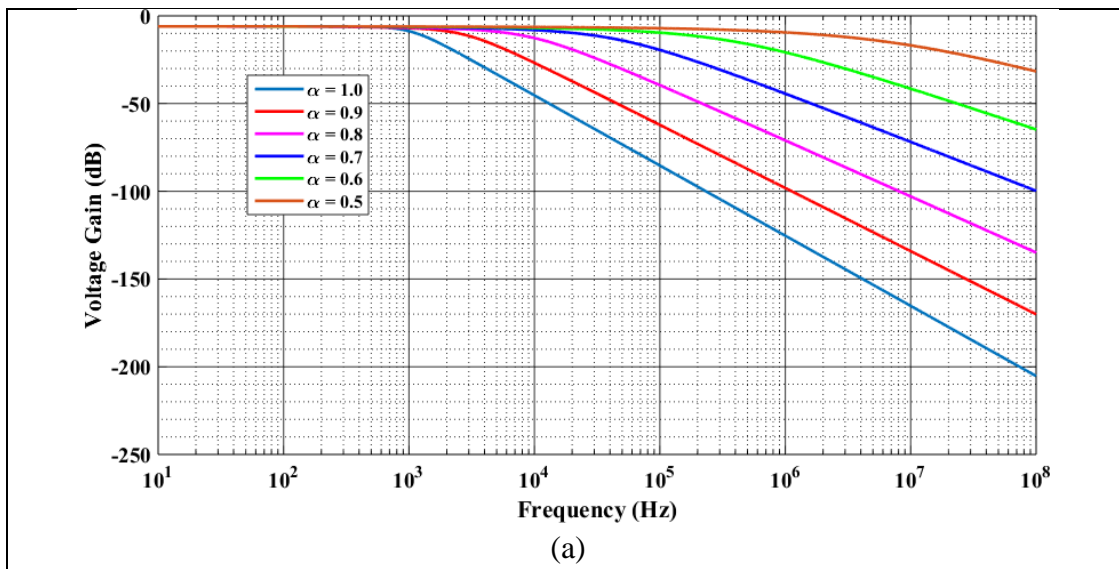


Figure 3.17 Frequency responses of FOFs using PSPICE (a) FOLP filter (b) FOBP filter (c) FOHP filter



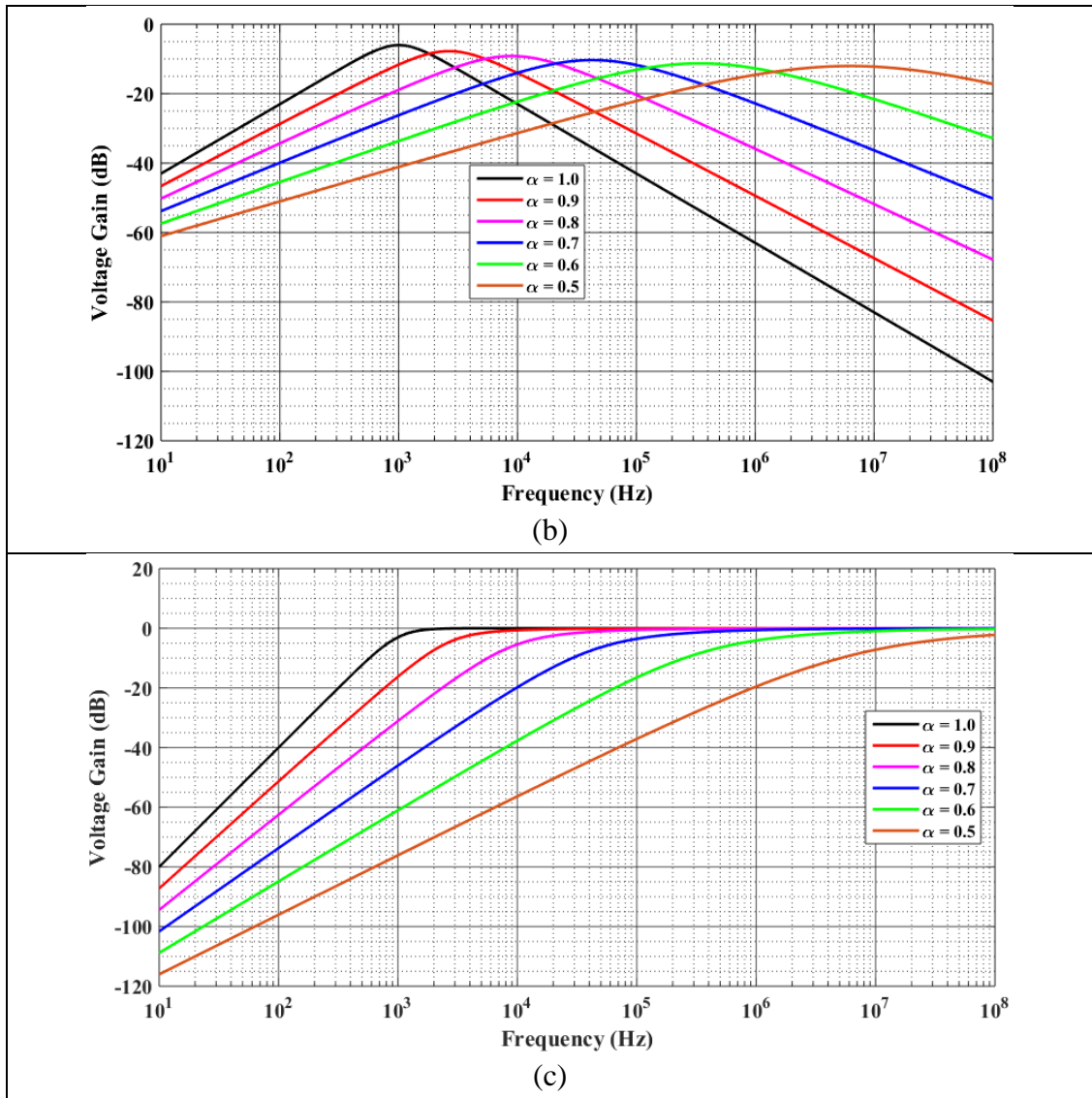


Figure 3.18 Frequency responses of FOFs using MATLAB (a) FOLP filter (b) FOBP filter (c) FOHP filter

A brief summary of simulation results of proposed FOFs of Fig. 3.16 with PSPICE and MATLAB are tabulated in Table 3.24 and Table 3.25 respectively.

Table 3.24 Simulation results for half power/maximum frequency (kHz)

Frequency (in KHz)		Value of α					
		1.0	0.9	0.8	0.7	0.6	0.5
Half power	PSPICE	1.000	2.042	5.012	16.22	81.13	891.30
	MATLAB	1.038	2.100	5.008	15.70	77.40	783.00

frequency (FOLP)	Theoretical	1.041	2.112	5.014	15.75	77.65	785.65
Half power frequency (FOHP)	PSPICE	1.00	3.71	16.98	120.00	1445	61660
	MATLAB	0.998	3.39	16.18	116.98	1528	36410
	Theoretical	1.001	3.46	16.68	121.64	1605.8	54859.86
Maximum frequency (FOBP)	PSPICE	0.997	2.60	9.49	41.62	277.44	5131
	MATLAB	0.998	2.65	8.974	40.76	310.4	5950
	Theoretical	1.006	2.66	8.97	42.82	344.17	6365.86

Table 3.25 Simulation results for stop band attenuation (dB/decade)

Attenuation (dB/decades)		Value of α					
		1.0	0.9	0.8	0.7	0.6	0.5
Attenuation (FOLP)	PSPICE	40.33	35.10	32.19	26.36	22.07	09.00
	MATLAB	39.97	35.39	31.51	27.53	22.46	12.39
	Theoretical	40.00	36.00	32.00	28.00	24.00	20.00
Attenuation (FOHP)	PSPICE	39.78	35.26	30.67	25.5	20.09	14.98
	MATLAB	39.43	35.06	31.40	27.65	23.81	19.98
	Theoretical	40.00	36.00	32.00	28.00	24.00	20.00
Attenuation (FOBP)	PSPICE	19.85	16.97	14.93	12.38	09.25	05.84
	MATLAB	20.20	18.09	16.06	14.57	12.08	10.08
	Theoretical	20	18	16	14	12	10

From Table 3.24 and 3.25, it is observed that the PSPICE and MATLAB results are in close proximity of theoretical findings. Thus, these results confirm the validity of the proposed FOFs of Fig. 3.16.

3.5. Current Mode Fractional Order Filter Configuration Using a Single CFOA

A new current mode fractional order filter using a single CFOA is shown in Fig 3.19, in which both input and output signals are current. A current source I_{in} is applied at node V_2 and output current (I_{out}) can be obtained at z-terminal of the CFOA.

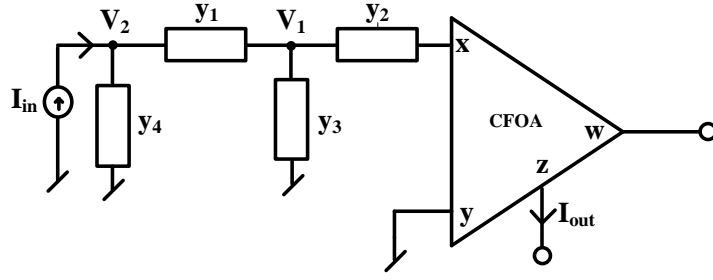


Figure 3.19 Proposed current mode fractional order generalized filter structure

A routine circuit analysis (assuming ideal CFOA) of Fig. 3.19 yields the following transfer function:

$$\frac{I_{out}}{I_{in}} = - \frac{y_1 y_2}{y_4 (y_1 + y_2 + y_3) + y_1 (y_2 + y_3)} \quad (3.46)$$

where $y_i, i=1-4$ are the branch admittances.

Equation (3.46) can now be used to realize various fractional order filters by appropriately selecting the various admittances as given in Table 3.26.

Table 3.26 Various fractional order filter transfer function derived from equation (3.46)

FOFs	y_1	y_2	y_3	y_4	$\frac{V_0}{V_{in}}$
FOLP	$\frac{1}{R_1}$	$\frac{1}{R_2}$	$s^\alpha C_3$	$s^\alpha C_4$	$-\frac{K_1}{D_1(s)}$
FOBP	$\frac{1}{R_1}$	$s^\alpha C_2$	$\frac{1}{R_3}$	$s^\alpha C_4$	$-\frac{K_2 s^\alpha}{D_2(s)}$
FOHP	$s^\alpha C_1$	$s^\alpha C_2$	$\frac{1}{R_3}$	$\frac{1}{R_4}$	$-\frac{K_3 s^{2\alpha}}{D_3(s)}$

where $D_1(s) = s^{2\alpha} + a_1 s^\alpha + b_1$, $D_2(s) = s^{2\alpha} + a_2 s^\alpha + b_2$, $D_3(s) = s^{2\alpha} + a_3 s^\alpha + b_3$ and $K_1 =$

$$\frac{1}{R_1 R_2 C_3 C_4}, K_2 = \frac{1}{R_1 C_4} \text{ and } K_3 = 1$$

The coefficients a_1 - a_3 and b_1 - b_3 for the FOLP, FOBP and FOHP filters are mapped with the values of various passive elements as given below in Table 3.27:

Table 3.27 Mapping of the coefficients of the characteristic equation with the passive components of the fractional order filters

a_1	$\frac{1}{C_3} \left(\frac{1}{R_1} + \frac{1}{R_2} \right) + \frac{1}{R_1 C_4}$	b_1	$\frac{1}{R_1 R_2 C_3 C_4}$
a_2	$\frac{1}{C_2} \left(\frac{1}{R_1} + \frac{1}{R_3} \right) + \frac{1}{R_1 C_4}$	b_2	$\frac{1}{R_1 R_3 C_2 C_4}$
a_3	$\frac{1}{C_2} \left(\frac{1}{R_3} + \frac{1}{R_4} \right) + \frac{1}{R_4 C_1}$	b_3	$\frac{1}{R_3 R_4 C_1 C_2}$

Thus, from Table 3.26, it is noted that the FOLP, FOBP and FOHP can be realized using two resistors and two fractional order capacitors only.

The ω_h of fractional order low pass and high pass filters, and ω_m of fractional order band pass filter can be obtained from the equations (3.42), (3.43) and (3.44) respectively.

3.5.1. MATLAB and PSPICE Simulation Results

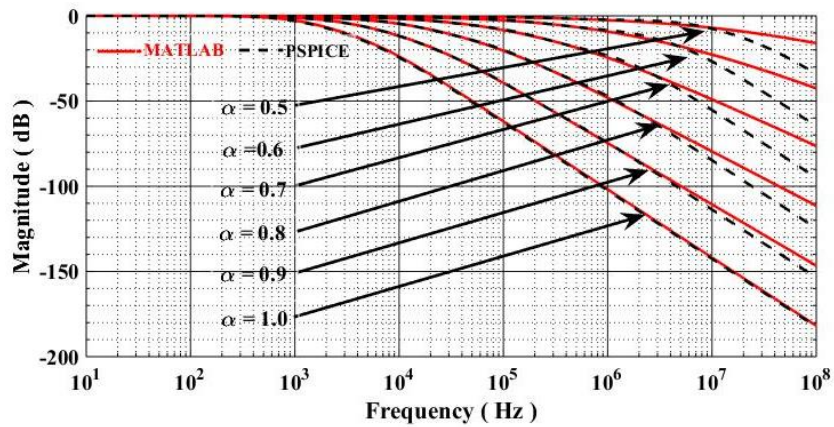
The workability of the presented fractional order filters of Fig. 3.19 has been validated through PSPICE simulations and MATLAB results. The values of passive resistances and fractional order capacitors used in the design of FOFs are provided in Table 3.28. The macro-model of AD844 type CFOA has been used to simulate all the filters in PSPICE.

Table 3.28 Component values for the realization of fractional order filter used in PSPICE simulation

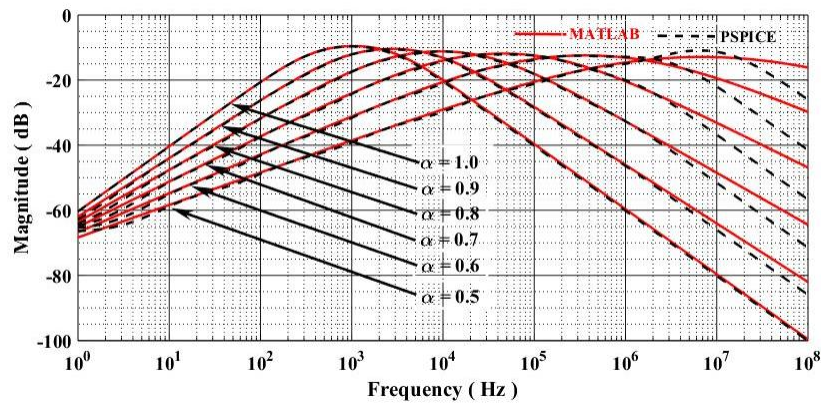
Type of Filter	Resistors	Fractional Order Capacitors
FOLP	$R_1 = 585\Omega$ $R_2 = 585\Omega$	$C_3 = 0.0955\mu\text{F}/\text{sec}^{(\alpha-1)}$ $C_4 = 0.0955\mu\text{F}/\text{sec}^{(\alpha-1)}$
FOBP	$R_1 = 1.598\text{K}\Omega$ $R_3 = 1.598\text{K}\Omega$	$C_4 = 0.0955\mu\text{F}/\text{sec}^{(\alpha-1)}$ $C_2 = 0.0955\mu\text{F}/\text{sec}^{(\alpha-1)}$

FOHP	$R_3 = 4.42\text{K}\Omega$ $R_4 = 4.42\text{K}\Omega$	$C_1 = 0.0955\mu\text{F}/\text{sec}^{(\alpha-1)}$ $C_2 = 0.0955\mu\text{F}/\text{sec}^{(\alpha-1)}$
-------------	----------------------------------------------------------	--------------------------------------------------------------------------------------------------------

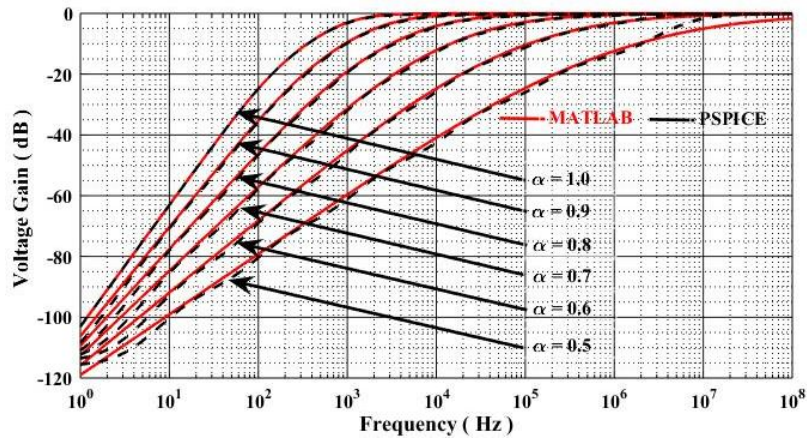
The fractional order capacitors were designed using Valsa, Dvorak and Friedl Method [89], having 2% ripple in the phase response for the frequency range of 10Hz – 1MHz for different values of α (varied from 0.5 to 0.9 in step of 0.1). The PSPICE and MATLAB simulation results of proposed current mode fractional order filters are shown in Fig. 3.20. The half power / maximum frequency and stop band attenuation of presented fractional order filters using MATLAB and PSPICE simulations along with theoretical results are presented in Table 3.29 and Table 3.30 respectively.



(a)



(b)



(c)

Figure 3.20 PSPICE and MATLAB simulation results of current mode FOFs (a) FOLP filter (b) FOBP filter (c) FOHP filter

Table 3.29 Simulation results for half power/maximum frequency (kHz)

Frequency (in KHz)		Value of α					
		1.0	0.9	0.8	0.7	0.6	0.5
Half power frequency (FOLP)	PSPICE	1.023	2.273	6.022	21.38	134.9	2800
	MATLAB	1.060	2.273	6.022	21.5	122.1	1456
	Theoretical	1.07	2.832	6.12	21.6	123.21	1530
Half power frequency (FOHP)	PSPICE	1.023	3.631	15.14	107.0	1230	6760
	MATLAB	1.009	3.301	14.38	92.50	1067	31180
	Theoretical	1.012	3.421	15.21	95.62	1160	32160
Maximum frequency (FOBP)	PSPICE	1.023	2.69	9.55	40.47	309	6600
	MATLAB	1.038	2.70	8.70	41.13	354	5988
	Theoretical	1.041	2.76	9.37	45.02	364.83	6827.10

Table 3.30 Simulation results for stop band attenuation (dB/decade)

Attenuation (dB/decades)		Value of α					
		1.0	0.9	0.8	0.7	0.6	0.5
Attenuation (FOLP)	PSPICE	39.85	35.24	27.10	21.51	18.7	14.02
	MATLAB	40.00	35.36	31.45	27.33	19.79	18.63
	Theoretical	40.00	36.00	32.00	28.00	24.00	20.00
Attenuation (FOHP)	PSPICE	39.00	35.01	31.52	27.59	23.09	19.90
	MATLAB	39.03	35.00	31.47	27.89	23.74	20.04
	Theoretical	40.00	36.00	32.00	28.00	24.00	20.00
Attenuation (FOBP)	PSPICE	19.75	17.78	15.84	13.91	11.95	09.96
	MATLAB	19.71	17.79	15.79	13.86	11.90	09.95
	Theoretical	20	18	16	14	12	10

From Tables 3.29 and Table 3.30 it is observed that the PSPICE and MATLAB results are in good agreement with the theoretical propositions. Therefore, these simulation results confirm the validity of the proposed current mode fractional order filters.

3.6. Conclusions

After presenting a detailed account of the fundamental concepts related to the fractional order filters and extensive literature review of fractional order filters with different properties, realized with various active building blocks, we have presented CFOA-based realization of fractional order filters in (i) voltage mode and (ii) current mode. Two different structures of voltage mode fractional order filters in which the fractional order low pass filter, fractional order band pass filter and fractional order high pass filter are realised by selecting the branch admittances appropriately. Both the structures employ only a single CFOA and five passive components (three/two passive resistors and two/three fractional order capacitors). The presented current mode fractional order filter structure, on the other hand, uses only a single CFOA, two resistors and two fractional order capacitors. Various transfer functions of FOLP, FOBP and FOHP can be obtained by appropriately selecting the branch admittances of the proposed structure(s). The performance of all the presented FOF circuits have been verified by theoretical calculation, MATLAB and PSPICE simulations for various values of ' α ' ($0 < \alpha < 1$).

References

- [1] A. G. Radwan, A. M. Soliman and A. S. Elwakil, "First-order filters generalized to the fractional domain," J. Circ. Syst. Comput. vol. 17, no. 1, pp. 55–66. July 2008.

- [2] A. G. Radwan, A. M. Soliman and A. S. Elwakil, "On the generalization of second-order filters to the fractional-order domain," *J. Circ. Syst. Comput.* vol.18, no. 2, pp. 361–386, Mar. 2009.
- [3] T. J. Freeborn, B. Maundy and A. S. Elwakil, "Towards the realization of fractional step filters," In *Proc IEEE Int. Symp. Circuits Syst. (ISCAS)*, pp. 1037–1040, May. -Jun.2010.
- [4] B. Maundy, A.S. Elwakil and T. J. Freeborn, "On the practical realization of higher-order filters with fractional stepping," *Signal Process*, vol. 91, no. 3, pp. 484–491, Mar. 2011.
- [5] A. Soltan, A. G. Radwan and A. M. Soliman, "Fractional order filters with two fractional elements of dependent orders," *Microelectron. J.*, vol. 43, no. 11, pp. 818–827, Nov. 2012.
- [6] P. Ahmadi, B. Maundy, A. S. Elwakil and L. Belostotski, "High-quality factor asymmetric-slope band-pass filters: a fractional-order capacitor approach," *IET Circ. Devices Syst.*, vol. 6, no. 3, pp. 187-197, May. 2012.
- [7] T. J. Freeborn, B. Maundy and A. S. Elwakil, "Fractional-step Tow-Thomas biquad filters," *Nonlinear Theory and Its Applications, IEICE*, vol.3, no. 3, pp. 357-374, Jul. 2012.
- [8] M. C. Tripathy, K. Biswas and S. Sen, "A design example of a fractional-order Kerwin-Huelsman-Newcomb biquad filter with two fractional capacitors of different order," *Circ. Syst. Signal Process*, vol. 32, no. 4, pp. 1523-1536, Aug. 2013.
- [9] A. S. Ali, A. G. Radwan and A. M. Soliman, "Fractional order Butterworth filter: active and passive realizations," *IEEE J. Emerging Selected Topics Circ. Syst.*, vol. 3, no. 3, pp. 346–354, Jun. 2013.

- [10] A. Soltan, A. G. Radwan and A. M. Soliman, "Fractional order Sallen-Key and KHN filters stability and poles allocation," *Circ. Syst Signal Process*, vol. 34, no. 5, pp. 1461–80, Aug. 2014.
- [11] C. Psychalinos, G. Tsirimokou and A. S. Elwakil, "Switched-Capacitor Fractional-Step Butterworth Filter Design," *Circ. Syst. Signal Process*. vol. 35, pp. 1377-1393, Apr. 2016.
- [12] M. C. Tripathy, "Experimental Realization of Fractional order filter using PMMA coated constant phase elements," *Int. J. Engineering and Advanced Research Technology (IJEART)*, vol. 1, no. 5, pp. 14-17, Nov. 2015.
- [13] T. J. Freeborn, "Comparison of $(1+\alpha)$ fractional-order transfer functions to approximate low pass Butterworth magnitude responses," *Circ. Syst Signal Process*. vol. 35, no. 6, 1983–2002, Jun. 2016.
- [14] J. Baranowski, M. Pauluk and A. Tutaj, "Analog realization of fractional filters: Laguerre approximation approach," *AEU-Int. J. Electron Commun*, vol. 81, pp. 1–11, Nov. 2017.
- [15] D. Kubanek, T. Freeborn and J. Koton, "Fractional-order band-pass filter design using fractional-characteristic specimen functions," *Microelectron. J.*, vol. 86, pp. 77-86, Apr. 2019.
- [16] K. Sengar and A. Kumar, "Fractional order capacitor in first order and second order filter," *Micro and nano systems*, vol. 12, no. 2, pp.1-4, 2020
- [17] A. Tutaj, P. Piątek, W. Bauer, J. Baranowski, T. Petropoulos, G. Moustos, P. Bertsias and C. Psychalinos, "Approximating fractional filters with analogue Active filter structures," *Int. Conf. on Telecommun. Signal Process. (TSP)* pp. 440-444, doi: 10.1109/TSP.2019.8768817

- [18] A.Soltan, A. G. Radwan and A. M. Soliman, "Butterworth passive filter in the fractional order," In: Proc IEEE Int. Conf. Microelectron. (ICM). pp. 1–4, 19-22 December 2011.
- [19] T. J. Freeborn, A. S Elwakil and B. Maundy, "Approximated fractional-order inverse Chebyshev lowpass filters," *Circ. Syst. Signal Process*, vol. 35, no.6, pp. 1973–1982, 2015.
- [20] M. C. Tripathy, D. Mondal, K. Biswas and S. Sen, "Experimental studies on realization of fractional inductors and fractional-order bandpass filters," *Int. J. Circ. Theory Appl.*, vol. 43, no. 9, pp. 1183–1196, 2015.
- [21] T. Khanna, and D. K. Upadhyay, "Design and realization of fractional order butterworth low pass filters," *Int. Conf. Signal Process., Comp. and Control*, vol. 978, no.1, pp. 356-361, 2015.
- [22] A. Marathe, B. Maundy and A.S. Elwakil, "Design of fractional notch filter with asymmetric slopes and large values of notch magnitude," *Int. Midwest Symp. Circuits Syst. (MWSCAS)*., pp. 388–391, 2013
- [23] M. C. Tripathy, D Mondal, K Biswas and S Sen, "Design and performance study of phase-locked loop using fractional-order loop filter," *Int. J. Circ. Theory Appl.*, vol. 43, pp. 773-792, 2014, doi:10.1002/cta.1972.
- [24] S. Mahata, S. K. Saha, R. Kar, and D. Mandal, "Optimal design of fractional order low pass Butterworth filter with accurate magnitude response," *Digital Signal Process.*, vol. 72, pp. 96-114, 2018.
- [25] A. M. AbdelAty, A. Soltan, W. A. Ahmed and A. G. Radwan, "On the analysis and design of fractional-order Chebyshev complex filter," *Circ. Syst. Signal Process.*, vol. 37, no. 3, pp.915-938, 2018.

- [26] D. Kubanek, T. J. Freeborn, J. Koton, and J. Dvorak, "Validation of fractional-order low pass elliptic responses of $(1+\alpha)$ -Order analog filters," *Applied Sciences*, vol. 8, no. 2603, pp. 1-17, 2018.
- [27] G. Tsirimokou, S. Koumoussi and C. Psychalinos "Design of fractional-order filters using current feedback operational amplifiers," *J. Eng. Sci. Technol. Rev.*, vol. 9, no. 4, pp. 77–81, Jan. 2016.
- [28] R. Verma, N. Pandey and R. Pandey, "CFOA based low pass and high pass fractional step filter realization," *AEU-Int. J Electron Commun.*, vol. 99, pp. 161-176, Feb. 2019.
- [29] S. Mahata, R. Kar and D. Mandal, "Optimal approximation of asymmetric type fractional order band passes Butterworth filter using decomposition Technique," *Int. J. Circ. Theor. Appl.*, pp. 1-7, 2017.
- [30] A. Soltan, A. G. Radwan and A. M. Soliman, "CCII based KHN fractional order filter," *Int. Midwest symp. Circ. Syst. (MWSCAS)*, pp. 197-200. IEEE, 2013.
- [31] A. Soltan, A. G. Radwan and A. M. Soliman, "CCII based fractional filters of different orders," *J. advanced research*, vol. 5, no. 2, pp. 157-164, Mar. 2014.
- [32] J. Koton, O. Sladok, J. Salasek and P. Ushakov, "Current-mode fractional low- and high pass filters using current conveyors", 8th Int. Congress on Ultra-Modern Telecommunications and Control Systems and Workshops (ICUMT), Lisbon, Portugal, pp. 231–234, 18–20 Oct. 2016.
- [33] L. A. Said, S. M. Ismail, A. G. Radwan, A. H. Median, El Yazeed MFA and A. M. Soliman, "On the optimization of fractional order low pass filter," *Circ. Syst. Signal Process.* vol. 35, no. 6, pp. 2017–2039. 2016.: 2017-2039. *Process.* vol. 35, no. 6, pp. 2017–2039, Jun. 20

- [34] S. Mahata, R. Kar and D. Mandal, "Optimal fractional-order high pass Butterworth magnitude characteristics realization using current mode filter," *AEU-Int J Electron Commun.*, vol. 102, pp. 78-89, Apr. 2019.
- [35] N. A. Khalil, L. A. Said, A. G. Radwan and A. M. Soliman, "Generalized two-port network based fractional order filters," *AEU-Int J Electron Commun.* vol. 104, pp. 128-146, May. 2019.
- [36] E. M. Hamed, A. M. Abdelaty, L. A. Said and A. G. Radwan, "Effect of different approximation techniques on fractional-order KHN filter design," *Circ. Syst Signal Process.*, vol. 37, pp. 5222–5252, Dec. 2018
- [37] L.A Said, S. M. Ismail, A. G. Radwan, A. H. Madian, M. F. Abu El Yazeed and A. M. Soliman, "On the optimization of fractional order low pass filters," *Circ., Syst. Signal Process*, vol. 35, no. 6, pp. 2017–2039, 2016.
- [38] G. Kaur, A. Q. Ansari and M. S. Hashmi, "Fractional order multifunction filter with 3degrees of freedom," *AEU-Int J Electron Commun.*, vol. 82, pp. 127–35, 2017.
- [39] G. Kaur, A. Q. Ansari, and M. S. Hashmi, "Fractional order high pass filter based on operational transresistance amplifier with three fractional capacitors of different order," *Advances in Electrical and Electronic Engineering*, vol. 17 n0. 2, pp. 155–166, 2019.
- [40] R. Verma, N. Pandey and R. Pandey, "Realization of a higher fractional order element based on novel OTA based IIMC and its application in filter," *Analog Integ. Circ. Signal Process.* vol. 97, pp. 177–191, Oct. 2018.
- [41] J. Jerabek, R. Sotner, J. Dvorak, J. Polak, D. Kubanek, N. Herencsar and J. Koton, "Reconfigurable fractional-order filter with electronically controllable slope of

- attenuation, pole frequency and type of approximation,” *J. Circ. Syst. Comput.*, vol. 26, no. 10, pp. 1–21, Oct. 2017.
- [42] T. Suksang, V. Pirajanchai and W. Loedhammacakra, “Tunable OTA Low Pass Filter with the Fractional-Order step Technique,” *Int. Conf. Advances in Electron Electr. Engg. (AEEE)*, pp. 29-32, 2012.
- [43] G. Tsirimokou, C. Psychalinos, and A. S. Elwakil, “Fractional-order electronically controlled generalized filters,” *Int. J. Circ. Theor. Appl.*, vol. 45, pp. 595–612, May. 2017.
- [44] L. Langhammer, J. Dvorak, R. Sotner and J. Jerabek, “Electronically tunable fully differential fractional-order low-pass filter,” *Elektron Elektrotech*, vol. 23, no. 3, pp. 47-54, Jun. 2017.
- [45] R. Verma, N. Pandey and R. Pandey, “Electronically tunable fractional order all pass filter,” *IOP Conf. Ser. Mater Sci. Eng.*, vol. 225, pp. 1–9, 2017.
- [46] R. Verma, N. Pandey and R. Pandey, “Electronically tunable fractional order filter,” *Arabian J. Science and Engineering*, vol. 42, no. 8, pp. 3409-3422, Aug. 2017.
- [47] L. Langhammer, J. Dvorak, R. Sotner, J. Jerabek and P. Bertsiyas, “Reconnection-less reconfigurable low pass-filtering technology suitable for higher order fractional order design,” *Journal of advanced research*, vol.25, pp. 257-274, 2020
- [48] G. Varshney, N. Pandey and R. Pandey, “ Electronically tunable multifunction transadmittance mode fractional order filter,” *Arabian J. Science and Engineering*, 2020, <https://doi.org/10.1007/s13369-020-04841-8>.
- [49] I. E. Sacu and M. Alci, "A current mode design of fractional order universal filter," *Advances in Electrical and Computer Engineering*, vol.19, no.1, pp.71-78, 2019, doi:10.4316/AECE.2019.01010

- [50] E. Kaskouta, T. Kamilaris, R. Sotner, J. Jerabek and C. Psychalinos, "Single- input multiple-output and multiple-input single-output fractional-order filter designs," Int. Conf. Telecommun. Signal Process. (TSP), Athens, 2018, pp. 1-4, doi: 10.1109/TSP.2018.8441348.
- [51] Gopal Singh, Garima and Pragati Kumar, "Fractional order capacitors based filters using three OTAs," Int. Conf. on Control Automation and Robotics (ICCAR), pp. 638-643, 2020.
- [52] J. Jerabek, R. Sotner, J. Dvorak, L. Langhammer and J. Koton, "Fractional-order high pass filter with electronically adjustable parameters," Int. Conf. Applied Electronics (APPEL), 6–7 September 2016, Pilsen, Czech Republic, pp. 111–116, 2016.
- [53] M. R. Dar, N. A. Kant, F. A. Khanday and C. Psychalinos, "Fractional-order filter design for ultra-low frequency applications," Int. Conf. Recent Trends in Electron., Information Commun. Tech. (RTEICT), pp. 1727-1730, 2016.
- [54] J. Dvorak, J. Jerabek, Z. Polesakova, D. Kubanek and P. Blazek, "Multifunctional Electronically Reconfigurable and Tunable Fractional-Order Filter," Elektronika ir Elektrotechnika, vol. 25, no. 1, pp.26-30, 2019.
- [55] P. Bertias, C. Psychalinos, A. S. Elwakil and B. J. Maundy, "Simple Multi-Function Fractional-Order Filter Designs," Int. Conf. Modern Circ. Systems Technologies (MOCASST), pp. 1-4, 2019.
- [56] T. J. Freeborn, B. Maundy and A. S. Elwakil, "Field programmable analogue array implementation of fractional step filters," IET Circ. Devices Syst., vol. 4, no. 6, pp. 514-524, Nov. 2010.

- [57] D. Kubanek, J. Koton, J. Jerabek, P. Ushakov and A. Shadrin, "Design and properties of fractional order multifunction filter with DVCCs," Int. Conf. Telecommunications Signal Process. (TSP), pp. 620-624, Jun. 2016
- [58] F. Khateb, D. Kubanek, G. Tsirimokou, and C. Psychalinos, "Fractional order filters based on low-voltage DDCCs," *Microelectron. J.*, vol. 50, pp. 50-59, 2016.
- [59] J. Koton, D. Kubanek, O. Sladok and K. Vrba, "Fractional-order low- and high-pass filters using UVCs," *J Circ. Syst Comput.*, vol. 26, no. 12, pp. 1–23, 2017.
- [60] P. Bertias, F. Khateb, D. Kubanek, F. A. Khanday, and C. Psychalinos, "Capacitorless digitally programmable fractional-order filters," *AEU-Int. J. Electron Commun.*, vol. 78, pp. 228-237, 2017.
- [61] D. Kubanek and T. Freeborn, " $(1+\alpha)$ Fractional-order transfer functions to approximate low-pass magnitude responses with arbitrary quality factor," *AEU-Int J Electron Commun.*, vol. 83, pp. 570-578, 2018.
- [62] S. K. Mishra, M. Gupta and D. K. Upadhyay, "Active realization of fractional order Butterworth lowpass filter using DVCC," *J. King Saud University Engineering Sciences*, vol. 32, no. 2, pp. 158-165, 2020.
- [63] T. Comedang and P. Intani, " $A \pm 0.2$ V, 0.12 μ W CCTA using VT MOS and an application fractional-order universal filter," *J. Circ. Syst. Comp.*, vol. 23, no. 8, 2014.
- [64] J. Koton, D. Kubanek, K. Vrba, A. Shadrin and P. Ushakov, "Universal voltage conveyors in fractional-order filter design," Int. Conf. Tele-communications and Signal Process. (TSP), Vienna, Austria. June 2016, pp. 1–5, 2016.

- [65] P. Rani and R. Pandey, "Voltage differencing transconductance amplifier based fractional order multiple input single output universal filter," *Solid State Electron. Letters* 1, pp. 110-118, 2019
- [66] T. Helie, "Simulation of fractional-order low-pass filters," *IEEE/ACM Trans. Audio Speech Lang. Process.*, vol. 22, no. 11, pp. 1636–1647, 2014.
- [67] P. Bertias, C. Psychalinos, A. S. Elwakil and K. Biswas, "Single transistor fractional order filter using multi-walled carbon nanotube device," *Analog Integrated Circ. Signal Process*, vol. 100, pp. 215-219, 2018.
- [68] J. Dvorak, L. Langhammer, J. Jerabek, J. Koton, R. Sotner, and J. Polak, "Synthesis and analysis of electronically adjustable fractional-order low-pass filter," *J. Circ. Systems Comp.*, vol. 27, no. 02, pp 1-18, 2018.
- [69] G. Tsirimokou, C. Psychalinos and A. S. Elwakil, "Digitally programmed fractional-order Chebyshev filters realizations using current-mirrors," *Int. Symp. Circ. Syst. (ISCAS)*, pp. 2337-2340, 2015.
- [70] S. Mahata, R. Kar and D. Mandal, "Optimal fractional-order highpass Butterworth magnitude characteristics realization using current mode filter," *AEU-Int J Electron Commun.*, vol. 102, pp. 78-89, 2019.
- [71] A. Acharya, S. Das, I. Pan, and S. Das, "Extending the concept of analog Butterworth filter for fractional order systems," *Signal process.*, vol. 94, pp. 409-420, 2014.
- [72] R. Tanwar and S. Kumar, "Analysis & design of fractance based fractional order filter," *Int. J. Innovative Research in Electrical, Electronics, Instrumentation and Control Engineering*, vol. 1, no. 3, 2013.

- [73] S. Mahata, S. K. Saha, R. Kar and D. Mandal, "Approximation of fractional-order low-pass filter," *IET Signal Processing*, vol. 13, no. 1, pp. 112-124, 2018.
- [74] I. El Gammoudi and M. Feki, "Synchronization of integer order and fractional order Chua's systems using robust observer," *Communications in Nonlinear Science and Numerical Simulation*, vol. 18, no. 3, pp. 625-638, 2013.
- [75] K. Baxevanaki, S. Kapoulea, C. Psychalinos and A. S. Elwakil, "Electronically tunable fractional-order highpass filter for phantom electro encephalographic system model implementation," *AEU-Int. J. Electron. Commun.*, vol. 110, 2019.
- [76] P. Bertias and C. Psychalinos, "Partial Fraction Expansion Based Fractional-Order Filter Designs," *Panhellenic Conference on Electronics & Telecommunications (PACET)*, pp. 1-4, 2019.
- [77] Z. Zalevsky and D. Mendlovic, "Fractional wiener filter," *Applied Optics*, vol. 35, no. 20, pp. 3930-3936, 1996.
- [78] A. Q. Ansari, G. Kaur and M. S. Hashmi, "Current Differencing Buffered Amplifier (CDBA) based Current Mode Universal Fractional Order Filter," *Nat. Conf. Adv. Microelectron. Instrumen. Commun. (MICOM 2015)*, India, 2015.
- [79] Y. Tao, W. Jiang, B. Han, X. Li, Y. Luo and L. Zeng, "A novel piecewise frequency control strategy based on fractional-order filter for coordinating vibration Isolation and positioning of supporting system," *Sensors*, vol. 20, no. 18, pp.5307, 2020.
- [80] O. Imik, B. B. Alagoz, A. Ates and C. Yeroglu, "Fractional order filter discretization by particle swarm optimization method," *Mathematical Methods in Engineering*, pp. 133-144, 2019. Springer, Cham.

- [81] D. Kubanek, T. Freeborn, J. Koton and N. Herencsar, "Evaluation of $(1+\alpha)$ fractional-order approximated Butterworth high-pass and band-pass filter transfer functions," *Elektronika ir Elektrotechnika*, vol. 24, no. 2, pp. 37-41, 2018.
- [82] S. Mahata, S. K. Saha, R. Kar and D. Mandal, "Accurate integer-order rational approximation of fractional-order low-pass Butterworth filter using a metaheuristic optimisation approach," *IET Signal Process.*, vol. 12, no. 5, pp. 581-589, 2018.
- [83] L. Langhammer, R. Sotner, J. Dvorak and T. Dostal, "Fully-differential multifunctional electronically configurable fractional-order filter with electronically adjustable parameters," *Elektronika ir Elektrotechnika*, vol. 24, no. 5, pp. 42-45, 2018.
- [84] Y. Zhang and J. Li, "An improvement method of fractional-order filter approximation," *Int. Conf. Computer Education, Simulation and Modeling*, pp. 101-106, 2011. Springer, Berlin, Heidelberg.
- [85] A. Soni and M. Gupta, "Analysis and Design of Optimized Fractional Order Low-Pass Bessel Filter," *J. Circ. Syst. Comp.*, 2150035, 2020.
- [86] A. Soni and M. Gupta, "Performance evaluation of different order fractional chebyshev filter using optimisation techniques," *Int. J. Electron. Letters*, vol. 8, no. 2, pp. 205-222, 2020.
- [87] A. Soni, N. Sreejeth, V. Saxena and M. Gupta, "Series optimized fractional order low pass butterworth filter," *Arabian J. Science Engineering*, vol. 45, no. 3, pp. 1733-1747, 2020.
- [88] G. Tsirimokou, C. Psychalinos and A. Elwakil, "Design of CMOS Analog Integrated Fractional Order Circuits Application in Medicine", Cham: Springer International Publishing, Springer, 2017, ISBN 9783319556338.

- [89] J. Valsa, P. Dvorak, and M. Friedl, "Network Model of the CPE," *Radioengineering*, Vol. 20, pp.619–626, Sep. 2011
- [90] R. Senani, D. R. Bhaskar, V. K. Singh and A. K. Singh, "Current feedback operational amplifiers and their applications. New York: Springer, 2013, ISBN 978-1-4614-5187-7.

Realization of Fractional Order Inverse Filters

This chapter begins with the introduction of fractional order inverse filters and their transfer functions (along with their magnitude and phase responses), an overview of inverse active filters reported by various researchers employing different active building blocks and subsequently introduces new configurations of fractional order inverse active filters using op-amp, CFOAs and OTRA along with conventional resistors and simulated fractional order capacitors.

4.1. Fractional Order Inverse Filters

An inverse filter is a type of frequency selective circuit, whose frequency response characteristics are inverse of the frequency response of the corresponding conventional filter viz., low pass, high pass, band pass and band reject. Inverse filters play an important role in the areas of communication, instrumentation and control systems where the distortion of the signal caused by transmission system or the signal processor can be eliminated by the inverse filters [1]. The fractional order inverse filters (FOIFs) have transfer functions similar to their integer order counterparts, the difference is only in the order of the FOIF; the order 'n' is non-integer, in case of fractional order inverse filters whereas it is an integer for integer order inverse filters. Since the present chapter deals with analog circuit implementation of fractional order inverse filters using different active building blocks, in the following, we have outlined the fundamentals related to the fractional order inverse filters before presenting the proposed new circuits.

The general transfer function of a fractional order filter can be written as [2]:

$$T(s) = \left(\frac{As^{\alpha+\beta} + Bs^{\beta} + C}{s^{\alpha+\beta} + Ds^{\beta} + E} \right) \quad (4.0)$$

Therefore, the transfer function of FOIF can be expressed as:

$$T(s)_{\text{FOIF}} = \frac{1}{T(s)} = \frac{1}{\left(\frac{As^{\alpha+\beta} + Bs^{\beta} + C}{s^{\alpha+\beta} + Ds^{\beta} + E} \right)} \quad (4.1)$$

where $0 < \alpha < 1$, $0 < \beta < 1$, and A, B, C, D, E are the constants.

From the above transfer function of FOIF (equation (4.1)), different fractional order inverse active filters i.e., fractional order inverse lowpass (FOILP), fractional order inverse high pass (FOIHP), fractional order inverse band pass (FOIBP) and fractional order inverse band reject (FOIBR) filters can be obtained by appropriate selection(s) of the constants A, B, C, D and E. In the following, we describe the various transfer functions along with the corresponding magnitude and phase responses.

4.1.1. Fractional Order Inverse Low Pass Filter

In equation (4.1), if we take the $A = 0$ and $B = 0$, the transfer function of a fractional order inverse low pass filter is obtained as:

$$T(s)_{\text{FOILP}} = \frac{1}{\left(\frac{C}{s^{\alpha+\beta} + Ds^{\beta} + E} \right)} \quad (4.2)$$

Using equation (4.2), the expressions for magnitude and phase of a FOILP filter can be obtained as:

$$|T(j\omega)_{\text{FOILP}}| = \frac{\left[\omega^{2(\alpha+\beta)} + 2D\omega^{(\alpha+2\beta)} \cos\left(\frac{\alpha\pi}{2}\right) + D^2\omega^{2\beta} + 2E\omega^{(\alpha+\beta)} \cos\left(\frac{(\alpha+\beta)\pi}{2}\right) + 2DE\omega^\beta \cos\left(\frac{\beta\pi}{2}\right) + E^2 \right]^{\frac{1}{2}}}{C} \quad (4.3a)$$

$$\angle T(j\omega)_{\text{FOILP}} = \tan^{-1} \left(\frac{\omega^{(\alpha+\beta)} \sin\left(\frac{(\alpha+\beta)\pi}{2}\right) + D\omega^\beta \sin\left(\frac{\beta\pi}{2}\right)}{\omega^{(\alpha+\beta)} \cos\left(\frac{(\alpha+\beta)\pi}{2}\right) + D\omega^\beta \cos\left(\frac{\beta\pi}{2}\right) + E} \right) \quad (4.3b)$$

The DC gain (low frequency gain) of FOILP filter can be obtained from equation (4.2) which is equal to $\frac{E}{C}$. The expression of half power frequency ω_h (frequency at which the gain of the transfer function becomes $\sqrt{2}$ times of the low frequency gain i.e, $(\sqrt{2}\frac{E}{C})$ of FOILP filter can be obtained by equating the equation (4.3a) with $\sqrt{2}\frac{E}{C}$, as given by:

$$\omega_h^{2(\alpha+\beta)} + 2D\omega_h^{(\alpha+2\beta)} \cos\left(\frac{\alpha\pi}{2}\right) + D^2\omega_h^{2\beta} + 2E\omega_h^{(\alpha+\beta)} \cos\left(\frac{(\alpha+\beta)\pi}{2}\right) + 2DE\omega_h^\beta \cos\left(\frac{\beta\pi}{2}\right) - E^2 = 0 \quad (4.4)$$

Solution of equation (4.4) yields the half power frequency of FOILP filter.

From equation (4.3b), we have obtained the expression of right phase frequency (the frequency at which the phase of transfer function becomes $\pm \frac{\pi}{2}$) [2]. Equating the phase of the $T(j\omega)_{\text{FOILP}}$ as given in equation (4.3b) with $\pm \frac{\pi}{2}$ yields:

$$\tan^{-1} \left(\frac{\omega_{\text{rp}}^{(\alpha+\beta)} \sin\left(\frac{(\alpha+\beta)\pi}{2}\right) + D\omega_{\text{rp}}^\beta \sin\left(\frac{\beta\pi}{2}\right)}{\omega_{\text{rp}}^{(\alpha+\beta)} \cos\left(\frac{(\alpha+\beta)\pi}{2}\right) + D\omega_{\text{rp}}^\beta \cos\left(\frac{\beta\pi}{2}\right) + E} \right) = \pm \frac{\pi}{2} \quad (4.5)$$

which can be further simplified into

$$\omega_{rp}^{\alpha+\beta} \cos\left(\frac{(\alpha+\beta)\pi}{2}\right) + D\omega_{rp}^{\beta} \cos\left(\frac{\beta\pi}{2}\right) + E = 0 \quad (4.6)$$

From equation (4.6), the right phase frequency of FOILP filter can be obtained.

The magnitude and phase responses, as given in equation (4.3) have been plotted using MATLAB for a FOILP filter designed to have a half power frequency of 1KHz (for $\alpha = 1, \beta = 1$) by selecting the coefficients C, D, and E as 39438400, 8882.748 and 39438400 respectively, so that the response is maximally flat. The magnitude and phase responses for different values of α and β are shown in Fig. 4.1

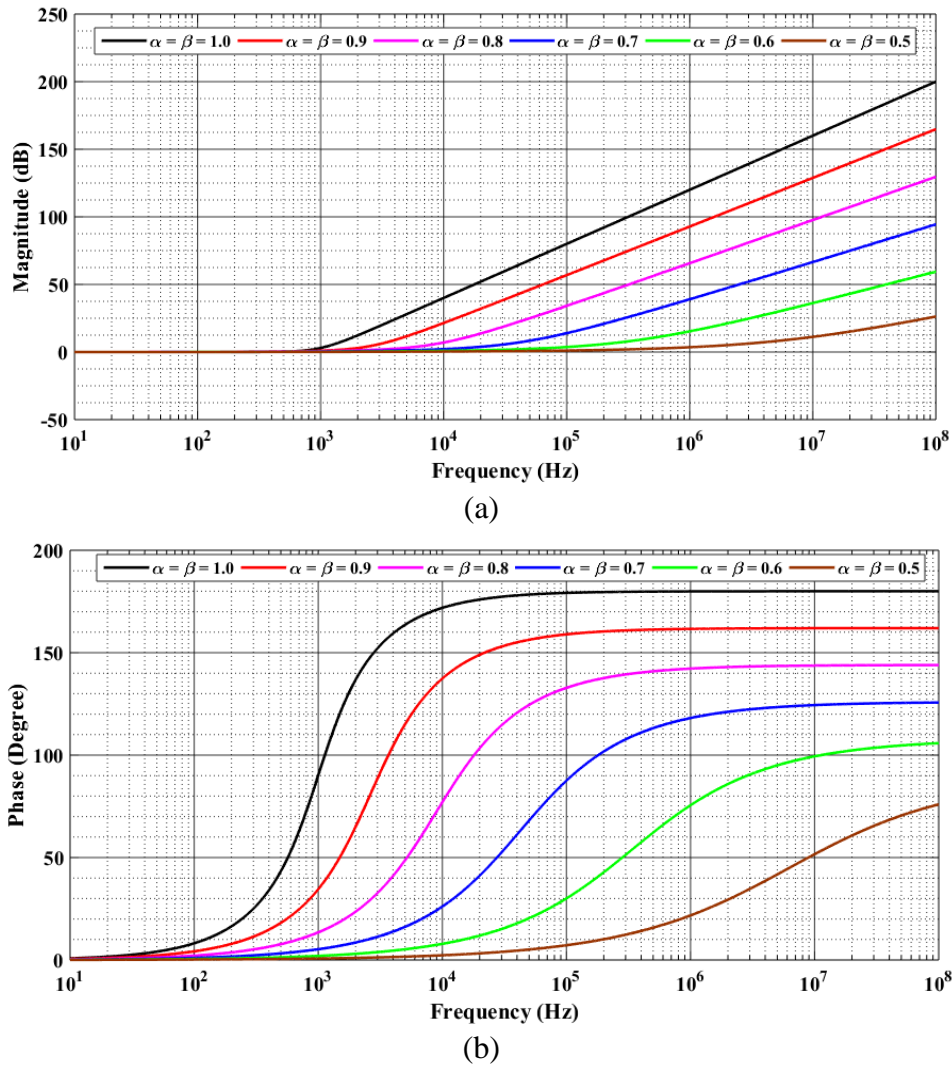


Figure 4.1 MATLAB simulations of FOILP (a) Magnitude responses (b) Phase responses

The slope of the magnitude response, half power frequency and right phase frequency as obtained from Fig. 4.1 are given below in Table 4.1, from where it may be noted that the slope of the magnitude characteristics and the characterising frequency may be varied by appropriately choosing the values of α and β . In contrast, for an integer order inverse filter, the slope and the half power frequency can not be varied.

Table 4.1 Various parameters of FOILP filter

α of FOILP	Filter parameters		
	ω_h (kHz)	ω_{rp} (kHz)	Attenuation (dB)
1.0	1.00	1.00	40
0.9	2.01	3.06	36
0.8	4.75	13.68	32
0.7	14.78	110.60	28
0.6	72.23	2860	24
0.5	717.3	8.03×10^8	20

4.1.2. Fractional Order Inverse High Pass Filter

If we put $B = 0$ and $C = 0$ in equation (4.1), the transfer function of FOIHP filter can be obtained as:

$$T(s)_{\text{FOIHP}} = \frac{1}{\left(\frac{A s^{\alpha+\beta}}{s^{\alpha+\beta} + D s^{\beta} + E} \right)} \quad (4.7)$$

From equation (4.7), the magnitude and phase of FOIHP filter may be deduced as:

$$|T(j\omega)_{\text{FOIHP}}| = \frac{1}{A} \frac{\left[\omega^{2(\alpha+\beta)} + 2D\omega^{(\alpha+2\beta)} \cos\left(\frac{\alpha\pi}{2}\right) + D^2\omega^{2\beta} + \right]^{\frac{1}{2}}}{\omega^{(\alpha+\beta)} \left[2E\omega^{(\alpha+\beta)} \cos\left(\frac{(\alpha+\beta)\pi}{2}\right) + 2DE\omega^{\beta} \cos\left(\frac{\beta\pi}{2}\right) + E^2 \right]} \quad (4.8a)$$

$$\angle T(j\omega)_{\text{FOIHP}} = \tan^{-1} \left(\frac{\omega^{(\alpha+\beta)} \sin\left(\frac{(\alpha+\beta)\pi}{2}\right) + D\omega^{\beta} \sin\left(\frac{\beta\pi}{2}\right)}{\omega^{(\alpha+\beta)} \cos\left(\frac{(\alpha+\beta)\pi}{2}\right) + D\omega^{\beta} \cos\left(\frac{\beta\pi}{2}\right) + E} \right) - (\alpha + \beta) \frac{\pi}{2} \quad (4.8b)$$

From equation (4.7), the high frequency gain of FOIHP filter is found to be equal to $\frac{1}{A}$.

The expression for half power frequency of FOIHP filter can now be derived by equating equation (4.8a) with $\sqrt{2}\frac{1}{A}$ as:

$$D^2\omega_h^{2\beta} + 2D\omega_h^{(\alpha+2\beta)}\cos\left(\frac{\alpha\pi}{2}\right) + 2E\omega_h^{(\alpha+\beta)}\cos\left(\frac{(\alpha+\beta)\pi}{2}\right) + 2DE\omega_h^\beta\cos\left(\frac{\beta\pi}{2}\right) + E^2 - \omega_h^{2(\alpha+\beta)} = 0 \quad (4.9)$$

Real solution of equation (4.9) for the given values of α and β , yields the expression of half power frequency for FOIHP filter.

Similarly, the expression for right phase frequency of FOIHP can be derived from equation (4.8b) by equating the phase angle to $\pm\frac{\pi}{2}$ as:

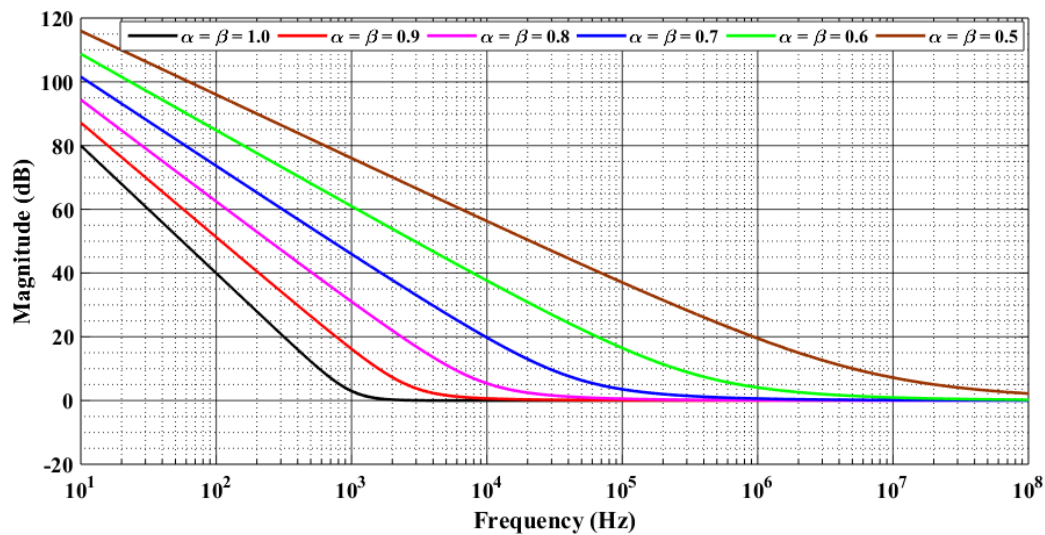
$$\tan^{-1}\left(\frac{\omega_{rp}^{(\alpha+\beta)}\sin\left(\frac{(\alpha+\beta)\pi}{2}\right) + D\omega_{rp}^\beta\sin\left(\frac{\beta\pi}{2}\right)}{\omega_{rp}^{(\alpha+\beta)}\cos\left(\frac{(\alpha+\beta)\pi}{2}\right) + D\omega_{rp}^\beta\cos\left(\frac{\beta\pi}{2}\right) + E}\right) - (\alpha+\beta)\frac{\pi}{2} = \pm\frac{\pi}{2} \quad (4.10)$$

Which can further be simplified as:

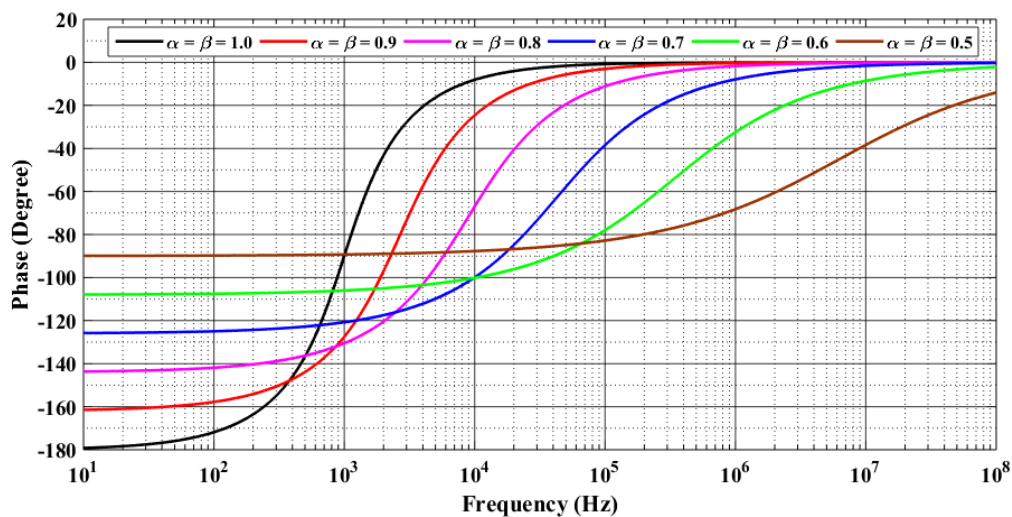
$$\omega_{rp}^{\alpha+\beta} + D\omega_{rp}^\beta\sin\left(\frac{(\alpha+1)\pi}{2}\right) + E\sin\left(\frac{(\alpha+\beta+1)\pi}{2}\right) = 0 \quad (4.11)$$

The solution of the above equation will yield right phase frequency (ω_{rp}).

The magnitude and phase responses, as given by equation (4.8) have been plotted using MATLAB for a FOIHP designed to have a half power frequency of 1KHz (for $\alpha = 1$, $\beta = 1$) by selecting the coefficients A, D, and E as 1, 8882.748 and 39438400 respectively, so that the response is maximally flat. The magnitude and phase responses for different values of α and β are displayed in Fig. 4.2



(a)



(b)

Figure 4.2 MATLAB simulations of FOIHP (a) Magnitude responses (b) Phase responses

The slope of the magnitude response, half power frequency and right phase frequency as obtained from Fig. 4.2 are given below in Table 4.2, from where it may be noted that the slope of the magnitude characteristics and the characterising frequency may be varied by appropriately choosing the values of α and β . In contrast, for an integer order inverse high filter, the slope as well as the half power frequency can not be varied.

Table 4.2 Various Parameters of FOIHP filter

α	Filter parameters		
	ω_h (kHz)	ω_{rp} (kHz)	Attenuation (dB)
1.0	1.00	1.00	40
0.9	3.44	2.26	36
0.8	16.60	5.76	32
0.7	121	16.29	28
0.6	1596	40.43	24
0.5	54600	-	20

4.1.3. Fractional Order Inverse Band Pass Filter

The substitution of $A = 0$ and $C = 0$ in equation (4.1), yields the transfer function of FOIBP as:

$$T(s)_{\text{FOIBP}} = \frac{1}{\left(\frac{Bs^\beta}{s^{\alpha+\beta} + Ds^\beta + E} \right)} \quad (4.12)$$

The expressions for the magnitude response and phase response of a FOIBP filter from equation (4.12) can be derived as:

$$|T(j\omega)_{\text{FOIBP}}| = \frac{\left[\omega^{2(\alpha+\beta)} + 2D\omega^{(\alpha+2\beta)} \cos\left(\frac{\alpha\pi}{2}\right) + D^2\omega^{2\beta} + \right]^{\frac{1}{2}}}{B\omega^\beta} \quad (4.13a)$$

$$\angle T(j\omega)_{\text{FOIBP}} = -\frac{\beta\pi}{2} + \tan^{-1} \left(\frac{\omega^{(\alpha+\beta)} \sin\left(\frac{(\alpha+\beta)\pi}{2}\right) + D\omega^\beta \sin\left(\frac{\beta\pi}{2}\right)}{\omega^{(\alpha+\beta)} \cos\left(\frac{(\alpha+\beta)\pi}{2}\right) + D\omega^\beta \cos\left(\frac{\beta\pi}{2}\right) + E} \right) \quad (4.13b)$$

From equation (4.13a), the high frequency gain as well as DC gain of FOIBP filter may be estimated to be infinity, while, minimum frequency gain is found to be $\frac{D}{B}$. The minimum frequency ω_m of fractional order inverse band pass filter is the frequency at which magnitude response of fractional order inverse band pass filter attains a minima. This frequency is given by

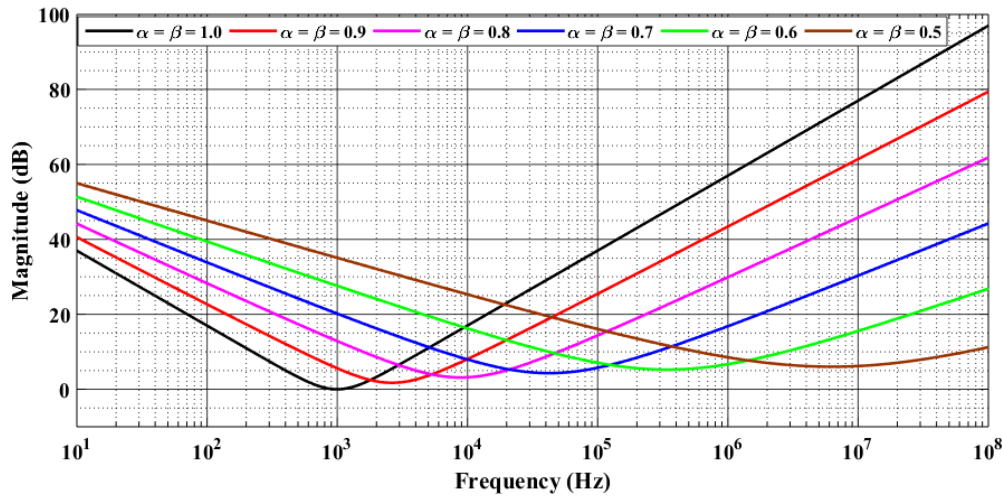
$$\omega_m = E^{\frac{1}{\alpha+\beta}} \quad (4.14)$$

While, equating the equation (4.13b) with $\pm \frac{\pi}{2}$, the expression for right phase frequency (ω_{rp}) of FOIBP can be derived as:

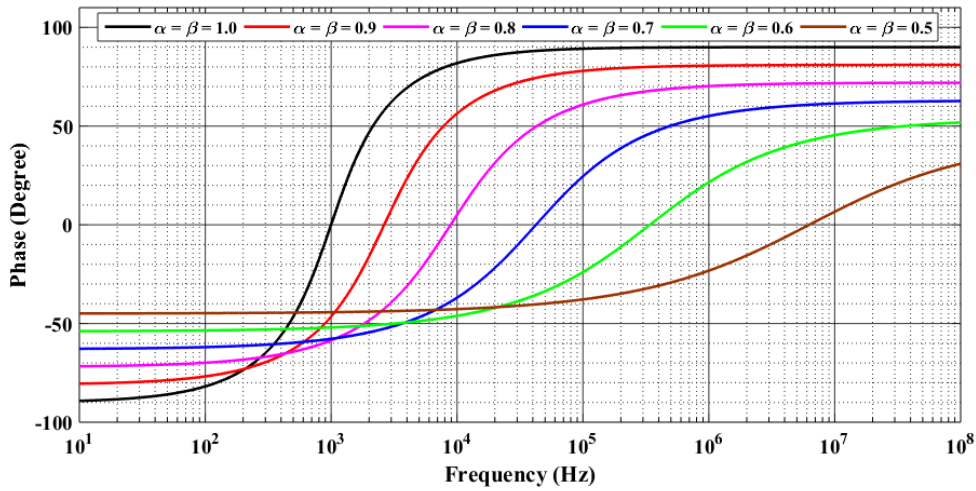
$$\omega_{rp}^{\alpha+\beta} \sin\left(\frac{(1-\alpha)\pi}{2}\right) E + D\omega_{rp}^\alpha + E \sin\left(\frac{(\beta+1)\pi}{2}\right) = 0 \quad (4.15)$$

Solution of equation (4.15), provides the value of ' ω_{rp} ' of FOIBP

The frequency responses of a FOIBP designed to have a minimum frequency (ω_m) of 1kHz (for $\alpha = 1, \beta = 1$), designed for the values of α and β by choosing the coefficients B, D, and E as 8882.748, 8882.748 and 39438400 respectively, have been plotted using MATLAB for different values of α and β and shown in Fig.4.3.



(a)



(b)

Figure 4.3 MATLAB simulations of FOIBP (a) Magnitude responses (b) Phase responses

The slope of the magnitude response and minimum frequency (ω_m) as obtained from Fig. 4.3 are given below in Table 4.3, from where it may be observed that be noted that the slope of the magnitude characteristics and the characterising frequency may be tuned by appropriately choosing the values of α and β .

Table 4.3 Various Parameters of FOIBP filter

α	Filter parameters	
	ω_m (kHz)	Attenuation (dB)
1.0	1.00	20
0.9	3.44	18
0.8	16.60	16
0.7	121	14
0.6	1596	12
0.5	54600	10

4.1.4. Fractional Order Inverse Band Reject Filter

The fractional order inverse band reject (FOIBR) filter response may be obtained from equation (4.1) by taking $B = 0$, $C = A.C$ and $C = E$ as:

$$T(s)_{\text{FOIBR}} = \frac{1}{A} \left[\frac{s^{\alpha+\beta} + Ds^\beta + E}{s^{\alpha+\beta} + E} \right] \quad (4.16)$$

The magnitude and phase responses of FOIBR filter can be derived from equation (4.16), as:

$$|T(j\omega)_{\text{FOIBR}}| = A \left[\frac{\omega^{2(\alpha+\beta)} + 2D\omega^{(\alpha+2\beta)} \cos\left(\frac{\alpha\pi}{2}\right) + D^2\omega^{2\beta} + 2E\omega^{(\alpha+\beta)} \cos\left(\frac{(\alpha+\beta)\pi}{2}\right) + 2DE\omega^\beta \cos\left(\frac{\beta\pi}{2}\right) + E^2}{\omega^{2(\alpha+\beta)} + 2C\omega^{(\alpha+\beta)} \cos\left(\frac{(\alpha+\beta)\pi}{2}\right) + E^2} \right]^{\frac{1}{2}} \quad (4.17a)$$

$$\begin{aligned} \angle T(j\omega)_{\text{FOIBR}} = & \tan^{-1} \left(\frac{\omega^{(\alpha+\beta)} \sin\left(\frac{(\alpha+\beta)\pi}{2}\right) + D\omega^\beta \sin\left(\frac{\beta\pi}{2}\right)}{\omega^{(\alpha+\beta)} \cos\left(\frac{(\alpha+\beta)\pi}{2}\right) + D\omega^\beta \cos\left(\frac{\beta\pi}{2}\right) + E} \right) \\ & - \tan^{-1} \left(\frac{\omega^{(\alpha+\beta)} \sin\left(\frac{(\alpha+\beta)\pi}{2}\right)}{\omega^{(\alpha+\beta)} \cos\left(\frac{(\alpha+\beta)\pi}{2}\right) + E} \right) \end{aligned} \quad (4.17b)$$

Using equation (4.16), the high frequency gain as well as DC gain are found to be $\frac{1}{A}$.

The peak frequency (ω_p) at which magnitude response of FOIBR filter attains its peak is given by:

$$\omega_p = E^{\frac{1}{(\alpha+\beta)}} \quad (4.18)$$

Similarly, the expression for right phase frequency of FOIBR can be derived from equation (4.17b) by equating the phase angle to $\pm \frac{\pi}{2}$ as:

$$\begin{aligned} \omega_{rp}^{2(\alpha+\beta)} + D\omega_{rp}^{\alpha+2\beta} \cos\left(\frac{\alpha\pi}{2}\right) + \omega_{rp}^{\alpha+\beta} \cos\left(\frac{(\alpha+\beta)\pi}{2}\right) (2E) \\ + C * D\omega_{rp}^\beta \cos\left(\frac{\beta\pi}{2}\right) + E^2 = 0 \end{aligned} \quad (4.19)$$

Solving equation (4.19), we can get the right phase frequency (ω_{rp}) of FOIBR.

In Fig. 4.4, we have shown the magnitude and phase responses of the FOIBR filter designed to have the peak frequency (ω_p) of 1kHz (for $\alpha = 1, \beta = 1$).

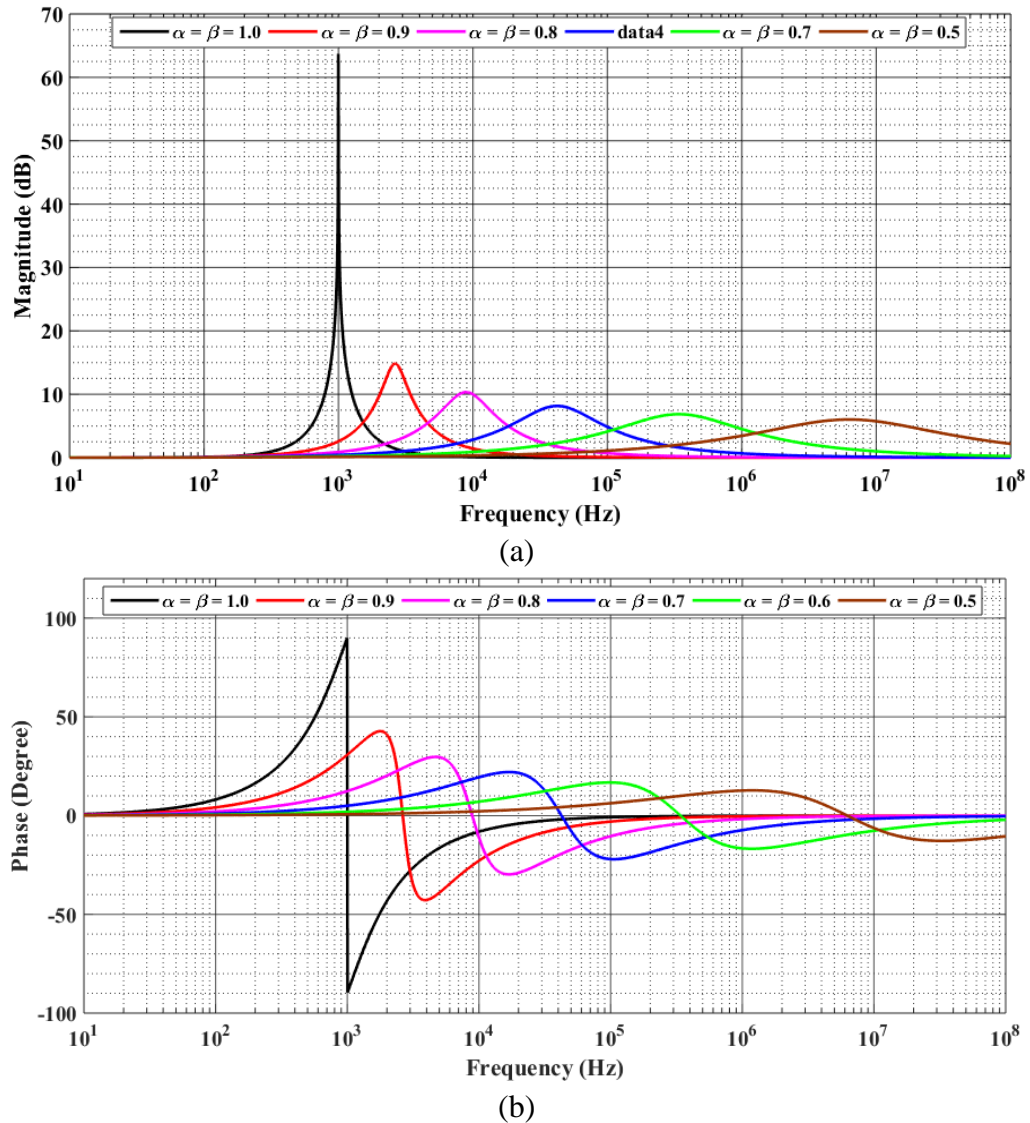


Figure 4.4 MATLAB simulations of FOIBP (a) Magnitude responses (b) Phase responses

The peak frequencies (ω_p) obtained from Fig.4.4 for different values of α are given in Table 4.4 and observed that ω_p vary with the value of ' α '.

Table 4.4 Peak frequency (ω_p) of FOIBR for different value of ' α '

α	Peak Frequency (ω_p) of FOIBR (kHz)
1.0	1.00
0.9	2.64
0.8	8.88
0.7	42.30
0.6	339.50
0.5	6260

From Fig. 4.1-Fig. 4.4, it may be noted that the fractional order inverse filters (FOILP, FOIHP, FOIBP and FOIBR) have a frequency response which is reciprocal of the frequency response of their conventional filter counterparts and the variable slopes of magnitude characteristics can be obtained by appropriate selections of the fractional order parameters, α and β . Similarly, by appropriate choices of the values of α and β the right phase frequencies and maximum frequencies as well as half power frequencies can be adjusted.

Before describing the formulation of various fractional order inverse active filter configurations realizable with op-amp, CFOAs and OTRA, it is useful to present an overview of various conventional inverse active filters proposed in the literature earlier.

4.2. Literature Overview of Conventional Inverse Active Filters

Nullor-based inverse active filter functions have been proposed earlier in [1] and [3]. Other works in which a four terminal floating nullor (FTFN) was used to realize inverse active filters were presented in [4-5]. On the other hand, the current feedback operational amplifier (CFOA) has been employed for the realization of inverse active filters in [6-9], while in [10], a current differencing buffered amplifier (CDBA) based universal inverse active filter structure was presented. In [11-12],

another building block, named as current differencing trans-conductance amplifier (CDTA) was used to realize inverse active filters, while second generation current conveyors (CCII) were employed in [13] to realize inverse all pass filter function. Differential difference current conveyor (DDCC) based inverse active filters were proposed in [14] whereas, three modified CFOAs were employed in [15] to realize the inverse active filters. Multiple output trans-conductance amplifiers have been used to realize inverse active filters operating in both voltage-mode (VM) and current-mode (CM) in [16]. Singh, Gupta and Senani [17] presented an OTRA-based multifunction inverse active filter configuration which was capable of realizing low pass, band pass and high pass filters in the voltage mode from the same structure.

From the survey of the existing literature as detailed above, it may be noted that no fractional order inverse active filter configurations employing any active element/device was reported in the open literature prior to the commencement of the present research work in 2015. Subsequent to the publication of the work reported³ in the following section of the thesis, few other works on the realization of fractional order inverse filters using CFOAs [18], CCII [19] and log-domain techniques [20] have also been reported.

Thus, in this chapter, we have proposed new structures of multi-functional fractional order inverse filters (FOIFs) realized with active building blocks such as, op-amp, CFOAs and OTRA. All the proposed topologies can realize fractional order inverse low pass, inverse high pass and inverse band pass responses from the same configuration as special cases.

³ D. R. Bhaskar, Manoj Kumar and P. Kumar “Fractional order inverse filters using operational amplifier”, *Analog Integrated Circuits and Signal Processing*, vol. 97, no. 1, pp. 149-158, 2018.

4.3. Fractional Order Inverse Active Filters using an Operational Amplifier

In this section, we have presented three new configurations of fractional order inverse active filters using single op-amp. The first structure of FOIF realizes FOILP, FOIBP and FOIHP responses in inverting mode whereas, the second structure yields FOILP, FOIBP and FOIHP responses in non-inverting mode. The third structure, on the other hand, is a minimal component realization (it uses minimum number of active and passive components) and, has infinite input impedance. These features are desirable from the point of view of reliability, power consumption and easy cascadability [21-22].

4.3.1. Fractional Order Inverse Active Filters Employing an Op-amp⁴

This section presents two new multifunctional fractional order inverse active filter configurations using a single op-amp. The first structure of FOIF uses op-amp in inverting mode while, in second configuration, op-amp has been configured in non-inverting mode to realise various inverse active filter responses.

4.3.1.1. Inverting Mode Multifunctional Fractional Order Inverse Filter Configuration

The generalized structure of multifunctional fractional order inverse filter has been shown in Fig.4.5.

⁴ The work presented in this section has been published in : D. R. Bhaskar, Manoj Kumar and P. Kumar “Fractional order inverse filters using operational amplifier”, Analog Integrated Circuits and Signal Processing, vol. 97, no. 1, pp. 149-158, 2018.

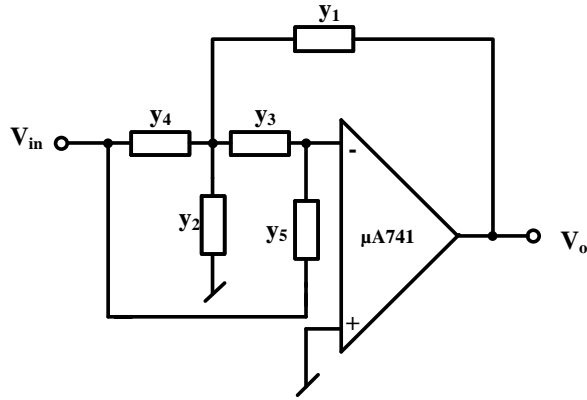


Figure 4.5 Inverting mode multifunctional FOIF configuration

Assuming ideal op-amp, the transfer function of FOIF of the circuit shown in Fig. 4.5 is derived as:

$$\frac{V_0}{V_{in}} = -\frac{y_3 y_4 + y_5 (y_1 + y_2 + y_3 + y_4)}{y_1 y_3} \quad (4.20)$$

where $y_i, i = 1-5$ are the branch admittances.

Equation 4.20 can now be used to realize various fractional order inverse active filters by appropriately selecting the admittances. These admittances, for different types FOIF realizations and the corresponding transfer functions are given below in Table 4.5.

Table 4.5 Transfer functions of the proposed FOIF structure shown in Fig. 4.5

Admittances Filter Responses	y₁	y₂	y₃	y₄	y₅	$\frac{V_0}{V_{in}}$
FOILP	$\frac{1}{R_1}$	$s^\alpha C_2$	$\frac{1}{R_3}$	$\frac{1}{R_4}$	$s^\alpha C_5$	$-\frac{D_1(s)}{K_1}$
FOIBP	$s^\alpha C_1$	$\frac{1}{R_2}$	$\frac{1}{R_3}$	$\frac{1}{R_4}$	$s^\alpha C_5$	$-\frac{D_2(s)}{K_2 s^\alpha}$
FOIHP	$s^\alpha C_1$	$\frac{1}{R_2}$	$s^\alpha C_3$	$s^\alpha C_4$	$\frac{1}{R_5}$	$-\frac{D_3(s)}{K_3 s^{2\alpha}}$

where

$$D_1(s) = s^{2\alpha} + a_1s^\alpha + b_1,$$

$$D_2(s) = s^{2\alpha} + a_2s^\alpha + b_2,$$

$$D_3(s) = s^{2\alpha} + a_3s^\alpha + b_3,$$

$$K_1 = \frac{1}{R_1R_3C_2C_5}, K_2 = \frac{1}{R_3C_5} \text{ and } K_3 = \frac{C_1}{C_4}$$

The coefficients a_1 – a_3 and b_1 – b_3 for the FOILP, FOIBP and FOIHP filters have been mapped with various passive components, which have been provided in Table 4.6.

Table 4.6 Mapping of the coefficients of the characteristic equation with the passive components of the fractional order inverse filters

Filter Coefficients			
a_1	$\frac{1}{C_2} \left(\frac{1}{R_1} + \frac{1}{R_3} + \frac{1}{R_4} \right)$	b_1	$\frac{1}{C_2C_5R_3R_4}$
a_2	$\frac{1}{C_1} \left(\frac{1}{R_2} + \frac{1}{R_3} + \frac{1}{R_4} \right)$	b_2	$\frac{1}{C_1C_5R_3R_4}$
a_3	$\frac{1}{R_5C_3C_4} (C_1 + C_3 + C_4)$	b_3	$\frac{1}{C_3C_4R_2R_5}$

From Table 4.5, it is noted that three different FOIFs viz. FOILP, FOIHP and FOIBP filters have been realized. The FOILP and FOIBP can be realized using three passive resistors and two fractional order capacitors ($0 < \alpha < 1$), while for FOIHP, two passive resistors and three fractional order capacitors are required. The filter parameters of the realized FOIFs i.e., half power frequency (ω_h) (for fractional order inverse low pass and inverse high pass filter) and minimum/peak frequency (ω_m or ω_p) (for fractional order inverse band pass filter) may be obtained by solving the following equations:

$$\text{FOILP: } \omega_h^{4\alpha} + 2a_1\omega_h^{3\alpha} \cos\left(\frac{\alpha\pi}{2}\right) + \omega_h^{2\alpha}(a_1^2 + 2b_1\cos(\alpha\pi)) + 2a_1b_1\omega_h^\alpha \cos\left(\frac{\alpha\pi}{2}\right) - b_1^2 = 0 \quad (4.21)$$

$$\text{FOIHP: } b_3^2 + 2a_3\omega_h^{3\alpha} \cos\left(\frac{\alpha\pi}{2}\right) + \omega_h^{2\alpha}(a_3^2 + 2b_3\cos(\alpha\pi)) + 2a_3b_3\omega_h^\alpha \cos\left(\frac{\alpha\pi}{2}\right) - \omega_h^{4\alpha} = 0 \quad (4.22)$$

$$\text{FOIBP: } \omega_m = (b_2)^{\frac{1}{2\alpha}} \quad (4.23)$$

4.3.1.1.1 PSPICE Simulations and MATLAB Evaluations

To evaluate the performance of proposed FOIF circuits, PSPICE simulations using SPICE macro model of $\mu A741$ have been carried out. The simulated results have also been verified with numerical evaluations using MATLAB.

PSPICE simulations: The FOIF structure shown in Fig.4.5 was designed to have a half power frequency or minimum frequency of 50 Hz for $\alpha = 1$. The choice of the half power frequency was dictated by the gain bandwidth product of the op-amp. The power supply voltages used to bias the op-amp were $\pm 12V$ DC. The values of passive components and the fractional order capacitors used in the simulations are given below in Table 4.7

Table 4.7 Component values used in PSPICE simulations

FOILP	FOIHP	FOIBP
$R_1 = 23576.88\Omega$	$R_2 = 3930.07\Omega$	$R_1 = 8336.95\Omega$
$R_3 = 11788.44\Omega$	$R_5 = 17688.00\Omega$	$R_2 = 20137.55\Omega$
$R_4 = 23576.88\Omega$	$C_1 = 0.382 \mu F/sec^{(\alpha-1)}$	$R_5 = 11788.44\Omega$
$C_2 = 0.382 \mu F/sec^{(\alpha-1)}$	$C_3 = 0.382 \mu F/sec^{(\alpha-1)}$	$C_3 = 0.382 \mu F/sec^{(\alpha-1)}$
$C_5 = 0.0955 \mu F/sec^{(\alpha-1)}$	$C_4 = 0.382 \mu F/sec^{(\alpha-1)}$	$C_4 = 0.382 \mu F/sec^{(\alpha-1)}$

The fractional order capacitors used in the simulations were designed using the method proposed by Valsa, Dvorak and Friedl [23], which uses a ladder network, as shown in Fig. 4.6. All passive component values to design FCs (for a fifth order approximation) have been calculated for different values of ' α ' (0.5, 0.6, 0.7, 0.8, 0.9) are given in Table 4.8.

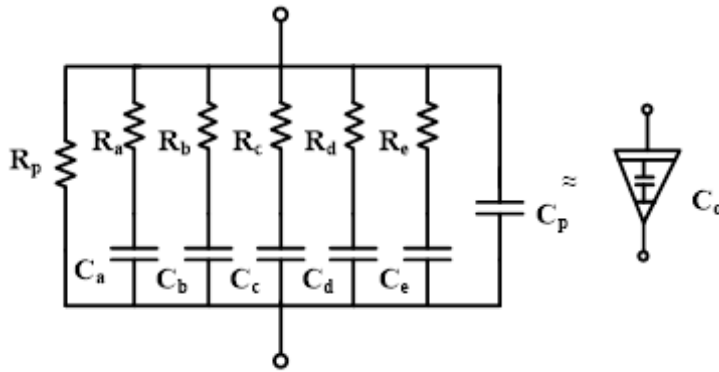
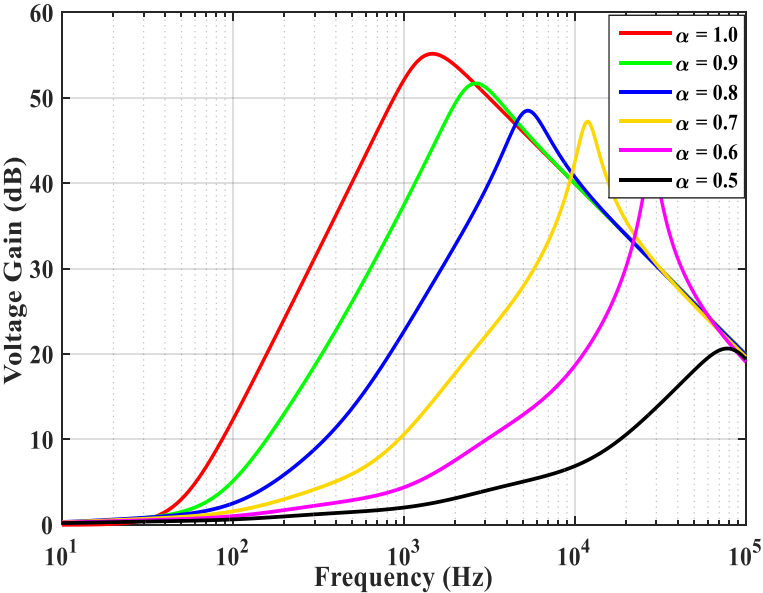


Figure 4.6 R-C ladder structure used to realize fractional order capacitors for the values 0.382 $\mu\text{F}/\text{sec}^{(\alpha-1)}$ and 0.0955 $\mu\text{F}/\text{sec}^{(\alpha-1)}$

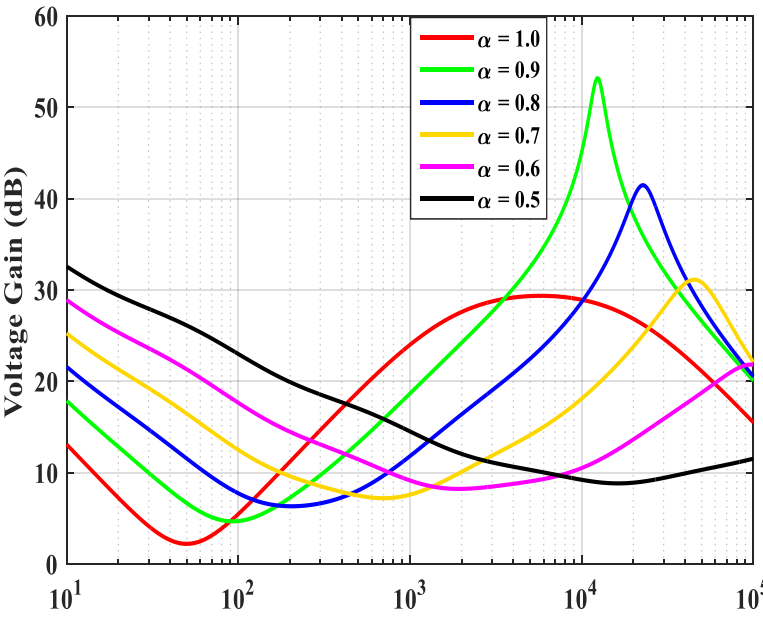
Table 4.8 Components value for the realization of FCs

α	$C_f = 0.0955 \mu\text{F}/\text{sec}^{(\alpha-1)}$	
	Resistors	Capacitors
0.9	$R_a = 676.34, R_b = 69.65, R_c = 7.17,$ $R_d = 0.74, R_e = 0.08, R_p = 5890.9$	$C_a = 14.79, C_b = 11.49, C_c = 8.92,$ $C_d = 6.93, C_e = 5.38, C_p = 18.736$
0.8	$R_a = 569.89, R_b = 75.56, R_c = 10.02,$ $R_d = 1.33, R_e = 0.18, R_p = 3728.7$	$C_a = 17.55, C_b = 10.59, C_c = 6.39,$ $C_d = 3.86, C_e = 2.33, C_p = 3.5397$
0.7	$R_a = 662.09, R_b = 113, R_c = 19.29,$ $R_d = 3.29, R_e = 0.56, R_p = 3217.2$	$C_a = 15.1, C_b = 7.08, C_c = 3.32, C_d = 1.56,$ $C_e = 0.73, C_p = 0.6429$
0.6	$R_a = 897.74, R_b = 197.24, R_c = 43.34,$ $R_d = 9.52, R_e = 2.09, R_p = 3188.2$	$C_a = 11.14, C_b = 4.06, C_c = 1.48, C_d = 0.54,$ $C_e = 0.2, C_p = 0.11211$
0.5	$R_a = 1355.8, R_b = 383.5, R_c = 108.5,$ $R_d = 30.7, R_e = 8.7, R_p = 3437.8$	$C_a = 7.375, C_b = 2.086, C_c = 0.59, C_d = 0.167,$ $C_e = 0.047, C_p = 0.018617$
α	$C_f = 0.382 \mu\text{F}/\text{sec}^{(\alpha-1)}$	
	Resistors	Capacitors
0.9	$R_a = 168.95, R_b = 17.40, R_c = 1.79,$ $R_d = 0.18, R_e = 0.019, R_p = 1471.36$	$C_a = 59, C_b = 46, C_c = 35, C_d = 27, C_e = 21,$ $C_p = 75$
0.8	$R_a = 142.47, R_b = 8.89, R_c = 2.5,$ $R_d = 0.33, R_e = 0.04, R_p = 932.16$	$C_a = 70.19, C_b = 42.35, C_c = 25.56, C_d = 15.42,$ $C_e = 9.31, C_p = 14.15$
0.7	$R_a = 165.52, R_b = 28.25, R_c = 4.82,$ $R_d = 0.82, R_e = 0.14, R_p = 804.3$	$C_a = 60.41, C_b = 28.32, C_c = 13.27, C_d = 6.22,$ $C_e = 2.92, C_p = 2.57$
0.6	$R_a = 224.43, R_b = 49.31, R_c = 10.83,$ $R_d = 2.38, R_e = 0.52, R_p = 797.06$	$C_a = 44.56, C_b = 16.22, C_c = 5.91, C_d = 2.15,$ $C_e = 0.78, C_p = 0.48$
0.5	$R_a = 338.96, R_b = 95.87, R_c = 27.12,$ $R_d = 7.67, R_e = 2.17, R_p = 859.45$	$C_a = 29.5, C_b = 8.34, C_c = 2.36, C_d = 0.67, C_e =$ $0.19, C_p = 0.074$
All resistors are in $\text{k}\Omega$ and capacitors are in nF .		

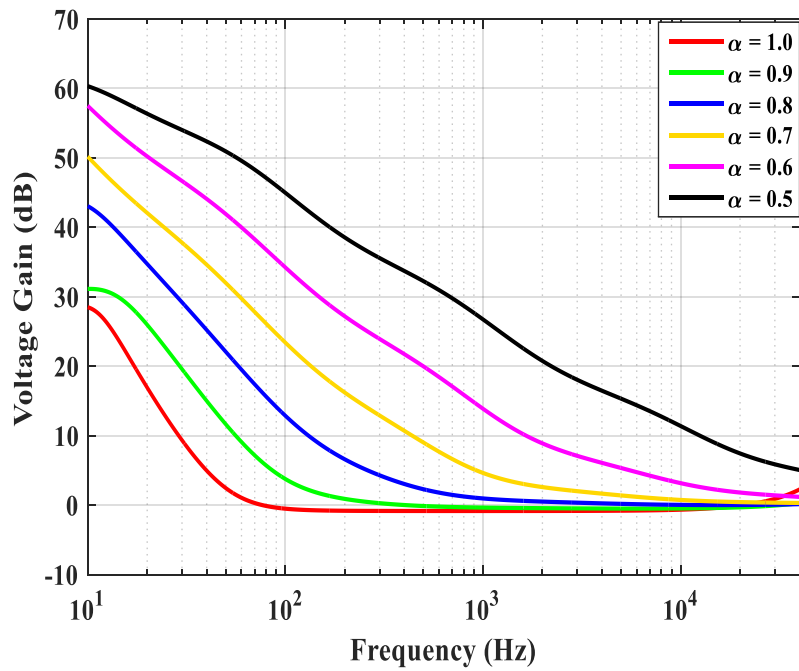
The magnitude responses of FOILP, FOIBP and FOIHP filter circuits derived from Fig.4.5 have been displayed in Fig. 4.7, in which, we have varied ' α ' from 0.5 to 1.0 in step of 0.1.



(i)



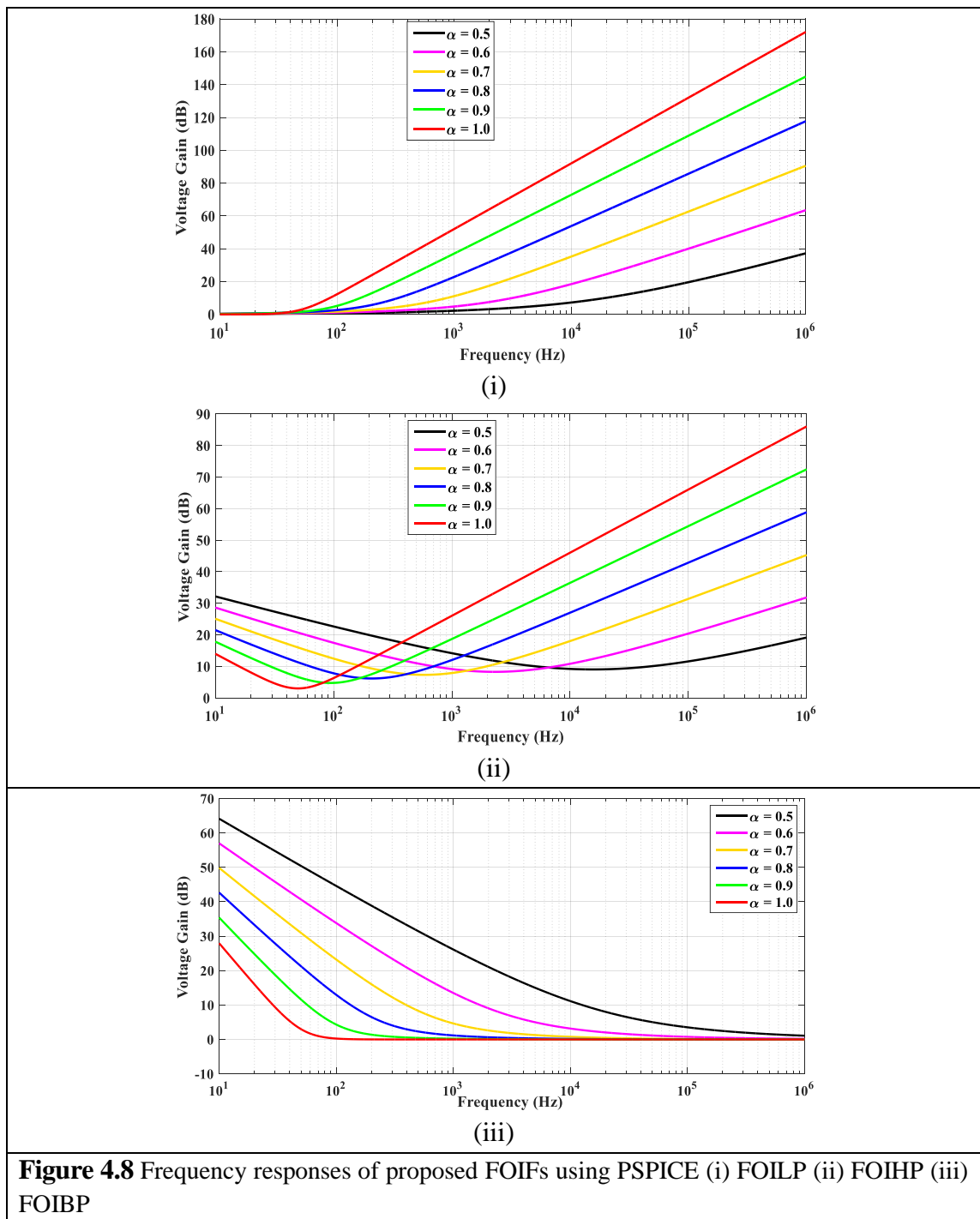
(ii)



(iii)

Figure 4.7 Frequency responses of proposed FOIFs using PSPICE (i) FOILP (ii) FOIHP (iii) FOIBP

MATLAB Evaluations: The frequency responses of all the FOIF circuits derived from Fig.4.5 were also evaluated using MATLAB for the same values of components which were used in PSPICE simulations. To validate the theoretical propositions, we have plotted magnitude responses of FOILP, FOIBP and FOIHP filter in MATLAB for different values of α ($\alpha = 0.5$ to 1.0). The resulting graphs have been displayed in Fig.4.8.



It may be pointed out that frequency responses, as obtained from MATLAB represent the ideal case(s) for different FOIF, whereas the PSPICE results reflect the real cases, in which, the gain bandwidth product of the operational amplifier limits the high frequency response. In the low frequency range of operation there is good correspondence between the MATLAB and PSPICE results. We have summarized the presented FOIFs results

obtained from PSPICE and MATLAB in terms of half power frequency, minimum frequency and stop band attenuation and presented in Tables 4.9 and 4.10 respectively.

Table.4.9 Summary of the simulation results for ω_h and ω_m for the FOIF of Fig. 4.5

Frequency (in Hz)		Values of α					
		1.0	0.9	0.8	0.7	0.6	0.5
Half power frequency (FOILP)	PSPICE	50.12	77.62	123.00	218.80	631.00	2138.00
	MATLAB	50.15	76.23	121.80	224.50	557.60	2101.00
	Theoretical	50.00	76.43	131.8	268.9	750.0	3236
Half power frequency (FOIHP)	PSPICE	51.29	121.60	402.70	1349.00	6310.00	17580.00
	MATLAB	50.04	124.00	394.30	1396.00	5716.00	19830.00
	Theoretical	50.00	110.3	313.6	1168	6494	68350
Minimum frequency (FOIBP)	PSPICE	50.12	95.50	204.20	707.90	1950.00	17780.00
	MATLAB	49.25	95.71	207.80	584.20	2293.00	16110.00
	Theoretical	50.00	94.73	210.5	588	2312	15725

Table 4.10 Summary of the simulation results for stop band attenuation (dB/decade)

Attenuation (dB/decades)		Value of α					
		1.0	0.9	0.8	0.7	0.6	0.5
Attenuation (FOILP)	PSPICE	39.76	36.35	33.46	31.89	29.70	14.54
	MATLAB	39.71	36.00	31.82	27.35	21.57	17.53
	Theoretical	40.00	36.00	32.00	28.00	24.00	20.00
Attenuation (FOIHP)	PSPICE	40.28	35.10	30.22	25.83	23.03	18.27
	MATLAB	39.44	34.90	30.90	25.56	22.75	18.46
	Theoretical	40.00	36.00	32.00	28.00	24.00	20.00
Attenuation (FOIBP)	PSPICE	18.52	17.87	15.91	13.80	10.86	09.47
	MATLAB	19.92	18.18	15.76	13.52	10.80	09.41
	Theoretical	20	18	16	14	12	10

From Table 4.9, it is seen that the half power/ minimum frequency evaluated from PSPICE and MATLAB concur with the theoretical values. From Table 4.10, the PSPICE and MATLAB stop band attenuation for different FOIFs are also in good agreement with the theoretical propositions.

4.3.1.2. Non-Inverting Fractional Order Inverse Filter Configuration

In the previous section, we have presented a FOIF structure which has a phase shift of 180° (for $\alpha = 1$) between input and output voltages. In this section, we present a non-inverting generalized configuration of multifunctional FOIF which has been shown in Fig.4.9.

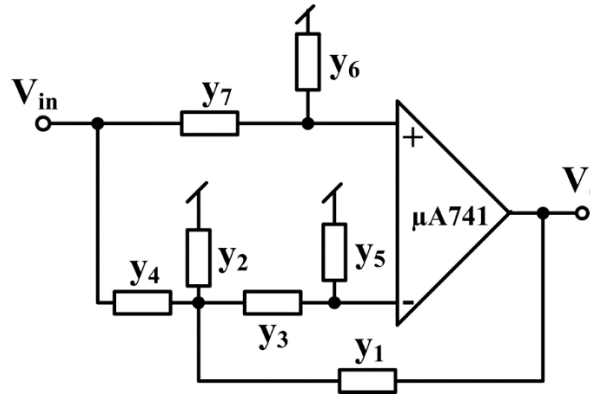


Figure 4.9 Proposed non-inverting multifunctional FOIF configuration

Assuming ideal op-amp, a routine circuit analysis of the circuit of Fig. 4.9 yields the following transfer function:

$$\frac{V_o}{V_{in}} = \frac{(y_3 + y_5)(y_1 + y_2 + y_4) + y_3y_5 - ky_3y_4}{ky_1y_3} \quad (4.24)$$

where $k = \left(1 + \frac{y_6}{y_7}\right)$, where $y_i, i = 1 - 7$ are the branch admittances.

Using Equation 4.24, the various FOIF transfer functions can be realized by appropriately selecting the various admittances as given below in Table 4.11.

Table 4.11 Branch admittances and transfer functions of FOIFs realized from Fig. 4.9

Admittances Filter Responses	y_1	y_2	y_3	y_4	y_5	y_6	y_7	$\frac{V_o}{V_{in}}$
FOILP	$\frac{1}{R_1}$	$\frac{1}{R_2}$	$\frac{1}{R_3}$	$s^\alpha C_4$	$s^\alpha C_5$	$\frac{1}{R_6}$	$\frac{1}{R_7}$	$\frac{D_1(s)}{K_1}$

FOIBP	$\frac{1}{R_1}$	$s^\alpha C_2$	$s^\alpha C_3$	$\frac{1}{R_4}$	$\frac{1}{R_5}$	$\frac{1}{R_6}$	$\frac{1}{R_7}$	$\frac{D_2(s)}{K_2 s^\alpha}$
FOIHP	$s^\alpha C_1$	$\frac{1}{R_2}$	$s^\alpha C_3$	$\frac{1}{R_4}$	$\frac{1}{R_5}$	$\frac{1}{R_6}$	$\frac{1}{R_7}$	$\frac{D_3(s)}{K_3 s^{2\alpha}}$

where

$$D_1(s) = s^{2\alpha} + a_1 s^\alpha + b_1, D_2(s) = s^{2\alpha} + a_2 s^\alpha + b_2, D_3(s) = s^{2\alpha} + a_3 s^\alpha + b_3,$$

$$K_1 = \frac{k}{R_1 R_3 C_4 C_5}, K_2 = \frac{k}{R_1 C_2}, K_3 = k \text{ and } k = \left(1 + \frac{R_7}{R_6}\right)$$

From Table 4.11, it may be noted that three different inverse filter functions i.e., FOILP, FOIBP and FOIHP can be realized from the structure shown in Fig. 4.9 employing five conventional resistors and two simulated FCs.

We have mapped the coefficients of the $D_1(s)$, $D_2(s)$ and $D_3(s)$ with the values of various passive components for FOILP, FOIBP and FOIHP filters respectively and tabulated them in Table 4.12

Table 4.12 Mapping of the coefficients of the characteristic equation with the passive components of the fractional order inverse filters

a_1	$\frac{1}{C_4} \left(\frac{1}{R_1} + \frac{1}{R_2} \right) + \frac{1}{C_4 R_3} + \frac{1}{C_5 R_3} - \frac{k}{C_5 R_3}$	b_1	$\frac{1}{C_4 C_5 R_3} \left(\frac{1}{R_1} + \frac{1}{R_2} \right)$
a_2	$\frac{1}{C_2} \left(\frac{1}{R_1} + \frac{1}{R_4} \right) + \frac{1}{C_3 R_5} + \frac{1}{C_2 R_5} - \frac{k}{C_2 R_4}$	b_2	$\frac{1}{C_2 C_3 R_5} \left(\frac{1}{R_1} + \frac{1}{R_4} \right)$
a_3	$\frac{1}{C_1} \left(\frac{1}{R_2} + \frac{1}{R_4} \right) + \frac{1}{C_3 R_5} + \frac{1}{C_1 R_5} - \frac{k}{C_1 R_4}$	b_3	$\frac{1}{C_1 C_3 R_5} \left(\frac{1}{R_2} + \frac{1}{R_4} \right)$

4.3.1.2.1 PSPICE Simulations and MATLAB Evaluations

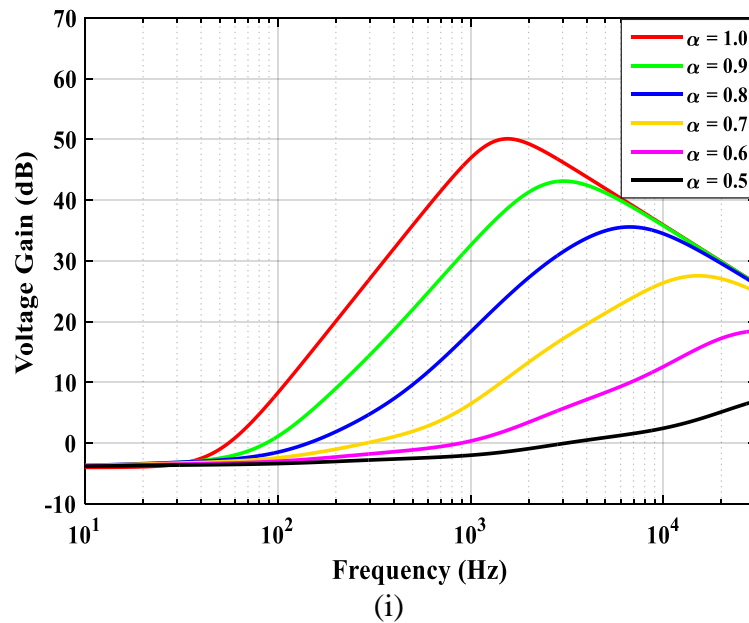
The performance of the FOIFs realized from the configuration of Fig. 4.9, has been evaluated using SPICE simulations and compared these results with the frequency response of the corresponding circuits obtained using MATLAB.

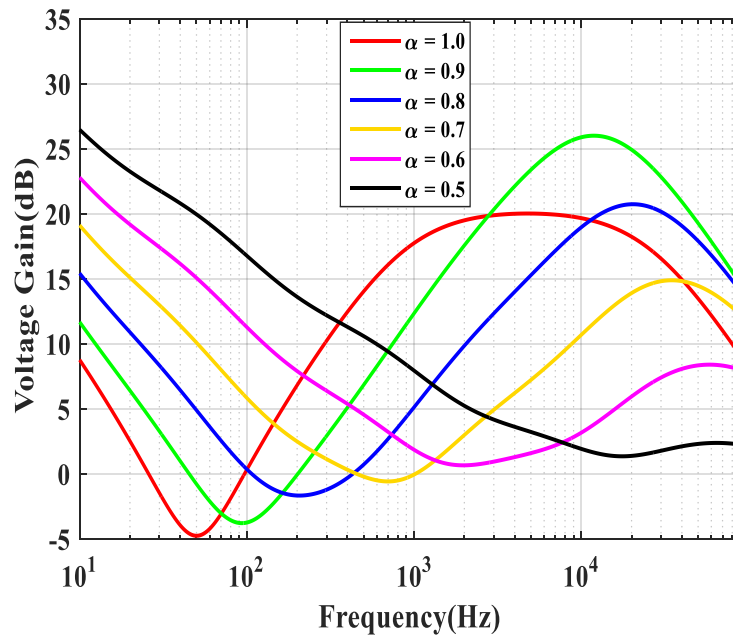
PSPICE simulations: All the FOIF circuits were designed for half power frequency (minimum frequency for FOIBP) of 50 Hz for $\alpha = 1$. Op-amp was biased with ± 12 V DC power supply. Values of passive resistors and FCs used to simulate the different FOIFs have been provided in Table.4.13.

Table.4.13 Component values used in PSPICE simulations

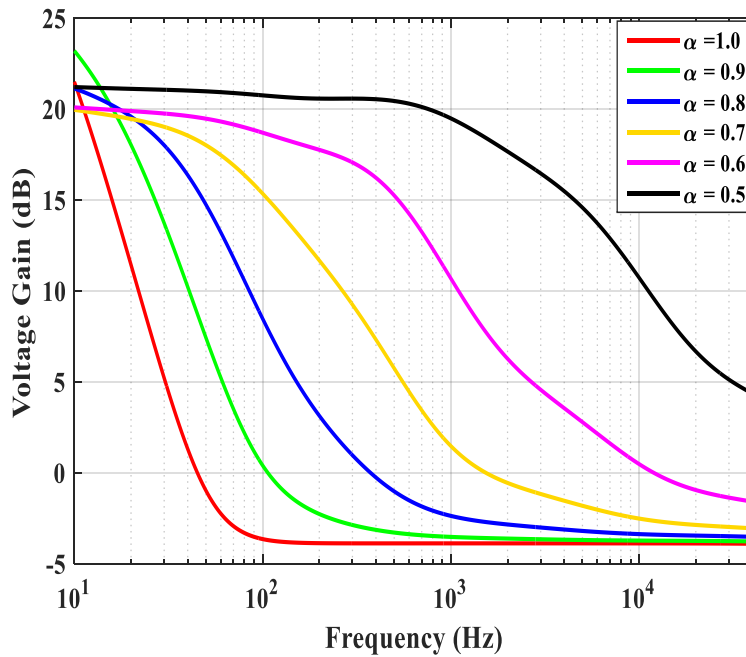
Components		
FOILP	FOIHP	FOIBP
$R_1 = 8324.61\Omega$	$R_2 = \infty$	$R_1 = 8324.61\Omega$
$R_2 = \infty$	$R_4 = 8324.61\Omega$	$R_4 = 8324.61\Omega$
$R_3 = 8324.61\Omega$	$R_5 = 8324.61\Omega$	$R_5 = 16649.21\Omega$
$R_6 = 8324.61\Omega$	$R_6 = 8324.61\Omega$	$R_6 = 8324.61\Omega$
$R_7 = 4876.661\Omega$	$R_7 = 4876.66\Omega$	$R_7 = 4876.66\Omega$
$C_5 = 0.382 \mu\text{F}/\text{sec}^{(\alpha-1)}$	$C_1 = 0.382 \mu\text{F}/\text{sec}^{(\alpha-1)}$	$C_2 = 0.382 \mu\text{F}/\text{sec}^{(\alpha-1)}$
$C_4 = 0.382 \mu\text{F}/\text{sec}^{(\alpha-1)}$	$C_3 = 0.382 \mu\text{F}/\text{sec}^{(\alpha-1)}$	$C_3 = 0.382 \mu\text{F}/\text{sec}^{(\alpha-1)}$

The magnitude responses for different FOIFs for $\alpha = 0.5, 0.6, 0.7, 0.8, 0.9$ and 1 have been demonstrated in Fig.4.10.





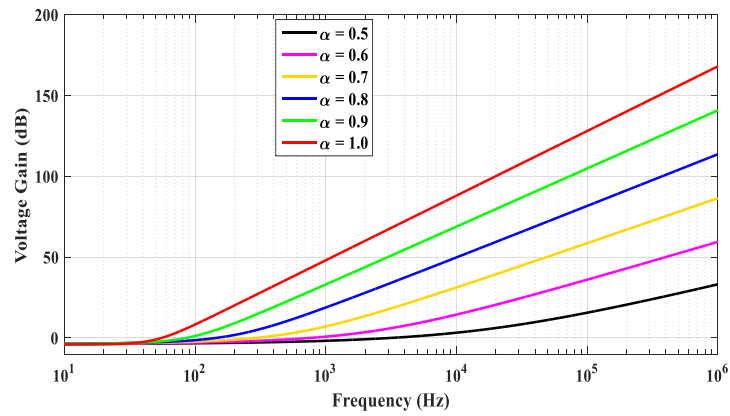
(ii)



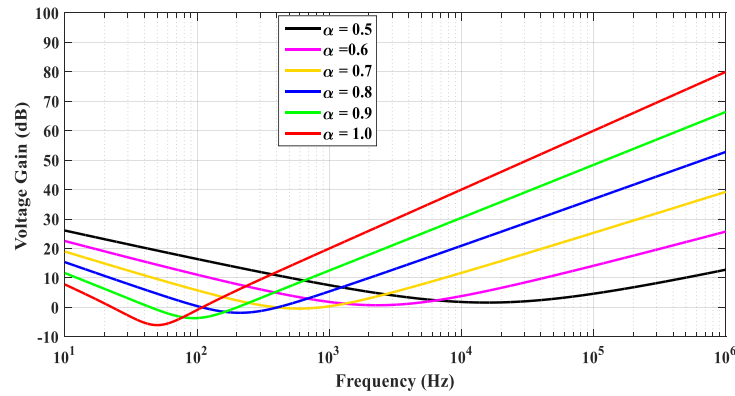
(iii)

Figure 4.10 Frequency responses of FOIFs using PSPICE (i) FOILP (ii) FOIBP (iii) FOIHP filter

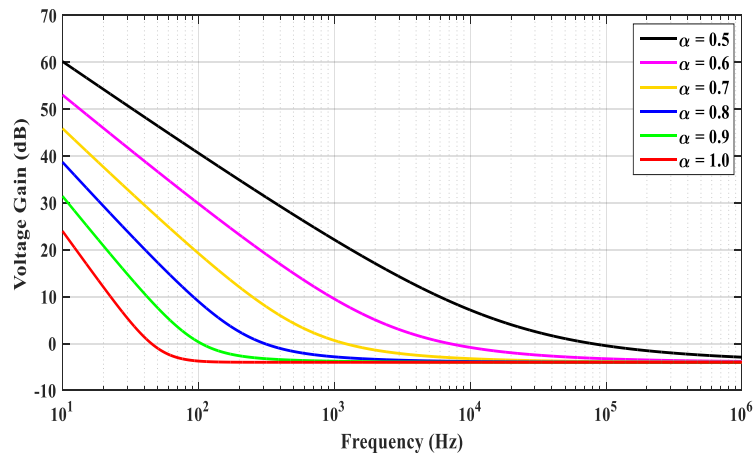
MATLAB evaluations: The performance of all the proposed FOIF circuits has also been verified using MATLAB for the same values of components which were used in PSPICE simulations. The MATLAB simulation results of the proposed fractional order inverse filters for different values of α ($\alpha = 0.5$ to 1.0) are shown in Fig. 4.11.



(i)



(ii)



(iii)

Figure 4.11 Frequency responses of FOIFs using MATLAB (i) FOILP (ii) FOIBP (iii) FOIHP filter

In Tables. 4.14 - 4.15, the summary of the simulation results with PSPICE and MATLAB has been provided.

Table 4.14 Summary of the simulation results for ω_h and ω_m (Hz)

Frequency (in Hz)		Value of α					
		1.0	0.9	0.8	0.7	0.6	0.5
Half power frequency (FOILP)	PSPICE	51.29	77.62	123.00	218.80	631.00	2188.00
	MATLAB	50.15	75.60	121.30	225.00	553.00	1848.00
	Theoretical	50.00	76.43	131.8	268.9	750.0	3236
Half power frequency (FOIHP)	PSPICE	49.50	120.20	407.40	1514.00	5370.00	17380.00
	MATLAB	50.25	124.60	396.00	1414.00	4137.00	17150
	Theoretical	50.00	110.3	313.6	1168	6494	68350
Minimum frequency (FOIBP)	PSPICE	50.12	93.33	204.20	691.90	1950.00	17780.00
	MATLAB	50.04	93.96	208.30	588.70	2293.00	16110.00
	Theoretical	50.00	94.73	210.5	588	2312	15725

Table 4.15 Summary of the simulation results for stopband attenuation (dB/decade)

Attenuation (dB/decades)		Value of α					
		1.0	0.9	0.8	0.7	0.6	0.5
Attenuation (FOILP)	PSPICE	38.63	32.73	26.30	19.93	13.83	6.97
	MATLAB	40.02	35.99	31.83	27.36	23.24	16.83
	Theoretical	40.00	36.00	32.00	28.00	24.00	20.00
Attenuation (FOIHP)	PSPICE	38.14	32.50	26.12	19.78	12.25	11.39
	MATLAB	39.22	34.90	31.06	27.29	23.50	19.69
	Theoretical	40.00	36.00	32.00	28.00	24.00	20.00
Attenuation (FOIBP)	PSPICE	19.50	17.40	14.30	11.69	11.41	09.52
	MATLAB	20.10	17.91	15.53	13.61	10.93	08.90
	Theoretical	20	18	16	14	12	10

4.3.2. Minimal Realization of Fractional Order Inverse Filters⁵

The fractional order inverse filter structures presented in previous sections suffer from the following limitations: (i) not having high input impedance and (ii) employment of non-canonic number of passive components. Therefore, in the following, we present a novel structure of the FOIFs which employs minimum number of active and passive elements with ideally infinite input impedance. The generalized filter configuration to realize multifunction fractional order inverse active filters is shown in Fig. 4.12.

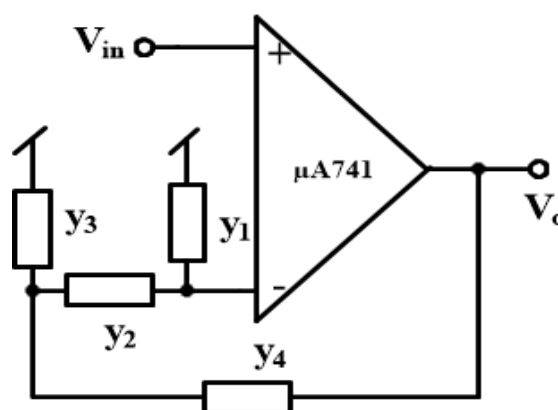


Figure 4.12 Proposed structure of multifunctional FOIFs

This configuration can realize (i) fractional order inverse low pass filter (ii) fractional order inverse high pass filter and (iii) fractional order inverse band pass filter by appropriate choice(s) of different branch admittances (y_1 - y_4).

Assuming ideal op-amp, a routine circuit analysis of the circuit shown in Fig.4.12 gives the following transfer function:

$$\frac{V_o}{V_{in}} = \frac{y_1(y_2 + y_3 + y_4) + y_2(y_3 + y_4)}{y_2y_4} \quad (4.25)$$

⁵ The work presented in this section has been published in: D. R. Bhaskar, Manoj Kumar and P.Kumar, "Minimal realization of fractional order inverse filters," IETE Journal of Research, 2020, DOI: 10.1080/03772063.2020.1803770.

Equation (4.25) can now be used to realize various inverse fractional order active filters by appropriately selecting the branch admittances as given below in Table 4.16.

Table 4.16 Various fractional order inverse filter transfer function derived from equation (4.25)

Admittances Filter Responses	y₁	y₂	y₃	y₄	$\frac{V_0}{V_{in}}$
FOILP	$s^\alpha C_1$	$\frac{1}{R_2}$	$s^\alpha C_3$	$\frac{1}{R_4}$	$\frac{D_1(s)}{K_1}$
FOIBP	$s^\alpha C_1$	$\frac{1}{R_2}$	$\frac{1}{R_3}$	$s^\alpha C_4$	$\frac{D_2(s)}{K_2 s^\alpha}$
FOIHP	$\frac{1}{R_1}$	$s^\alpha C_2$	$\frac{1}{R_3}$	$s^\alpha C_4$	$\frac{D_3(s)}{K_3 s^{2\alpha}}$
where $D_1(s) = s^{2\alpha} + a_1 s^\alpha + b_1$, $D_2(s) = s^{2\alpha} + a_2 s^\alpha + b_2$, $D_3(s) = s^{2\alpha} + a_3 s^\alpha + b_3$ and $K_1 = \frac{1}{R_2 R_4 C_1 C_3}$, $K_2 = \frac{1}{R_2 C_1}$ and $K_3 = 1$					

Thus, from Table 4.16 it is seen that the FOILP, FOIBP and FOIHP can be realized using only two passive resistors and two fractional order capacitors ($0 < \alpha < 1$).

The ω_h of FOILP, FOIHP, and ω_m for FOIBP can be obtained from equations (4.21) - (4.23) respectively.

The coefficients a_1 - a_3 and b_1 - b_3 for the FOILP, FOIBP and FOIHP filters are mapped with the values of various passive components as given below in Table 4.17.

Table 4.17 Mapping of the coefficients of the characteristic equation with the passive components of the fractional order inverse filters

a_1	$\frac{1}{C_3} \left(\frac{1}{R_2} + \frac{1}{R_4} \right) + \frac{1}{R_2 C_1}$	b_1	$\frac{1}{C_1 C_3 R_2 R_4}$
a_2	$\frac{1}{C_4} \left(\frac{1}{R_2} + \frac{1}{R_3} \right) + \frac{1}{R_2 C_1}$	b_2	$\frac{1}{C_1 C_4 R_2 R_3}$
a_3	$\frac{1}{C_4} \left(\frac{1}{R_1} + \frac{1}{R_3} \right) + \frac{1}{R_1 C_2}$	b_3	$\frac{1}{C_2 C_4 R_1 R_3}$

4.3.2.1. PSPICE and MATLAB Simulation Results

The proposed fractional order inverse active filter circuits have been simulated in PSPICE. The simulated results have also been verified with numerical simulations carried out in MATLAB. In PSPICE simulations, we have used a $\mu A741$ type op-amp, two fractional order capacitors and two passive resistors. The component values which are used in the design of fractional order inverse active filters for a half power/minimum frequency of 50 Hz for $\alpha = 1$ (half power frequency for FOILP, FOIHP and minimum frequency for FOIBP filters) are shown in Table 4.18. The fractional order capacitors used were designed using Valsa, Dvorak and Friedl method [23], having 2% ripple in the phase response in the frequency range (10Hz – 1MHz) for different values of α used in simulations. The equivalent RC ladder circuit, simulating the fractional order capacitor is shown in Fig. 4.6. We have listed the values of all components required to design a fractional order capacitor of value $0.382\mu\text{F}/\text{sec}^{(\alpha-1)}$ for different values of α in Table 4.18. The simulated phase responses of the fractional order capacitors for different values of α (from 0.5 to 0.9 in step of 0.1) are depicted in Fig. 4.13.

Table 4.18 Component values for the realization of fractional order inverse filters used in PSPICE

Type of filter	Resistor	Fractional Capacitor
FOILP	$R_2 = 3113\Omega, R_4 = 3113\Omega$	$C_1 = 0.382\mu\text{F}/\text{sec}^{(\alpha-1)}, C_3 = 0.382\mu\text{F}/\text{sec}^{(\alpha-1)}$
FOIBP	$R_2 = 8324.6\Omega, R_3 = 8324.6\Omega$	$C_1 = 0.382 \mu\text{F}/\text{sec}^{(\alpha-1)}, C_4 = 0.382 \mu\text{F}/\text{sec}^{(\alpha-1)}$
FOIHP	$R_1 = 23545\Omega, R_3 = 23545\Omega$	$C_2 = 0.382\mu\text{F}/\text{sec}^{(\alpha-1)}, C_4 = 0.382\mu\text{F}/\text{sec}^{(\alpha-1)}$

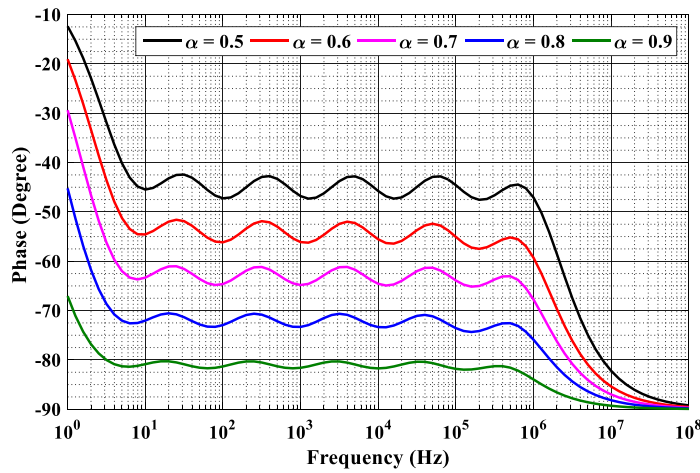
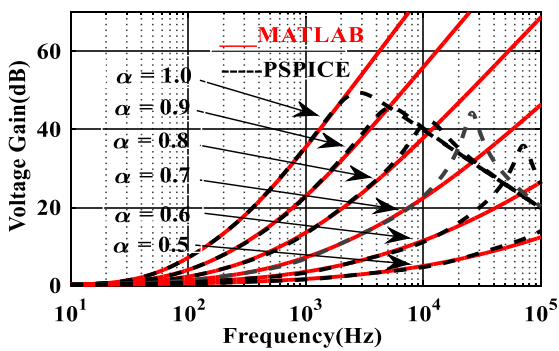
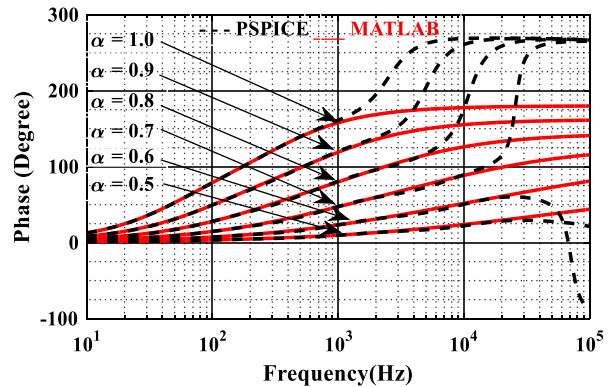


Figure 4.13 Phase responses of fractional order capacitor of value $0.382 \mu\text{F}/\text{sec}^{(\alpha-1)}$ for different values of α

The PSPICE and MATLAB frequency responses (magnitude and phase) of the proposed fractional order inverse active filters of Fig. 4.12 are shown in Fig. 4.14. The magnitude responses are shown in Fig.4.14 (a-c) while the corresponding phase responses have been demonstrated in Fig.4.14 (d-f) respectively. A brief summary of simulated results using PSPICE and MATLAB along with theoretical values for half power/minimum frequency and stop band attenuation of FOIFs are given in Table 4.19 and 4.20 respectively.



(a)



(d)

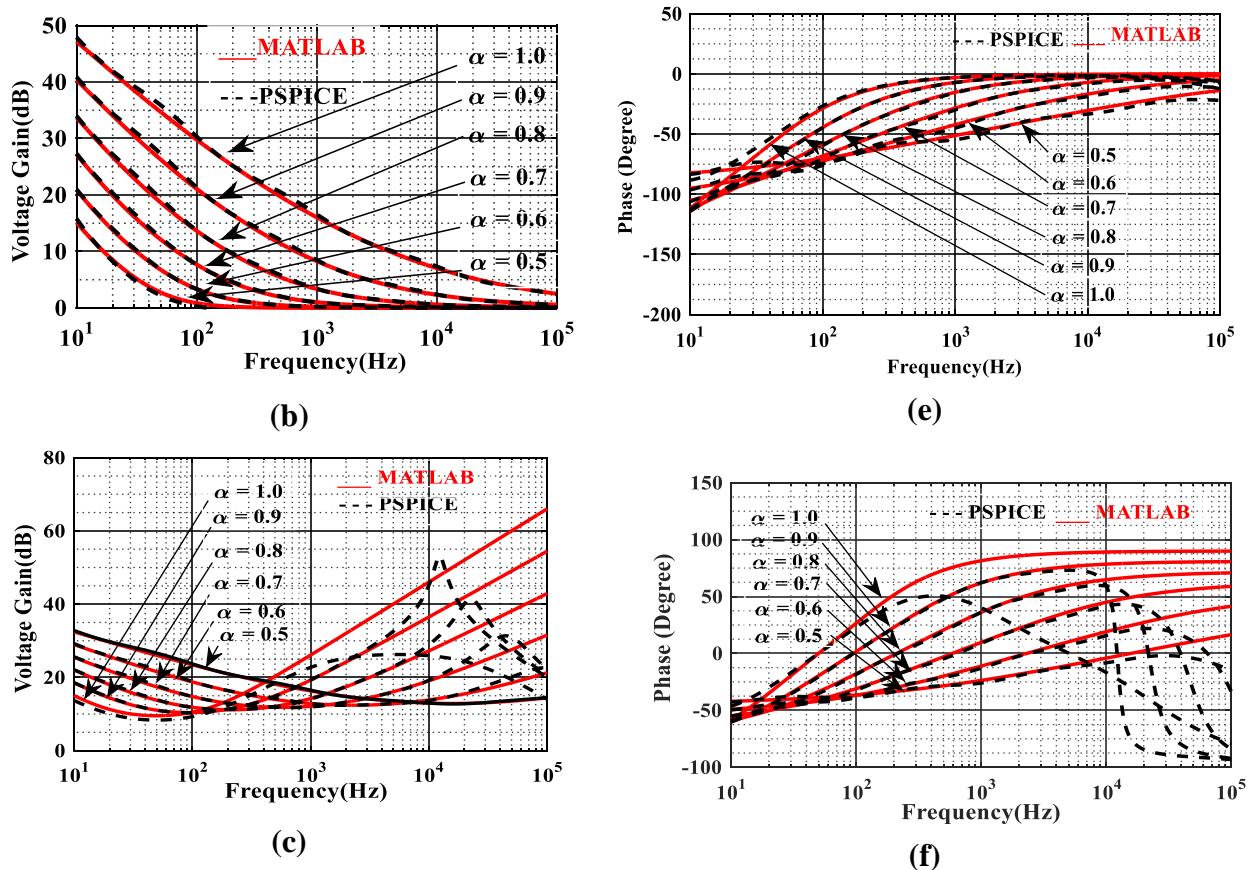


Figure 4.14 Frequency responses of FOIFs (a) Magnitude responses of FOILP (b) Magnitude responses of FOIHP (c) Magnitude responses of FOIBP filter (d) Phase responses of FOILP (e) Phase responses of FOIHP (f) Phase responses of FOIBP

Table.4.19 PSPICE, MATLAB and theoretical results for half power/minimum frequency (Hz)

Frequency (in Hz)		Value of α					
		1.0	0.9	0.8	0.7	0.6	0.5
Half power frequency (FOILP)	PSPICE	50.12	79.43	134.9	275.4	856.3	3311
	MATLAB	49.95	76.23	131.8	272.4	745.3	3320
	Theoretical	50.00	76.43	131.8	268.9	750.0	3236
Half power frequency (FOIHP)	PSPICE	49.95	107.2	323.6	1147	7200	67700
	MATLAB	47.33	110.2	314.7	1161	6515	68320
	Theoretical	50.00	110.3	313.6	1168	6494	68350
Minimum frequency (FOIBP)	PSPICE	50.12	97.72	208.9	676.6	1905	15140
	MATLAB	51.10	95.71	207.8	628.9	2289	15610
	Theoretical	50.00	94.73	210.5	588	2312	15725

Table 4.20 Summary of the simulation results for stop band attenuation (dB/decade)

Attenuation (dB/decades)		Value of α					
		1.0	0.9	0.8	0.7	0.6	0.5
Attenuation (FOILP)	PSPICE	32.27	29.95	28.18	18.92	13.46	5.40
	MATLAB	39.54	34.69	31.79	26.29	21.40	15.40
	Theoretical	40.00	36.00	32.00	28.00	24.00	20.00
Attenuation (FOIHP)	PSPICE	34.37	28.63	24.85	24.35	23.56	19.51
	MATLAB	34.87	29.92	21.35	17.62	12.81	13.79
	Theoretical	40.00	36.00	32.00	28.00	24.00	20.00
Attenuation (FOIBP)	PSPICE	17.44	15.05	13.74	10.90	09.42	06.93
	MATLAB	19.18	17.31	14.36	12.65	11.16	07.98
	Theoretical	20	18	16	14	12	10

From the PSPICE and MATLAB simulation results as shown in Fig. 4.14 and summarized in Tables 4.19 and 4.20, it is observed that there is very little deviation in the two results up to 1 kHz. Since the inverse filters tend to have a very large gain around the cut-off frequencies, the difference in the values of attenuation and half power/minimum frequencies for different values of α , obtained from MATLAB and PSPICE simulations may be attributed to the non-ideal behaviour of the op-amp (mainly due to its finite gain bandwidth product).

The power consumption of the proposed FOILP, FOIBP and FOIHP filters is found to be 50 mW using PSPICE simulations. Performance of proposed fractional order band pass filter was analyzed using intermodulation distortion (IMD) method [25-26]. In PSPICE simulations, 1 Volt sinusoidal signal of frequency 676 Hz with parasitic signal of 0.1 V with variable frequencies were applied at input node of the designed FOIBP filter. The obtained % THD for different frequencies of parasitic signal of FOIBP is given in Table 4.21.

Table 4.21 IMD results of the proposed FOIBP for $\alpha = 0.7$

Frequency of parasitic signal (KHz)	THD (%)	Frequency of parasitic signal (KHz)	THD (%)	Frequency of parasitic signal (KHz)	THD (%)
0.10	1.670	1	6.090	10	3.108
0.20	1.709	2	11.900	11	1.140
0.30	1.236	3	13.440	12	2.140
0.40	2.620	4	15.080	13	0.805
0.50	3.490	5	16.630	14	2.430
0.60	1.620	6	17.46	16	2.470
0.70	0.752	7	5.010	18	2.580
0.80	3.070	8	2.249	20	2.650
0.90	4.260	9	1.967	22	2.730

4.3.2.2. Experimental Results of the Proposed FOIFs

For the experimental verification of the proposed fractional-order inverse active filter responses, we have bread boarded the circuit as shown in Fig. 4.15 using a fractional-order capacitor of value $0.382 \mu\text{F}/\text{sec}(\alpha-1)$ for $\alpha = 0.7$ and an op-amp $\mu\text{A}741$. The power supply voltages used were $\pm 15\text{V}$. The fractional-order capacitor was realized using RC-ladder circuit as shown in Fig.4.6 whose component values were given in Table 4.8. The values of other passive components required for the realization of different fractional order inverse active filters are provided in Table 4.18. A snapshot of the experimental setup is displayed in Fig.4.15.

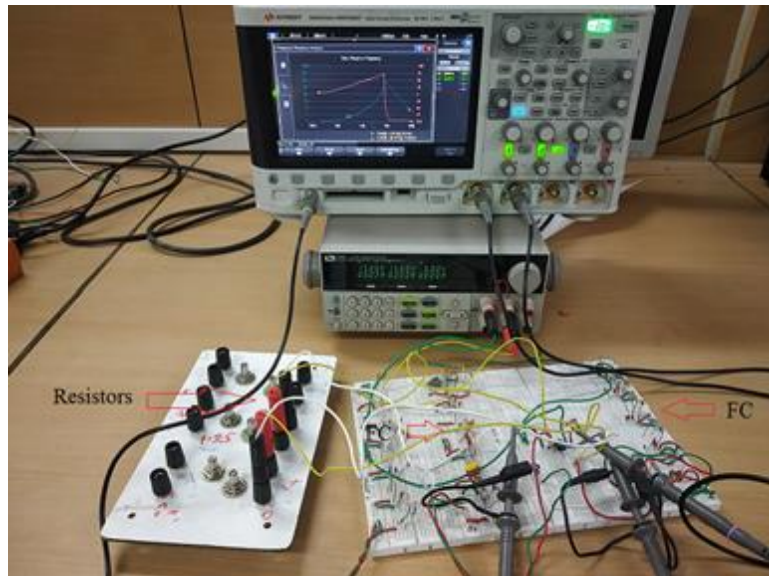


Figure 4.15 Experimental set up for FOILP filter for $\alpha = 0.7$

The frequency responses of all the three fractional order inverse active filters were obtained using KEYSIGHT DSOX-3034T. We have shown an exemplary frequency response plot of FOILP filter in Fig.4.16.

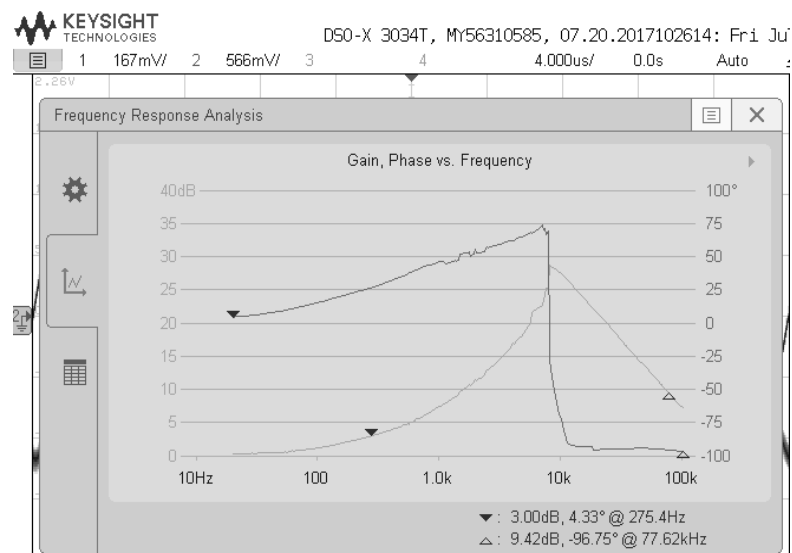


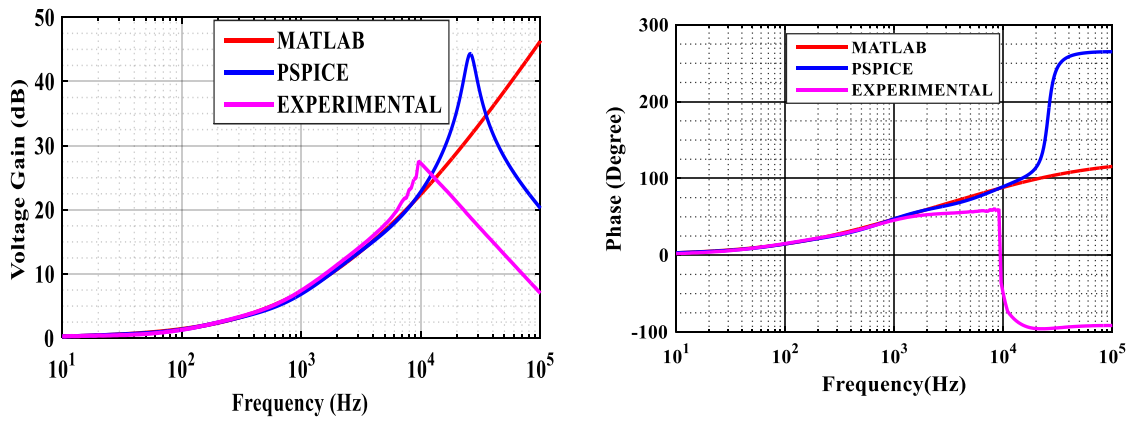
Figure 4.16 Experimental results of FOILP filter

The experimentally obtained half power/minimum frequency and phase at half power/minimum frequency along with their values obtained from MATLAB and PSPICE simulations for FOILP, FOIHP and FOIBP filters are presented in Table 4.22.

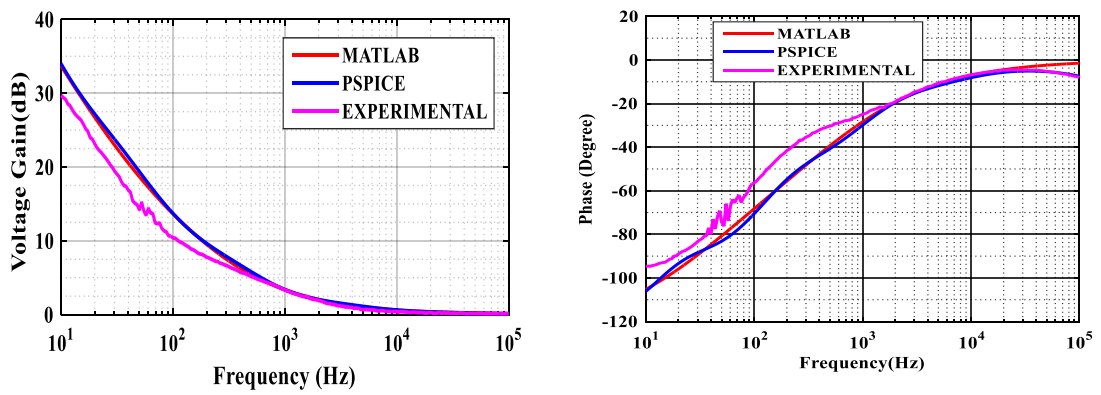
Table 4.22 Summary of results of FOIs for $\alpha = 0.7$

FOILP	Half power frequency (Hz)	Phase at half power frequency (Degree)
MATLAB	272.2	26.26
PSPICE	275.4	25.00
Experimental	275.4	25.78
FOIBP	Minimum Frequency (Hz)	Phase at Minimum Frequency (Degree)
MATLAB	628.9	01.23
PSPICE	676.6	0.829
Experimental	660.7	-1.29
FOIHP	Half power Frequency (Hz)	Phase at half power frequency (Degree)
MATLAB	1161	-26.22
PSPICE	1147	-27.61
Experimental	1124	-24.30

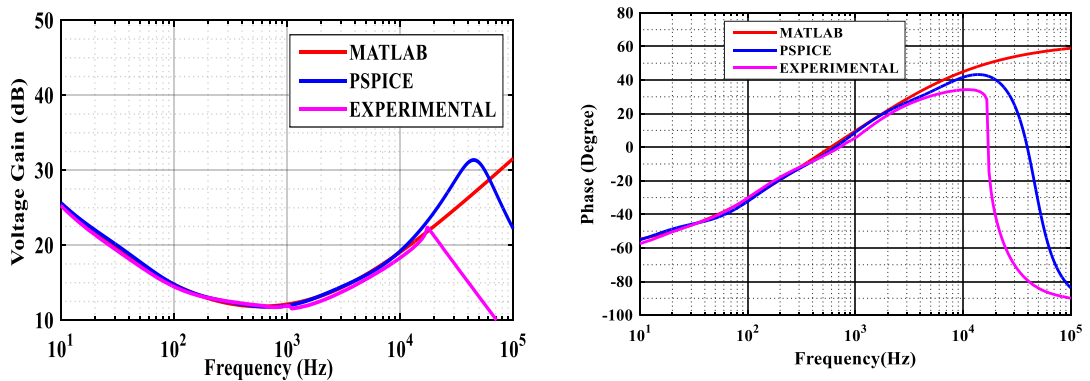
The experimentally obtained frequency and phase responses of the proposed fractional order active inverse filters superimposed on the corresponding MATLAB and PSPICE responses for $\alpha = 0.7$ are shown in Fig. 4.17 (a-c). Also from these figures, it may be noted that the three responses obtained are in close agreement with each other in the frequency range of 10Hz-1KHz indicating satisfactory performance of the fractional order inverse active filters. The degradation in the performance of the filters at higher frequencies may be attributed to the finite unity gain bandwidth of the operational amplifier used.



(a)



(b)



(c)

Figure 4.17 Frequency responses of proposed FOIFs superimposed on MATLAB and PSPICE obtained results for $\alpha = 0.7$ (a)FOILP (b) FOIHP (c) FOIBP filter

4.3.2.3. Sensitivity Analysis of the Proposed Fractional Order Inverse Active Filters

Sensitivity is an important property, which is used to evaluate the system behaviour (characteristic) with respect to the variation of component values of the system. The system sensitivity is described mathematically [24] by:

$$S_x^y = \frac{x}{y} \frac{\partial y}{\partial x} \quad (4.26)$$

where y is system characteristic (transfer function of inverse active filters in our case), which can be varied with the variation of x (component values) of the designed system. We have derived the expressions for sensitivity of the proposed fractional order inverse active filter transfer functions with respect to R_i , C_i ($i = 1-4$) and α . Fig. 4.18 displays the plots of the various fractional order inverse filter transfer functions with α . We have also computed the numerical values of the magnitude of the sensitivity function for $\alpha = 0.7$ and half power frequency and minimum frequency and presented them in Table 4.19.

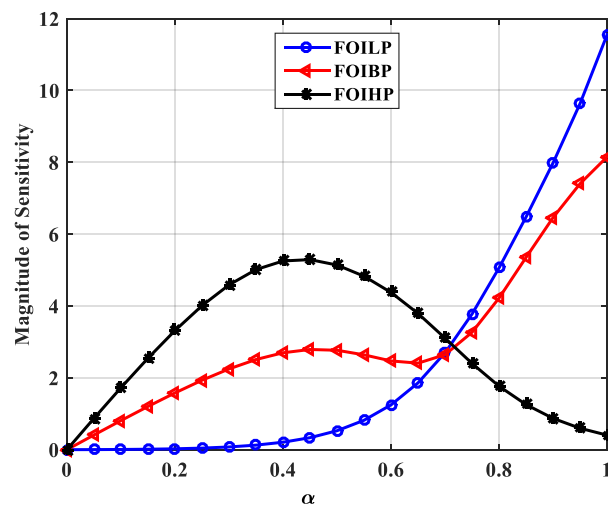


Figure 4.18 Sensitivity of magnitude of transfer functions for the proposed FOIFs

Table 4.23 Sensitivity of the proposed fractional order inverse filters

Sensitivity	Expression for sensitivity	Numerical value of magnitude of sensitivity at $\alpha = 0.7$
$S_{\alpha}^{TF_{FOILP}}$	$\frac{s^{\alpha} (C_3 R_4 + C_1 (R_2 + R_4 + 2C_3 R_2 R_4 s^{\alpha})) \alpha \ln(s)}{1 + C_3 R_4 s^{\alpha} + C_1 s^{\alpha} (R_2 + R_4 + C_3 R_2 R_4 s^{\alpha})}$	2.698
$S_{R_2}^{TF_{FOILP}}$	$\frac{C_1 R_2 s^{\alpha} (1 + C_3 R_4 s^{\alpha})}{1 + C_3 R_4 s^{\alpha} + C_1 s^{\alpha} (R_2 + R_4 + C_3 R_2 R_4 s^{\alpha})}$	0.175
$S_{R_4}^{TF_{FOILP}}$	$\frac{R_4 s^{\alpha} (C_1 + C_3 + C_1 C_3 R_2 s^{\alpha})}{1 + C_3 R_4 s^{\alpha} + C_1 s^{\alpha} (R_2 + R_4 + C_3 R_2 R_4 s^{\alpha})}$	0.330
$S_{C_1}^{TF_{FOILP}}$	$\frac{C_1 s^{\alpha} (R_2 + R_4 + C_3 R_2 R_4 s^{\alpha})}{1 + C_3 R_4 s^{\alpha} + C_1 s^{\alpha} (R_2 + R_4 + C_3 R_2 R_4 s^{\alpha})}$	0.330
$S_{C_3}^{TF_{FOILP}}$	$\frac{C_3 R_4 s^{\alpha} (1 + C_1 R_2 s^{\alpha})}{1 + s^{\alpha} (C_1 R_2 + C_1 R_4 + C_3 R_4) + C_1 C_3 R_2 R_4 s^{2\alpha}}$	0.175
$S_{\alpha}^{TF_{FOIHP}}$	$-\frac{(2 + C_4 R_3 s^{\alpha} + C_2 (R_1 + R_3) s^{\alpha}) \alpha \ln(s)}{1 + C_4 R_3 s^{\alpha} + C_2 s^{\alpha} (R_1 + R_3 + C_4 R_1 R_3 s^{\alpha})}$	3.262
$S_{R_1}^{TF_{FOIHP}}$	$-\frac{1 + (C_2 + C_4) R_3 s^{\alpha}}{1 + s^{\alpha} (C_4 R_3 + C_2 (R_1 + R_3 + C_4 R_1 R_3 s^{\alpha}))}$	0.340
$S_{R_3}^{TF_{FOIHP}}$	$-\frac{1 + C_2 R_1 s^{\alpha}}{1 + s^{\alpha} (C_4 R_3 + C_2 (R_1 + R_3 + C_4 R_1 R_3 s^{\alpha}))}$	0.180
$S_{C_2}^{TF_{FOIHP}}$	$-\frac{1 + C_4 R_3 s^{\alpha}}{1 + s^{\alpha} (C_4 R_3 + C_2 (R_1 + R_3 + C_4 R_1 R_3 s^{\alpha}))}$	0.180
$S_{C_4}^{TF_{FOIHP}}$	$-\frac{1 + C_2 (R_1 + R_3) s^{\alpha}}{1 + s^{\alpha} (C_4 R_3 + C_2 (R_1 + R_3 + C_4 R_1 R_3 s^{\alpha}))}$	0.340
$S_{\alpha}^{TF_{FOIBP}}$	$\frac{(-1 + C_1 C_4 R_2 R_3 s^{2\alpha}) \alpha \ln(s)}{1 + s^{\alpha} (C_4 R_3 + C_1 (R_2 + R_3 + C_4 R_2 R_3 s^{\alpha}))}$	2.762
$S_{R_2}^{TF_{FOIBP}}$	$-\frac{C_1 R_2 s^{\alpha} (1 + C_4 R_3 s^{\alpha})}{1 + s^{\alpha} C_4 R_3 + C_1 s^{\alpha} (R_2 + R_3 + C_4 R_2 R_3 s^{\alpha})}$	0.469
$S_{R_3}^{TF_{FOIBP}}$	$-\frac{1 + C_1 R_2 s^{\alpha}}{1 + s^{\alpha} (C_4 R_3 + C_1 (R_2 + R_3 + C_4 R_2 R_3 s^{\alpha}))}$	0.404
$S_{C_1}^{TF_{FOIBP}}$	$-\frac{C_1 s^{\alpha} (R_2 + R_3 + C_4 R_2 R_3 s^{\alpha})}{1 + s^{\alpha} (C_4 R_3 + C_1 (R_2 + R_3 + C_4 R_2 R_3 s^{\alpha}))}$	0.695
$S_{C_4}^{TF_{FOIBP}}$	$-\frac{1 + C_1 (R_2 + R_3) s^{\alpha}}{1 + s^{\alpha} (C_4 R_3 + C_1 (R_2 + R_3 + C_4 R_2 R_3 s^{\alpha}))}$	0.639

From Table 4.19, it is observed that the magnitude of sensitivity of the fractional order inverse filter transfer functions with respect to various resistors and fractional order capacitors are less than one while the magnitude of sensitivity of various

fractional order inverse filter transfer functions with respect to the parameter α is more than 1 and are consistent with the results presented in [24] for the various fractional order filter transfer function sensitivities.

4.4. Fractional Order Inverse Active Filters using Current Feedback Operational Amplifiers

Current feedback operational amplifier is a very versatile active analog circuit building block, implementing the architecture of trans-impedance amplifier and is characterized by very high slew rate and constant, gain-independent bandwidth [30]. It has been extensively used for the realization of various analog signal processing circuits both in integer order domain as well as in fractional order domain. In this section, we present the realization of fractional order inverse active filters using CFOAs.

The CFOA is a four terminal analog active building block characterized by the matrix equation (4.27):

$$\begin{bmatrix} i_y \\ v_x \\ i_z \\ V_w \end{bmatrix} = \begin{bmatrix} 0 & 0 & 0 \\ 1 & 0 & 0 \\ 0 & 1 & 0 \\ 0 & 0 & 1 \end{bmatrix} \begin{bmatrix} V_y \\ i_x \\ V_z \\ i_w \end{bmatrix} \quad (4.27)$$

From matrix equation (3.39), terminal equations can be deduced as:

$$i_y = 0, v_x = v_y, i_z = I_x \text{ and } v_w = v_z \quad (4.28)$$

The circuit symbol of CFOA is shown in Fig. 4.19.

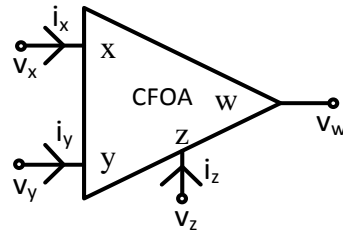


Figure 4.19 Circuit symbol of CFOA

4.4.1. Generalized (Inverting Mode) Fractional Order Inverse Active Filter Configuration

A generalized structure of fractional order inverse active filters is shown in Fig. 4.20.

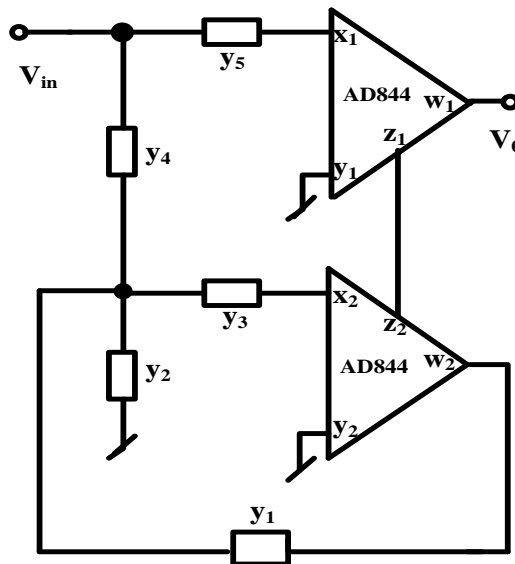


Figure 4.20 Proposed generalized FOIF structure

The routine circuit analysis of the generalized structure of Fig. 4.20 (assuming ideal CFOAs), yields a transfer function as:

$$\frac{V_0}{V_{in}} = -\frac{y_3 y_4 + y_5 (y_1 + y_2 + y_3 + y_4)}{y_1 y_3} \quad (4.29)$$

where y_i , $i = 1-5$ are the branch admittances.

From equation (4.29) different inverse fractional order active filters can now be obtained by appropriately selecting the various admittances as given below in Table 4.20.

Table 4.24 Various fractional order inverse filter transfer functions derived from equation (4.29)

Admittances Filter Responses	y₁	y₂	y₃	y₄	y₅	$\frac{V_0}{V_{in}}$
FOILP	$\frac{1}{R_1}$	$s^\alpha C_2$	$\frac{1}{R_3}$	$\frac{1}{R_4}$	$s^\alpha C_5$	$-\frac{D_1(s)}{K_1}$
FOIBP	$\frac{1}{R_1}$	$\frac{1}{R_2}$	$s^\alpha C_3$	$s^\alpha C_4$	$\frac{1}{R_5}$	$-\frac{D_2(s)}{K_2 s^\alpha}$
FOIHP	$s^\alpha C_1$	$\frac{1}{R_2}$	$s^\alpha C_3$	$s^\alpha C_4$	$\frac{1}{R_5}$	$-\frac{D_3(s)}{K_3 s^{2\alpha}}$

where $D_1(s) = s^{2\alpha} + a_1 s^\alpha + b_1$, $D_2(s) = s^{2\alpha} + a_2 s^\alpha + b_2$, $D_3(s) = s^{2\alpha} + a_3 s^\alpha + b_3$ and $K_1 = \frac{1}{R_1 R_3 C_2 C_5}$, $K_2 = \frac{1}{R_1 C_4}$ and $K_3 = \frac{C_1}{C_4}$ where a_i and b_i ($i = 1-3$) are the coefficients.

Thus, from Table 4.24, it is seen that the FOILP and FOIBP can be realized using three resistors and two fractional order capacitors ($0 < \alpha < 1$), while for FOIHP, two resistors and three fractional order capacitors are required. Using equations (4.21) - (4.23) ω_h of FOILP, FOIHP and ω_m of FOIBP filters can be determined.

The coefficients a_1 - a_3 and b_1 - b_3 for the FOILP, FOIBP and FOIHP filters are mapped with the values of various passive components which are given below in Table 4.25.

Table 4.25 Mapping of the coefficients of the characteristic equation with the passive components of the fractional order inverse filters

Filter Coefficients			
a₁	$\frac{1}{C_2} \left(\frac{1}{R_1} + \frac{1}{R_3} + \frac{1}{R_4} \right)$	b₁	$\frac{1}{C_2 C_5 R_3 R_4}$

a_2	$\frac{1}{R_5} \left(\frac{1}{C_3} + \frac{1}{C_4} \right)$	b_2	$\frac{1}{R_5 C_3 C_4} \left(\frac{1}{R_1} + \frac{1}{R_2} \right)$
a_3	$\frac{1}{R_5 C_3 C_4} (C_1 + C_3 + C_4)$	b_3	$\frac{1}{C_3 C_4 R_2 R_5}$

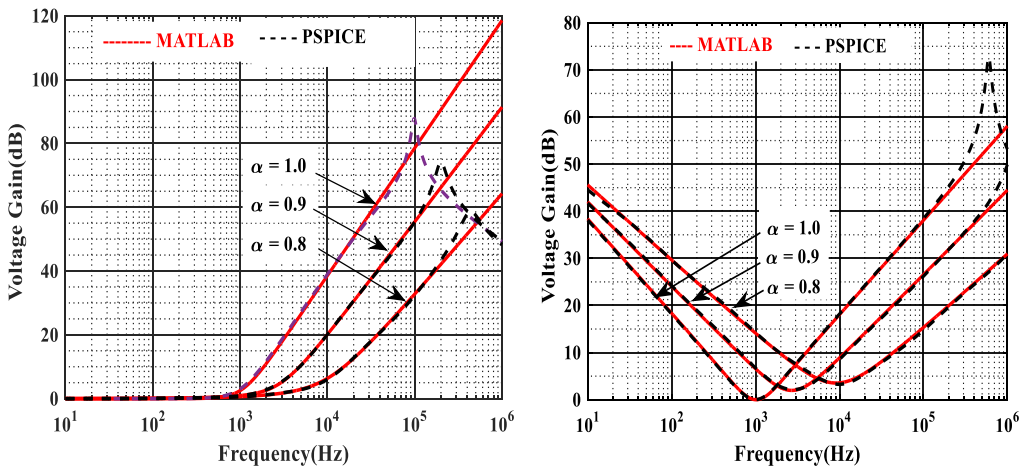
4.4.1.1. PSPICE and MATLAB Simulation Results

The PSPICE and MATLAB simulations were performed on proposed fractional order inverse active filters. The fractional order inverse filters were designed to have a ω_h or ω_m of 1kHz for $\alpha = 1$ for FOILP, FOIHP FOIBP filter. The component values used to design fractional order inverse active filters are provided in Table 4.26.

Table 4.26 Component values used in the design of FOIFs

FOILP	FOIHP	FOIBP
$R_1 = 1060\Omega$	$R_2 = 754.3\Omega$	$R_1 = 1280\Omega$
$R_3 = 530\Omega$	$R_5 = 3395.3\Omega$	$R_2 = 3865.6\Omega$
$R_4 = 1060\Omega$	$C_1 = 0.0995 \mu\text{F}/\text{sec}^{(\alpha-1)}$	$R_5 = 2560\Omega$
$C_2 = 0.382 \mu\text{F}/\text{sec}^{(\alpha-1)}$	$C_3 = 0.0995 \mu\text{F}/\text{sec}^{(\alpha-1)}$	$C_3 = 0.0995 \mu\text{F}/\text{sec}^{(\alpha-1)}$
$C_5 = 0.0955 \mu\text{F}/\text{sec}^{(\alpha-1)}$	$C_4 = 0.0995 \mu\text{F}/\text{sec}^{(\alpha-1)}$	$C_4 = 0.0995 \mu\text{F}/\text{sec}^{(\alpha-1)}$

The PSPICE and MATLAB simulation results of proposed fractional order inverse active filters of Fig. 4.20 for different values of α are shown in Fig. 4.21.



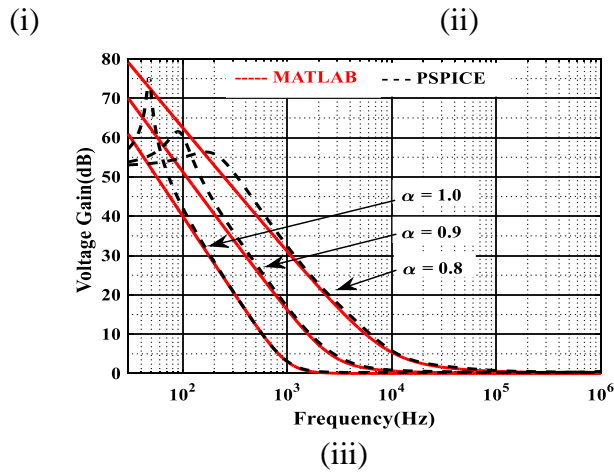


Figure 4.21 Frequency responses of FOIFs of Fig. 4.20 (i) FOILP (ii) FOIBP (iii) FOIHP filter

The comparative results of ω_h and ω_m of proposed fractional order inverse active filters along with integer order counterparts are shown in Table 4.23. The stop band attenuations are provided in Table 4.24.

Table 4.27 Half power frequency and maximum frequency (Hz) of proposed FOIFs of Fig. 4.20

Order	FOILP		FOIHP		FOIBP	
	PSPICE	MATLAB	PSPICE	MATLAB	PSPICE	MATLAB
2.0	1000	1065	977	1000	1000	1008
1.8	2089	2163	3715	3455	2727	2818
1.6	5248	5144	16600	16630	9772	9193

Table 4.28 Stop band attenuation (dB/decade) of proposed FOIFs

Order	FOILP		FOIHP		FOIBP	
	PSPICE	MATLAB	PSPICE	MATLAB	PSPICE	MATLAB
2.0	37.40	39.99	39.50	40.36	20.27	20.03
1.8	35.30	35.65	35.56	36.26	17.58	17.50
1.6	31.20	31.50	29.22	31.06	15.40	15.56

From Table 4.23 and Table 4.24, it is observed that the PSPICE and MATLAB simulation results of proposed FOIFs are in good agreement. Thus, these simulation results confirm the validity of proposed formulations.

4.4.2. Generalized (Non-Inverting Mode) Fractional Order Inverse Active Filter Configuration⁶

The proposed generalized structure of a fractional order inverse filters having ideally infinite input impedance is shown in Fig. 4.22.

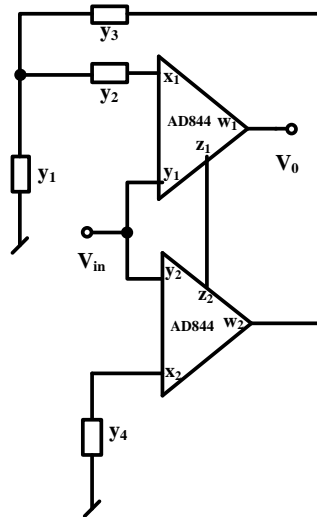


Figure 4.22 Proposed generalized FOIF structure

A routine circuit analysis for the generalized structure of Fig. 4.22 (assuming ideal CFOAs), yields a voltage transfer function:

$$\frac{V_0}{V_{in}} = \frac{y_4(y_1 + y_2 + y_3) + y_2(y_1 + y_3)}{y_2 y_3} \quad (4.30)$$

where y_i , $i = 1-4$ are the branch admittances. Using equation (4.30) various types of inverse fractional order active filters may be realized by appropriate selection of different admittances as given below in Table 4.25.

⁶ The work presented in this section has been published in : Manoj Kumar, D. R. Bhaskar and P. Kumar, “ CFOA based new structure of fractional order inverse filters,” International Journal of Recent Technology and Engineering, vol. 8, no. 5, pp. 4501-4504, 2020.

Table 4.29 Transfer functions of proposed FOIFs

Admittances Filter Responses	y₁	y₂	y₃	y₄	$\frac{V_0}{V_{in}}$
FOILP	$s^\alpha C_1$	$\frac{1}{R_2}$	$\frac{1}{R_3}$	$s^\alpha C_4$	$\frac{D_1(s)}{K_1}$
FOIBP	$\frac{1}{R_1}$	$\frac{1}{R_2}$	$s^\alpha C_3$	$s^\alpha C_4$	$\frac{D_2(s)}{K_2 s^\alpha}$
FOIHP	$\frac{1}{R_1}$	$s^\alpha C_2$	$s^\alpha C_3$	$\frac{1}{R_4}$	$\frac{D_3(s)}{K_3 s^{2\alpha}}$

where $D_1(s) = s^{2\alpha} + a_1 s^\alpha + b_1$, $D_2(s) = s^{2\alpha} + a_2 s^\alpha + b_2$, $D_3(s) = s^{2\alpha} + a_3 s^\alpha + b_3$ and
 $K_1 = \frac{1}{R_2 R_3 C_1 C_4}$, $K_2 = \frac{1}{R_2 C_4}$ and $K_3 = 1$

The FOILP, FOIBP and FOIHP filters been realized using two resistors and two fractional order capacitors only ($0 < \alpha < 1$).

The ω_h of FOILP, FOIHP and ω_m of FOIBP filters can be obtained from the following equations (4.21) -(4.23) respectively.

The coefficients a_1 - a_3 and b_1 - b_3 for the FOILP, FOIBP and FOIHP filters are mapped with the values of various passive components as given below in Table 4.26

Table 4.30 Mapping of the coefficients of the characteristic equation with the passive components of the fractional order inverse filters

a_1	$\frac{1}{C_1} \left(\frac{1}{R_2} + \frac{1}{R_3} \right) + \frac{1}{R_2 C_4}$	b_1	$\frac{1}{C_1 C_4 R_2 R_3}$
a_2	$\frac{1}{C_3} \left(\frac{1}{R_1} + \frac{1}{R_2} \right) + \frac{1}{R_2 C_4}$	b_2	$\frac{1}{R_1 R_2 C_3 C_4}$
a_3	$\frac{1}{C_3} \left(\frac{1}{R_1} + \frac{1}{R_4} \right) + \frac{1}{R_4 C_2}$	b_3	$\frac{1}{C_2 C_3 R_1 R_4}$

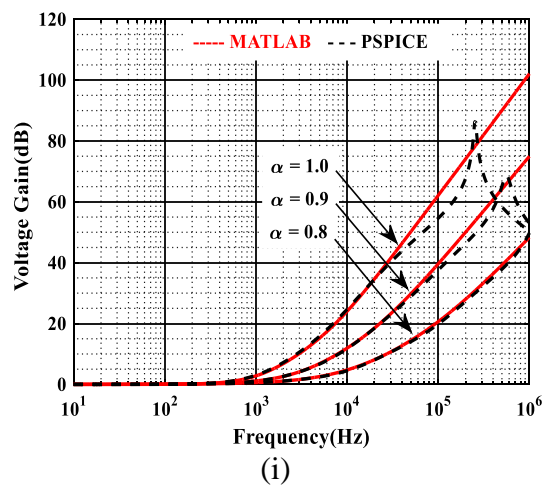
4.4.2.1. PSPICE and MATLAB Simulation Results

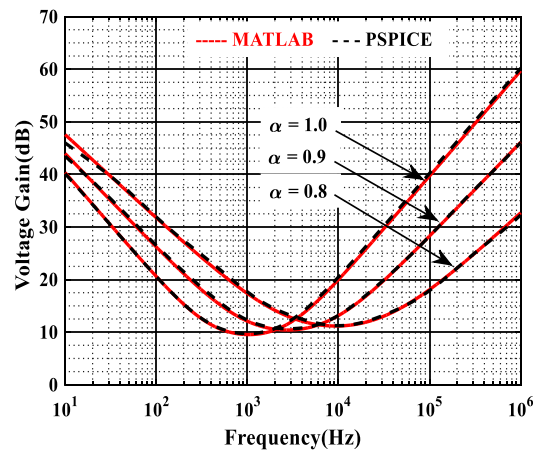
The performance of the proposed FOIFs for $\alpha = 0.8$ and 0.9 and integer order inverse filters ($\alpha = 1.0$) of Fig. 4.22 was validated through PSPICE and MATLAB simulations. The FOIFs were designed to have a $\omega_h = \omega_m$ of 1 kHz for $\alpha = 1$. The component values used to design fractional order inverse active filters are provided in Table 4.27.

Table 4.31 Component values used in the design of FOIFs

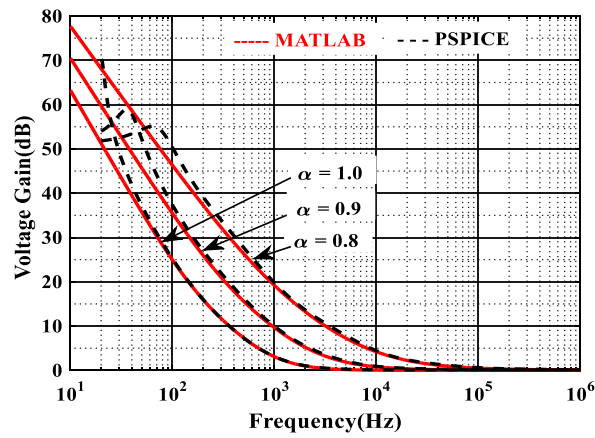
Low pass	High pass	Band pass
$R_2 = 570\Omega$	$R_1 = 4200\Omega$	$R_1 = 1540\Omega$
$R_3 = 570\Omega$	$R_4 = 4200\Omega$	$R_2 = 1540\Omega$
$C_1 = 0.0995 \mu\text{F}/\text{sec}^{(\alpha-1)}$	$C_2 = 0.0995 \mu\text{F}/\text{sec}^{(\alpha-1)}$	$C_3 = 0.0995 \mu\text{F}/\text{sec}^{(\alpha-1)}$
$C_4 = 0.0995 \mu\text{F}/\text{sec}^{(\alpha-1)}$	$C_3 = 0.0995 \mu\text{F}/\text{sec}^{(\alpha-1)}$	$C_4 = 0.0995 \mu\text{F}/\text{sec}^{(\alpha-1)}$

The PSPICE simulation results of proposed FOIFs and integer order inverse filters are shown in Fig. 4.23





(ii)



(iii)

Figure 4.23 Frequency responses of proposed FOIFs (i) FOILP (ii) FOIBP (iii) FOIHP filter

The simulated results of ω_h and ω_m of proposed fractional order inverse active filters along with integer order counterparts are shown in Table 4.28. The stop band attenuations are given in Table 4.29.

Table 4.32 Half power frequency and minimum frequency (Hz) of proposed FOIFs of Fig. 4.20

Order	Low Pass		High Pass		Band Pass	
	PSPICE	MATLAB	PSPICE	MATLAB	PSPICE	MATLAB
2.0	1000	1043	1026	1017	1000	1038
1.8	2239	2245	3639	3342	2630	2697
1.6	6310	5898	15170	14560	9550	9903

Table 4.33 Stop band attenuation (dB/decade) of proposed FOIFs

Order	Low Pass		High Pass		Band Pass	
	PSPICE	MATLAB	PSPICE	MATLAB	PSPICE	MATLAB
2.0	30.00	38.07	38.44	40.10	19.71	19.70
1.8	26.85	35.37	32.29	35.08	17.75	17.82
1.6	15.04	28.21	30.25	31.44	14.64	14.59

From Table 4.28 and Table 4.29, it is noted that the PSPICE and MATLAB simulation results of proposed FOIFs are in good agreement.

4.5. Fractional Order Inverse Active Filters using a Single Operational Trans-resistance Amplifier

In section 4.4, two different FOIF structures were presented using a two CFOAs, in this section, a new configuration of FOIFs employing single operational trans-resistance amplifier (OTRA) has been presented. The proposed configuration is capable of realizing FOILP, FOIBP and FOIHP filters from the same configuration with appropriate choice(s) of different branch admittances. The performance of the

proposed circuit topology of FOIFs has been validated through PSPICE and MATLAB simulations.

4.5.1. Operational Trans-Resistance Amplifier

An operational trans-resistance amplifier (OTRA) is a differential current-controlled voltage source, characterized by ideally zero input impedance (looking into its both input terminals p and n) and zero output impedance. The port relations of an ideal OTRA are given in equation (4.31).

$$\begin{bmatrix} V_p \\ V_n \\ V_o \end{bmatrix} = \begin{bmatrix} 0 & 0 & 0 \\ 0 & 0 & 0 \\ R_m & -R_m & 0 \end{bmatrix} \begin{bmatrix} I_p \\ I_n \\ I_o \end{bmatrix} \quad (4.31)$$

$$V_p = 0, V_n = 0 \text{ and } V_o = R_m(I_p - I_n)$$

The symbolic representation and equivalent circuit of OTRA are shown in Fig. 4.24.

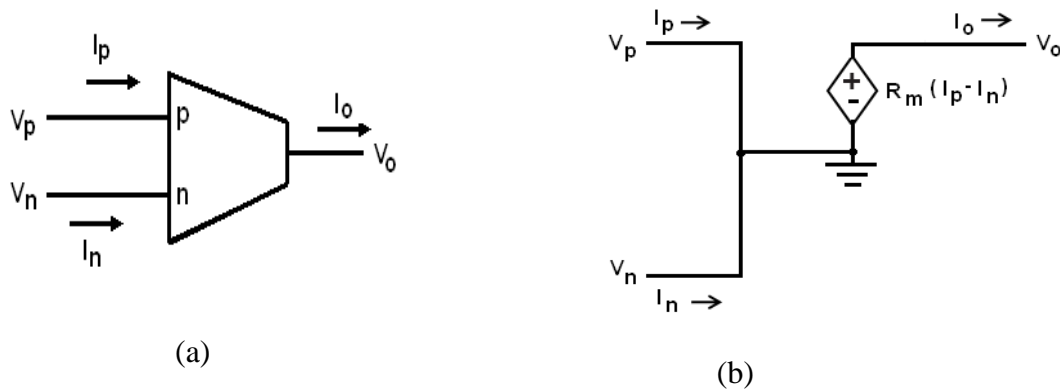


Figure 4.24 (a) Symbolic representation (b) Equivalent circuit of OTRA

The output voltage V_o can be expressed by:

$$V_o = R_m (I_p - I_n) \quad (4.32)$$

Since both the input and output terminals are having low (ideally zero) impedance, this eliminates the response limitations incurred by capacitive time constants leading

to circuits which are insensitive to the parasitic capacitances at the input ports, while its low output impedance enables the OTRA-based circuits to be cascaded easily. Ideally, the trans-resistance gain R_m approaches infinity thereby forcing the two input currents to be equal i.e., $I_p = I_n$. Therefore, the OTRA must be used in a negative feedback structure in a way similar to op-amp.

4.5.2. Proposed Fractional Order Inverse Filter Structure

The proposed FOIF configuration implemented with a single OTRA is shown in Fig.4.25.

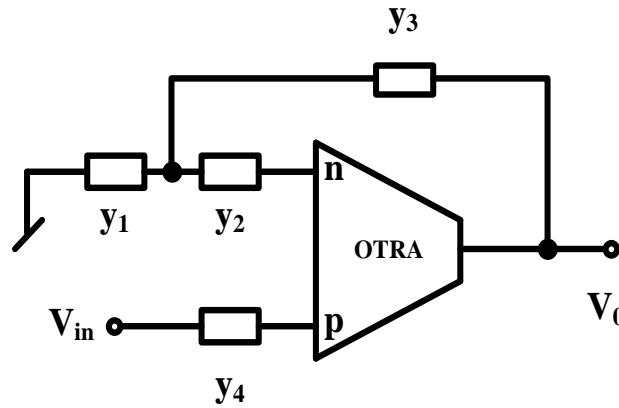


Figure 4.25 Proposed structure of OTRA based FOIFs

Assuming ideal OTRA, a routine circuit analysis yields the following transfer function:

$$\frac{V_0}{V_{in}} = \frac{y_4(y_1 + y_2 + y_3)}{y_2 y_3} \quad (4.33)$$

where y_i , $i = 1-4$ are the branch admittances

From equation (4.33), various responses of FOIFs viz. FOILP, FOIBP and FOIHP can be realized by appropriate selection of the branch admittances. Table 4.30 shows the specific choices of branch admittances for realization of different FOIFs.

Table 4.34 Transfer functions of proposed FOIFs

Admittances Filter Responses	y₁	y₂	y₃	y₄	$\frac{V_0}{V_{in}}$
FOILP	$s^\alpha C_1$	$\frac{1}{R_2}$	$\frac{1}{R_3}$	$s^\alpha C_4 + \frac{1}{R_4}$	$\frac{D_1(s)}{K_1}$
FOIBP	$\frac{1}{R_1}$	$s^\alpha C_2$	$\frac{1}{R_3}$	$s^\alpha C_4 + \frac{1}{R_4}$	$\frac{D_2(s)}{K_2 s^\alpha}$
FOIHP	$\frac{1}{R_1}$	$s^\alpha C_2$	$s^\alpha C_3$	$s^\alpha C_4 + \frac{1}{R_4}$	$\frac{D_3(s)}{K_3 s^{2\alpha}}$
where $D_1(s) = s^{2\alpha} + a_1 s^\alpha + b_1$, $D_2(s) = s^{2\alpha} + a_2 s^\alpha + b_2$, $D_3(s) = s^{2\alpha} + a_3 s^\alpha + b_3$ and $K_1 = \frac{1}{R_2 R_3 C_1 C_4}$, $K_2 = \frac{1}{R_3 C_4}$ and $K_3 = \frac{C_2 C_3}{C_4 (C_2 + C_3)}$					

Thus, from Table 4.30, it is seen that the FOILP and FOIBP filters and can be realized using three resistors and two fractional order capacitors ($0 < \alpha < 1$), while FOIHP filter can be realized with two resistors and three fractional order capacitors.

The half power frequency (ω_h) of fractional order inverse low pass and inverse high pass filters, and minimum/peak frequency (ω_m/ω_p) of fractional order inverse band pass filter can be obtained from equations (4.21)-(4.23) respectively.

The coefficients a_1 - a_3 and b_1 - b_3 for the FOILP, FOIBP and FOIHP filters are mapped with the values of various passive components as given below in Table 4.31.

Table 4.35 Mapping of the coefficients of the characteristic equation with the passive components of the fractional order inverse filters

Filter Coefficients			
a_1	$\frac{1}{C_1} \left(\frac{1}{R_2} + \frac{1}{R_3} \right) + \frac{1}{R_4 C_4}$	b_1	$\frac{1}{C_1 C_4 R_4} \left(\frac{1}{R_2} + \frac{1}{R_3} \right)$
a_2	$\frac{1}{C_2} \left(\frac{1}{R_1} + \frac{1}{R_3} \right) + \frac{1}{R_4 C_4}$	b_2	$\frac{1}{C_2 C_4 R_4} \left(\frac{1}{R_1} + \frac{1}{R_3} \right)$
a_3	$\frac{1}{R_1 (C_2 + C_3)} + \frac{1}{R_4 C_4}$	b_3	$\frac{1}{R_1 R_4 C_4 (C_2 + C_3)}$

4.5.3. PSPICE and MATLAB Simulation Results

We have carried out PSPICE and MATLAB simulations to validate the performance of proposed fractional order inverse active filters. In PSPICE simulations, CMOS OTRA implementation with TSMC 0.18 μ m CMOS technology parameters, proposed by Mostafa and Soliman [27], shown below in Fig.4.26 was used. The aspect ratios of MOSFETs used in the design of OTRA are given in Table 4.32.

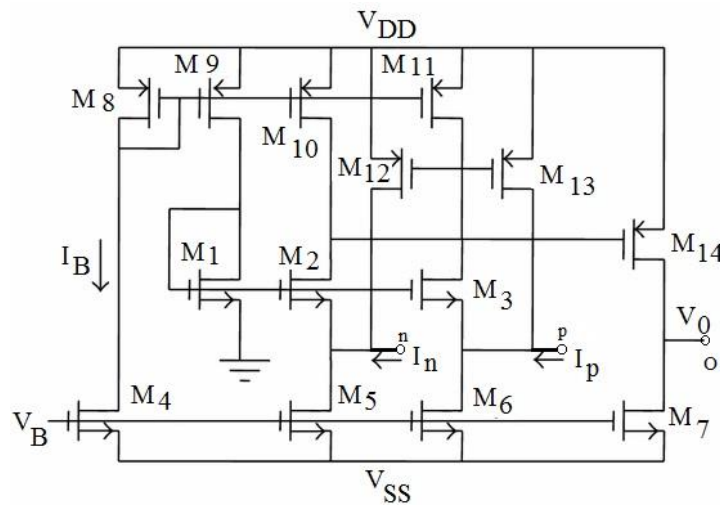


Figure 4.26 Exemplary CMOS OTRA proposed by Mostafa and Soliman [27]

Table 4.36 Aspect ratios of various MOSFETs for the OTRA circuit of Fig. 4.26

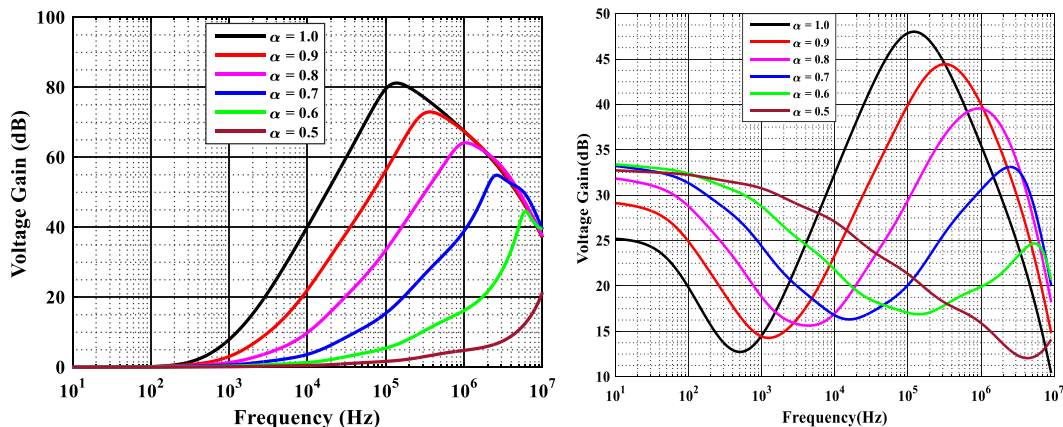
MOSFETs	W (μm)	L(μm)
M ₁ ,M ₂ , M ₃ , M ₁₂ , M ₁₃	100	2.5
M ₄	10	2.5
M ₅ , M ₆	30	2.5
M ₇	10	2.5
M ₈ ,M ₉ , M ₁₀ , M ₁₁ ,	50	2.5
M ₁₄	50	0.5

Fractional order capacitors are designed using Valsa, Dvorak and Friedl method [23] and the equivalent RC ladder circuit used is shown in Fig. 4.6. The component values of RC ladder structure of fractional capacitors for different values of ‘ α ’ are provided in Table.4.4. The fractional order inverse active filters have been designed for the half power frequency/ minimum frequency of 500 Hz, for $\alpha = 1$ (half power frequency for FOILP, FOIHP and minimum frequency for FOIBP filter). The various passive component values, used in PSPICE simulations are provided in Table 4.33.

Table 4.37 Component values used in the design of FOIFs

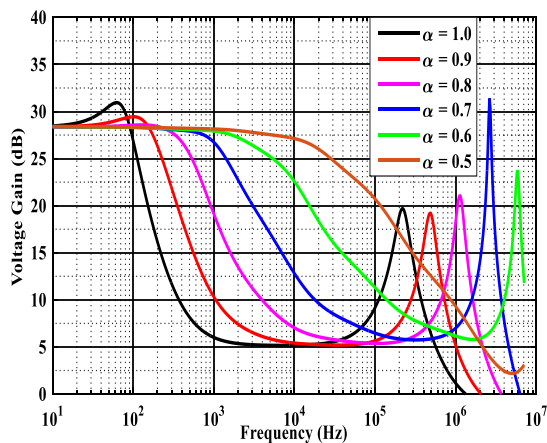
Type of filter	Resistor	Fractional Capacitor
FOILP	R ₂ = 1597 Ω	C ₁ = 0.0995 $\mu\text{F}/\text{sec}^{(\alpha-1)}$
	R ₃ = 1597 Ω	C ₄ = 0.0995 $\mu\text{F}/\text{sec}^{(\alpha-1)}$
	R ₄ = 3195 Ω	
FOIBP	R ₁ = 3850 Ω	C ₂ = 0.0995 $\mu\text{F}/\text{sec}^{(\alpha-1)}$
	R ₃ = 7700 Ω	C ₄ = 0.0995 $\mu\text{F}/\text{sec}^{(\alpha-1)}$
	R ₄ = 3850 Ω	
FOIHP	R ₁ = 1000 Ω	C ₂ = 0.0995 $\mu\text{F}/\text{sec}^{(\alpha-1)}$
	R ₄ = 1000 Ω	C ₃ = 0.0995 $\mu\text{F}/\text{sec}^{(\alpha-1)}$
		C ₄ = 0.0995 $\mu\text{F}/\text{sec}^{(\alpha-1)}$

PSPICE and MATALB simulation results of the proposed fractional order inverse active filters, for different values of ' α ' (varied from 1.0 to 0.5 in step of 0.1) are shown in Fig.4.27 and Fig.4.28 respectively.



(i)

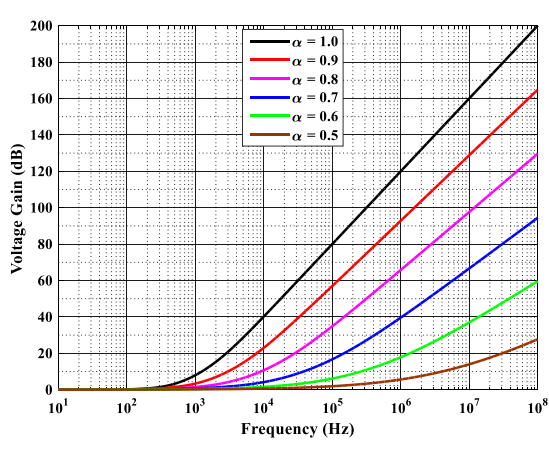
(ii)



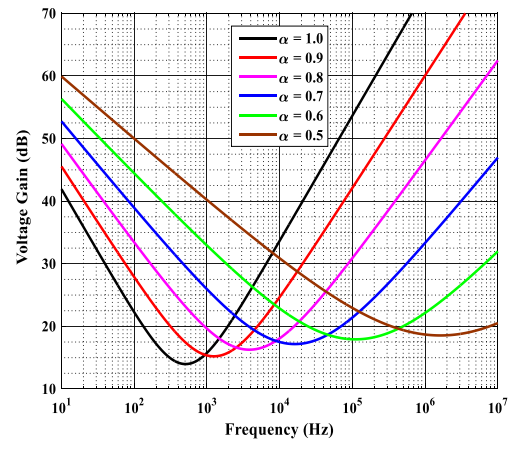
(iii)

Figure 4.27 Frequency responses of OTRA-based FOIFs using PSPICE (i) FOILP

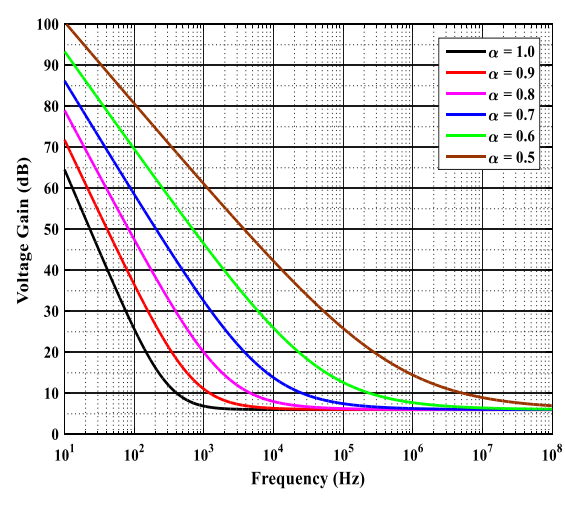
(ii) FOIBP (iii) FOIHP



(i)



(ii)



(iii)

Figure 4.28 Frequency responses of OTRA-based FOIFs using MATLAB (i) FOILP (ii) FOIBP (iii) FOIHP

The summary of simulated results with MATLAB and PSPICE are given in Table 4.34 and Table 4.35 respectively. These results, thus, establish the validity of the proposed fractional order inverse active filters employing an OTRA.

Table 4.38 PSPICE and MATLAB simulations results for half power and maximum frequency (Hz)

Order	Low Pass		High Pass		Band Pass	
	PSPICE	MATLAB	PSPICE	MATLAB	PSPICE	MATLAB
2.0	478	474	494	490	503	504
1.8	1000	910	1550	1446	1234	1268
1.6	2188	2092	6047	5474	4359	3983
1.4	7588	6327	27340	32540	15744	16200
1.2	30900	28860	196450	304000	140940	110400
1.0	302000	255400	2070000	5581000	4359000	1696000

Table 4.39 Stop band attenuation (dB/decade) of proposed FOIFs

Order	Low Pass		High Pass		Band Pass	
	PSPICE	MATLAB	PSPICE	MATLAB	PSPICE	MATLAB
2.0	36.20	37.22	20.63	39.74	19.12	19.88
1.8	34.08	33.92	19.11	35.40	16.45	17.84
1.6	23.5	31.09	16.41	27.50	15.68	16.11
1.4	15.50	29.00	13.95	26.00	10.56	13.77
1.2	11.00	18.23	14.26	20.60	07.45	11.62
1.0	16.42	08.32	10.00	16.33	05.56	09.63

From the above tables, it may be noticed that both the PSPICE and MATLAB simulation results of the proposed FOIFs are in good agreement.

4.6. Stability Analysis of Fractional Order Inverse Active Filters

Stability is an important property of any dynamic system, which can be analyzed in various domains [28]. The roots of characteristic equation of any system in s-plane describe the stability of the system. If all roots of characteristic equation (CE) lie in left half of the s-plane ($\theta_p \geq |\pi/2|$, θ_p is root angle), the system would be stable, otherwise

unstable [30]. It is convenient to find roots of integer order filter in frequency domain (s-plane) using characteristic equation of the system. But it becomes difficult to find the roots of characteristic equation in case of fractional order system in s-plane (as in case of proposed fractional order inverse filters) which is of the form:

$$s^{2\alpha} + bs^\alpha + c = 0, 0 < \alpha < 1 \quad (4.34)$$

Therefore, we transform the fractional order transfer function from s-plane to w-plane [30] by replacing $s = w^m$ and $\alpha = \frac{k}{m}$ (where k and m are positive integers). Now equation (4.34) can be represented in w-domain as:

$$w^{2k} + bw^k + c = 0 \quad (4.35)$$

The s-plane, defined by $\theta_s = \pm\pi$, is shown in Fig. 4.29(a) and its equivalent w-plane (physical region) is defined by $\theta_w \leq |\pi/m|$ is shown in Fig.4.29 (b). The non physical region in w-plane is defined by $\theta_w \geq |\pi/m|$ as shown in Fig.4.29 (b) and this region can not be mapped into s-plane.

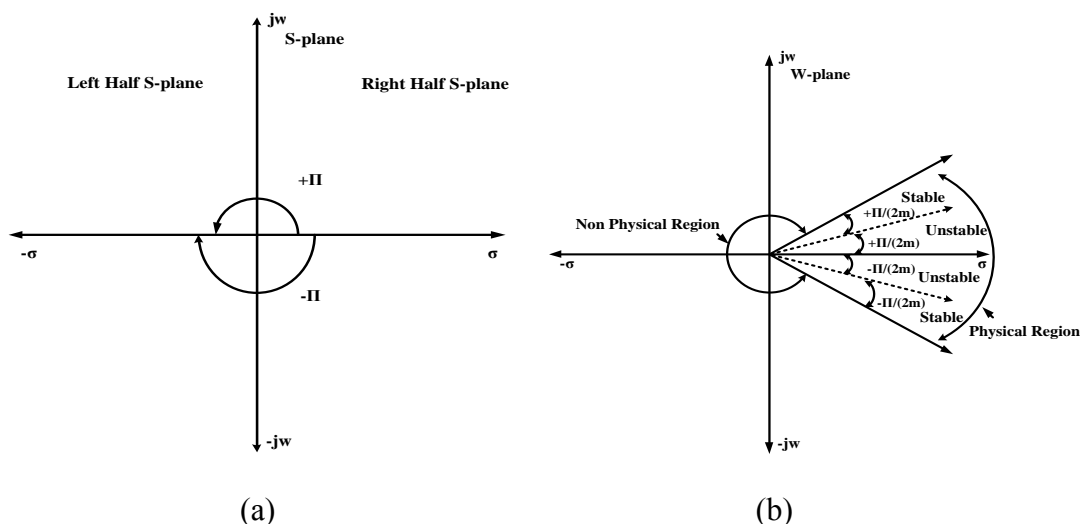


Figure 4.29 Stability analysis of fractional order system (a) s-plane (b) w-plane

The left half of s-plane ($\theta_s \geq |\pi/2|$) is mapped in w-plane by $\theta_w \geq |\pi/2m|$, as shown in Fig.4.29 (b). After transforming the fractional order system characteristic equation

(CE) from s-domain to w-domain, the resulting CE becomes an integer order CE in w-domain. Therefore, the stability of the system in w-domain can now be determined on the basis of location of roots in w- plane. If all roots of equation (4.35) lie in the stable region ($\theta_w \geq |\pi/2m|$) of w-plane (as shown in Fig. 4.29(b)), the system will be stable, otherwise system will be unstable. The stable system in w-plane will also be stable in s-plane, because physical region of w-plane can be mapped onto s-plane. For example, if $\alpha = 0.9$, the equation (4.34) can be written as:

$$s^{1.8} + bs^{0.9} + c = 0 \quad (4.36)$$

If we take $m = 10$, the physical region of w-plane is defined by $\theta_w \leq \left| \frac{\pi}{10} \right|$ and stable

region is represented by $\left| \frac{\pi}{20} \right| \leq \theta_w \leq \left| \frac{\pi}{10} \right|$ as shown in Fig. 4.29 (b). The equation (4.36)

can be transformed into w-pane and will be represented as:

$$w^{18} + bw^9 + c = 0 \quad (4.37)$$

The system will be stable iff, angle of all roots of above characteristic equation (CE) in w-plane are greater than 9° .

The proposed fractional order inverse filters are stable because all roots of fractional order filters lie in stable region of w-plane. The exemplary plot of roots of CE of the proposed fractional order inverse band pass filters ($\alpha = 0.9$) for fractional order filter structures of Fig. 4.5, Fig. 4.9, Fig.4.20 and Fig. 4.22 are shown in Fig.4.30, Fig.4.31, Fig.4.32 and Fig.4.33 respectively.

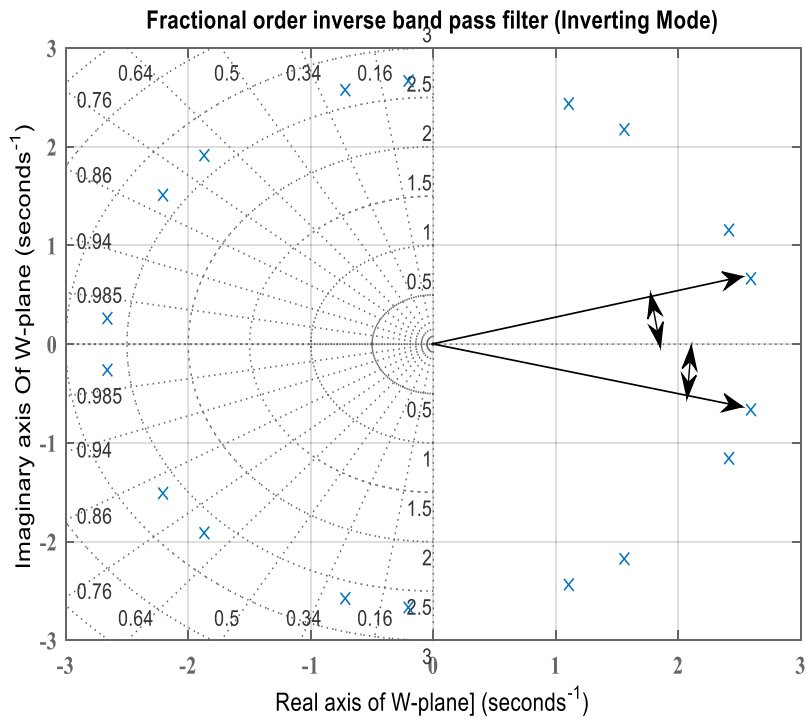


Figure 4.30 Polar plots of CE of FOIBP filter of Fig. 4.5 in w-plane for $\alpha = 0.9$

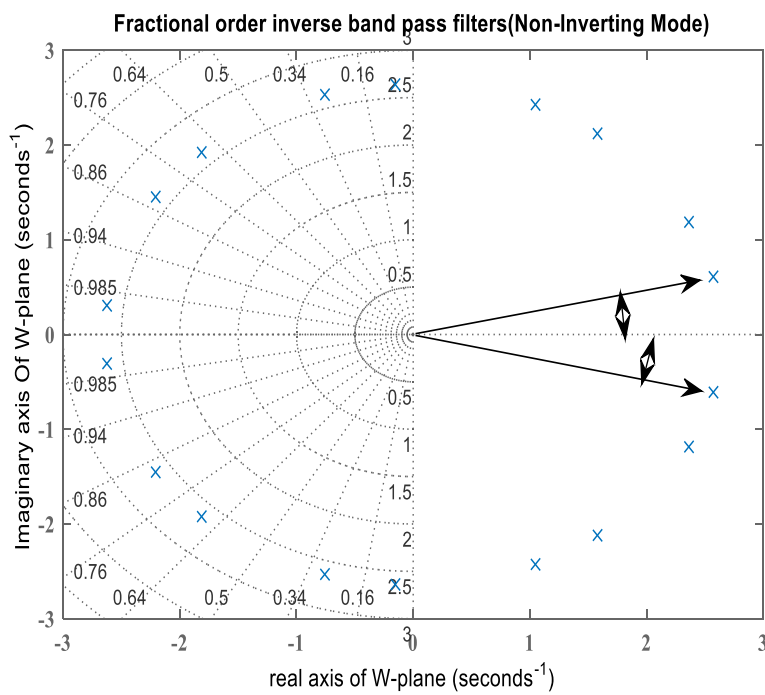


Figure 4.31 Polar plots of CE of FOIBP filter of Fig. 4.9 in w-plane for $\alpha = 0.9$

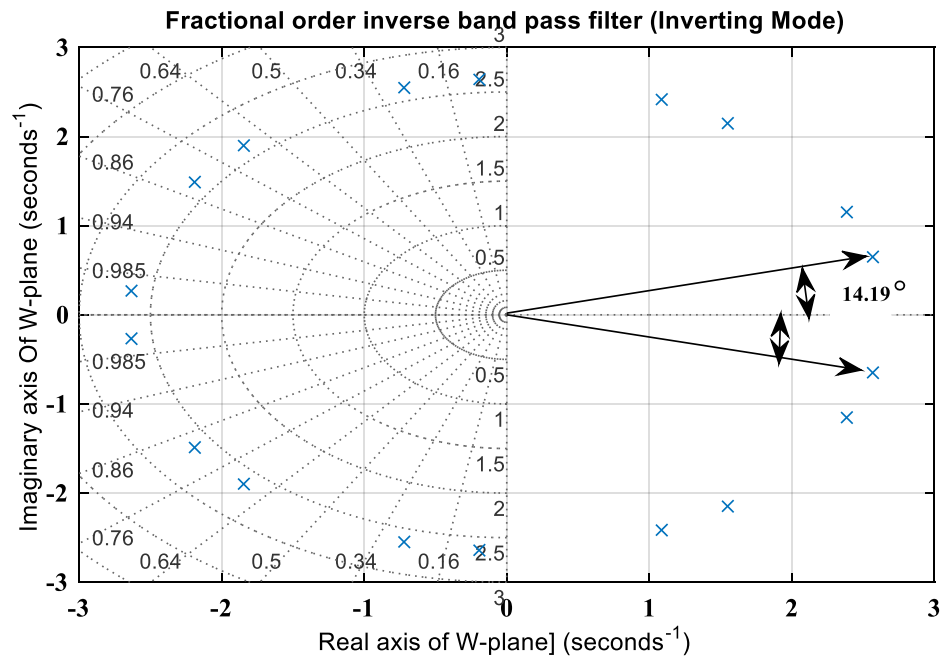


Figure 4.32 Polar plots of CE of FOIBP filter of Fig. 4.20 in w-plane for $\alpha = 0.9$

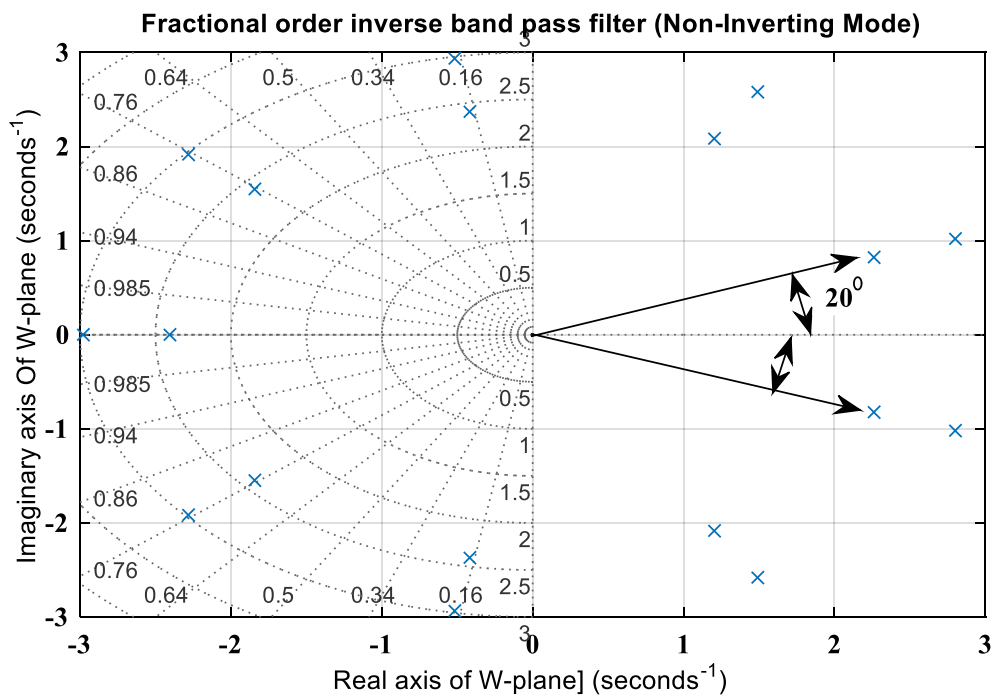
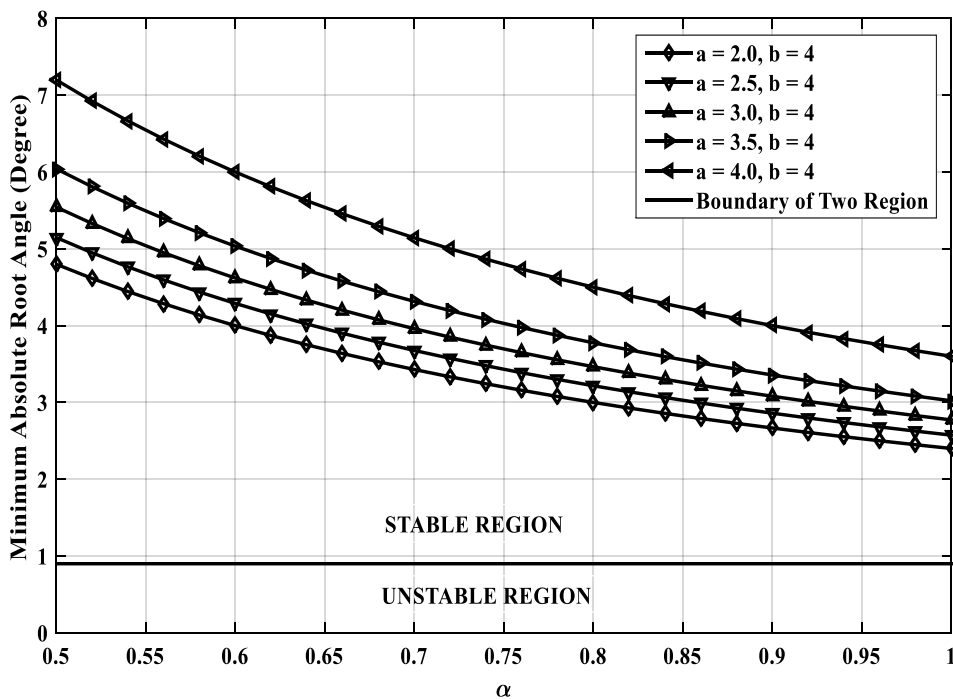


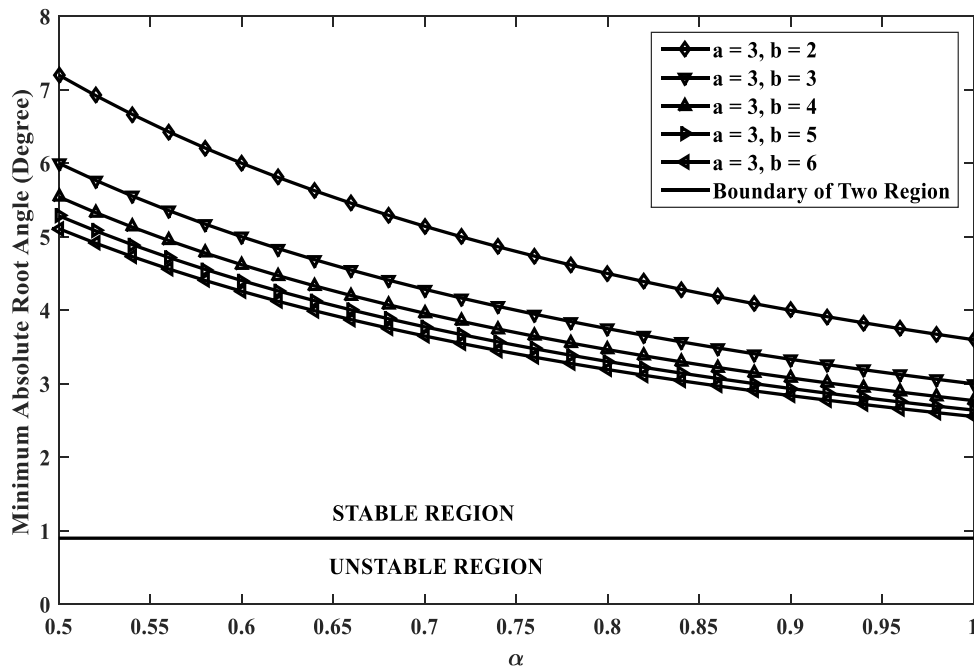
Figure 4.33 Polar plots of CE of FOIBP filter of Fig. 4.22 in w-plane for $\alpha = 0.9$

It is observed that minimum root angles are $\pm 13.34^\circ$, $\pm 14.38^\circ$; $\pm 14.19^\circ$ and $\pm 20.00^\circ$ for fractional order band pass filters of Fig. 4.5, Fig. 4.9, Fig. 4.20, and Fig. 4.22 respectively.

Alternative approach to show the stability of fractional order systems (fractional order inverse filter or fractional order filter) is described in [31]. As per the stability criteria described in [31], if the minimum of the absolute value of angles for all the roots of the CE (Equation (4.37)) in the w-plane when α is varied, is more than $\frac{180^\circ}{2m}$, signifying that none of the roots of the CE in the s-plane has positive real part, the system is stable. We have selected $m = 100$ and varied ' α ' in steps of 0.02 between 0.5 and 1, and plotted the minimum of the absolute values of angles of roots of CE for different values of α , a and b, and shown them in Fig.4.34.



(a)



(b)

Figure 4.34 Minimum absolute root angles for fractional order inverse filters: (a) $b = 4$, $a = 2.0, 2.5, 3.0, 3.5, 4.0$ (b) for $a = 4$ and $b = 2, 3, 4, 5, 6$

For stability of system the coefficients ‘a’ and ‘b’ should be positive and $a^2 \geq b$. From the above figures, it may be observed that none of the roots have angle whose absolute value is less than $\frac{180^\circ}{2m} = 9^\circ$.

4.7. Conclusions

In this chapter, a brief literature overview of conventional inverse filters, designed using various active building blocks has been presented. We have presented several structures of fractional order inverse filters, designed with different active building blocks (viz. op-amp, CFOA and OTRA), passive resistors and simulated fractional order capacitors. Three structures of fractional order inverse active filters using a single op-amp and two configurations employing two CFOAs are implemented, while one fractional order inverse active filter topology is implemented using an OTRA. From the same configuration of all the proposed fractional order inverse filters, three filter functions of

fractional order inverse active filters viz. FOILP, FOIBP and FOIHP filters can be obtained by appropriate selection of the branch admittances. The performance of all the presented circuits has been verified by theoretical calculation, MATLAB and PSPICE simulations for different values of ' α ' ($0 < \alpha < 1$). One of the op-amp-based fractional order inverse filter configuration (minimal realization of fractional order inverse filters) has also been verified experimentally for $\alpha = 0.7$. The sensitivity and stability analyses of the presented fractional order inverse active filters are also described in this chapter.

Reference

- [1] A. Leuciuc, "Using nullors for realization of inverse transfer functions and characteristics," *Electron. Lett.*, vol. 33, no. 11, pp. 949–951, 1997.
- [2] A. G. Radwan, A. M. Soliman and A. S. Elwakil, "On the generalization of second-order filters to the fractional-order domain," *J. Circ. Syst. Comput.* vol.18, no. 2, pp. 361–386, Mar. 2009.
- [3] B. Chipipop and W. Surakamponorn, "Realization of current-mode FTFN-based inverse filter," *Electron. Lett.*, vol. 35, no. 9, pp. 690–692, 1999.
- [4] H. Y. Wang and C. T. Lee, "Using nullors for realization of current-mode FTFN based inverse filters," *Electron. Lett.*, vol. 35, no. 22, pp. 1889–1890, 1999.
- [5] M. T. Abuelma'atti, "Identification of cascadable current-mode filters and inverse-filters using single FTFN," *Frequenz*, vol. 54, no. 11–12, pp. 284–289, 2000.

- [6] S. S.Gupta, D. R. Bhaskar and R. Senani, "New analogue inverse filters realized with current feedback op-amp," *Int. J. Electron.*, vol. 98, no. 8, pp. 1103–1113, 2011.
- [7] S. S.Gupta, D. R. Bhaskar, R. Senani and A. K. Singh, "Inverse active filters employing CFOAs," *Electrical Engineering*, vol. 91, no. 1, pp. 23-26, 2009.
- [8] H. Y.Wang, S. H.Chang, T. Y. Yang and P. Y. Tsai, "A novel multifunction CFOA based inverse filter," *Circ. Syst.*, vol. 2, no. 1, pp. 14–17, 2011.
- [9] V. N. Patil, R. K. Sharma, "Novel inverse active filters employing CFOAs," *Int. J. Scientific Research & Development*, vol. 3, no.7, pp. 359–360, 2015.
- [10] R. Pandey, N. Pandey, T. Negi and V. Garg, "CDBA based universal inverse filter," *ISRN Electronics*, 2013.
- [11] A. Sharma, A. Kumar and P. Whig, "On performance of CDTA based novel analog inverse low pass filter using 0.35 μm CMOS parameter," *Int. J. Science, Technology & Management*, vol. 4, no. 1, pp. 594–601, 2015.
- [12] N. A. Shah, M. Quadri and S. Z. Iqbal, "High output impedance current-mode all pass inverse filter using CDTA," *Indian Journal of pure and applied physics*, vol. 46, no. 12, pp. 893–896, 2008.
- [13] N. A. Shah and M. F. Rather, (2006). Realization of voltage-mode CCII-based all pass filter and its inversion version. *Indian Journal of Pure & Applied Physics*, vol. 44, no. 3, pp. 269–271, 2006.
- [14] N. Herencsar, A. Lahiri, J. Koton, and K. Vrba, K, "Realizations of second-order inverse active filters using minimum passive components and DDCCs," *Int. Conf. Telecommunications and Signal Process.(TS)*, pp. 38-41, 2010.

- [15] K. Garg, R. Bhagat and B. Jaint, "A novel multifunction modified CFOA based inverse filter," *Int. Conf. Power Electronics (IICPE)*, pp. 1-5, 2012
- [16] T. Tsukutani, Y. Sumi and N. Yabuki, "Electronically tunable inverse active filters employing OTAs and grounded capacitors," *Int. J. Electron. Lett.*, vol. 4, no. 2, pp. 166–176, 2016.
- [17] A. K. Singh, A. Gupta and R. Senani, "OTRA-based multi-function inverse filter configuration," *Advances in Electrical and Electronic Engineering*, vol. 15, no. 5, pp. 846-856, 2018.
- [18] E. M. Hamed, L. A. Said, H. M. Ahmed and A. G. Radwan, "On the Approximations of CFOA-Based Fractional-Order Inverse Filters," *Circ. Syst. Signal Process.*, vol. 39, pp. 2-29, 2019.
- [19] N. A. Khalil, L. A. Said, A. G. Radwan and A. M. Soliman, "Fractional Order Inverse Filters Based on CCII Family, *Int. Conf. Advances in Computational Tools for Engineering Applications (ACTEA)*, Beirut, Lebanon, pp. 1-4, Sep. 2019.
- [20] P. Bertias, G. Tsirimokou, C. Psychalinos and A. S. Elwakil, "Fully Electronically Tunable Inverse Fractional-Order Filter Designs," *Novel Intelligent and Leading Emerging Sciences Conference (NILES)*, Giza, Egypt, 2019, pp. 42-45, doi: 10.1109/NILES.2019.8909317.
- [21] H. P. Chen, "High-input impedance voltage-mode multifunction filter with four grounded components and only two plus type DDCCs," *Active and Passive Electronic Components*, vol. 2010, Article ID 362516, Dec. 2010.
- [22] C. T. Lee and H. Y. Wang, "Minimum realization for FTFN-based SRCO," *Electron. Lett., IEE (UK)*, vol. 37, no. 20, pp. 1207-1208, Sep. 2001

- [23] J. Valsa, P. Dvorak and M. Friedl, "Network model of the CPE," *Radioengineering*, vol. 20, no. 3, pp. 619–626, 2011.
- [24] R. Verma, N. Pandey and R. Pandey, "Electronically tunable fractional order filter," *Arabian J. Science and Engineering*, Vol. 42, no. 8, pp. 3409-3422, Aug. 2017.
- [25] P. Prommee, and M. Somdunyanok, "CMOS-based current-controlled DDCC and its applications to capacitance multiplier and universal filter," *AEU-Int. J. Electron. Commun.*, vol. 65, no. 1, pp. 1–8, Jan. 2011.
- [26] A. Kumar, and S. K. Paul, " N^{th} order current mode universal filter using MOCCCIIs," *Analog Integr Circ. Signal Process*, vol. 95, pp. 181-193, Apr. 2018.
- [27] H. Mostafa and A.M. Soliman, "A modified realization of the OTRA," *Frequenz*, vol. 60, pp. 3-4, 2006.
- [28] A. G. Radwan, A. M. Soliman, A. S. Elwakil, and A. Sedeek, "On the stability of linear systems with fractional-order elements," *Chaos, Solitons and Fractals*, vol. 40, no. 5, pp. 2317-2328, 2009.
- [29] S. Mahata, R. Kar and D. Mandal, "Optimal fractional-order highpass Butterworth magnitude characteristics realization using current mode filter," *AEU-Int J Electron Commun.*, vol. 102, pp. 78-89, Apr. 2019.
- [30] R. Senani, D. R. Bhaskar, V. K. Singh and A. K. Singh, "Current feedback operational amplifiers and their applications," New York: Springer, 2013, ISBN 978-1-4614-5187-7.

Chapter 5

Realization of Fractional Order Sinusoidal Oscillators Using a Single Analog Active Building Block

In the previous chapter, we have presented a number of fractional order analog inverse active filter configurations realized with different active building blocks viz., op-amp, CFOAs and OTRA.

In this chapter, we present two different structures of fractional order sinusoidal oscillators (FOSO), realized with single active building block. The first structure employs a single OTRA along with two fractional order capacitors (FCs) and four resistors, while the other structure utilizes a single CFOA, two fractional order capacitors and three resistors. It may be pointed out that both the structures are new and have not been presented earlier as conventional integer order oscillators. The functionality of implemented fractional order oscillators has been verified with PSPICE simulation results, where the employed FCs have been designed using the methods suggested by Valsa, Dvorak, Friedl [1] and Oustaloup, Levron, Maithew and Nanot [2]. The CFOA-based fractional order oscillator is also tested experimentally for $\alpha = \beta = 0.8$ using off-the-shelf available IC AD844 and simulated fractional order capacitors.

5.1. Fractional Order Sinusoidal Oscillators

Oscillators are broadly classified into two categories according to the shape of their output waveforms: sinusoidal and non-sinusoidal (relaxation). In analog signal processing, an oscillator is used in various applications such as wireless communication, electronic computers, biological systems, temperature measurement systems and radar system [3]-[4]. Fractional order harmonic oscillators are sinusoidal oscillators in which, the reactive element, instead of being an integer order capacitor/inductor is a fractional order reactive element. The interest in these fractional order oscillators has stemmed from the fact that, unlike a conventional RC oscillator, the frequency and phase relationship in a fractional order oscillator is a function of the fractional order parameters α , β and γ , defining the constant phase element (CPE). Though the concept of a fractional order oscillator was introduced in the context of an FM demodulation system long back [4], it could not gather much attention till the early 2000s. The detailed theoretical framework for the general fractional order oscillator, however, was developed during the early years of the last decade [6], when the design equations for CO and FO of a fractional order oscillator were presented. Since then, many fractional order oscillator circuits employing different types of amplifiers and other active building blocks have been presented. The general theoretical framework for the design of fractional order oscillator with n-fractance devices was developed by Radwan, Elwakil and Soliman [6]-[7], and since then, a number of fractional order oscillator circuits [4]-[28], realized, either by replacing the conventional capacitors with fractional order capacitors [7]-[15] or designed ab-initio [16]-[28] have appeared in open literature. The fractional order oscillators which were not designed by replacing the conventional capacitor(s) of an existing oscillator, different active building blocks such as current controlled current follower trans-conductance

amplifier [16], second generation current conveyors and operational amplifier [17], differential voltage current conveyor [18], operational trans-resistance amplifiers (OTRA) [19]-[20], operational trans-conductance amplifiers [21]-[22], differential difference current conveyor [23], multiplication mode current conveyor [24] have been used to propose fractional order oscillators with different properties.

5.1.1. Design Procedure of Fractional Order Sinusoidal Oscillators

A fractional order linear system, designed with two fractance devices can be modelled [6] as:

$$\begin{bmatrix} D^\alpha X_1 \\ D^\beta X_2 \end{bmatrix} = \begin{bmatrix} a_{11} & a_{12} \\ a_{21} & a_{22} \end{bmatrix} \begin{bmatrix} X_1 \\ X_2 \end{bmatrix} \quad (5.1)$$

Laplace transform of equation (5.1), assuming zero initial conditions can be written as:

$$\begin{bmatrix} s^\alpha X_1(s) \\ s^\beta X_2(s) \end{bmatrix} = \begin{bmatrix} a_{11} & a_{12} \\ a_{21} & a_{22} \end{bmatrix} \begin{bmatrix} X_1(s) \\ X_2(s) \end{bmatrix} \quad (5.2)$$

The characteristic equation (CE) of fractional order system can be derived from equation (5.2) as:

$$s^{\alpha+\beta} - a_{22}s^\alpha - a_{11}s^\beta + |A| = 0 \quad (5.3)$$

where, $|A| = a_{11}a_{22} - a_{12}a_{21}$, is the determinant of coefficient matrix of fractional order system. The fractional order system can sustain sinusoidal oscillations at any frequency ' ω ', if and only if the value of ' ω ' can satisfy the following equations simultaneously.

$$\omega^{\alpha+\beta} \cos\left((\alpha + \beta) \frac{\pi}{2}\right) - a_{11} \omega^\beta \cos\left(\beta \frac{\pi}{2}\right) - a_{22} \omega^\alpha \cos\left(\alpha \frac{\pi}{2}\right) + |A| = 0 \quad (5.4)$$

$$\omega^{\alpha+\beta} \sin\left((\alpha + \beta) \frac{\pi}{2}\right) - a_{11} \omega^\beta \sin\left(\beta \frac{\pi}{2}\right) - a_{22} \omega^\alpha \sin\left(\alpha \frac{\pi}{2}\right) = 0 \quad (5.5)$$

The phase difference between two state variables X_1 and X_2 can be expressed as:

$$\phi = \tan^{-1} \left(\frac{\omega^\alpha \sin\left(\alpha \frac{\pi}{2}\right)}{\omega^\alpha \cos\left(\alpha \frac{\pi}{2}\right) - a_{11}} \right) - \frac{\pi}{2} (1 - \text{sgn}(a_{12})) \quad (5.6)$$

$$\text{or } \phi = \frac{\pi}{2} (1 - \text{sgn}(a_{12})) - \tan^{-1} \left(\frac{\omega^\beta \sin\left(\beta \frac{\pi}{2}\right)}{\omega^\beta \cos\left(\beta \frac{\pi}{2}\right) - a_{22}} \right) \quad (5.7)$$

where $\text{sgn}(\cdot) = \pm 1$

It may be noted from equations (5.4) – (5.7) that the frequency of oscillation ‘ ω ’ and phase difference ‘ ϕ ’ are, not only the function of the elements of the matrix A, namely a_{11} , a_{12} , a_{21} and a_{22} , these equations also depend on α as well as β . Thus, the circuit designers have additional degree of freedom in meeting the given specifications on ω and ϕ .

Before we present the proposed new fractional order sinusoidal oscillator circuits, a brief summary of earlier works done in the field of fractional order sinusoidal oscillators (FOSO) is presented in following section, so that the work presented in this thesis should be put in the proper prospective.

5.2. Literature Overview of Fractional Order Sinusoidal Oscillators

Although, the concept of fractional order sinusoidal oscillator (FOSO) is not new, as it was first mentioned by Oustaloup in 1981, in the context of generation of low frequency sinusoids for FM application. In [5], a fractional-order Wien bridge oscillator was reported, wherein, the conventional capacitors were replaced by fractional order capacitors. It was shown that the FO and CO of FOSO were dependent not only on the values of resistors and capacitors, but also, on the values of α , β , the parameters, defining the fractional order capacitors. Numerical simulations

were carried out for $\alpha = 0.3, 0.5, 0.7$ and 1 . The variation of phase shift between two state variables, X_1 and X_2 with α was also shown.

Later on, the general theoretical framework for the design of fractional order sinusoidal oscillators with n- fractance devices was developed by Radwan, Elwakil and Soliman [6] – [7]. In [6], the authors have derived the Barkhausen criterion to oscillate a linear non-integer dynamical system. It was shown that the CO and FO of the classical oscillators like the Wien bridge, Colpitts, phase-shift and LC tank oscillators can be obtained as special cases from their generalised formulations in the fractional order domain, whereas, in [7], the authors have presented the analysis and design of four well known oscillators, namely, the Wien bridge oscillator, negative resistor oscillator, Twin-T and Hartley oscillators. Numerical analysis and PSPICE simulations for different values of α and β were carried out for all the proposed fractional order oscillator circuits. Experimental results were also given for one of the fractional order oscillator (Wien bridge oscillator) using one fractional order capacitor and one passive capacitor.

In [8], a two-port autonomous network, described by its transmission parameters and three impedances has been used to illustrate the design methodology of a fractional-order oscillator. Two different structures of two port networks, one using an op-amp and three passive resistors, while, the other employing a CCII-based realization of a non-ideal gyrator along with two FCs and an additional resistor, have been used to design fractional-order oscillators.

Said, Madian, Radwan and Soliman [9] proposed fractional-order oscillators based on CFOAs, in which, two existing integer order oscillator circuits

were generalised in fractional-order domain by replacing the conventional capacitors with FCs. Three different cases ($\alpha = \beta$, $\alpha \neq \beta = 1$, $\beta \neq \alpha = 1$) have been studied and the variation of controlling parameter (resistor) and FO against fractional parameters (α or β) have also been presented.

In yet another publication [10], the same authors have presented a fractional-order oscillator circuit configuration using a single CCII-, three resistors and three fractional order capacitors. Four cases of fractional-order sinusoidal oscillators have been studied and their PSPICE simulation results have been presented to validate the performance of these oscillators.

A four-phase classical oscillator circuit has been generalized in fractional domain and presented in [11]. A double integrated loop method was used in the design of this oscillator circuit using two op-amps, two fractional order capacitors and four resistors. The proposed fractional order sinusoidal oscillator offered an independent control of CO and FO through separate resistors.

Single CFOA-based FOSO circuits employing four resistors and two fractional order capacitors were presented by Said, Radwan, Madian and Soliman in [12] by generalizing the design of an existing single-CFOA based integer order oscillator topology presented earlier by Soliman in [29], whereas, in [13], they have presented the realization of three FC-based fractional-order sinusoidal oscillators. These circuits were based on replacement of conventional capacitors in the existing third order quadrature oscillator circuits realized with op-amps, CFOAs, and CCII- [30].

In [14] and [23], Mishra, Upadhaya and Gupta presented a simple technique to approximate fractance device (FD). The proposed technique utilizes an elementary mathematical tool of impedance equalization at a particular frequency for the design of FD having lesser number of passive components than any other existing approximation of FD. Using this technique, fractional order oscillators were designed for a specified FO and phase which employed the fixed frequency FD, implementing the Wien bridge oscillator using the continued fraction expansion method. The performance of fractional order Wien bridge oscillator implemented using proposed FD was found to be better in respect of phase noise, figure of merit, total harmonic distortions, settling time, peak to peak voltage, power dissipation and hardware compactness.

In [15], Pradhan and Sharma have presented two fractional order oscillator circuits using three OTAs and two fractional order capacitors. It may again be mentioned here that the proposed structures were mere generalization of already published OTA-based integer order oscillators [31].

A current controlled CFTA based quadrature oscillator using three FCs of order 0.5 has been reported in [16], whereas in [17], the generalized design concept of two-port network based oscillator design in fractional order domain was presented. The authors have expanded their earlier work presented in [8] and presented all possible fractional order oscillator circuits from an autonomous two-port network and three impedances. Experimental results using TL082 type op-amp were provided to validate the performance of some of the proposed oscillator circuits.

A new structure of fractional order oscillator circuit, implemented with two DVCCs, two resistors and two grounded fractional order capacitors was proposed in [18]. Experimental results as well as PSPICE results of proposed fractional order oscillators were also presented to verify the performance of fractional order oscillator circuit.

Said, Madian, Radwan and Soliman have presented fractional order oscillator circuits employing OTRAs in [19]. The expressions for FO, CO and phase deviation between the different voltages in terms of circuit parameters and fractance parameters (order of FCs) have been derived. Different cases ($\alpha = \beta$, $\alpha \neq \beta = 1$, $\beta \neq \alpha = 1$) have been studied for proposed oscillator circuits. Total eight fractional order oscillator circuits have been proposed along with their respective COs and FOs. Also, the stability analysis has been carried out for the proposed fractional order oscillators.

In [20], authors have reported a fractional order oscillator circuit using two OTRAs. Four different cases of proposed oscillator were studied and the expressions for various parameters of oscillator circuit like FO, CO and phase differences were derived.

A voltage mode fractional order oscillator implemented with two OTAs, two inverting voltage buffers and two FCs was introduced in [21]. The circuit was implemented with 12 MOS transistors and two fractional order capacitors.

In [22], Kartci, Herencsar, Koton, Brancik, Vrba, Tsirimokou and Psychalinos presented CMOS realization of an OTA-based fractional order oscillator in which two-OTAs, two-flipped voltage followers-based voltage buffers, two FCs and a resistor was employed. Variation of different parameters like FO, CO and phase with respect to passive components and fractional order parameters were presented using numerical as well as PSPICE simulations.

In [24] and [25], fractional order current mode, voltage controlled oscillators (VCO) were presented using multiplication mode current conveyors (MMCCs). These oscillator circuits were derived using state variable approach. PSPICE simulations employing the MMCC realized with macro modal of AD844 and AD835 along with numerical simulations in MATLAB for different cases, have been presented in support of the theoretical findings.

In [26], an electronically tunable fractional order oscillator, employing operational trans-conductance amplifiers and two fractional order capacitors was presented by Singh and Kumar. In this circuit, the FO and the phase difference between the output voltages could be controlled electronically by changing the trans-conductance of different OTAs for specified values of the fractional order parameters α and β .

From the detailed discussion of the existing analog circuit realization of the fractional order oscillators, it emerges that compared to fractional order filters, comparatively less attention has been paid on the realization of single-active element based fractional order oscillators. Also, very few new realizations of fractional order oscillator circuits, which have not been derived from the existing integer order oscillator circuits (replacing the passive capacitors by FCs) exist in open literature.

Therefore, the main objective of this chapter is to introduce two new structures of fractional order sinusoidal oscillators using single active device namely, OTRA and CFOA. The single OTRA-based fractional order sinusoidal oscillator has the property

of single resistance controlled FO, for the specified values of fractional order parameters α and β .

5.3. Realization of Fractional Order Sinusoidal Oscillator Employing Single Operational Trans-Resistance Amplifier

We now present a fractional order sinusoidal oscillator (FOSO) implemented with two fractional order capacitors (FCs), four resistors and a single operational trans-resistance amplifier (OTRA). The characteristic equation of the proposed fractional order sinusoidal oscillator has been derived using nodal analysis and the expressions for frequency of oscillation, condition of oscillation and phase relationship between the two voltages V_1 and V_2 are obtained. In one special case, when $\alpha = \beta = 1$, the oscillator circuit behaves as a classical single resistance controlled sinusoidal oscillator (SRCO) in which the frequency of oscillation and the condition of oscillation can be varied through separate resistors. These properties are retained even when the values of α and β lie in the range of $0 < \alpha, \beta < 1$. Since the input terminals of an OTRA are at virtual ground, the proposed FOSO circuit is also insensitive to parasitic input capacitances and input resistances. Circuit simulations employing CMOS OTRA [32] with TSMC 0.18 μ m CMOS technology and fractional order capacitors realized using the method proposed by Valsa, Dovrak and Friedl [1] have been included to confirm the workability of the proposed FOSO.

5.3.1. Proposed Structure of Fractional Order Oscillator

The proposed single OTRA-based fractional order sinusoidal oscillator circuit is shown in Fig. 5.1.

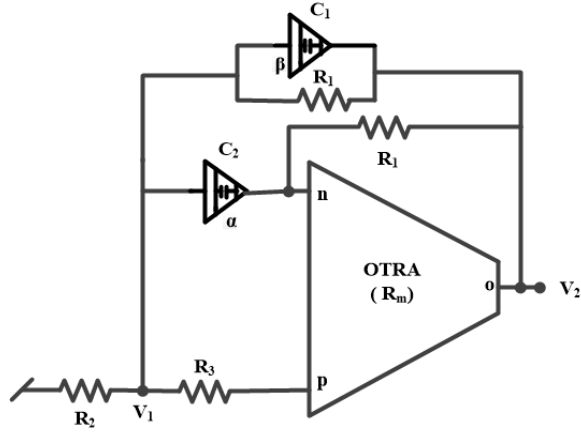


Figure 5.1 The proposed OTRA based fractional order oscillator

Considering an ideal OTRA, (characterized by $V_p = V_n = 0$ and $I_p = I_n$), a routine analysis of the circuit shown in Fig. 5.1, results in the following characteristic equation (CE):

$$s^{\alpha+\beta} + \frac{2}{R_1 C_1} s^\alpha + \frac{1}{C_2} \left(\frac{1}{R_1} - \frac{1}{R_3} \right) s^\beta + \frac{1}{R_1 C_1 C_2} \left(\frac{1}{R_1} + \frac{1}{R_2} \right) = 0 \quad (5.8)$$

Application of Euler's theorem on equation (5.8) for $s = j\omega$ yields:

$$\begin{aligned} & \omega^{\alpha+\beta} \cos((\alpha + \beta)\pi/2) + \frac{2\omega^\alpha}{R_1 C_1} \cos(\alpha\pi/2) \\ & + \frac{1}{C_2} \left(\frac{1}{R_1} - \frac{1}{R_3} \right) \omega^\beta \cos(\beta\pi/2) + \frac{1}{R_1 C_1 C_2} \left(\frac{1}{R_1} + \frac{1}{R_2} \right) \\ & + j \left[\omega^{\alpha+\beta} \sin((\alpha + \beta)\pi/2) + \frac{2\omega^\alpha}{R_1 C_1} \sin(\alpha\pi/2) \right. \\ & \left. + \frac{1}{C_2} \left(\frac{1}{R_1} - \frac{1}{R_3} \right) \omega^\beta \sin(\beta\pi/2) \right] = 0 \end{aligned} \quad (5.9)$$

The circuit represented by the above CE can support sustained oscillations, if, for the given values of the passive components and the fractional order parameters α and β , equations (5.10) and (5.11), obtained by equating the real and imaginary parts of the CE given in equation (5.9) admits a real solution.

$$\omega^{\alpha+\beta} \cos((\alpha + \beta)\pi/2) + \frac{2\omega^\alpha}{R_1 C_1} \cos(\alpha\pi/2) + \frac{1}{C_2} \left(\frac{1}{R_1} - \frac{1}{R_3} \right) \omega^\beta \cos(\beta\pi/2) + \frac{1}{R_1 C_1 C_2} \left(\frac{1}{R_1} + \frac{1}{R_2} \right) = 0 \quad (5.10)$$

$$\omega^{\alpha+\beta} \sin((\alpha + \beta)\pi/2) + \frac{2\omega^\alpha}{R_1 C_1} \sin(\alpha\pi/2) + \frac{1}{C_2} \left(\frac{1}{R_1} - \frac{1}{R_3} \right) \omega^\beta \sin(\beta\pi/2) = 0 \quad (5.11)$$

The CO can be obtained by solving equation (5.11) for R_3 , for the specified values of FO and $R_1, R_2, C_1, C_2, \alpha$ and β while the FO can be found by using the value of R_3 , thus obtained, in equation (5.10). Therefore, the expressions for FO and CO are given below in equations (5.12) and (5.13) respectively.

$$\text{FO: } C_2 \omega^{\alpha+\beta} (-\sin(\alpha\pi/2)) + \frac{2\omega^\alpha C_2}{R_1 C_1} \sin((\beta - \alpha)\pi/2) + \frac{1}{R_1 C_1} \left(\frac{1}{R_1} + \frac{1}{R_2} \right) \sin(\beta\pi/2) = 0 \quad (5.12)$$

$$\text{CO: } \frac{1}{R_3} = \frac{C_2 \omega^\alpha \sin((\alpha+\beta)\pi/2)}{\sin((\beta)\pi/2)} + \frac{2C_2 \omega^{\alpha-\beta} \sin((\alpha)\pi/2)}{R_1 C_1 \sin((\beta)\pi/2)} + \frac{1}{R_1} \quad (5.13)$$

It is interesting to note that when $\alpha = \beta = 1$, the circuit can operate like an integer order sinusoidal oscillator for which the FO and CO can be given by:

$$\text{FO: } \left(\frac{1}{R_1 C_2 C_1} \left(\frac{1}{R_1} + \frac{1}{R_2} \right) \right)^{\frac{1}{2}} \quad \text{and} \quad \text{CO: } \frac{1}{R_3} = \frac{1}{R_1} \left(1 + 2 \frac{C_2}{C_1} \right) \quad (5.14)$$

Thus, from equation (5.14), it is clear that FO can be varied by controlling the value of R_2 without disturbing the CO. Similarly, by controlling R_3 , CO can be adjusted independently without affecting FO. Thus, the circuit can be operated as a single resistance controlled oscillator. It may be mentioned that such SRCO has not been reported earlier.

The phase relationship between V_1 and V_2 can be found as:

$$\phi = \tan^{-1} \left(\frac{R_1 C_2 \omega^\alpha \sin(0.5\alpha\pi)}{R_1 C_2 \omega^\alpha \cos(0.5\alpha\pi) - \frac{R_1}{R_3}} \right) \quad (5.15)$$

From equation (5.15), it may be observed that the phase can be varied by varying the value of ‘ α ’

5.3.2. Simulation and Numerical Results

The proposed structure of fractional order sinusoidal oscillator of Fig. 5.1 was simulated in PSPICE using CMOS OTRA structure [32] as shown in Fig. 5.2. The power supplies used to bias the CMOS OTRA were $\pm 1.5V$ DC. The circuit was designed for a nominal frequency of oscillation of 11.24 kHz (for $\alpha = \beta = 1$) by selecting the passive components as $R_1 = R_2 = 20K\Omega$, and $C_1 = C_2 = 1nF$. Fractional order capacitors, $C_1 = C_2 = 1nF/s^{(\alpha-1)}$, with different values of $\alpha = \beta = 0.8, 0.9$ were used in the simulation of the proposed fractional order sinusoidal oscillator using the method proposed by Valsa, Dovrak and Friedl [1]. The ladder structure (with a fifth order approximation), along with the passive component values of the ladder elements are shown in Fig.5.3 and Table 5.1 respectively.

Table.5.1 Component values of FC for ($\alpha = \beta = 0.8, 0.9$)

Order	$C_f = 1nF/s^{(\alpha-1)}$	
	Resistor	Capacitor
0.9	$R_a = 76.44M\Omega$ $R_b = 11.339M\Omega$ $R_c = 1.682M\Omega$ $R_d = 0.25M\Omega$ $R_e = 0.037M\Omega$ $R_p = 436.86M\Omega$	$C_a = 0.138nF$ $C_b = 0.1058nF$ $C_c = 0.856nF$ $C_d = 0.0693nF$ $C_e = 0.056nF$ $C_p = 0.2372nF$
0.8	$R_a = 64.029M\Omega$ $R_b = 11.471M\Omega$ $R_c = 2.153M\Omega$ $R_d = 0.395M\Omega$ $R_e = 0.072M\Omega$ $R_p = 285.14M\Omega$	$C_a = 0.156nF$ $C_b = 0.15058nF$ $C_c = 0.0669nF$ $C_d = 0.0438nF$ $C_e = 0.0286nF$ $C_p = 0.0542nF$

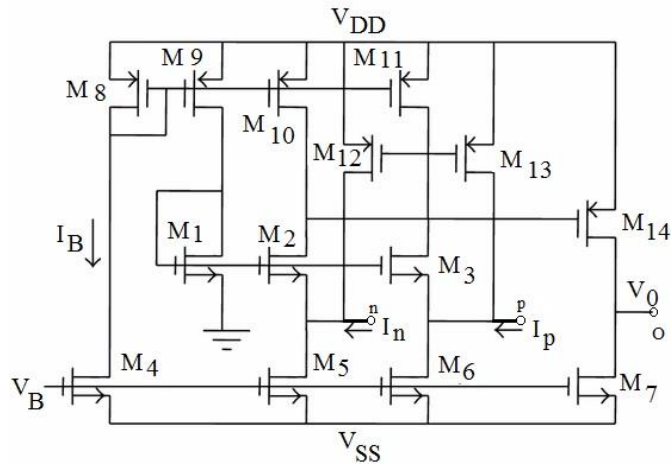


Figure 5.2 CMOS OTRA circuit proposed by Mostafa and Soliman [32]

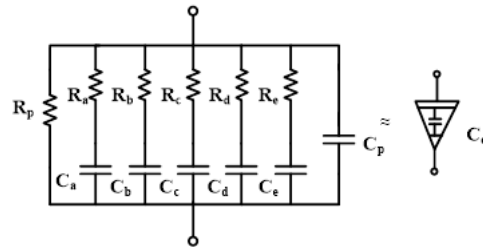
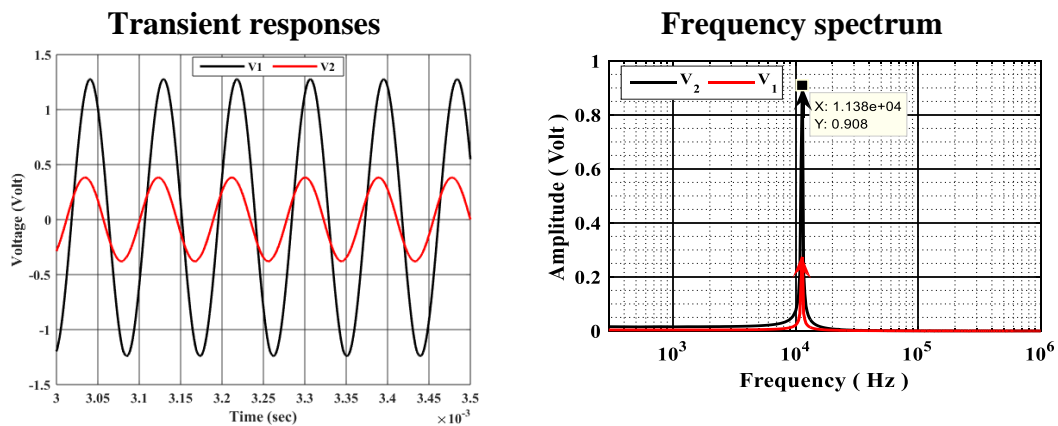
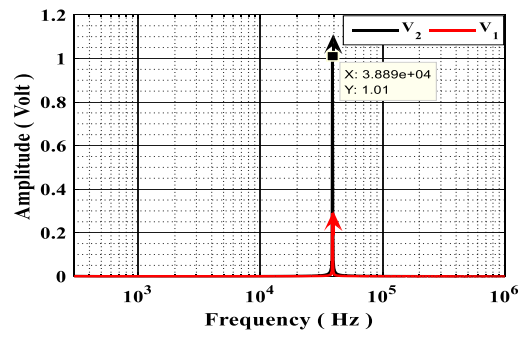
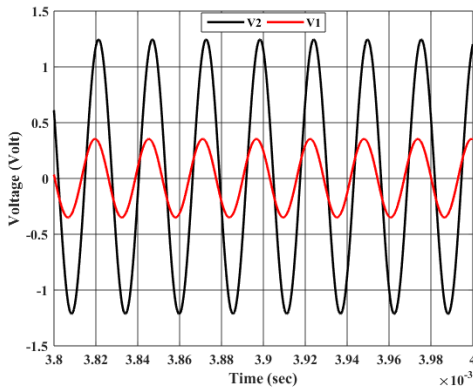


Figure 5.3 R-C ladder circuit of fractional order capacitor

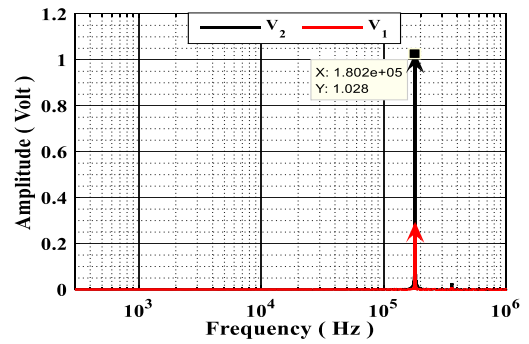
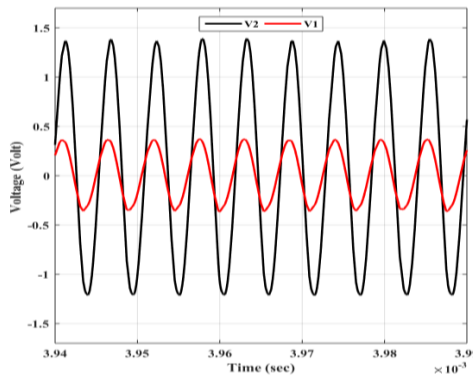
Eight different cases of fractional order sinusoidal oscillator (for different combinations of α and β) were simulated in PSPICE. The transient responses and frequency spectrums of the proposed fractional order sinusoidal oscillator are displayed in Fig.5.4. The simulation results (SM) and theoretical results (TH) showing frequency of oscillation, and the phase difference between V_1 and V_2 for different values of α and β , along with the value of R_3 , are shown in Table 5.2.



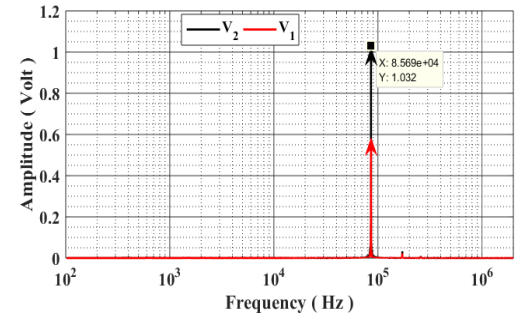
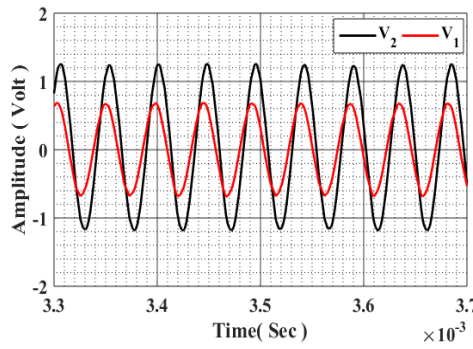
(a) $\alpha = 1.0 \beta = 1.0$



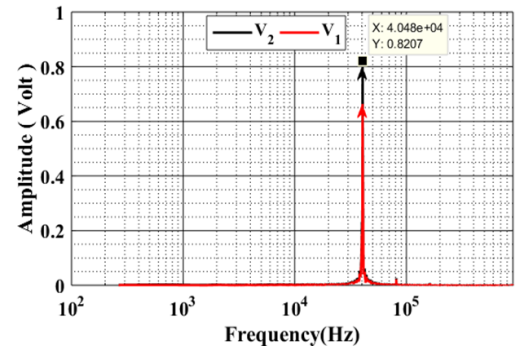
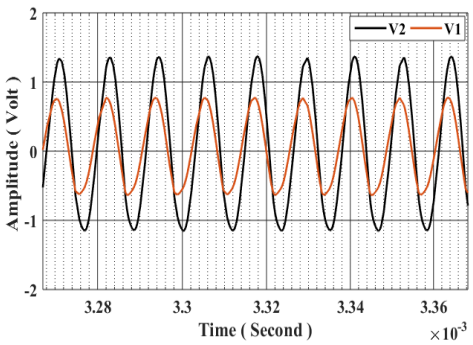
(b) $\alpha = 0.9 \beta = 0.9$



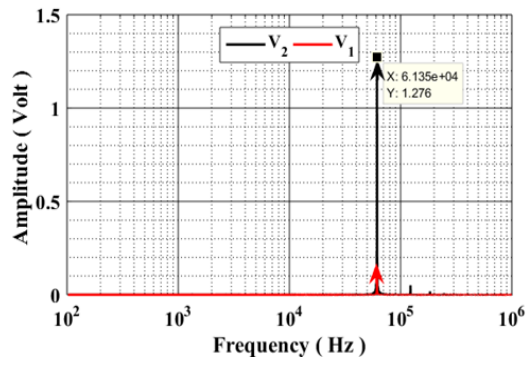
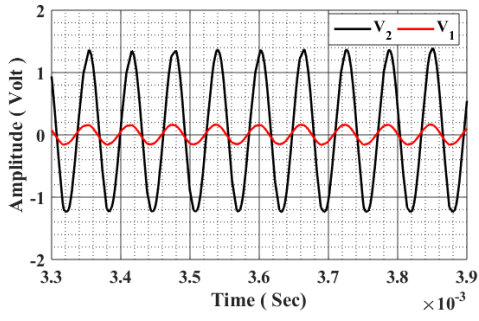
(c) $\alpha = 0.8 \beta = 0.8$



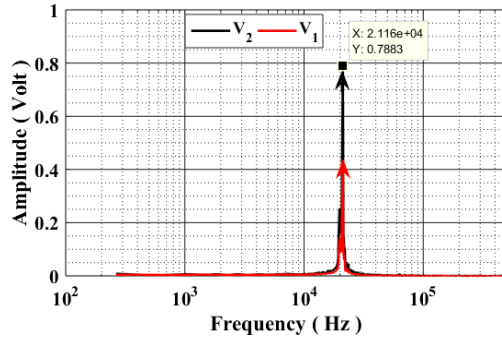
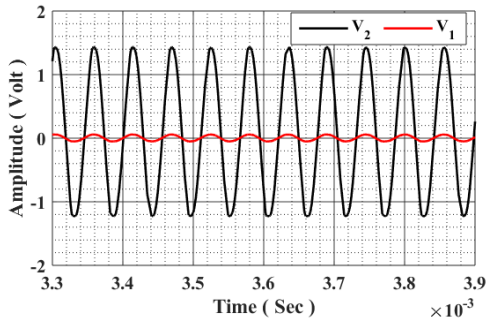
(d) $\alpha = 0.8, \beta = 0.9$



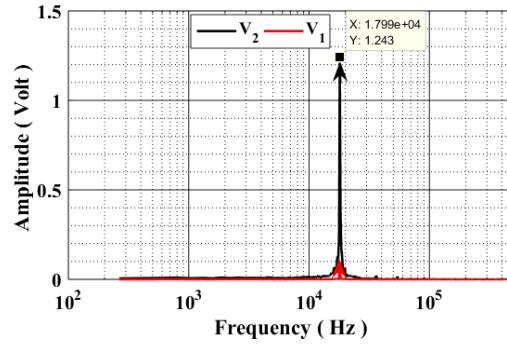
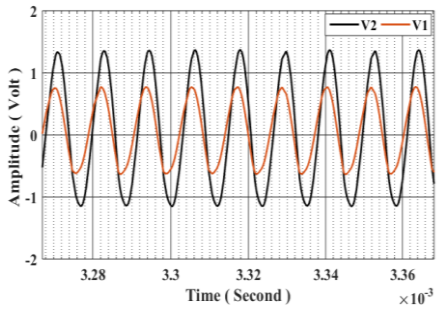
(e) $\alpha = 0.8, \beta = 1.0$



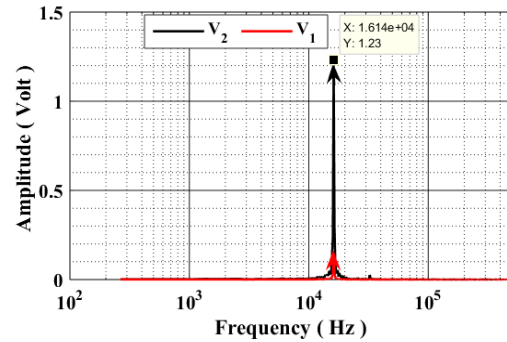
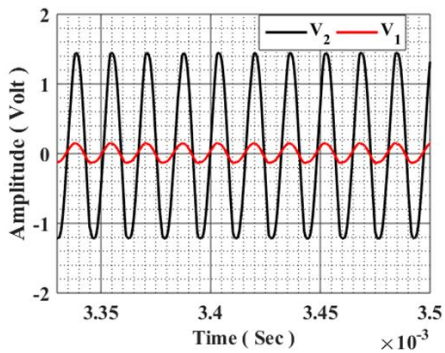
(f) $\alpha = 0.9, \beta = 0.8$



(g) $\alpha = 0.9, \beta = 1.0$



(h) $\alpha = 1.0, \beta = 0.8$



(i) $\alpha = 1.0, \beta = 0.9$

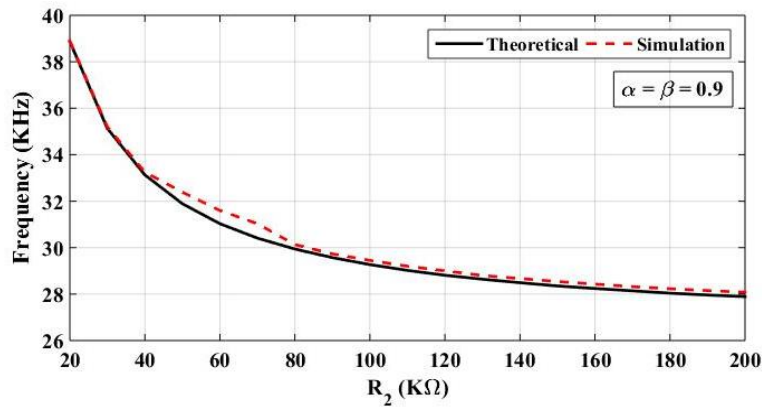
Figure 5.4 Transient responses and frequency spectra of proposed fractional order oscillator

Table 5.2 Simulation and theoretical results of fractional order sinusoidal oscillator

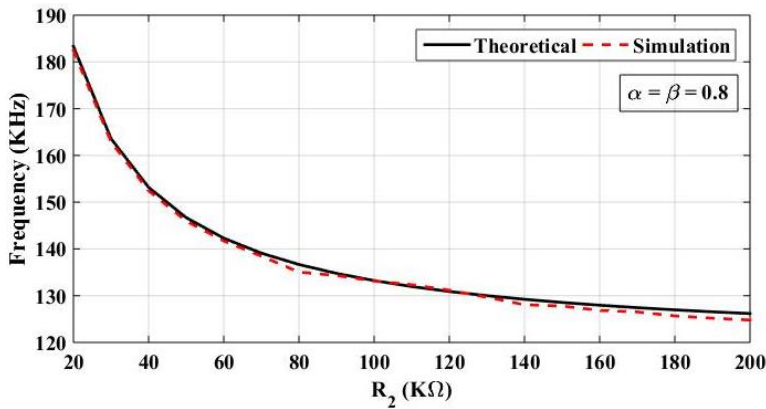
Values of α and β	FO (SM/TH) (KHz)	Phase (SM/TH) (Degree)	R_3 (K Ω)
$\alpha = 1.0, \beta = 1.0$	11.25/11.24	25.52/25.08	6.63
$\alpha = 0.9, \beta = 0.9$	38.90/38.88	21.01/20.84	5.85
$\alpha = 0.8, \beta = 0.8$	181.27/183.3	26.01/21.73	5.30
$\alpha = 0.8, \beta = 0.9$	86.32/88.39	22.22/20.62	10.5
$\alpha = 0.8, \beta = 1.0$	40.40/42.92	18.73/18.74	15.26
$\alpha = 0.9, \beta = 0.8$	61.23/61.22	17.66/12.5	2.016
$\alpha = 0.9, \beta = 1.0$	20.17/21.37	25.80/25.12	11.42
$\alpha = 1.0, \beta = 0.8$	18.00/18.02	7.72/5.39	0.82
$\alpha = 1.0, \beta = 0.9$	16.45/16.34	13.60/14.57	2.533

5.3.3. Operation of the Proposed Fractional Order Oscillator as SRCO

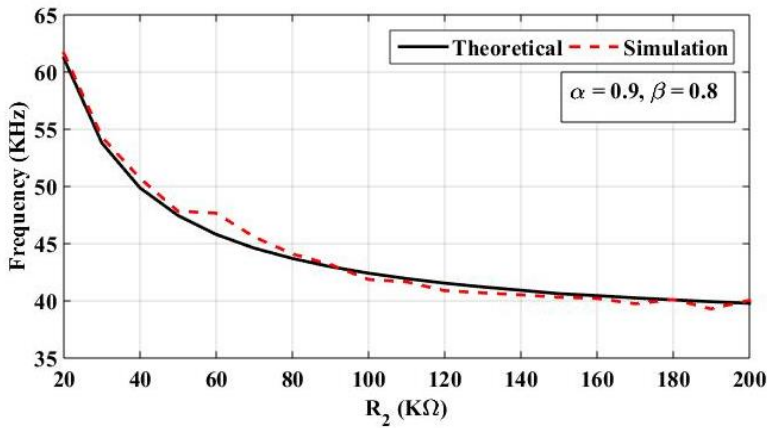
It may be observed from equations (5.12) and (5.13) that the FO of the proposed FOSO can be varied by changing the value of R_2 without disturbing the CO for the given values of α and β , thus, the fractional order sinusoidal oscillator provides the single resistance controllability of the FO. We can fix the value of fractional parameters (α and β) and other passive components for a particular oscillation frequency. Subsequently, we can vary the frequency of oscillation (FO) by varying the resistor (R_2) without affecting the CO. This property of FOSO was verified through PSPICE simulations as well as numerically using MATLAB for two different cases (i) when both α and β have equal values ($\alpha = \beta = 0.8$ and $\alpha = \beta = 0.9$) and (ii) when both ' α ' and ' β ' have different values ($\alpha = 0.9$ and $\beta = 0.8$). The PSPICE simulations and MATLAB results in both the cases are shown graphically in Fig. 5.5 to verify the performance of the proposed SRCO.



(a)



(b)



(c)

Figure 5.5 Variation of FO with R_2 (a) $\alpha = \beta = 0.9$ (b) $\alpha = \beta = 0.8$ (c) $\alpha = 0.9, \beta = 0.8$

5.4. Fractional Order Sinusoidal Oscillator Implemented with a Single CFOA and Two Fractional Order Capacitors

In this section, we present a new structure of a fractional order sinusoidal oscillator employing a single CFOA, two FCs and three resistors. The workability of the

proposed FOSO circuit has been corroborated by the PSPICE simulation and hardware implementation results employing AD844-type IC CFOA. The fractional order capacitors used in simulation and experimental verification have been designed using the method suggested by Oustaloup, Levron, Mathieu and Nanot [2]

5.4.1. Proposed Single CFOA Based FOSO Circuit

The proposed structure of fractional order sinusoidal oscillator employing a single CFOA, three resistors and two simulated fractional order capacitors is shown in Fig. 5.6.

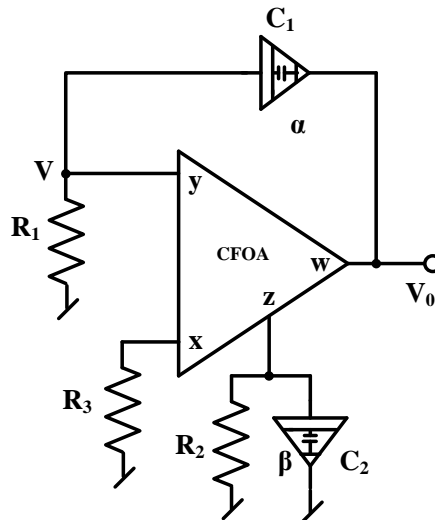


Figure 5.6 Proposed configuration of single CFOA based fractional order oscillator

Using the terminal equations of an ideal CFOA, a straight forward analysis of the FOSO circuit presented in Fig. 5.6 yields:

$$V_0(C_1s^\alpha) = V\left(\frac{1}{R_1} + C_1s^\alpha\right) \quad (5.16)$$

$$V\left(\frac{1}{R_3}\right) = V_0\left(\frac{1}{R_2} + C_2s^\beta\right) \quad (5.17)$$

Solving equations (5.16) and (5.17), the characteristic equation (CE) of the FOSO can be expressed as:

$$s^{\alpha+\beta} + \left(\frac{1}{R_1 C_1} s^\beta + \frac{1}{R_2 C_2} s^\alpha - \frac{1}{R_3 C_2} s^\alpha \right) + \frac{1}{R_1 R_2 C_1 C_2} = 0 \quad (5.18)$$

Application of Euler's theorem on Equation (5.18) for $s = j\omega$, gives:

$$\begin{aligned} \omega^{\alpha+\beta} \cos((\alpha + \beta)\pi/2) + \frac{\omega^\beta}{R_1 C_1} \cos(\beta\pi/2) + \frac{1}{C_2} \left(\frac{1}{R_2} - \frac{1}{R_3} \right) \omega^\alpha \cos(\alpha\pi/2) + \\ \frac{1}{R_1 R_2 C_1 C_2} + j(\omega^{\alpha+\beta} \sin((\alpha + \beta)\pi/2) + \frac{\omega^\beta}{R_1 C_1} \sin(\beta\pi/2) + \frac{1}{C_2} \left(\frac{1}{R_2} - \frac{1}{R_3} \right) \omega^\alpha \sin(\alpha\pi/2)) = 0 \end{aligned} \quad (5.19)$$

Now, to produce the sustained oscillations for the given values of passive components and the fractional order parameters α and β , the following equations are obtained by equating the real and imaginary parts of the CE given in equation (5.19), admits a real solution.

$$\begin{aligned} \omega^{\alpha+\beta} \cos((\alpha + \beta)\pi/2) + \frac{\omega^\beta}{R_1 C_1} \cos(\beta\pi/2) + \frac{1}{C_2} \left(\frac{1}{R_2} - \frac{1}{R_3} \right) \omega^\alpha \cos(\alpha\pi/2) \\ + \frac{1}{R_1 R_2 C_1 C_2} = 0 \end{aligned} \quad (5.20)$$

$$\omega^{\alpha+\beta} \sin((\alpha + \beta)\pi/2) + \frac{\omega^\beta}{R_1 C_1} \sin(\beta\pi/2) + \frac{1}{C_2} \left(\frac{1}{R_2} - \frac{1}{R_3} \right) \omega^\alpha \sin(\alpha\pi/2) = 0 \quad (5.21)$$

Solving equations (5.20) and (5.21), the FO and CO are obtained as:

$$C_2 \omega^\beta (-\sin(\beta\pi/2)) + \frac{\omega^{\beta-\alpha} C_2}{R_1 C_1} \sin((\alpha - \beta)\pi/2) + \frac{1}{R_1 C_1 R_2 \omega^\alpha} \sin(\alpha\pi/2) = 0 \quad (5.22)$$

$$\frac{1}{R_3} = \frac{C_2 \omega^\beta \sin((\alpha + \beta)\pi/2)}{\sin(\alpha)\pi/2} + \frac{C_2 \omega^{\beta-\alpha} \sin((\beta)\pi/2)}{R_1 C_1 \sin((\alpha)\pi/2)} + \frac{1}{R_2} \quad (5.23)$$

From equations (5.22) and (5.23), it is observed that for $\alpha = \beta = 1$, the circuit functions as an integer order oscillator for which the FO and CO are given by:

$$\text{FO: } \omega = \left(\frac{1}{R_1 R_2 C_1 C_2} \right)^{\frac{1}{2}} \quad \text{CO: } \frac{1}{R_3} = \frac{1}{R_2} + \frac{C_2}{R_1 C_1} \quad (5.24)$$

The phase angle between V and V₀ can be evaluated from equation (5.16) as:

$$\phi = \frac{\alpha \pi}{2} - \tan^{-1} \left(\frac{R_1 C_1 \omega^\alpha \sin(0.5\alpha\pi)}{1 + R_1 C_1 \omega^\alpha \cos(0.5\alpha\pi)} \right) \quad (5.25)$$

5.4.2. PSPICE Simulation and Numerical Results

PSPICE Simulation: The proposed structure of Fig. 5.6 was simulated in PSPICE using the macro-modal of AD844 type CFOA. The oscillator circuit was designed for a nominal frequency of 15.9 kHz (for $\alpha = \beta = 1$) by selecting the passive components as $R_1 = R_2 = 1\text{K}\Omega$, and $C_1 = C_2 = 10\text{ nF}$. The transient and frequency spectrum of this oscillator circuit are depicted in Fig. 5.8. Fractional order capacitors, $C_1 = C_2 = 10\text{ nF/s}^{(\alpha-1)}$, with different values of α and β (0.8, 0.9) used in the simulation of proposed fractional order oscillator of Fig. 5.6 were realized using the method proposed by Oustaloup, Levron, Mathieu and Nanot (assuming $n = 8$) [2]. The R-C ladder structure of simulated FC is shown in Fig. 5.7 and component values of ladder elements are given in Table 5.3.

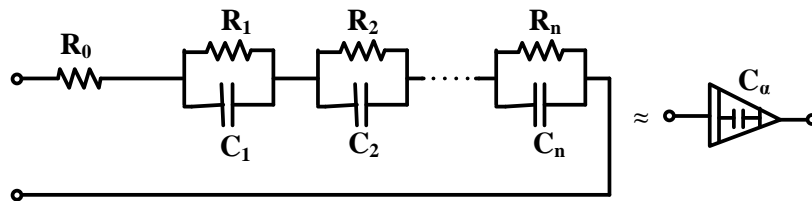


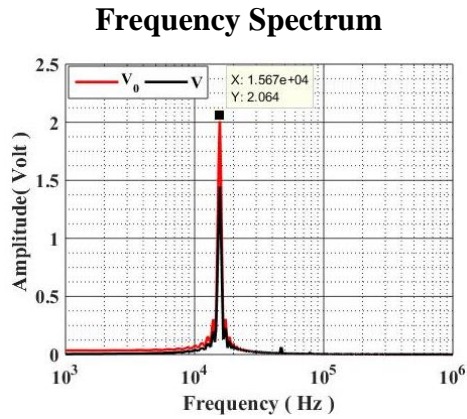
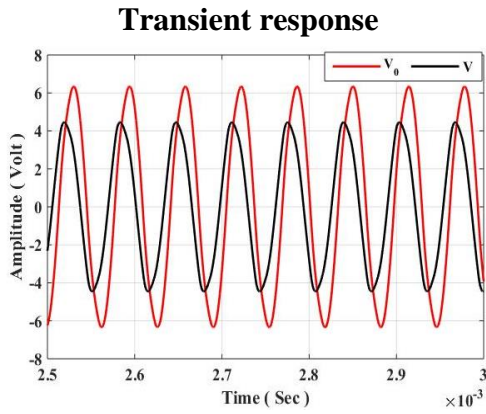
Figure 5.7 R-C ladder circuit to realize fractional order capacitors

Table 5.3 Component values of FC for $\alpha = 0.8$ and 0.9

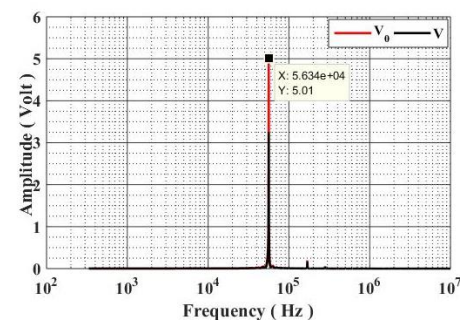
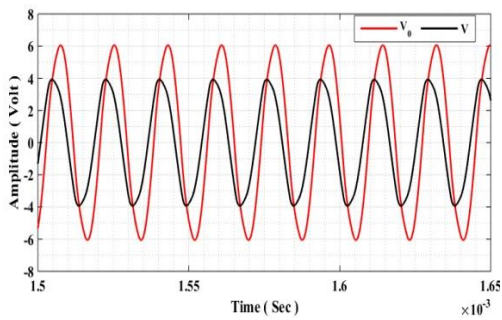
Order	$C_f = 10\text{nF/s}^{(\alpha-1)}$			
	Resistor		Capacitor	
0.9	$R_0 = 1.20\Omega$	$R_1 = 1.116\Omega$	$C_1 = 9.25\text{nF}$	$C_2 = 10.03\text{nF}$
	$R_2 = 8.07\Omega$	$R_3 = 50.23\Omega$	$C_3 = 12.08\text{nF}$	$C_4 = 14.75\text{nF}$
	$R_4 = 308.66\Omega$	$R_5 = 1.895\text{K}\Omega$	$C_5 = 18.00\text{nF}$	$C_6 = 21.75\text{nF}$
	$R_6 = 11.76\text{K}\Omega$	$R_7 = 79.52\text{K}\Omega$	$C_7 = 24.14\text{nF}$	$C_8 = 6.21\text{nF}$
	$R_8 = 2.315\text{M}\Omega$			

0.8	$R_0 = 8.957\Omega$	$R_1 = 12.89\Omega$	$C_1 = 0.757\text{nF}$	$C_2 = 1.0009\text{nF}$
	$R_2 = 72.56\Omega$	$R_3 = 368.96\Omega$	$C_3 = 1.48\text{nF}$	$C_4 = 2.22\text{nF}$
	$R_4 = 1.85\text{K}\Omega$	$R_5 = 9.3\text{K}\Omega$	$C_5 = 3.319\text{nF}$	$C_6 = 4.918\text{nF}$
	$R_6 = 47.1\text{K}\Omega$	$R_7 = 254.4\text{K}\Omega$	$C_7 = 6.82\text{nF}$	$C_8 = 3.9\text{nF}$
	$R_8 = 3.33\text{M}\Omega$			

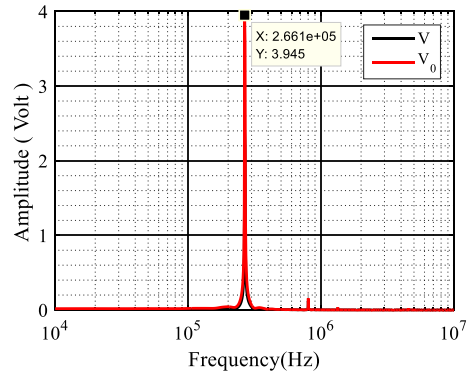
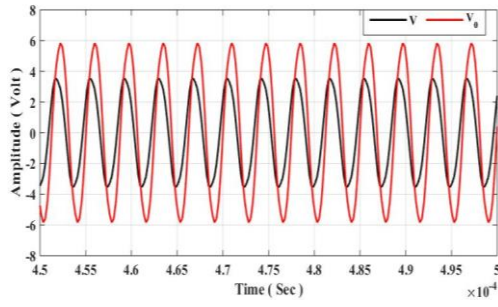
Eight different cases of fractional order oscillators (for different combinations of α and β) were simulated in PSPICE using the macro modal of AD844 type CFOA. The transient responses and frequency spectrums of proposed fractional order oscillators are displayed in Fig.5.8 (b) - Fig.5.8 (i).



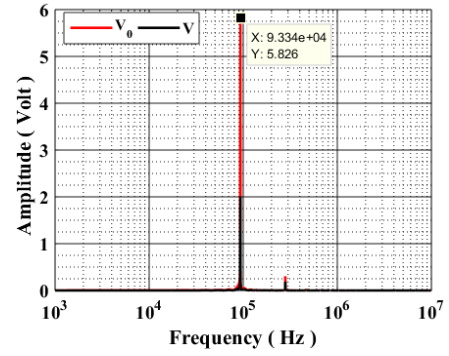
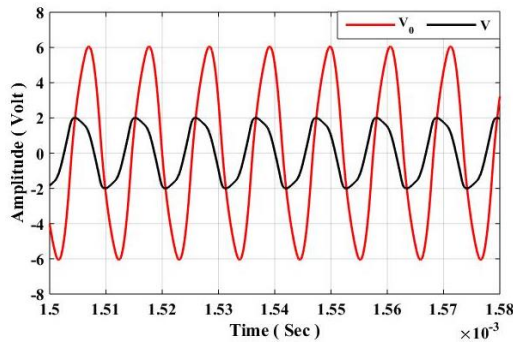
(a) $\alpha = 1.0, \beta = 1.0$



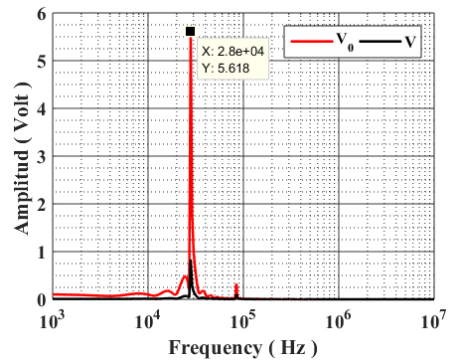
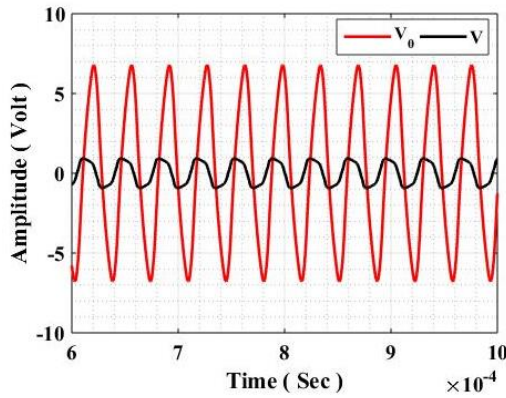
(b) $\alpha = 0.9, \beta = 0.9$



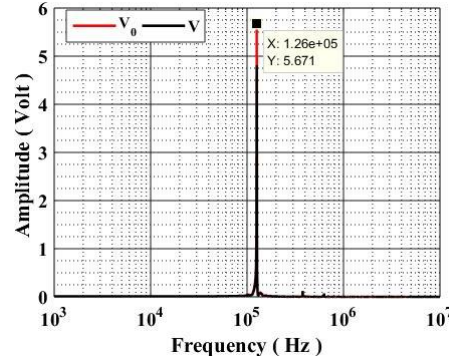
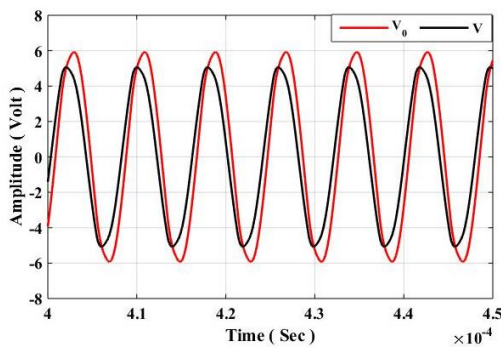
(c) $\alpha = 0.8, \beta = 0.8$



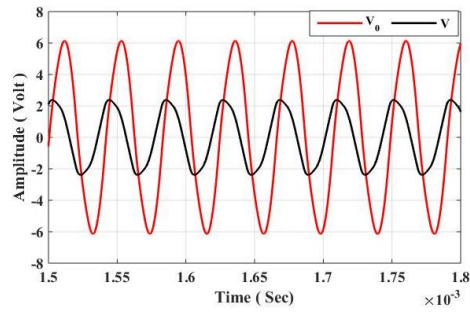
(d) $\alpha = 0.8, \beta = 0.9$



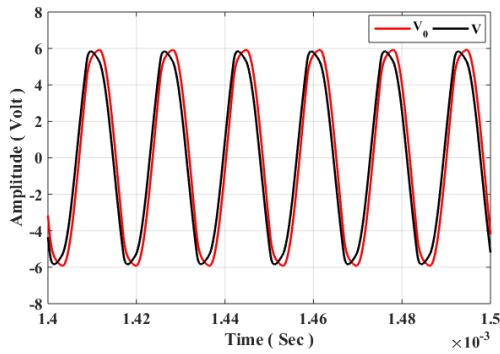
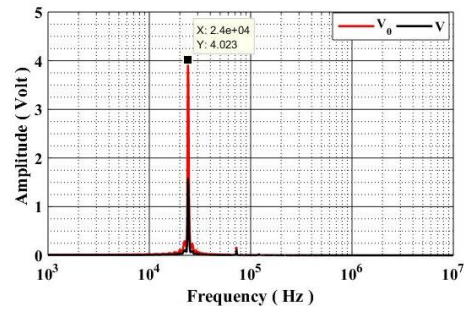
(e) $\alpha = 0.8, \beta = 1.0$



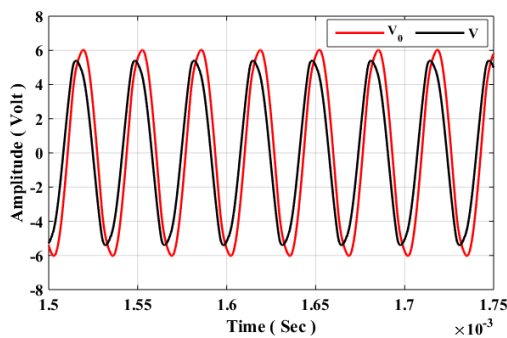
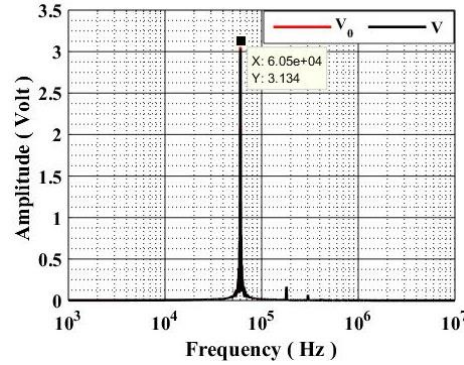
(f) $\alpha = 0.9, \beta = 0.8$



(g) $\alpha = 0.9, \beta = 1.0$



(h) $\alpha = 1.0, \beta = 0.8$



(i) $\alpha = 1.0, \beta = 0.9$

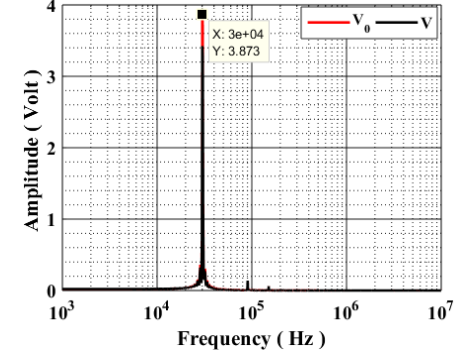


Figure 5.8 Transient responses and frequency spectra of proposed fractional order oscillator of Fig. 5.6

The simulation results (SM) and theoretical (MATLAB) results (TH) exhibiting FO and the phase difference for different values of α and β , along with the values of R_3 which are used in simulation of the circuit of Fig. 5.6 are shown in Table 5.4.

Table 5.4 Simulation and theoretical results of fractional order sinusoidal oscillator

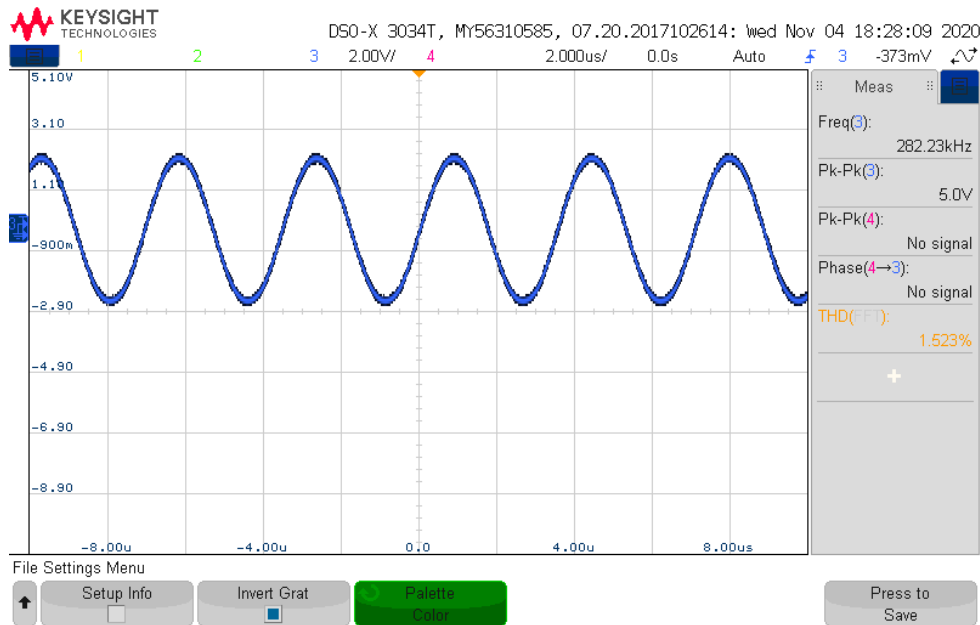
α and β	FO (SM/TH) (kHz)	Phase (SM/TH) (Degree)	$R_3(\Omega)$
$\alpha = 1.0, \beta = 1.0$	15.79/15.9	43.20/44.95	445.09
$\alpha = 0.9, \beta = 0.9$	56.82/57.04	39.24/40.42	390
$\alpha = 0.8, \beta = 0.8$	271.36/282.74	34.29/36.02	340.79
$\alpha = 0.8, \beta = 0.9$	98.37/98.52	47.87/52.10	143.7
$\alpha = 0.8, \beta = 1.0$	30.03/27.699	54.04/63.9	52.59
$\alpha = 0.9, \beta = 0.8$	126.85/130.09	23.84/23.69	629.5
$\alpha = 0.9, \beta = 1.0$	24.61/24.91	53.99/57.40	187.2
$\alpha = 1.0, \beta = 0.8$	61.25/61.68	27.09/14.57	669
$\alpha = 1.0, \beta = 0.9$	30.42/30.68	26.29/27.43	668

From the Table 5.4, it may be observed that the simulated results are in good agreement with the theoretical results in most of the cases.

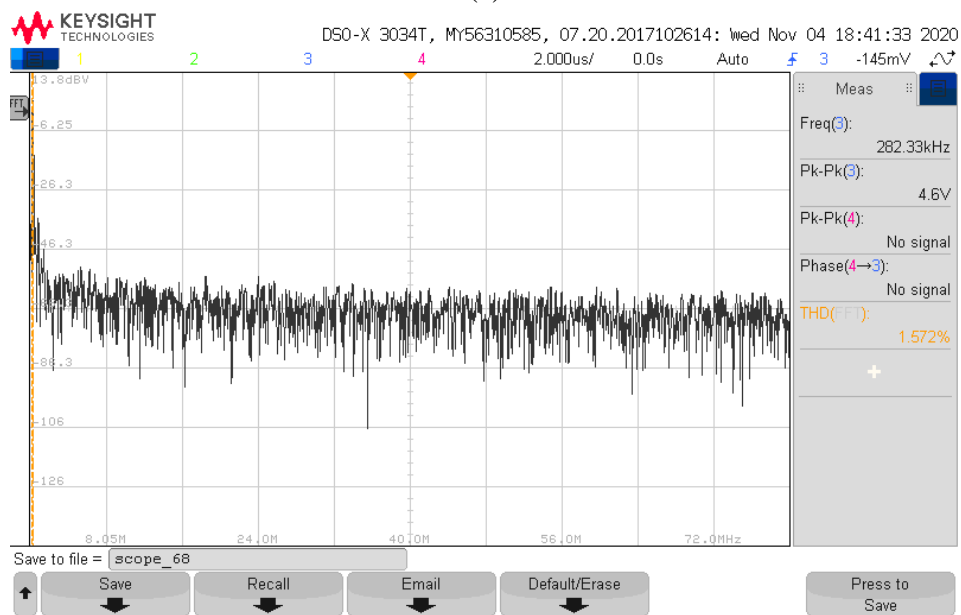
5.4.3. Experimental Results of Proposed Fractional Order Sinusoidal Oscillator

To validate the simulation results, the FOSO circuit was bread-boarded using off-the-shelf available IC AD844 type CFOA with 5% tolerance RC components. The power supplies used to bias the AD844 were $\pm 12V$ DC. The fractional order capacitors of value $10nF/(s^{1-\alpha})$ (for $\alpha = \beta = 0.8$) were simulated using the RC ladder as shown in Fig. 5.7 whose component values are presented in Table 5.3. The FOSO circuit was designed for a nominal frequency of 282.74 kHz, by selecting $R_1 = R_2 = 1K\Omega$. The value of R_3 required for meeting the CO was obtained as 340Ω . The experimentally obtained value of FO was found to be 282.23 kHz, which is very close to the designed value. The %THD of proposed FOSO circuit was found to be 1.52%. The transient response and frequency

spectrum of the oscillator have been displayed in Fig. 5.9, while frequency of oscillation and phase are given in Table. 5.5.



(a)



(b)

Figure 5.9 Experimentally obtained transient response and frequency spectrum of the oscillator of Fig. 5.6

Table 5.5. Frequency of oscillation and phase difference between the outputs of fractional order oscillator for $\alpha = \beta = 0.8$

Parameter of FOSO	Theoretical	Experimental	PSPICE Simulation
FO (kHz)	282.74	283.3	271.34

The above experimental results, thus, establish the workability of the proposed FOSO circuit.

5.5. Stability Analysis

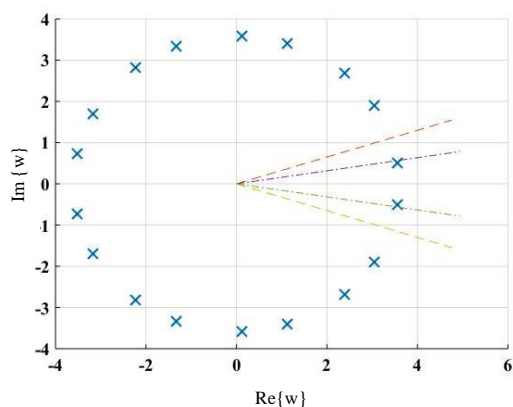
The stability of the proposed fractional order sinusoidal oscillators has been investigated using the method given in [33]. For stability of fractional order oscillator, at least one root of CE in w -plane must lie on $|\theta_w| = \frac{\pi}{2k}$ and remaining other roots lie in stable region (region shown in w -plane) [33]. Even if, a single root lies in unstable region, the fractional order oscillator becomes unstable. The location of roots of CE of FOSOs of Fig. 5.1 and Fig.5.6 have been plotted (for $k = 10$) in w -plane for different values of α and β , and these have been shown in Fig. 5.10 and Fig. 5.11 respectively. From the observation of Fig. 5.10 and Fig. 5.11, it is confirmed that the implemented fractional order sinusoidal oscillators are stable in nature.

Values of
 α and
 β

$$\alpha = 0.9,$$

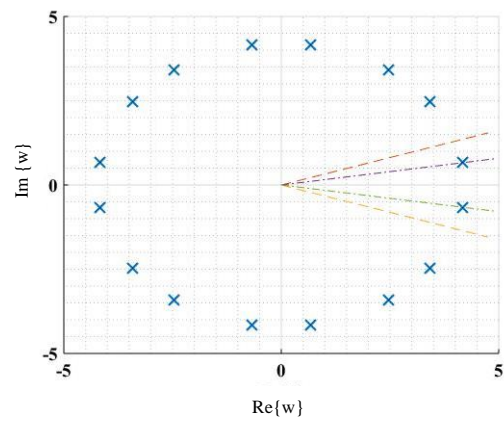
$$\beta = 0.9$$

Poles in w -plane of fractional order oscillator of Fig. 5.1



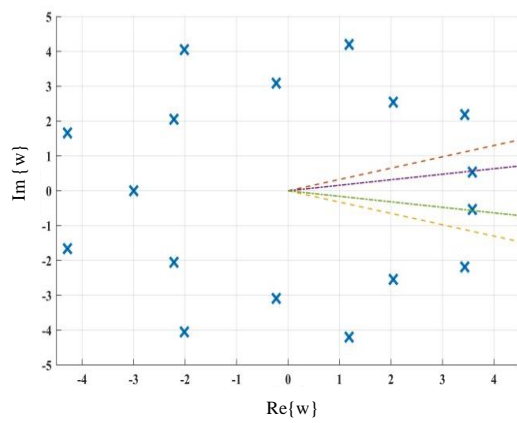
$\alpha = 0.8$

$\beta = 0.8$



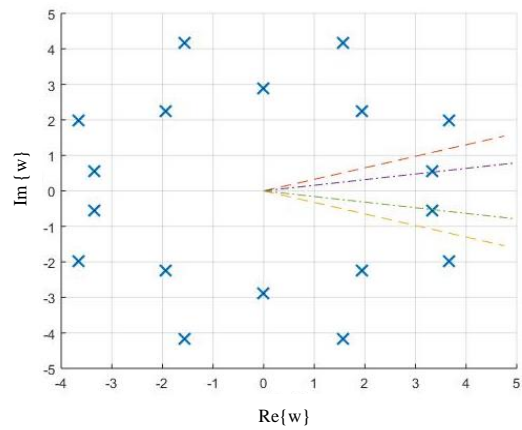
$\alpha = 0.8$

$\beta = 0.9$



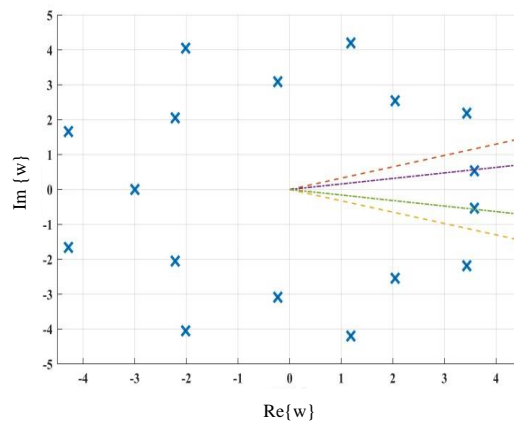
$\alpha = 0.8$

$\beta = 1.0$



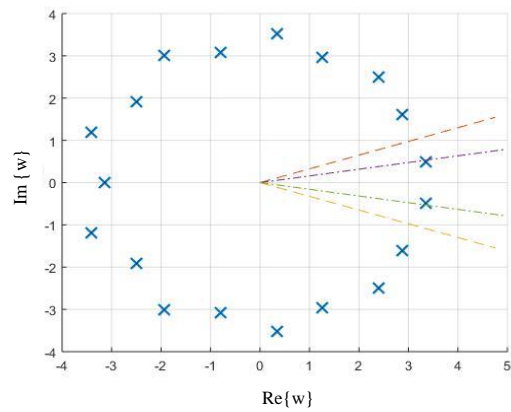
$\alpha = 0.9$

$\beta = 0.8$



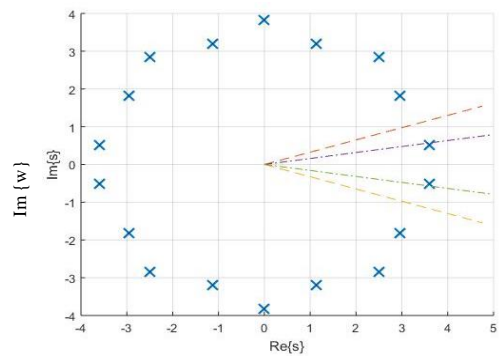
$$\alpha = 0.9$$

$$\beta = 1.0$$



$$\alpha = 1.0$$

$$\beta = 0.8$$



$$\alpha = 1.0$$

$$\beta = 0.9$$

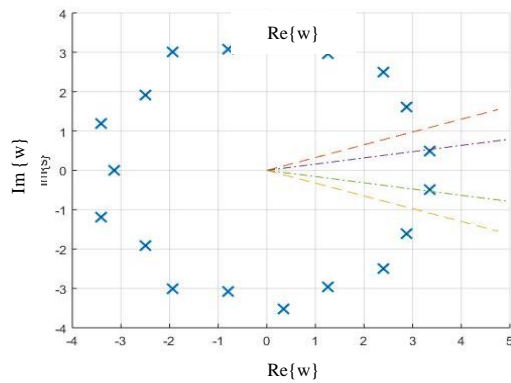


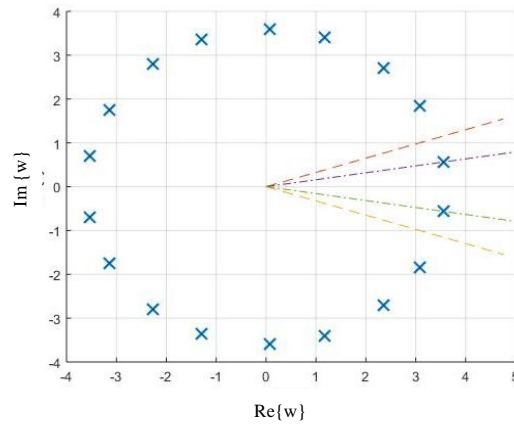
Figure 5.10. Polar plot of the poles of the CE in w-plane of the oscillator of Fig. 5.1

Values of
 α and
 β

$\alpha = 0.9$

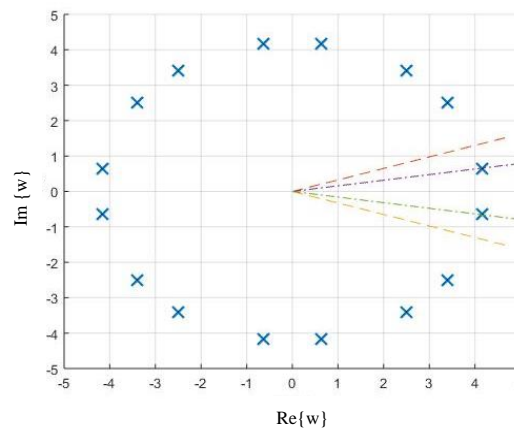
$\beta = 0.9$

Poles of fractional order oscillator of Fig. 5.1 in w-plane



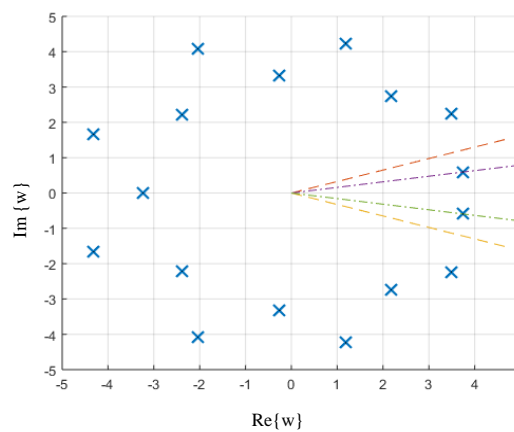
$\alpha = 0.8$

$\beta = 0.8$



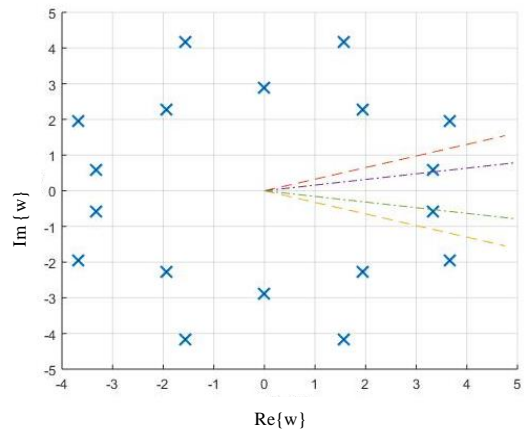
$\alpha = 0.8$

$\beta = 0.9$



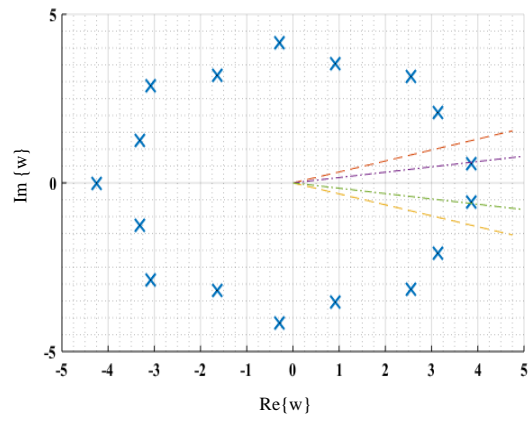
$$\alpha = 0.8$$

$$\beta = 1.0$$



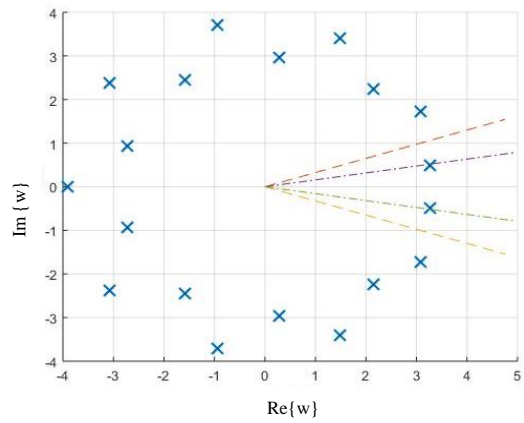
$$\alpha = 0.9$$

$$\beta = 0.8$$



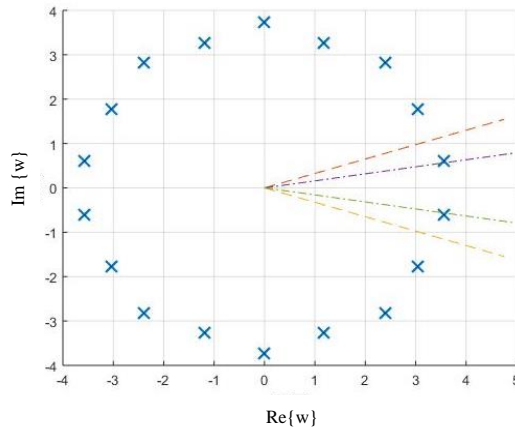
$$\alpha = 0.9$$

$$\beta = 1.0$$



$$\alpha = 1.0$$

$$\beta = 0.8$$



$$\alpha = 1.0$$

$$\beta = 0.9$$

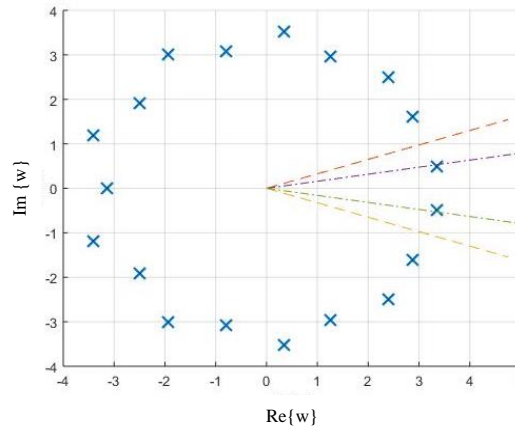


Figure 5.11. Polar plot of the poles of the CE in w -plane of the oscillator of Fig. 5.6

5.6. Conclusions

In this chapter, we have presented an extensive literature review of fractional order oscillator circuits, which are designed by replacing conventional capacitors by fractional order capacitors or designed ab-initio using various active building blocks. Two new configurations of fractional order sinusoidal oscillators are implemented using single active device with other passive components viz. passive resistors and fractional order capacitors. One of the structures of FOSO is realized with a single OTRA, three resistors and two fractional order capacitors. Nine different cases of OTRA-based fractional order sinusoidal oscillator for different combinations of α and β ((i) $\alpha = \beta = 1.0$ (ii) $\alpha = \beta = 0.9$ (iii) (i) $\alpha = \beta = 0.8$ (iv) $\alpha = 0.8$ and $\beta = 0.9$ (v) $\alpha =$

0.8 and $\beta = 1.0$ (vi) $\alpha = 0.9$ and $\beta = 0.8$ (vii) $\alpha = 0.9$ and $\beta = 1.0$ (viii) $\alpha = 1.0$ and $\beta = 0.9$ and (ix) $\alpha = 1.0$ and $\beta = 0.8$) were simulated in PSPICE. While, the second structure employs a single CFOA, three resistors and two fractional order capacitors. Again nine different cases of CFOA based FOSO circuit were considered for different values of α and β ((i) $\alpha = \beta = 1.0$ (ii) $\alpha = \beta = 0.9$ (iii) (i) $\alpha = \beta = 0.8$ (iv) $\alpha = 0.8$ and $\beta = 0.9$ (v) $\alpha = 0.8$ and $\beta = 1.0$ (vi) $\alpha = 0.9$ and $\beta = 0.8$ (vii) $\alpha = 0.9$ and $\beta = 1.0$ (viii) $\alpha = 1.0$ and $\beta = 0.9$ and (ix) $\alpha = 1.0$ and $\beta = 0.8$), were simulated in PSPICE. For both the structures of FOSOs, PSPICE simulations were carried out, to validate the workability of the proposed FOSO structures. The performance of CFOA-based FOSO circuit was also examined experimentally for $\alpha = \beta = 0.8$. The study of stability analysis has also been carried out for both the proposed fractional order sinusoidal oscillators.

References

- [1] J. Valsa, P. Dvorak and M. Friedl, "Network model of the CPE," *Radioengineering*, vol. 20, no. 3, pp. 619–626, 2011.
- [2] A. Oustaloup, F. Levron, B. Mathieu and F. M. Nanot, "Frequency-band complex noninteger differentiator: characterization and synthesis," *IEEE Trans. Circ. Syst. I: Fundamental Theory and Applications*, vol. 47 no. 1, pp. 25-39, 2000.
- [3] R. Senani, D. R. Bhaskar V. K. Singh and R. K Sharma, "Sinusoidal Oscillators and Waveform Generators using Modern Electronic Circuit Building Blocks," Springer, Cham./doi.org/10.1007/978-3-319-23712-1_1

- [4] A. Oustaloup, "Fractional order sinusoidal oscillators: optimization and their use in highly linear FM modulation," *IEEE Trans. Circ. Syst.*, vol. 28, no. 10, pp. 1007-1009, 1981.
- [5] A. G. Radwan, A. M. Soliman and A. S. Elwakil, "Design equations for fractional-order sinusoidal oscillators: four practical circuits examples," *Int. J. Circ. Theory Appl.*, vol. 36, pp. 473-492, 2007.
- [6] W. Ahmad, R. El-Khazali, and A. S. Elwakil, "Fractional-order Wien-bridge oscillator," *Electron. Lett.*, vol. 37, no.18, pp. 1110-1112, 2001.
- [7] A. G. Radwan, A. S. Elwakil and A. M. Soliman, "Fractional-order sinusoidal oscillators: design procedure and practical examples," *IEEE Trans. Circ. Syst. I*, vol. 55, no. 7, pp. 2051-2063, 2008
- [8] L. A. Said, A. G. Radwan, A.H. Madian and A. M. Soliman, "Fractional order two port network oscillator with equal order," *Int. Conf. Microelectron. (ICM)*, pp. 156-159, 2014.
- [9] L. A. Said, A. H. Madian, A. G. Radwan and A. M. Soliman, "Current feedback operational amplifier (CFOA) based fractional order oscillators," *Int. Conf. Electron. Circ. Syst. (ICECS)*, Marseille, 2014, pp. 510-513, doi: 10.1109/ICECS.2014.7050034.
- [10] L. A. Said, A. G. Radwan, A. H. Madian and A. M. Soliman, "Fractional-order oscillator based on single CCII," *Int. Conf. Telecommun. Signal Process. (TSP)*, Vienna, 2016, pp. 603-606, doi: 10.1109/TSP.2016.7760952.
- [11] A. M. EL-Naggar, L. A. Said, A. G. Radwan, A. H. Madian, A. M. Soliman, "Fractional order four-phase oscillator based on double integrator topology," *IEEE Int. Conf. Modern Circ. and Syst. Technologies*, pp. 1-4, 2017.

- [12] L. A. Said, A. G. Radwan, A. H. Madian, and A. M. Soliman, "Generalized family of fractional-order oscillators based on single CFOA and RC network," *Int. Conf. Modern Circ. Syst. Technologies (MOCASST)*, pp. 1-4, 2017.
- [13] L. A. Said, A. G. Radwan, A. H. Madian, and A. M. Soliman, "Three fractional-order-capacitors-based oscillators with controllable phase and frequency," *J. Circ. Syst. Comp.*, 26(10), 1750160, 2017.
- [14] S. K. Mishra, D. K. Upadhyay, and M. Gupta, "An approach to improve the performance of fractional-order sinusoidal oscillators," *Chaos, Solitons & Fractals*, Elsevier, 116(C), pages 126-135, 2018.
- [15] A. Pradhan, and R. K. Sharma, "Generalized Fractional-Order Oscillators using OTA," *Int. Conf. Signal Process. Integrated Networks (SPIN)*, pp. 402-406, 2018.
- [16] T. Comedang, and P. Intani, "Current-Controlled CFTA Based Fractional Order Quadrature Oscillators," *Circ. Syst.*, vol.7, pp. 4201-4212, 2016
- [17] L. A. Said, A. G. Radwan, A. H. Madian and A. M. Soliman, "Fractional order oscillator design based on two-port network," *Circ. Syst. Signal Process.* vol. 35 pp. 3086–3112,2016.
- [18] D. Kubánek, F. Khateb, G. Tsirimokou, and C. Psychalinos, "Practical design and evaluation of fractional-order oscillator using differential voltage current conveyors," *Circ. Syst. Signal Process.*, vol. 35, no. 6, pp. 2003-2016, 2016.
- [19] L. A. Said, A. G. Radwan A. H. Madian and A. M. Soliman, "Fractional order Oscillators Based on Operational Transresistance Amplifiers," *Int. J. Electron. Comm. (AEÜ)*, vol.69, pp. 988-1003, 2015.

- [20] L. A. Said, A. H. Madian, A. G. Radwan and A. M. Soliman, "Fractional order oscillator with independent control of phase and frequency," *Int. Conf. Electronic Design (ICED)*, Penang, 2014, pp. 224-229, doi: 10.1109/ICED.2014.7015803.
- [21] A. Kartci, N. Herencsar, J. Koton and C. Psychalinos, "Compact MOS-RC voltage-mode fractional-order oscillator design," *European Conf. Circ. Theory and Design (ECCTD)*, Catania, 2017, pp. 1-4, doi: 10.1109/ECCTD.2017.8093281.
- [22] A. Kartci, N. Herencsar, J. Koton, L. Brancik, K. Vrba, G. Tsirimokou and C. Psychalinos, "Fractional-order oscillator design using unity-gain voltage buffers and OTAs," *Int. Midwest Symp. Circ. Syst. (MWSCAS)*, Boston, MA, pp. 555-558, , 2017, doi: 10.1109/MWSCAS.2017.8052983.
- [23] S. K. Mishra, M. Gupta and D. K. Upadhyay, "Design and implementation of DDCC-based fractional-order oscillator," *Int. J. Electron.*, vol. 106, no. 4, pp.581-598, 2019.
- [24] A. Pradhan, K. S. Subhadhra, N. Atique, R. K. Sharma and S. S. Gupta, "MMCC-based current-mode fractional-order voltage-controlled oscillators," *Int. Conf. Inventive Systems and Control (ICISC)*, pp. 763-768,2018.
- [25] K. S. Subhadhra, R. K. Sharma and S. S. Gupta, "Realisation of some current-mode fractional-order VCOs/SRCOs using multiplication mode current conveyors," *Analog Integr Circ Sig Process*, vol. 103, pp. 31–55, 2020. doi:10.1007/s10470-020-01590-4

- [26] V. Singh and P. Kumar, "Fractional Order Oscillator Using OTAs," Int. Conf. Control, Automation and Robotics (ICCAR), Singapore, 2020, pp. 27-32, 2020, doi: 10.1109/ICCAR49639.2020.9108095.
- [27] A. Kartci and L. Brancik, "CFOA-based fractional-order oscillator design and analysis with NILT method," Int. Conf. Radioelektronika (RADIOELEKTRONIKA), Brno, pp. 1-4, 2017 doi: 10.1109/RADIOELEK.2017.7937600.
- [28] M. R. Dar, F. A. Khanday and C. Psychalinos, "Multiphase Fractional-Order Sinusoidal Oscillator Design Using CFOA," Int. J. Advance Research in Science and Engineering, vol. 6, no. 10, pp. 926-934, 2017.
- [29] A. M. Soliman, "Three oscillator families using the current feedback opamp," Frequenz, vol. 54, no. 5-6, pp.126-131, 2000.
- [30] A. M. Soliman, "Generation of third-order quadrature oscillator circuits using NAM expansion," J. Circ. Syst. Comput., vol. 22 (2013) 1350060.
- [31] D. R. Bhaskar, M. P. Tripathi and R. Senani, "A Class of Three-OTA Two-Capacitor Oscillators with Non-interacting Controls," Int. J. Electron., Vol. 74, No. 3, pp. 459-463, 1993
- [32] H. Mostafa and A. M. Soliman, "A Modified CMOS Realization of the Operational Transresistance Amplifier (OTRA)," Frequenz, vol.60, no. (3-4), pp. 70-77, 2006.
- [33] A. G. Radwan, A. M. Soliman, A. S. Elwakil and A. Sedeek, "On the stability of linear systems with fractional-order elements," Chaos, Solitons Fractals, vol. 40, no. 5, pp. 2317-2328, 2009.

Chapter 6

Conclusions and Future Scope

This thesis has dealt with the realization of voltage-mode/current-mode fractional order analog circuits viz. fractional order filters, fractional order inverse filters and fractional order sinusoidal oscillators using different active building blocks such as op-amp, CFOAs and OTRA. In the following, we present a summary of the main contributions of this thesis.

6.1. Summary

In Chapter 1 of the thesis, a preliminary introduction of fractional order analog circuits, the objectives of the research work and the organization of the thesis has been presented.

Chapter 2 dealt with different types of fractional order elements (FOEs) available in open literature, viz. single component based and multicomponent-based FOEs. We have presented the details of some of the important works dealing with the realizations of the FOEs using single, as well as multi-component based realizations of the FOEs. We have also presented the details of the methodology and design of the fractional order capacitors, which we have used for the realization of various fractional order analog circuits in this thesis. The methods proposed by Valsa, Dvorak and Friedl and Oustaloup, Levron, Mathieu and Nanot, for implementation of fractional order capacitors have been explained in detail for finding the component values in the R-C ladder network. Using Valsa, Dvorak and Friedl's method,

fractional order capacitors of values $0.382\mu\text{F}/\text{sec}^{(\alpha-1)}$, $0.0955\mu\text{F}/\text{sec}^{(\alpha-1)}$ and $1\text{nF}/\text{sec}^{(\alpha-1)}$ for different values of α have been designed, whereas fractional order capacitors of value $10\text{nF}/\text{sec}^{(\alpha-1)}$ for $\alpha = 0.9$ and $\alpha = 0.8$ have been designed using Oustaloup, Levron, Mathieu and Nanot's method. To verify the performance of these fractional order capacitors, the magnitude and phase responses have also been presented. Experimentally obtained frequency response characteristics of a fractional order capacitor have also been presented.

In chapter 3, a brief literature overview of fractional order filters, designed using various active building blocks has been presented. This Chapter is also concerned with the design of CFOA-based fractional order filters in (i) voltage-mode and (ii) current-mode. Two different structures of voltage-mode fractional order filters have been presented in which the fractional order low pass filter, fractional order band pass filter and fractional order high pass filter can be realized by selecting the branch admittances appropriately. Both the presented structures employ only a single CFOA and five passive components (three/two conventional resistors and two/three fractional order capacitors). The proposed current-mode fractional order filter structure, on the other hand, employs only a single CFOA, two resistors and two fractional order capacitors. The various output responses viz, FOLP, FOBP and FOHP can be obtained by appropriate selection of the branch admittances. The workability of all the proposed circuits has been verified by theoretical calculations, MATLAB and PSPICE simulations for different values of ' α ' ($0 < \alpha < 1$). Experimental results for an exemplary single CFOA based fractional order filter operating in voltage mode (for $\alpha = \beta = 0.7$) have also been presented.

In chapter 4, a brief literature overview of conventional inverse filters, designed using various active building blocks has been presented. Prior to the commencement of this research work, no analog inverse active filter in fractional order domain was reported in open literature. In view of this, we have presented several structures of fractional order inverse active filters, designed with various active building blocks viz. op-amp, CFOAs and OTRA, passive resistors and simulated fractional order capacitors. Three circuits of op-amp-based fractional order multifunction inverse active filters, two circuits of CFOA-based multifunction inverse filters and one circuit of OTRA-based fractional order inverse filter have been presented. From the same topology, in all the presented configurations, FOILP, FOIBP and FOIHP filter responses can be obtained by appropriately selecting the branch admittances. The performance of all presented circuits has been verified by theoretical calculations, MATLAB and PSPICE simulations for various values of ' α ' ($0 < \alpha < 1$). One of the op-amp-based fractional order inverse filter circuit (minimal realization of fractional order inverse filter) has also been verified experimentally for $\alpha = 0.7$. The sensitivity and stability analysis of fractional order inverse active filters have also been described in this chapter.

In chapter 5, we have presented an extensive literature review of fractional order sinusoidal oscillators, which were designed by merely replacing the integer order capacitors by fractional order capacitors or designed ab-initio using various active building blocks. Two new configurations of fractional order sinusoidal oscillators have been implemented using single active device and other passive components viz. passive resistors and fractional order capacitors. One of the structures of FOSO is realized with a single OTRA, four resistors and two fractional

order capacitors. Nine different cases of OTRA-based fractional order oscillators for different combinations of α and β were simulated in PSPICE. The other structure was implemented using a single CFOA, three resistors and two fractional order capacitors. Nine different cases of CFOA-based fractional order oscillators for different combinations of α and β were simulated in PSPICE. For both the structures of FOSOs, PSPICE simulations were carried out to show the transient response and frequency spectra of the proposed FOSOs. For one case, ($\alpha = \beta = 0.8$) of CFOA based FOSO, experimental results have also been presented. The stability analysis has also been carried out for the presented fractional order sinusoidal oscillators.

6.2. Future Scope

Fractional order circuits and systems is an emerging interdisciplinary area of science and engineering. Several interesting developments have taken place in the area of fractional order analog active circuits during the last two decades resulting in appearance of various types of analog circuit implementation of fractional order filters, fractional order sinusoidal oscillators and fractional order PID controllers with different properties, which were not reported in their integer order counterparts, in open literature. When this research work was initiated, there were no fractional order inverse filter structure available in the open literature. We have proposed a new configuration of fractional order inverse filters in 2018 and proposed several other inverse active filters in fractional order domain. Apart from the work reported in this thesis, in the following, we suggest few other directions in which the work presented in this thesis can be extended:

1. The design and development of a compact fractance device, in which the order of

the FOE can be changed smoothly, by means of some electronic control (voltage /current), will be helpful in exploiting the real potential of the fractional order active circuits. This is still an open problem which can be taken up for further investigation.

2. Various approximation methods have been used for simulation of the FOE in general. A systematic evaluation of the performance of the realized FOE for a specific application will help in benchmarking of the different approximation methods for different applications, thus, will help in the development of commercially available FOEs, and therefore, is an interesting problem open for future research.
3. The inverse analog filters presented in this thesis have been realized using an approach wherein we have realized the transfer functions with the help of fractional order capacitor(s). These transfer functions could also be realized using any one of the standard methods of approximations of the fractional order Laplacian operator and the performance may be compared in terms of the tunability properties and other specifications.
4. The development of design tables and related softwares for the design of fractional order active filters for different values of the fractional order parameters and design specifications is an interesting problem which may be taken up for further research.
5. New structures of multiphase sinusoidal oscillators realized with different ABBs may be developed.

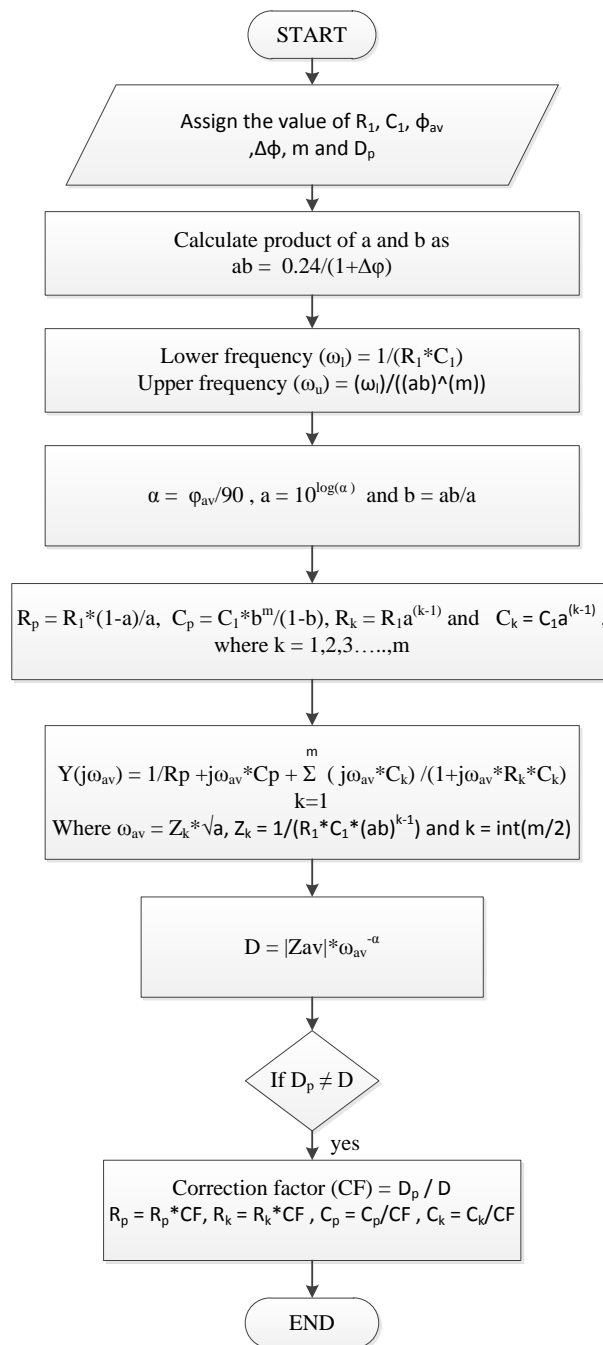
6. Analog circuit implementation of multi frequency fractional order oscillators is yet another area in which the work presented in this thesis may be extended.

Finally, it must be concluded that there is no dearth of new possibilities, problems and ideas to pursue, as far as the design of fractional order analog circuits is concerned and this is, undoubtedly, a very exciting area of research.

Appendix I:

**Realization of FC and Fractional Order Filter
and Inverse Filter**

**Flowchart for the design of Fractional order capacitor using Valsa,
Dvorak and Friedl Method**

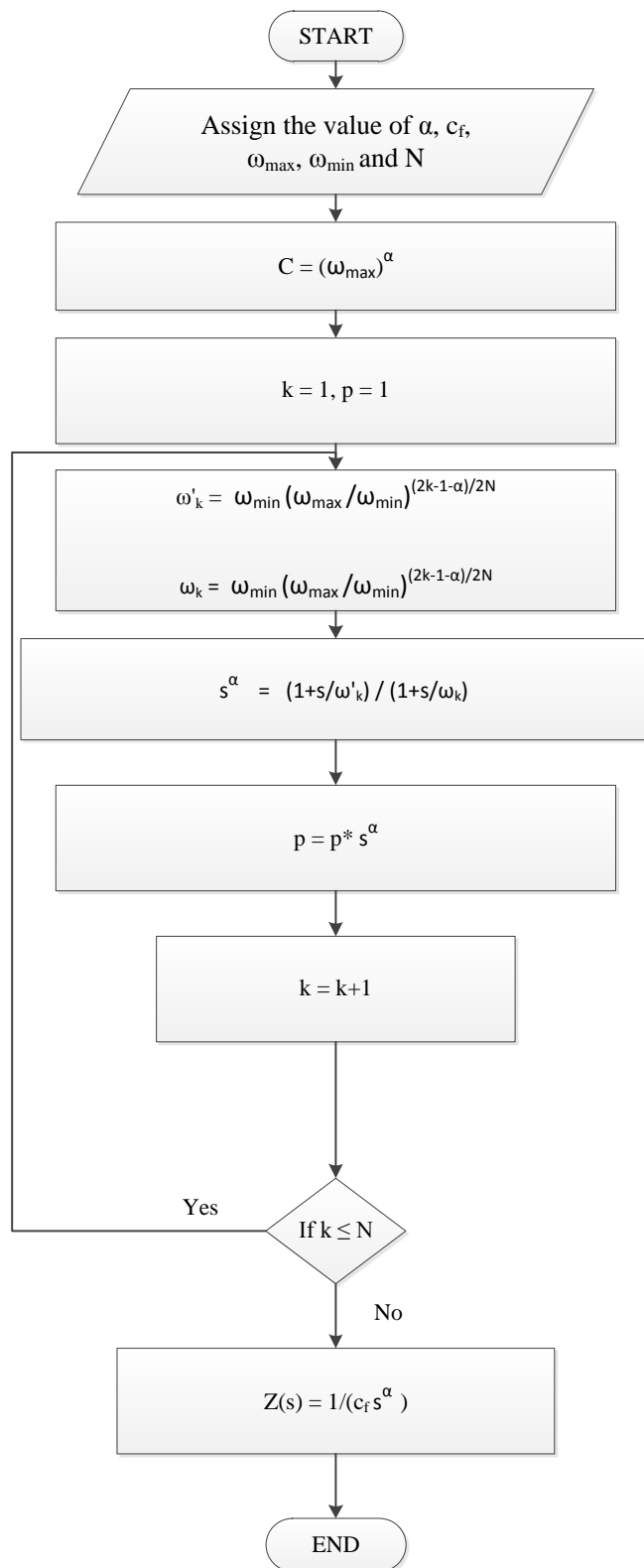


MATLAB code of Fractional Order Capacitor using Valsa, Dvorak and Friedl Method

```
clc;
clear all;
close all;

Dp=input('enter the value of capacitance of fractional capacitor');
al=input('enter the order of capacitor');
m=input('enter the no of branches m=');
err=input('enter % error in design');
c1=input('enter the value of c1');
r1=input('enter the value of r1');
wl=1/(c1*r1);
wu=wl/((a*b)^(m));
ab=0.24/(1+err);
p=al*log10(ab);
a=10^(p);
b=ab/a;
Rp=r1*(1-a)/a;
Cp=c1*b^(m)/(1-b);
Wav=(a/b)^(0.25)/(r1*c1*ab^(2));
e=1i*Wav*Cp;
sum=0;
f=1/Rp;
for n=1:m
    sum=sum+(1i*Wav*c1*b^(n-1))/(1+1i*Wav*r1*c1*ab^(n-1));
end
Yav=sum+1/Rp+e;
Zav=1/abs(Yav);
Dc=Zav*Wav^(al);
ml=Dp/Dc;
Rpm=Rp*ml;
Cpm=Cp/ml;
for n=1:m
    R(n)=r1*a^(n-1)*ml;
    C(n)=(c1*b^(n-1))/ml;
end
```

Flowchart of fractional order capacitor designed using Oustaloup, Levron, Mathieu and Nanot Method



MATLAB Code for Design of fractional order capacitor using Oustaloup, Levron, Mathieu and Nanot Method

```

clc;
close all;
clear all;
wmax=input('enter the value of maximum frequency in rad/sec = ');
wmin=input('enter the value of minimum frequency in rad/sec = ');
alpha=input('enter the value of alpha = ');
c1=input('enter the value of capacitor = ');
k1=(1/(c1*(wmax^alpha)));
n=input('the value of n =. ');

for l=1:n
z1(l)=-((wmin*((wmax/wmin)^((2*l)-1+alpha)/(2*n))))
p1(l)=-((wmin*((wmax/wmin)^((2*l)-1-alpha)/(2*n))))
end
z=z1';
p=p1';
[num den]=zp2tf(z,p,k1);
[c r k]=residue(num,den);
cap=1./c;
res=-c./r;

```

MATLAB Code of FOILP and FOLP

```

%%%%%%%%%%%%%%%%%%%%%%%%%%%%%%%%%%%%%%%%%%%%%%%%%%%%%%%%%%%%%%%%%%%%%%%%
%%%%%%%%%%%%%%%%%%%%%%%%%%%%%%%%%%%%%%%%%%%%%%%%%%%%%%%%%%%%%%%%%%%%%%%%
%          FOILP and FOLP of single fractance device          %
%%%%%%%%%%%%%%%%%%%%%%%%%%%%%%%%%%%%%%%%%%%%%%%%%%%%%%%%%%%%%%%%%%%%%%%%
%%%%%%%%%%%%%%%%%%%%%%%%%%%%%%%%%%%%%%%%%%%%%%%%%%%%%%%%%%%%%%%%%%%%%%%%
close all;
clear all;
clc;
b = 1:-0.1:.5;
w = logspace(1,9,5000);
f=.159*w;
%p=1:-.1:.5;
for i=1:1:6
Fr = @(w) (3140)./((1i*w).^(b(i))+3140);
figure(1)
semilogx(f,20*log10(abs(Fr(w))));
hold on
figure (2)
semilogx(f,(180/pi)*angle(Fr(w)));
hold on
figure(3)
semilogx(f,20*log10(abs(1./Fr(w))));
hold on
figure(4)
semilogx(f,(180/pi)*angle(1./Fr(w)));
hold on
end
%%%%%%%%%%%%%%%%%%%%%%%%%%%%%%%%%%%%%%%%%%%%%%%%%%%%%%%%%%%%%%%%%%%%%%%%
%%%%%%%%%%%%%%%%%%%%%%%%%%%%%%%%%%%%%%%%%%%%%%%%%%%%%%%%%%%%%%%%%%%%%%%%
%          End of FOILP and FOLP filter          %
%%%%%%%%%%%%%%%%%%%%%%%%%%%%%%%%%%%%%%%%%%%%%%%%%%%%%%%%%%%%%%%%%%%%%%%%

```



```
%%%%%%%%%%%%%%%%%%%%%%%%%%%%%%%%%%%%%%%%%%%%%%%%%%%%%%%%%%%%%%%%%%%%%%%%
%%%%%%%%%%%%%%%%%%%%%%%%%%%%%%%%%%%%%%%%%%%%%%%%%%%%%%%%%%%%%%%%%%%%%%%%
```

```
%%%%%%%%%%%%%%%%%%%%%%%%%%%%%%%%%%%%%%%%%%%%%%%%%%%%%%%%%%%%%%%%%%%%%%%%
%%%%%%%%%%%%%%%%%%%%%%%%%%%%%%%%%%%%%%%%%%%%%%%%%%%%%%%%%%%%%%%%%%%%%%%%
```

% FOILP and FOLP filter using two Fractance devices %

```
%%%%%%%%%%%%%%%%%%%%%%%%%%%%%%%%%%%%%%%%%%%%%%%%%%%%%%%%%%%%%%%%%%%%%%%%
%%%%%%%%%%%%%%%%%%%%%%%%%%%%%%%%%%%%%%%%%%%%%%%%%%%%%%%%%%%%%%%%%%%%%%%%
```

```
close all;
clear all;
clc;
b = 1:-0.1:.5;
w = logspace(1,9,5000);
f=.159*w;
p=1:-.15:.15;
for i=1:1:6
Fr = @(w) (6280*6280)./((1i*w).^p(i)+b(i))+1.414*6280*(1i*w).^p(i)+6280*6280);
figure(1)
semilogx(f,20*log10(abs(Fr(w))));
hold on
figure (2)
semilogx(f,(180/pi)*angle(Fr(w)));
hold on
figure(3)
semilogx(f,20*log10(abs(1./Fr(w))));
hold on
figure(4)
semilogx(f,(180/pi)*angle(1./Fr(w)));
hold on
end
```

```
%%%%%%%%%%%%%%%%%%%%%%%%%%%%%%%%%%%%%%%%%%%%%%%%%%%%%%%%%%%%%%%%%%%%%%%%
%%%%%%%%%%%%%%%%%%%%%%%%%%%%%%%%%%%%%%%%%%%%%%%%%%%%%%%%%%%%%%%%%%%%%%%%
```

```
%
% End of FOILP and FOLP filter %
%%%%%%%%%%%%%%%%%%%%%%%%%%%%%%%%%%%%%%%%%%%%%%%%%%%%%%%%%%%%%%%%%%%%%%%%
%%%%%%%%%%%%%%%%%%%%%%%%%%%%%%%%%%%%%%%%%%%%%%%%%%%%%%%%%%%%%%%%%%%%%%%%
```

MATLAB Code of FOIBP and FOBP filters

```
%%%%%%%%%%%%%%%%%%%%%%%%%%%%%%%%%%%%%%%%%%%%%%%%%%%%%%%%%%%%%%%%%%%%%%%%
%%%%%%%%%%%%%%%%%%%%%%%%%%%%%%%%%%%%%%%%%%%%%%%%%%%%%%%%%%%%%%%%%%%%%%%% FOIBP and FOBP using Single FC
```

```
%
%%%%%%%%%%%%%%%%%%%%%%%%%%%%%%%%%%%%%%%%%%%%%%%%%%%%%%%%%%%%%%%%%%%%%%%%
%%%%%%%%%%%%%%%%%%%%%%%%%%%%%%%%%%%%%%%%%%%%%%%%%%%%%%%%%%%%%%%%%%%%%%%%
```

```
close all;
clear all;
clc;
b = 1:-0.1:0.5;
w = logspace(1,9,5000);
f=.159*w;
p=0.8:-0.1:.3;
for i=1:1:6
```

```

Fr = @(w) ((1i*w).^p(i))./((1i*w).^b(i)+3140);
figure(1)
semilogx(f,20*log10(abs(Fr(w))));
hold on
figure (2)
semilogx(f,(180/pi)*angle(Fr(w)));
hold on
figure(3)
semilogx(f,20*log10(abs(1./Fr(w))));
hold on
figure(4)
semilogx(f,(180/pi)*angle(1./Fr(w)));
hold on
end
%%%%%%%%%%%%%%%%%%%%%%%%%%%%%%%%%%%%%%%%%%%%%%%%%%%%%%%%%%%%%%%%%%%%%%%%
%                               %
%           End of FOIBP and FOBP filter           %
%%%%%%%%%%%%%%%%%%%%%%%%%%%%%%%%%%%%%%%%%%%%%%%%%%%%%%%%%%%%%%%%%%%%%%%%

%%%%%%%%%%%%%%%%%%%%%%%%%%%%%%%%%%%%%%%%%%%%%%%%%%%%%%%%%%%%%%%%%%%%%%%%
%                               %
%           FOIBP and FOBP filter using two FC           %
%%%%%%%%%%%%%%%%%%%%%%%%%%%%%%%%%%%%%%%%%%%%%%%%%%%%%%%%%%%%%%%%%%%%%%%%

close all;
clear all;
clc;
b = 1:-0.1:.5;
w = logspace(1,15,5000);
f=.159*w;
p=1:-.15:.1;
for i=1:1:6
Fr=@(w)(1.414*6280*(1i*w).^p(i))./((1i*w).^(p(i)+b(i))+1.414*6280*(1i*w).^p(i)+3140*3140);
figure(5)
semilogx(f,20*log10(abs(Fr(w))));
hold on
figure (6)
semilogx(f,(180/pi)*angle(Fr(w)));
hold on
figure(7)
semilogx(f,20*log10(abs(1./Fr(w))));
hold on
figure(8)
semilogx(f,(180/pi)*angle(1./Fr(w)));
hold on
end
%%%%%%%%%%%%%%%%%%%%%%%%%%%%%%%%%%%%%%%%%%%%%%%%%%%%%%%%%%%%%%%%%%%%%%%%
%                               %
%           End of FOBP and FOIBP filter           %
%%%%%%%%%%%%%%%%%%%%%%%%%%%%%%%%%%%%%%%%%%%%%%%%%%%%%%%%%%%%%%%%%%%%%%%%

```

MATLAB Code for FOIHP and FOHP

```
%%%%%%%%%%%%%%%%%%%%%%%%%%%%%%%%%%%%%%%%%%%%%%%%%%%%%%%%%%%%%%%%%%%%%%%%%%%%%%  
FOIHP and FOHP filter using a single FC  
%
```

```
close all;  
clear all;  
clc;  
b = 1:-0.1:.5;  
w = logspace(1,9,5000);  
f=.159*w;  
for i=1:1:6  
Fr = @(w) ((1i*w).^b(i))./((1i*w).^b(i)+3140);  
figure(1)  
semilogx(f,20*log10(abs(Fr(w))));  
hold on  
figure (2)  
semilogx(f,(180/pi)*angle(Fr(w)));  
hold on  
figure(3)  
semilogx(f,20*log10(abs(1./Fr(w))));  
hold on  
figure(4)  
semilogx(f,(180/pi)*angle(1./Fr(w)));  
hold on  
end
```

```
%%%%%%%%%%%%%%%%%%%%%%%%%%%%%%%%%%%%%%%%%%%%%%%%%%%%%%%%%%%%%%%%%%%%%%%%%%%%%%  
% End of FOIHP and FOHP filter %  
%%%%%%%%%%%%%%%%%%%%%%%%%%%%%%%%%%%%%%%%%%%%%%%%%%%%%%%%%%%%%%%%%%%%%%%%%%%%%%
```

```
%%%%%%%%%%%%%%%%%%%%%%%%%%%%%%%%%%%%%%%%%%%%%%%%%%%%%%%%%%%%%%%%%%%%%%%%%%%%%%  
FOIHP and FOHP filter using two FC  
%
```

```
close all;  
clear all;  
clc;  
b = 1:-0.1:.5;  
w = logspace(1,15,5000);  
f=.159*w;  
p=1:-.1:.5;  
for i=1:1:6  
Fr = @(w) ((1i*w).^p(i)+b(i))./((1i*w).^p(i)+b(i)+0.5*3140*(1i*w).^p(i)+3140*3140);  
figure(9)  
semilogx(f,20*log10(abs(Fr(w))));  
hold on  
figure (10)  
semilogx(f,(180/pi)*angle(Fr(w)));
```

```

hold on
figure(11)
semilogx(f,20*log10(abs(1./Fr(w))));
hold on
figure(12)
semilogx(f,(180/pi)*angle(1./Fr(w)));
hold on
end
%%%%%%%%%%%%%%%%%%%%%%%%%%%%%%%%%%%%%%%%%%%%%%%%%%%%%%%%%%%%%%%%%%%%%%%%
%
%      End of FOIHP and FOHP filter      %
%%%%%%%%%%%%%%%%%%%%%%%%%%%%%%%%%%%%%%%%%%%%%%%%%%%%%%%%%%%%%%%%%%%%%%%%

%%%%%%%%%%%%%%%%%%%%%%%%%%%%%%%%%%%%%%%%%%%%%%%%%%%%%%%%%%%%%%%%%%%%%%%%
%
%      FOAP filter      %
%%%%%%%%%%%%%%%%%%%%%%%%%%%%%%%%%%%%%%%%%%%%%%%%%%%%%%%%%%%%%%%%%%%%%%%%

close all;
clear all;
clc;
b = 1:-0.1:5;
w = logspace(1,9,5000);
f=.159*w;
%p=-.8:-.1:3;
for i=1:6
Fr = @(w) ((1i*w).^b(i)-3140)./((1i*w).^b(i)+3140);
figure(1)
semilogx(f,20*log10(abs(Fr(w))));
hold on
figure (2)
semilogx(f,(180/pi)*angle(Fr(w)));
hold on
figure(3)
hold on
end
%%%%%%%%%%%%%%%%%%%%%%%%%%%%%%%%%%%%%%%%%%%%%%%%%%%%%%%%%%%%%%%%%%%%%%%%
%
%      End of FOAP filter      %
%%%%%%%%%%%%%%%%%%%%%%%%%%%%%%%%%%%%%%%%%%%%%%%%%%%%%%%%%%%%%%%%%%%%%%%%

```

List of Research Papers in Journals and Conferences

International Journals:

- [1] D. R. Bhaskar, M. Kumar and P. Kumar, "Fractional order inverse filters using operational amplifier," *Analog Integrated Circuits Signal Process*, Vol. 97, no. 1, pp. 149-158, Oct. 2018. (SCI Journal)
- [2] D. R. Bhaskar, M. Kumar and P. Kumar, "Minimal realization of Fractional order inverse filters," *IETE Journal of Research*, pp. 1-14, 2020. (SCI Journal)
- [3] M. Kumar, D. R. Bhaskar and P. Kumar, "A Multifunctional Voltage Mode Fractional Order Filters using a Single CFOA", *IJITEE*, ISSN: 2278-3075, Vol.9, n0. 4, February 2020 (Scopus Journal)
- [4] M. Kumar, D. R. Bhaskar and P. Kumar, "CFOA-Based New Structure of Fractional Order Inverse Filters ", *IJRTE*, Vol. 8, no. 5, January 2020. (Scopus Journal)

International Conferences:

- [5] M. Kumar, P. Kumar and D. R. Bhaskar, "Multifunction Voltage Mode Fractional Order Filters Using Single Current Feedback Operational Amplifier", 1st International conference on signal processing, VLSI and communication engineering (IEEE conference) 2019 at ECED, DTU, Delhi
- [6] M. kumar, D. R. Bhaskar, and P. Kumar, " Single OTRA-based fractional order inverse filters", International congress on recent advances in sciences and technology(international conferenece), Kuala Lumpur, Malaysia
- [7] M. kumar, D. R. Bhaskar and P. Kumar, "Fractional Order Sinusoidal Oscillator Using only a Single Operational Trans-resistance Amplifier," *IEEE International Conference on Computing, Communication, and Intelligent Systems (ICCCIS)*, Sharda University, Greater Noida, UP (India), 2021

Author's Biography



Manoj Kumar was born in Patna (Bihar), India on 15th December 1975. He received the B. E. degree in Electronics and Communication Engineering from Karnataka University, Dharwad, Karnataka (India) in 1999 and M. Tech. in Bio-Electronics from Tezpur Central University, Tezpur, Assam (India) in 2008. He worked as Lecturer in the Department of Electronics and Communication Engineering, IIMT, Meerut (UP), during July 2008 to January 2010 before joining the GBPIET, Pauri (Uttarakhand) as Assistant Professor in the Department of Electronics and Communication Engineering, from where he was deputed to pursue doctoral studies in the Department of Electrical Engineering at Delhi Technological University, Delhi (India) under MHRD (Government of India) scheme of quality improvement program (QIP). He has authored or co-authored 10 research papers in various International/National journals and conferences proceedings. His teaching and research interests are in the area of analog circuits, analog filter design and fractional order systems.